Université de Montréal

Régulation du facteur de transcription FOXK1 par O-GlcNAcylation : Implications dans la différenciation adipocytaire

par Nicholas Iannantuono

Département de Biochimie Médecine moléculaire

Faculté de médecine

Mémoire présentée à la Faculté de Médecine en vue de
l'obtention du grade de maîtrise en Biochimie et médecine moléculaire
Option génétique moléculaire

Août 2015

Tables des matières

RÉSUMÉ (EN FRANÇAIS) IV
RÉSUMÉ (EN ANGLAIS) V
LISTES DES FIGURES VI
LISTE DES SIGLES ET ABBRÉVIATIONS VII
DÉDICACE X
REMERCIEMENTS XI

CHAPITRE 1 1

1. REVUE DE LA LITTÉRATURE 1

1.1 LES MODIFICATIONS POST-TRADUCTIONNELLES 2
1.1.1 Le système ubiquitine 2
1.1.2 Le système de déubiquitination 3
1.1.2.2 La structure et la fonction de BAP1 5
1.1.2.3 Les partenaires d'interaction de BAP1 7
1.2 LES MODIFICATIONS POST-TRADUCTIONNELLES DU COMPLEXE BAP1 8
1.2.1 Ubiquitination 9
1.2.1.1 Ubiquitination de BAP1 10
1.2.1.2 Ubiquitination de HCF1 11
1.2.1.3 Ubiquitination d'OGT 14
1.2.2 Phosphorylation 16
1.2.2.1 Phosphorylation de BAP1 17
1.2.2.2 Phosphorylation de l'OGT 19
1.2.2.3 Phosphorylation de YY1 21
1.2.3 O-GlcNAcylation et le métabolisme 23
1.2.3.1 La O-GlcNAcylation et maturation de HCF-1 24
1.2.3.2 O-GlcNAcylation of YY1 26
1.3 LES FACTEURS DE TRANSCRIPTION FOXK 27
1.3.1 Structure et domaine des FOXK 28
1.3.2 FOXK1 30
1.3.2.1 Réseau de régulation de FOXK1 dans la myogenèse 30
1.3.2.2 Régulation de FOXK1 par mTOR et le métabolisme 34
1.3.3 FOXK2 35
1.3.3.1 Recrutement de BAP1 à la chromatine 35
1.3.3.1 Implication de FOXK2 dans la prolifération cellulaire 36
1.3.4. La redondance entre FOXK1 et FOXK2 37
1.4 MISE EN CONTEXTE DU PROJET DE RECHERCHE 38
1.5 HYPOTHÈSE 38

CHAPITRE 2 40

2. ARTICLE EN PRÉPARATION 40

2.1 CONTRIBUTION DE CHAQUE AUTEUR 42
2.2 ABSTRACT 43
2.3 INTRODUCTION 44
2.4 MATERIAL AND METHODS 46

2.4.1 Bacterial induction, purification and GST-Pulldown *46*
2.4.2 Cell culture and G0 synchronization *46*
2.4.3 Plasmids, transfections and siRNA treatments *47*
2.4.4 Immunoprecipitation and complex purification *47*
2.4.5 Site-directed mutagenesis *48*
2.4.6 Differentiation and starvation *48*
2.4.7 Oil Red O staining *49*
2.4.8 Immunoblotting and antibodies. *49*
2.5 RESULTS 50
2.5.1 BAP1 structural conformation and Thr493 residue but not HCF-1 and OGT are important for FHA-dependant FOXKs binding to BAP1. ..... *50*
2.5.2 FOXK1 but not FOXK2 is O-GlcNAcylated by OGT *53*
2.5.3 FOXK1 O-GlcNAcylation by OGT is BAP1-independent. *56*
2.5.4 FOXK1 O-GlcNAcylation is modulated during cell cycle entry and in response to starvation. *57*
2.5.5 Foxk1, but not Foxk2, is required for adipogenesis *61*
2.6 DISCUSSION 64
2.7 ACKNOWLEDGEMENTS 68

CHAPITRE 3 ..... **69**

3. DISCUSSION **69**

3.1 RÉSUMÉ DES TRAVAUX DE RECHERCHES 70
3.2 UN CONCERT D'INTERACTIONS PROTÉIQUES MÉDIENT L'ASSOCIATION ENTRE LES FACTEURS FOXK ET BAP1. 70
3.3 FOXK1 EST RÉGULÉ PAR O-GLCNACYLATION 72
3.4 L'IMPORTANCE DE LA DYNAMIQUE PHOSPHORYLATION/O-GLCNACYLATION DE FOXK1 74
3.5 FOXK1 DANS L'ADIPOGENÈSE ET LA MYOGENÈSE 75

4. CONCLUSION **80**

5. LISTES DES RÉFÉRENCES **81**

CHAPITRE 4 ..... **97**

4. ARTICLES EN ANNEXES **97**

4.1 ARTICLE 1 : UNDETECTABLE HISTONE O-GLCNACYLATION IN MAMMALIAN CELLS II
4.2 ARTICLE 2 : THE BAP1/ASXL2 HISTONE H2A DEUBIQUITINASE COMPLEX REGULATES CELL PROLIFERATION AND IS DISRUPTED IN CANCER* XLI

Résumé (en français)

Les modifications post-traductionnelles telles que la phosphorylation, l'O-GlcNAcylation et l'ubiquitination jouent des rôles critiques dans la coordination des fonctions protéiques et par conséquent influencent grandement de nombreux processus cellulaires. Il est à noter que ces modifications sont hautement dynamiques et finement regulées. Par exemple, l'ubiquitination peut être réversible via l'action des déubiquitinases comme le suppresseur de tumeurs BAP1. Parmis les gènes codant pour les déubiquitinases, BAP1 est la plus souvent mutée dans le cancer. Des études récentes ont démontré l'importance des dynamiques de modifications post-traductionnelles dans la régulation du complexe BAP1. En plus, BAP1 forme un complexe multi-protéiques contenant plusieurs régulateurs transcriptionnels comme la protéine polycomb OGT et les facteurs de transcription FOXK1 et FOXK2. OGT est une enzyme unique qui catalyze l'ajout d'un groupement O-GlcNAc sur ses substrats afin d'en moduler l'activité enzymatique, les interactions protéines-protéines et leur localisation cellulaire. Cette modification est aussi liée au métabolisme puisque son substrat donneur, l'UDP-GlcNAc, est dérivé de la voie biosynthétique des hexosamines. Parallèlement, FOXK1/2 ont aussi été démontrés comme étant critiques à des processus métaboliques telles que la myogenèse et l'autophagie. Lors de nos études, nous avons identifié FOXK1 comme un nouveau substrat d'OGT. De plus, les niveaux d'O-GlcNAcylation de FOXK1 fluctuent lors de l'entrée/sortie du cycle cellulaire. En uotre, nous avons identifié l'importance de FOXK1 dans l'adipogenèse et observé que l'interaction FOXK1/BAP1 est affectée par le métabolisme cellulaire. En résumé, nos études ont révélé l'importance d'OGT dans la régulation de certaines composantes du complexe BAP1, ce qui aidera à la compréhension de l'effet suppresseur de tumeur de BAP1 ainsi que son mécanisme d'action dans différents processus tel que le remodelage de la chromatine.

Mots clées : FOXK1, FOXK2, BAP1, OGT, Ubiquitination, O-GlcNAcylation, Adipogenèse, Cancer, Métabolisme, Polycomb

Résumé (en anglais)

Post-translational modifications such as phosphorylation, O-GlcNAcylation and ubiquitination play critical roles in coordinating protein function and are therefore involved in diverse cellular processes. Of relevance here, ubiquitination may be removed by deubiquitinases such as the tumour suppressor BAP1, which represents the most mutated deubiquitinase gene in the human genome. Recent studies have revealed that important and dynamic post-translational modifications regulate several functions of the BAP1 complex. Indeed, BAP1 has been shown to form a multi-protein complex with several transcriptional regulators including the polycomb group protein OGT and the transcription factors FOXK1 and FOXK2. OGT is a unique enzyme that catalyzes the addition of an O-GlcNAc moiety to target proteins, which impacts protein function including enzymatic activity, protein-protein interactions and subcellular localization. This modification is also highly linked to cellular metabolism, as the donor substrate for the reaction, UDP-GlcNAc, is derived from the hexosamine biosynthesis pathway. Similarly, FOXK1 and FOXK2 have been shown to be implicated in metabolic processes such as myogenesis and autophagy. During our studies, we identified FOXK1 but not FOXK2 as a novel substrate of OGT. Further, we found that this O-GlcNAcylation is modulated during the entry/exit of cell cycle. We also found that FOXK1 is critical for adipogenesis and that the interaction between FOXK1/BAP1 is compromised during nutrient starvation. Thus, our studies have revealed that OGT selectively modulates and regulates components of the BAP1 complex which may impact different cellular processes, notably chromatin remodelling and could help understanding how BAP1 acts as a tumor suppressor.

Key Words : FOXK1, FOXK2, BAP1, OGT, Ubiquitination, O-GlcNAcylation, Adipogenesis, Cancer, Metabolism, Polycomb

Listes des figures

Figure 1. Mutations somatiques de BAP1 causant le cancer sont retouvées sur toute la longueur de la séquence de la protéine. 5
Figure 2. Homologie de séquence et de structure entre BAP1 chez l'humain et Calypso chez la Drosophile**.** 6
Figure 3. Schéma du complexe de suppresseur de tumeur BAP1. 9
Figure 4. La séquence du signal de localisation nucléaire de BAP1 est bipartite et contient une région hydrophobe nécessaire à l'interaction avec UBE2O**.**. 10
Figure 5. HCF-1 est ubiquitinée via des chaînes K48 et K63. 13
Figure 6. Schéma de la voie biosynthétique des hexosamines. 14
Figure 7. Hiérarchie des déubiquitinases de la famille UCH démontrant les sites de phosphorylation de BAP1**.** 18
Figure 8. Structure de YY1 avec les sites de phosphorylation et de clivages identifiés**.**. 22
Figure 9. HCF-1 est O-GlcNAcylée sur plusieurs sites en N-terminal et l'O-GlcNAcylation joue un rôle critique dans sa maturation.. 24
Figure 10. Modèle proposé pour le mécanisme moléculaire du clivage de HCF-1 par OGT via l'UDP-GlcNAc**.** 25
Figure 11. Structure cristalline du domaine FH de FOXK1 démontrant l'importance de l'hélice 3 et de l'aile de FOXK1 pour l'interaction avec l'ADN**.** 28
Figure 12. Structure cristalline du domaine FHA de RAD53 démontre que le résidu pT+3 confère la spécificité de l'interaction**.**. 29
Figure 13. Schéma du réseau de signalisation de Foxk1 dans les MPC**.** 31
Figure 14. Le domaine FHA de FOXK2 interagit avec le T493 phosphorylé de BAP1.. 35
Figure 15. BAP1 structural conformation and Thr493 residue but not HCF-1 and OGT are important for FHA-dependant FOXKs binding to BAP1**.**. 53
Figure 16. FOXK1 but not FOXK2 is O-GlcNAcylated by OGT**.**. 55
Figure 17. FOXK1 O-GlcNAcylation by OGT is BAP1-independent**.**. 57
Figure 18. FOXK1 O-GlcNAcylation is modulated during cell cycle entry and in response to starvation**.** 61
Figure 19. Foxk1 but not Foxk2 is required for adipogenesis**.** 64
Figure 20. FOXK1 et FOXK2 forment deux complexes distincts avec BAP1 qui ont probablement des fonctions différentes**.**. 72
Figure 21. Modèles des différents groupes de modifications post-traductionnelles sur FOXK1 et leurs fonctions respectives**.** 74
Figure 22. Modèle spéculé de la fonction de la dynamique de phosphorylation et O-GlcNAcylation de FOXK1**.** 79

Liste des sigles et abbréviations

AMPK : *AMP-Activated Protein Kinase*

ASX : *Additional Sex Comb*

ASXL1/2 : *Additional Sex Comb-Like 1 et 2*

ATM : *Ataxia Telangiectasia Mutated*

BAP1 : *BRCA1-Associated Protein 1*

BCA : Acide Bicinchoninique

BRCA1 : *Breast Cancer Susceptibility Gene 1*

BSS : Syndrome de Brooke-Spiegler

CC : *Coiled-Coil*

ChIP : Immunoprécipitation de la Chromatine

COX7c : *Cytochrome C Oxidase subunit 7C*

CTD : Domaine en C-Terminal

CXXC1 : *CXXC-type zinc finger protein 1*

CYLD : *Cylindromatosis*

DMEM : *Dulbecco's Modified Eagle Medium*

DSB : Bris Double Brin

DTT: Dithiothreitol

DUBs : Déubiquitinases

DVL : *Dishevelled*

EcR: Récepteur à l'Ecdysone

EZH2 : *Enhancer of Zeste 2*

FH : *Forkhead*

FHA : *Forkhead Associated*

FHL3 : *Four and a Half Lim Domain 3*

FOXK1/2 : *Forkhead Box Proteins 1 et 2*

GMPS : Guanosine 5'-monophosphate synthétase

GST : *Gluthatione-S-Transferase*

H2AK119ub : Monoubiquitination de H2A K119

HAT1 : *Histone Acetyltransferase 1*

HBM: *HCF-1 Binding Motif*

HBP : La voie Biosynthétique des Hexosamine

HBSS : *Hank's Balanced Salt Solution*

HCF-1 : *Host-Cell Factor 1*

HDAC1/2 : *Histone Deacetylase 1 and 2*

HR : Recombinaison Homologue

IBMX : *Isobutylmethylxanthine*

INO80 : *INO80 Complex Subunit*

iPOND : *Isolation of Proteins On Nascent DNA*

IPTG: Isopropyl β-D-1-thiogalactopyranoside

IRS-1 : *Insulin Receptor Substrate 1*

JAMMs : JAB1/NPP/MOV34 métalloenzymes

KDM1B/LSD2 : Lysine (K)-Specific Demethylase 1B

MDS : Syndrome Myélodysplasique

MPC : Cellule Progénitrice Myogénique

MPM : *Malignant Pleural Mesothelioma*

MPTs Modifications Post-Traductionnelles

MYL2 : Chaine Légère de la Myosine 2

NLS : Signal de Localisation Nucléaire

O-GlcNAc : *O-Linked-β-N-Acetylglucosamine*

OGT : *O-linked-N-acetylglucosamine transferase*

OTU : *Ovarian Tumour Proteases*

PLA : Ligation par proximité

PAH : Hélice Amphipathique jumelée

PcG : *Polycomb Group Protein*

PEI : Polyéthylenimine

PH : *Polyhomeotic*

PHC1-3 : *Polyhomeotic-Like Proteins 1-3*

PLK1 : *Polo-like Kinase 1*

PMSF: Phenylmethanesulfonyl fluoride

PPPDE : *Permuted Papain Fold Peptidases of DsRNA Viruses and Eukaryotes*

PSMD14: *Proteasome 26S Non-ATPase Regulatory Subunit*

pT : Phospho-thréonine

RB : *Retinoblastoma*

RBBP4/7 : *Retinoblastoma-Binding Protein 4 and 7*

RI : Rayonnements Ionisants

RT : *Room Temperature*

SAP18/SAP30 :*Sin3-Associated Protein 18 and 30*

SBE : *Sox Binding Element*

Sds3 : *Sin3 Histone Deacetylase Corepressor Complex Component SDS3*

Ser : Serine

SIN3A : *Paired Amphipathic Helix Protein Sin3a*

SIN3B : *Paired Amphipathic Helix Protein Sin3b*

SMAD3/4 : *Mothers Against Decapentaplegic 3 et 4*

SRF : *Serum Response Factor*

STAT3 : *Signal Transducer and Activator of Transcription 3*

Thr : Thréonine

TNNC1 : *Troponine 1 Type C*

TPR : Répétitions de tétratricopeptides

UBE2O: *Ubiquitin Conjugating Enzyme E2O*

UCH : *Ubiquitine C-terminal Hydrolase*

USP : *Ubiquitine-Specific Protease*

YY1 : *Yin Yang 1*

Dédicace

Je dédie ce mémoire à mes parents

Qui m'ont toujours poussé à l'excellence,

Qui m'ont toujours soutenu dans mon cheminement

Qui m'ont montré qu'il faut travailler fort

Pour réaliser nos rêves

Remerciements

D'abord, je voudrais remercier mon directeur de recherche Dr. El Bachir Affar pour m'avoir offert cette opportunité de réaliser ma maîtrise dans son laboratoire. J'aimerais le remercier de m'avoir conseillé tout au long de mon cheminement et de m'avoir apporté son soutien scientifique et professionnel.

En plus, je voudrais remercier mes collègues de laboratoire et du centre de recherche pour m'avoir guidé et aidé tout au long de mon cheminement scientifique. Surtout, je voudrais les remercier de m'avoir transmis leurs connaissances et particulièrement leur curiosité scientifique.

J'aimerais remercier la Faculté de médecine, le département de Biochimie et médecine moléculaire et la Faculté des études supérieures pour m'avoir accepté dans leur programme en plus de m'avoir octroyé des bourses d'études pour faciliter ma recherche scientifique.

Finalement, j'aimerais remercier tous les membres de ma famille qui m'ont supporté, encouragé et qui ne cesse de me guidé durant mon développement en tant que scientifique.

Surtout, je veux remercier ma conjointe et partenaire de vie, qui n'a jamais cessé de me soutenir, de m'aimer, de s'impliquer dans ma recherche, de s'investir dans mon futur et plus particulièrement je la remercie pour sa passion pour la science et la découverte qui contribue à renforcer davantage mon amour pour la science.

Chapitre 1

1. Revue de la littérature

1.1 Les modifications post-traductionnelles

Le changement de l'état d'une protéine par l'ajout d'une modification post-traductionnelle telles que la méthylation, acétylation, la phosphorylation, l'O-GlcNAcylation, la sumoylation et l'ubiquitination a pour but principal de réguler sa fonction, sa localisation et/ou son activité catalytique. Certaines modifications peuvent même inhiber ou entrer en compétition avec d'autre. De telles compétitions sont bien connues dans le domaine de l'épigénétique, où l'acétylation, méthylation et/ou ubiquitination des histones, par exemple, peuvent influencer et contrôler la réponse transcriptionnelle. Parmi ces modifications, l'ubiquitination s'avère être critique pour l'homéostasie cellulaire, car elle sert de signal entre-autre pour la dégradation via le protéasome, un mécanisme important de recyclage cellulaire.

1.1.1 Le système ubiquitine

L'ubiquitination est une modification post-traductionnelle très abondante qui correspond à l'ajout, par liaison covalente, d'une protéine « ubiquitine » de 76 acides aminés aux lysines ou aux résidus N-terminaux des protéines substrats. La cascade enzymatique menant à l'ubiquitination d'un substrat comporte l'action séquentielle de trois classes d'enzymes, soit la *E1 ubiquitin-activating*, *E2 ubiquitin-conjugating* et enfin la *E3 ubiquitin-ligating [1-7]*. Dans la plupart des cas, les E3 ligases confèrent la spécificité de la réaction en reconnaissant le substrat, mais quelques exemples d'hybride E2/E3 ainsi que des E2 seules ont aussi été identifiés [8, 9]. Il existe aussi un groupe d'enzyme nommé E4 *Chain Elongation Factors* qui confère un niveau supplémentaire de régulation en participant à l'étape finale de l'ubiquitination en collaboration avec les E3 [10]. Cependant, la majorité des substrats sont ubiquitinés via la voie classique comprenant les enzymes E1, E2 et E3. Par ailleurs, l'ubiquitination d'une protéine cible peut se faire de différentes manières incluant la modification d'une seule lysine (mono-ubiquitination) ou de plusieurs lysines (multi-mono-ubiquitination) [7]. De plus, une des sept lysines (K6, K11, K27, K29, K33, K48 et K63) de la protéine d'ubiquitine elle-même peut aussi être ciblée pour ubiquitination (poly-ubiquitination) résultant en une multitude de chaînes d'ubiquitine homotypiques ou même hétérotopiques, chacune associée à différents signaux cellulaires spécifiques[7]. Par exemple, les chaines d'ubiquitine médiées par des liaisons K48 sont associés à la dégradation par le

protéasome tandis que celles médiées par les liaisons K63 sont associées à l'activation des kinases et l'assemblage transitoires des complexes protéiques [11-13]. Cependant, plusieurs questions mécanistiques au sujet de l'ubiquitination sont non résolues. Entre autres, qu'est-ce qui détermine la longueur spécifique des chaînes d'ubiquitine et est-ce la même E3 ligase qui ajoute progressivement les quatre ubiquitines sur un substrat, ou y-a-t'il y a relâchement du substrat après chaque ubiquitination? Par ailleurs, pour ce qui est de la mono-ubiquitination, bien que les lysines de l'ubiquitine conjuguée soient disponibles, il n'y a pas d'extension en chaîne même en présence d'E3 ligase non spécifiques. Des études récentes ont révélé que ces lysines peuvent être modifiées par acétylation, phosphorylation, ISG15ylation, etc ce qui ajoute un niveau de régulation supplémentaire à cette cascade[14-17].

1.1.2 Le système de déubiquitination

L'ubiquitination est une modification hautement dynamique puisqu'elle est toujours en compétition avec le processus inverse, soit la déubiquitination. Cette dynamique est régulée par les enzymes déubiquitinases (DUBs) qui servent à contrecarrer cette signalisation. De plus, les DUBs sont elles-mêmes très régulées. À ce jour, environ une centaine de gènes codant pour des DUBs dans le génome humain ont été identifiés[18, 19]. Ces DUBs sont sous-divisés en 6 familles, à savoir les *Ubiquitin C-terminal Hydrolases* (UCH), les *Ubiquitin-Specific Proteases* (USP), les *Ovarian Tumour Proteases* (OTUs), les Machado-*Josephin domain proteases (MJDs)*, les *JAB1/NPP/MOV34 métalloenzymes* (JAMMs) et la famille récemment découverte *Permuted Papain Fold Peptidases of DsRNA Viruses and Eukaryotes* (PPPDE)[7, 20-22]. Les DUBs des familles UCH, USP, OTU, Josephin et PPPDE utilisent différents domaines catalytiques, touts composes d'une triade catalytique basée sur une cystéine catalytique, afin de faire une attaque nucléophile sur la liaison isopeptidique entre l'ubiquitine et le substrat. Quant aux JAMM, il s'agit de métalloprotéases à base de zinc. Depuis la dernière décennie, l'étude de la fonction des déubiquitinases constitue un sujet de recherche d'un intérêt particulièrement éminent et de nouvelles découvertes ont mené à une meilleure compréhension de plusieurs maladies. Par exemple, la déubiquitinase USP7 s'est révélée être un antagoniste direct de l'activité de MDM2, la E3 ligase qui cible pour dégradation protéasomale le suppresseur de tumeurs p53, un facteur de transcription qui joue un rôle

important dans l'arrêt de la progression du cycle cellulaire et qui est considéré comme le gardien du génome [23]. La DUB *Proteasome 26S Non-ATPase Regulatory Subunit 14* (PSMD14) est une métalloprotéase de la sous-unité régulatrice 19S du protéasome capable d'antagoniser la signalisation RNF8/RNF168 lors des dommages à l'ADN [24]. D'autre part, les structures cristallines ont révélé l'importance de PSMD14 dans la déubiquitination des chaînes K48 sur les substrats avant leur entrée dans le canal de dégradation du protéasome et cela dans le but de maintenir les niveaux d'ubiquitines libres dans les cellules [24-26]. Enfin, des mutations dans le gène *Cylindromatosis* (CYLD), une DUB associée à la régulation de la signalisation NF-κB, ont été associées au syndrome Brooke-Spiegler (BSS) (ou Cylindromatose familiale), une maladie caractérisée par des néoplasmes annexielles, incluant les cylindromes et les glandes salivaires [27-32]. De toute évidence, la régulation des niveaux d'ubiquitines dans la cellule affecte un grand nombre, sinon la plupart des processus cellulaires [1, 3-7, 12, 18, 19, 33-41]. En outre, la déubiquitinase *BRCA1 Associated Protein-1* (BAP1) a été découverte pour la première fois dans un criblage double-hybride permettant d'identifier des partenaires d'interaction de *BReast CAncer type 1 susceptibility gene 1* (BRCA1) [42, 43]. En effet, ces études ont démontré que BAP1 agit de concert avec BRCA1 pour réguler la croissance des tissus mammaires et que cette interaction est souvent éliminée dans le cancer du sein [43]. De plus, plusieurs études ont tenté de cartographier les mutations de BAP1 dans des cancers provenant de divers tissus. Il est à noter que des mutations de BAP1 ont été associées au mésothéliome pleural malin (MPM) [44-46]. Souvent, les mutations causent une troncation du domaine C-terminal, délétant donc le signal de localisation nucléaire (NLS) de BAP1 et provoquant par la suite une séquestration de BAP1 dans le cytoplasme (figure 1). Il est à noter que plusieurs mutations affectent aussi l'activité catalytique de BAP1 (figure 1) [47, 48]. Un nombre important d'études continuent d'identifier des mutations de BAP1 dans un nombre toujours grandissant de cancers incluant les paragangliomes, carcinomes Neuro-endocrine, méningiomes, adénocarcinomes du poumon, mésothéliome, mélanome cutané, et carcinome rénal à cellules claires [48]. Le séquençage des exomes de diverses tumeurs a révélé que, parmi les centaines de gènes codant pour des DUBs, BAP1 est le plus mutée dans le génome humain (figure 1)[46, 47, 49]. Entre-autre, deux études indépendentes ont identifié

des mutations somatiques de BAP1 pouvant être liées au développement de mélanomes uvéaux (47 et 39 %)[46, 47, 49, 50]. Toutefois, à l'exception des carcinomes du rein, MPM et mélanomes uvéaux, moins de 10 % des cancers de la prostate, de l'ovaire, du côlon, du sein, du poumon, du pancréas, des voies biliaires, de l'estomac et des cancers du système nerveux central sont causés par des mutations somatiques BAP1. En fait, ces cancers sont plutôt liés à des mutations sporadiques de BAP1. Le vaste éventail de tissus touchés démontre que BAP1 est un important suppresseur de tumeurs qui régule des processus cellulaires très importants. Cependant la fonction exacte de BAP1 comme suppresseur de tumeurs demeure peu connue.

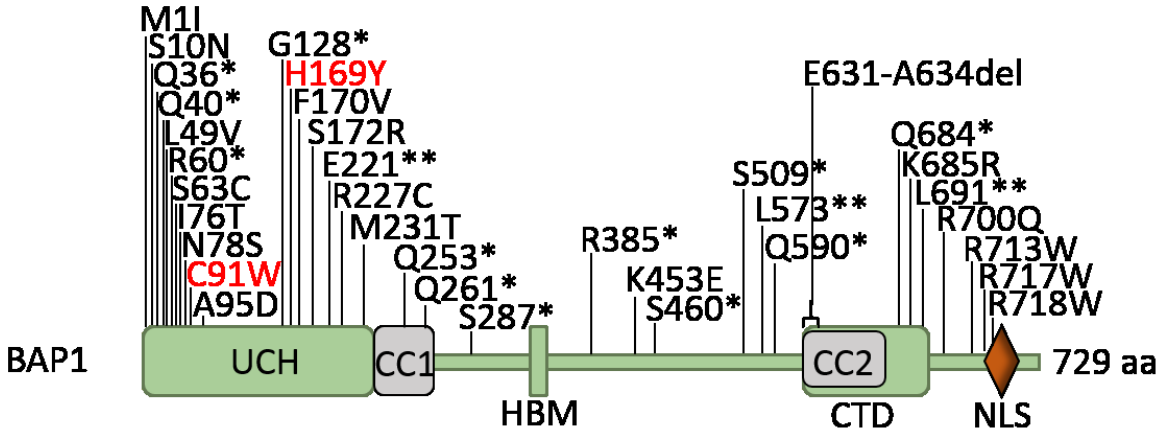

Figure 1. Mutations somatiques de BAP1 causant le cancer sont retouvées sur toute la longueur de la séquence de la protéine. Les mutations somatiques du répertoire *COSMIC* retrouvées aux moins deux fois ont été utilisées pour produire ce schéma. Des mutations sont retrouvées dans presque tous les domaines et les mutations causant un codon stop prématuré (annotées par un astérisque) élimine souvent le domaine CTD et NLS de BAP1 ce qui cause sa rétention dans le cytoplasme. Les mutations causant un changement de cadre de lecture sont annotées pas deux astérisques. Les mutations en rouge sont directement associées avec les acides aminés critiques pour le tryade catalytique de BAP1. Ces mutations engendrent la formation d'un BAP1 peu ou pas actif pouvant avoir des effets dominants négatifs. UCH: Ubiquitin C-Terminal Hydrolase, CC1/2: Coiled-Coil 1/2, HBM: *HCF-1-Interacting Motif*, NLS: *Nuclear Localization Signal*, CTD: *C-terminal Domain*.

1.1.2.2 La structure et la fonction de BAP1

La protéine BAP1 a une structure modulaire (figure 1-2). Brièvement, son domaine catalytique UCH se trouve en position N-terminale de la protéine, alors que son NLS, comme décrit précédemment, se retrouve dans l'extrémité C-terminale. Un petit motif de quatre acides aminés, soit le *HCF-1 Binding Motif* (HBM) dont l'importance et la fonction seront discutées plus tard, se trouve au centre de la protéine. Aussi, un domaine d'interaction protéique avec diverses protéines telles que BRCA1, *Yin Yang 1* (YY1) et *Ubiquitin Conjugating Enzyme E2O* (UBE2O) se trouve dans sa portion C-terminale (CTD) [9, 43, 51]. De manière

importante, la structure de BAP1 s'est grandement complexifiée chez les vertébrés en comparaison avec son orthologue, Calypso, chez la Drosophile [52]. Comme présenté à la figure 2, il y a eu apparition d'une extension contenant ce motif HBM entre le domaine catalytique et le domaine CTD. Cette extension, et donc son interaction avec *Host-Cell Factor 1* (HCF-1), a entraîné une grande complexification des fonctions de BAP1 en raison des interactions possibles avec une pléthore de facteurs associés à la chromatine.

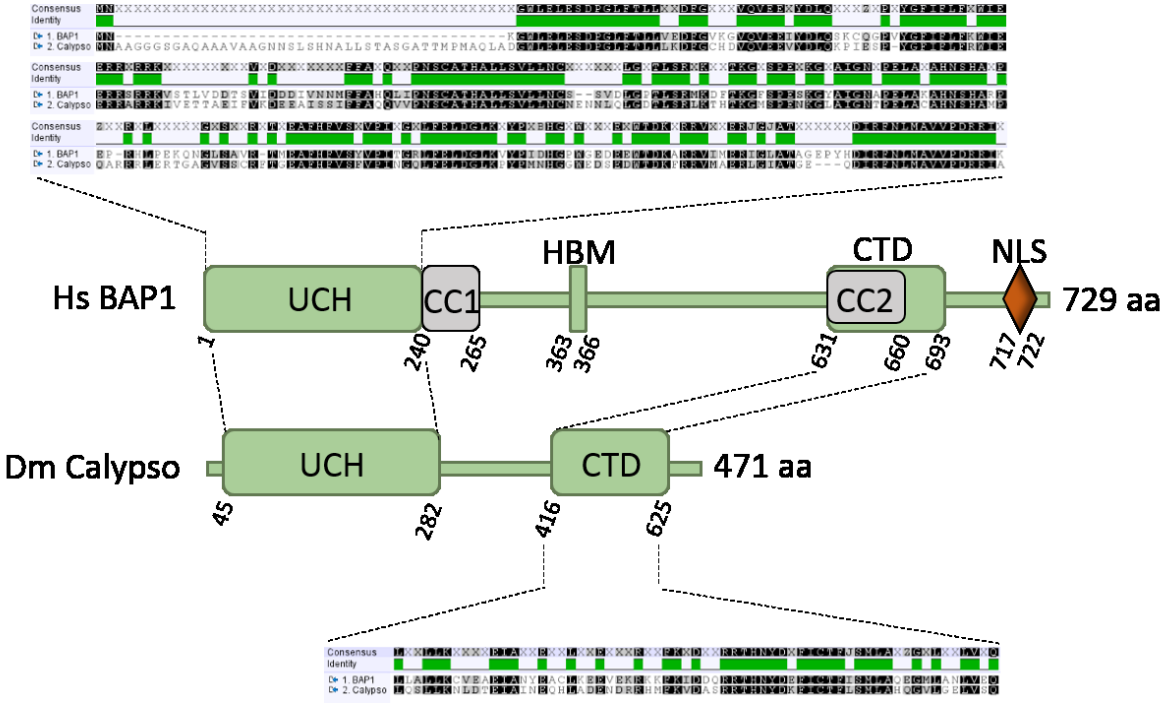

Figure 2. Homologie de séquence et de structure entre BAP1 chez l'humain et Calypso chez la Drosophile. BAP1 et Calypso contiennent des domaines hautement conservés, soit 66% d'identité entre les domaines UCH et un domaine CTD avec 54% d'identité. Contrairement à Calypso, BAP1 contient une extension au centre contenant le motif HBM, un motif permettant donc à BAP1 d'interagir avec HCF-1 et plusieurs autres partenaires tel OGT. UCH; Ubiquitin C-Terminal Hydrolase, CC1/2; Coiled-Coil 1/2, HBM; HCF-1 Interacting Motif, NLS; Nuclear Localization Signal, CTD; C-terminal Domain.

La fonction polycombe (PcG) du complexe BAP1 a d'abord été déterminée grâce aux études de Calypso chez la Drosophile. Ces études ont démontré que Calypso interagit de façon stable avec une protéine PcG *Additional Sex* Comb (ASX), homologue de *Additional Sex Comb-Like 1 et 2* (ASXL1 et ASXL2), pour former un complexe appelé *Polycomb Repressive-DUB* (PR-DUB) [52]. Chez la Drosophile, ce complexe est capable de déubiquitiner la mono-ubiquitination de la lysine 118 de l'histone H2A (H2AK118ub), une marque connue pour son importance dans la répression de l'expression des gènes HOX et de la régulation de l'expression génique [52]. Des

études similaires chez les mammifaires ont permis de démontrer que BAP1 en complexe avec ASXL1/2 est capable de déubiquitiner la lysine 119 (H2AK119ub) chez l'humain correspondant à H2AK118 chez la Drosophile [52].

En raison de la létalité embryonnaire des souris BAP1$^{-/-}$, l'étude de la fonction précise de BAP1 dans le développement s'est réalisée via des systèmes de *knockout* (KO) inductibles [42, 46]. Étonnamment, dans un délai très court d'environ 4 semaines, l'ablation complète de BAP1 après la naissance, provoque une splénomégalie chez les souris [46]. En fait, les souris BAP1$^{-/-}$ récapitulent le syndrome Myélodysplasique humain (MDS), impliquant le développement d'une hématopoïèse extramédullaire et une expansion de la lignée myéloïde [46]. Ces souris ont également montré des enrichissements des cellules myéloïdes au niveau des ganglions lymphatiques et de la moelle osseuse, ce qui peut être provoqué par une différenciation dysfonctionnelle de la lignée myéloïde [46]. Cependant, la façon précise dont BAP1 contrôle la différenciation hématopoïétique demeure inconnue, bien que les phénotypes observés soulignent son importance dans l'homéostasie de l'hématopoïèse.

Par ailleurs, outre son importance directe envers l'histone H2A et la régulation transcriptionnelle qui découle de cette activité, des études plus poussées de son activité enzymatique ont révélé qu'en fait, BAP1 reconnaît et peut déubiquitiner plusieurs autres substrats tels que son propres NLS et/ou d'autres régulateurs transcriptionnels [9, 51, 53-60]. L'importance de ces activités supplémentaires sera discutée plus tard.

1.1.2.3 Les partenaires d'interaction de BAP1

Afin de comprendre comment BAP1 régule les processus cellulaires dans une large gamme de tissus, plusieurs groupes dont le nôtre ont purifié le complexe BAP1 pour étudier ses partenaires d'interaction[45, 56, 57, 61, 62]. Ces purifications de complexe ont révélées l'importance de BAP1 dans l'expression génique puisque cette DUB s'associe principalement avec des régulateurs transcriptionnels. Chez les mammifères, BAP1 forme un complexe multi-protéique de 1,6 MégaDalton (MDa) contenant plusieurs co-régulateurs transcriptionnels, des facteurs de transcription et des protéines PcG tel que schématisé à la figure 3 ci-dessous[51, 56, 57]. Des analyses protéomiques plus approfondies ont révélé que presque toutes les

molécules BAP1 se trouvant dans le noyau sont en complexe avec HCF-1, les facteurs PcG ASXL1 et ASXL2, le facteur PcG *O-linked β-N-acetylglucosamine transferase* (OGT) et les facteurs de transcription *Forkhead Box K1 et K2* (FOXK1 et FOXK2)[52, 57, 61]. L'hybride E2-E3 ubiquitine ligase UBE2O, le facteur de transcription Yin Yang 1 (YY1), l'acétyltransférase de l'histone 1 (HAT1) et la déméthylase de l'histone H3K4 (KDM1B/LSD2) ont également été purifiés avec BAP1 malgré le fait qu'ils sont moins abondants. Cependant, il existe probablement d'autres partenaires qui n'ont pas été identifiés dans ces purifications de complexes dû au contexte biologique ou au type cellulaire. En effet, ces purifications ont été réalisées dans des cellules HEK293T et HeLa [51, 56, 57]. Il se peut donc que dans le contexte de ces cellules cancéreuses, l'interaction entre BAP1 et BRCA1 détectée dans les cellules du cancer du sein MCF-7 puisse être compromise dans ces types cellulaires.

1.2 Les Modifications post-traductionnelles du complexe BAP1

La présence d'un grand nombre de protéines modificatrices dans le complexe BAP1 (BAP1, UBE2O, HAT1, OGT, LSD2) suggère qu'une régulation très fine par modifications post-traductionnelles est nécessaire au bon fonctionnement de ce complexe. En effet, il est possible de spéculer que la diversité de ces protéines modificatrices au sein du complexe BAP1 agisse comme une plateforme où la collaboration entre les différentes modifications résulte en une régulation complexe de la transcription. Toutefois, ceci doit être vérifié. D'autre part, il est maintenant connu que ces modifications jouent un rôle dans la régulation de l'activité de ces composantes à même le complexe. En effet, l'ubiquitination, la phosphorylation et l'O-GlcNAcylation de plusieurs des sous-unités du complexe BAP1 sont critiques à leurs fonctions.

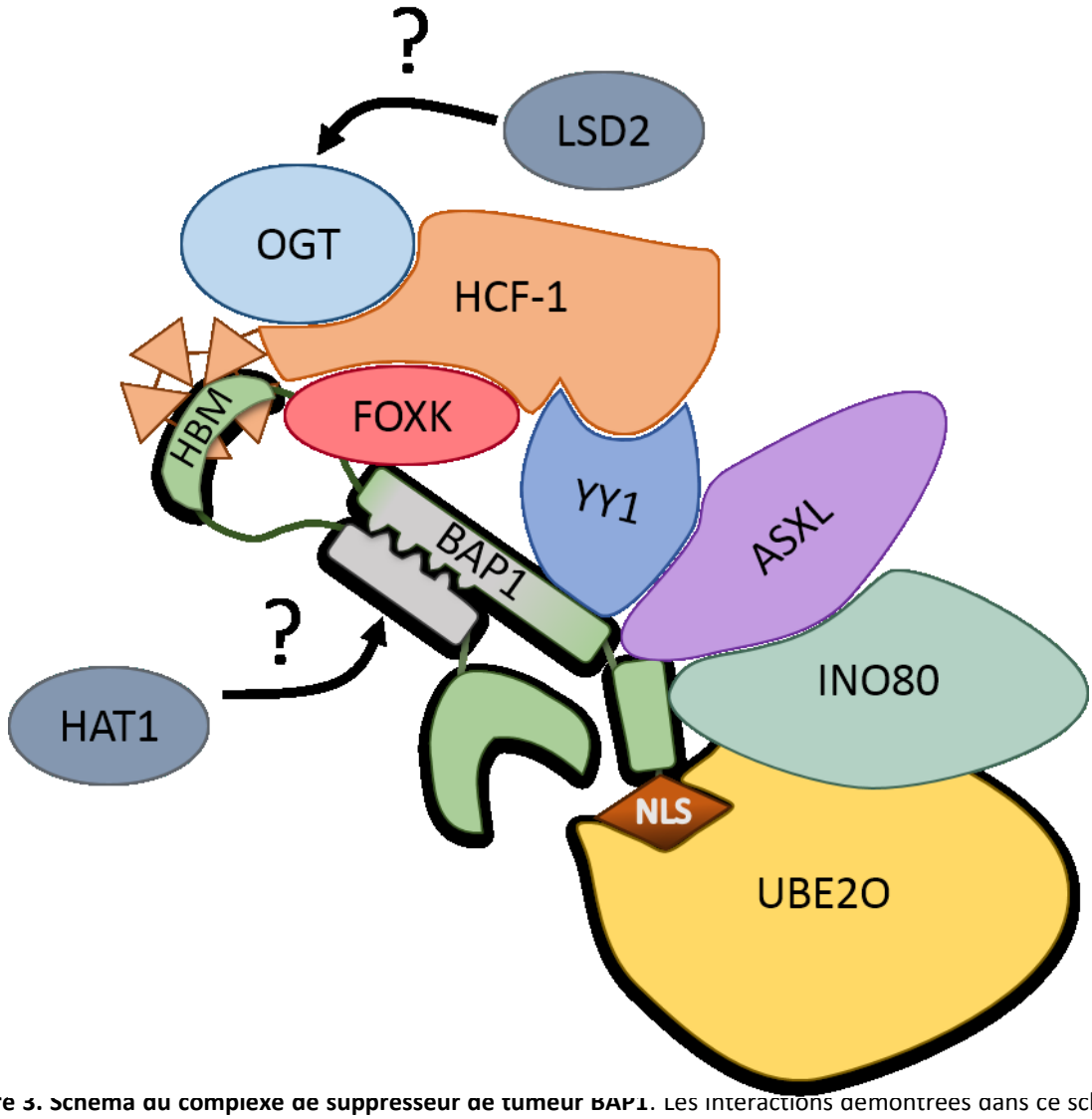

Figure 3. Schéma du complexe de suppresseur de tumeur BAP1. Les interactions démontrées dans ce schéma viennent de plusieurs études qui ont caractérisé leurs positions dans le complexe BAP1. Les études récentes sur les FOXKs ont démontré une interaction avec T493 de BAP1 et le domaine FHA de FOXKs. L'interaction avec LSD2 dans le complexe n'est pas caractérisée mais son activité E3 ligase envers OGT peut expliquer sa présence dans le complexe. Des études de spectrométrie de masse ont révélé la présence de HAT1 dans le complexe mais cette interaction n'a pas été étudiée.

1.2.1 Ubiquitination

Comme décris précédemment, l'ubiquitination d'une protéine peut avoir diverses répercussions, sur l'activité, la localisation cellulaire et les interactions protéiques de cette dernière. Dans le complexe BAP1, trois exemples illustrent bien ces différents effets de l'ubiquitination.

1.2.1.1 Ubiquitination de BAP1

Notre groupe a récemment démontré que BAP1 est constitutivement mono-ubiquitinée et que cette modification dépend de son activité catalytique [9]. De plus, nous avons démontré que l'ubiquitine ligase UBE2O interagit avec le NLS de BAP1 permettant ainsi l'ubiquitination de ce motif de manière indépendante de son ubiquitination constitutive [9]. Il

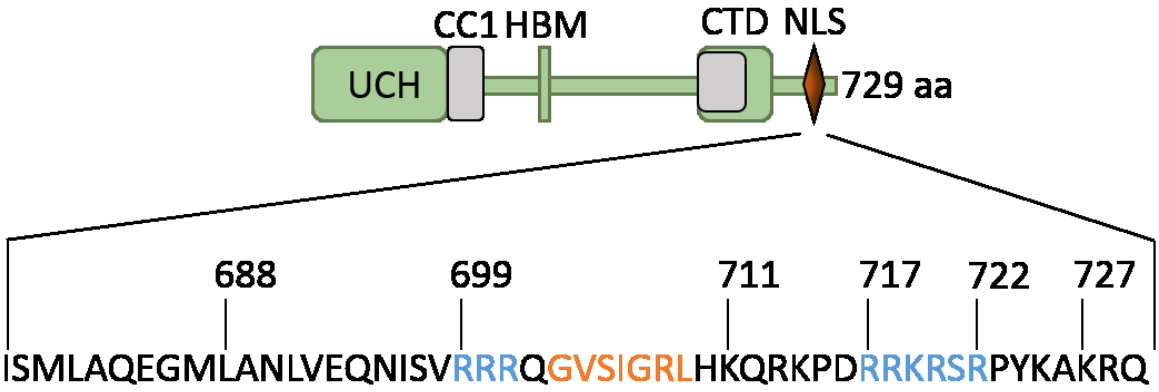

Figure 4. La séquence du signal de localisation nucléaire de BAP1 est bipartite et contient une région hydrophobe nécessaire à l'interaction avec UBE2O. Le NLS bipartite (en bleu) de BAP1 et la région hydrophobe (en orange) de BAP1 sont nécessaires à la multi-mono-ubiquitination par UBE2O. Cette ubiquitination masque le NLS afin de séquestrer BAP1 dans le cytoplasme. La localization nucléaire d'autres protéines ayant des NLS bipartite comme celui de BAP1 (ayant la région hydrophobe), comme la protéine nucléaire CXXC1 peut aussi être régulées par un mécanisme similaire impliquant UBE2O. Adapté de Mashtalir et al [9].

est à noter que UBE2O ne catalyse pas la poly-ubiquitination de BAP1, mais plutôt la multi-mono-ubiquitination de plusieurs lysines du NLS [9]. Plus spécifiquement, BAP1 comporte un NLS bipartite composé de deux lobes importants pour l'interaction avec UBE2O, séparé par une région hydrophobe contenant les acides aminés valine, isoleusine et leucine (Figure 4). L'ubiquitination du NLS mène à la séquestration de BAP1 dans le cytoplasme et résulte donc en l'inhibition de sa fonction en tant que régulateur transcriptionnel. Par contre, cette ubiquitination est activement contrecarrée par l'activité d'auto-déubiquitination de BAP1 dans les cellules prolifératives [9]. Des mutations affectant cette activité ont été identifiés dans différents cancers [9]. D'ailleurs, dans les cellules post-mitotiques comme les cellules adipocitaire 3T3L1 différenciées, un mécanisme encore inconnu permet le maintien de cette multi-mono-ubiquitination, séquestrant BAP1 dans le cytoplasme [9]. De cette manière, UBE2O provoque un arrêt du cycle cellulaire en inhibant la prolifération contrôlée par le complexe BAP1.

Il y a un éventail de répercussions cellulaires suite à la séquestration de BAP1 au cytoplasme. Par exemple, dans un contexte de prolifération normale, BAP1 régule l'activité du complexe de remodelage de la chromatine INO80. Plus précisément, en utilisant la technologie d'isolation des protéines sur les brins d'ADN naissants (iPOND) [63], une étude a démontré que BAP1 interagit avec et déubiquitine INO80. Ce complexe régit plusieurs processus cellulaires, y compris la transcription, la réplication et réparation de l'ADN afin de maintenir la stabilité génomique [64-66]. L'interaction entre BAP1 et INO80 s'est montrée critique à la bonne progression des fourches de réplication de l'ADN et cette fonction dépendait de leurs activités catalytiques [55]. Cette interaction permet de stabiliser les niveaux protéiques d'INO80 et ce, tout en le recrutant à la chromatine via l'interaction entre BAP1 et H2AK119ub [55]. Un criblage de mutants de cancer de INO80 et BAP1 a révélé une perte d'expression des deux protéines dans plus de 80% des Mésothéliome Pleural Malin (MPM). De plus, bien qu'il y avait plus souvent une perte d'expression de BAP1 dans les Mésothéliome Péritonéal Malin il y avait une forte corrélation entre les niveaux d'expression de BAP1 et INO80 dans ces cancers [55]. Ces données révèlent la nécessité d'un bon fonctionnement de l'autodéubiquitination par BAP1. En effet, si cette dynamique se trouve affectée par des mutations cancéreuses, BAP1 cytoplasmique ne peut exercer sa fonction sur INO80 ou toutes ces autres cibles nucléaires. Quant à INO80, les mutations de BAP1 pourraient conduire à une déstabilisation de ce facteur, entraînant ainsi l'effondrement des fourches de réplication, ce qui pourrait conduire à des aberrations chromosomiques. À noter que INO80 est associé avec l'échange de H2A pour l'isoforme H2A.Z près des sites de transcription hautement actifs [67]. À cet égard, par l'entremise d'une dynamique d'ubiquitination de BAP1 par UBE2O, il reste à déterminer si le complexe BAP1 pourrait réguler à la fois directement les niveaux de H2Aub et indirectement les niveaux de H2A.Z via la régulation de la stabilité de INO80 dans certains contextes cellulaires.

1.2.1.2 Ubiquitination de HCF1

Un des partenaires d'interaction majeur du complexe BAP1 est HCF-1. Elle s'avère être la composante la plus stœchiométrique du complexe où presque la totalité des molécules de BAP1 sont liées à des molécules de HCF-1 dans un ratio 1:1, ce qui suggère l'importance de

cette interaction pour la fonction du complexe [61, 68]. HCF-1 est composée d'une région N-terminale qui comporte cinq répétitions Kelch et une région contenant un motif *fibronectin type III-like* en C-terminal (figure 5). Par ailleurs, HCF-1 est soumise à un processus de maturation protéique impliquant une étape de clivage protéolytique d'une de ses six répétitions (HCF-1PRO) au centre de la protéine [51, 56, 57, 69-73]. Ce clivage produit une paire de polypeptides (HCF-1N et HCF-1C) qui interagissent par liaisons non-covalentes et qui sont associés à la régulation de la progression G1/S et à l'étape mitotique de cytocinèse [73]. De plus, HCF-1 régule la transcription génique en interagissant avec plusieurs facteurs et co-facteurs puisqu'elle ne peut pas lier l'ADN. Par exemple, HCF-1 participe à d'importantes interactions avec les membres de la famille E2F pour réguler le cycle cellulaire [73-76]. Dans le contexte du complexe BAP1, des études protéomiques ont révélé que HCF-1 sert de protéine d'échafaudage permettant le recrutement de plusieurs partenaires d'interaction [51]. Comme mentionné précédemment, à l'aide de ses domaines Kelch, HCF-1 interagit avec BAP1 via un motif de liaison de quatre acides aminés (NHNY) dans la région flexible de BAP1 nommé *HCF-1 Binding Motif* (HBM) [51]. Cette région est critique pour l'assemblage du complexe BAP1, car des études de mutagenèse dirigée ont révélé une perte presque totale des membres du complexe suite à une délétion de cette région [51]. D'autre part, une étude a démontré que HCF-1 est hautement régulée par ubiquitination sur les résidus K1807 et K1808 au niveau de son domaine C-terminal, via des chaînes K48 et K63 (figure 5) [57]. Cette étude a aussi révélé que BAP1 interagit avec HCF-1 via son HBM afin de réduire les niveaux d'ubiquitination K48 [57]. Une autre étude effectuée par Machida et al. [56] a permis l'identfication de d'autres sites d'ubiquitination, encore majoritairement K48 avec peu de K63 sur les résidus K105, K163, K244 et K363, se trouvant dans le domaine Kelch de HCF-1, plus précisément entre les répétitions (Figure 5). Cependant, contrairement à cell de Misaghi, l'équipe de Machida n'a pas observé d'effet sur la stabilité de HCF-1. Ceci suggère donc que BAP1 régulerait HCF-1 via déubiquitination, sans affecter sa stabilité. En effet, les sites d'ubiquitination en N-terminal sont au niveau du domaine Kelch de HCF-1 et c'est ce même domaine qui permet l'intéraction avec BAP1. Il est donc possible que l'enlèvement de ces ubiquitines permette le bon repliement de ce domaine. De ce fait, la déubiquitination de HCF-

1 par BAP1 permettrait une bonne liaison entre le domaine Kelch de HCF-1 et le HBM de BAP1. En déubiquitinant HCF-1, BAP1 stabiliserait la présence de ce système d'échafaudage dans le complexe.

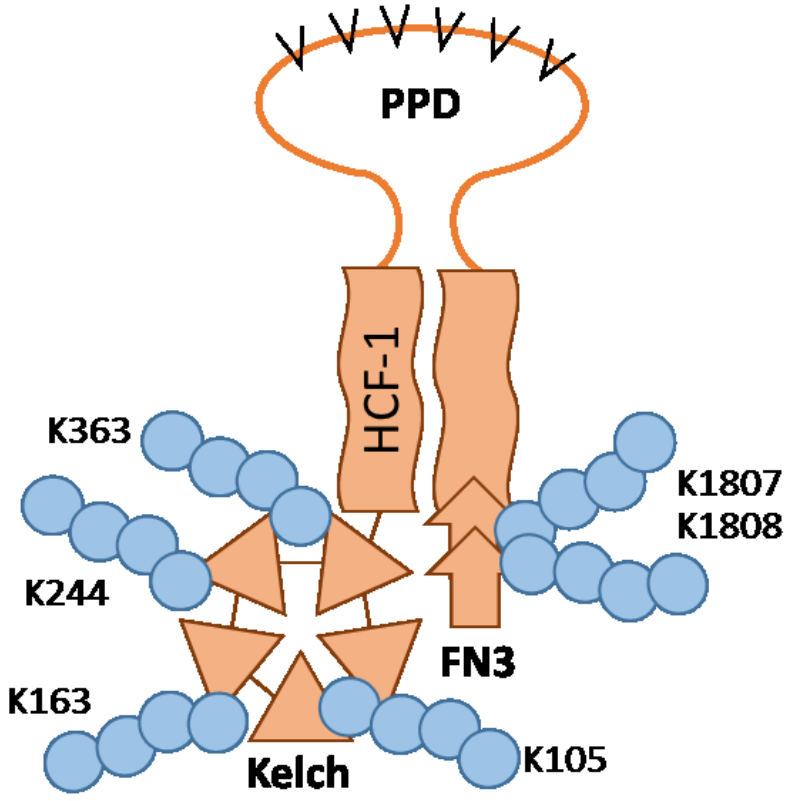

Figure 5. HCF-1 est ubiquitinée via des chaînes K48 et K63. Schéma de la structure de HCF-1 avec les domaines connus. Les sites d'ubiquitination ont été déterminés par analyse par spectrométrie de masse. Le domaine Kelch est ubiqutiné entre les feuillets béta et deux sites d'ubiquitination des répétitions de fibronectine type III ont été trouvés. PPD : Domaine de clivage protéolytique, FN3; *Fibronectlin-like type III.*

Toutefois, il est important de noter que cet échafaudage n'a pas d'impact sur l'activité enzymatique de BAP1. En fait, des études in vitro et in vivo ont montré que le mutant BAP1ΔHBM, où le motif HBM a été enlevé, peut déubiquitiner H2AK119ub [51]. Cependant, en l'absence de la majorité des partenaires d'interactions, il est possible que son action soit beaucoup moins spécifique entrainant ainsi une dérégulation de l'homéostasie cellulaire.

Par ailleurs, des lignées cellulaires BAP1$^{-/-}$ dans lesquelles on a restauré l'expression de BAP1 démontrent une meilleure progression de la transition G1/S [53]. D'autres études ont démontré que BAP1, via son interaction avec HCF-1, régule négativement le cycle cellulaire

[44, 46, 56, 77-79]. En résumé, la déubiquitination de HCF-1 par BAP1 démontre l'importance de cette modification et de sa dynamique dans le contrôle des signaux pro- et anti-prolifératifs, de sorte que BAP1 puisse agir en tant que suppresseur de tumeur en engendrant une prolifération cellulaire contrôlée.

1.2.1.3 Ubiquitination d'OGT

L'*O-Linked N-Acetylglucosamine (*O-GlcNAc) *Transferase* (OGT) est une enzyme unique dans le génome et extrêmement conservée de *C.elegans* à l'humain, capable de médier le transfert d'un groupement O-GlcNAc sur les sérines et thréonines des protéines substrats[80].

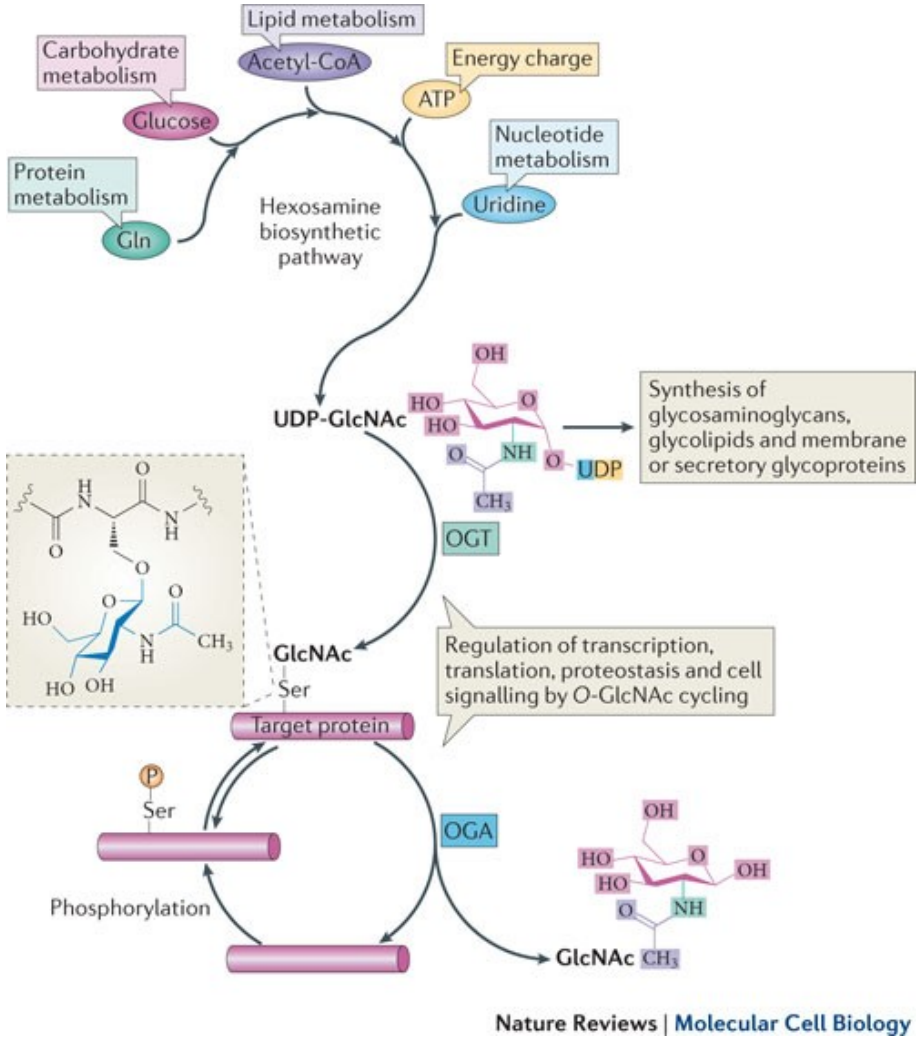

Figure 6. Schéma de la voie biosynthétique des hexosamines. La synthèse de la molécule d'UDP-GlcNAc est régulée par de multiples voies métaboliques incluant les acides aminés, les acides gras, l'ATP et les nucléotides. De plus, 5% du glucose cellulaire est dévié vers la voie des hexosamines. Aussi, lorsqu'OGA catalyse l'enlèvement de l'O-GlcNAc d'un substrat, l'O-GlcNAc peut être recyclé. Ce schéma est tiré de Hanover et al, 2012 [89].

Cette enzyme est critique pour la viabilité cellulaire [81, 82]. Un site consensus de liaison à son substrat n'a pas encore été identifié, mais OGT peut cibler une pléthore de substrats différents impliqués dans presque toutes les voies de signalisation. Par exemple, OGT régule la structure de la chromatine via la stabilisation de *Enhancer of Zeste 2* (EZH2), qui est une sous-unité critique du complexe polycomb répressif PRC2 [83] et via le contrôle de la polymérisation ordonnée de la protéine Polyhomeotic (Ph) chez la Drosophile, homologue des trois protéines humaines *Polyhomeotic-like protein 1-3* (PHC1-3). Ces dernières sont d'importantes sous-unités des complexes polycomb répressifs PRC1 [84]. De plus, OGT régule aussi la stabilité des protéines importantes pour le rythme circadien [85-88]. Finalement, OGT régule aussi la gluconéogenèse via la stabilisation de PGC-1α [58] et le cycle cellulaire via la régulation de la maturation de HCF-1, un processus qui sera discusté plus en détails subséquemment.

Un point de régulation primordiale d'OGT est la disponibilité de son substrat donneur, soit l'UDP-GlcNAc. Ce substrat, dérivé de moins de 5% du glucose cellulaire, est synthétisé via la voie biosynthétique des hexosamines (Figure 6)[89]. La particularité de cette voie est qu'elle est modulée par de multiples voies du métabolisme cellulaire, incluant entre-autres celles du glucose, des acides aminés, des acides gras et des nucléotides. De plus, cette voie est aussi sensible au niveau énergétique (ratio ATP/ADP) de la cellule[90]. De ce fait, OGT est décrite comme un senseur du métabolisme. Il est important de noter qu'OGT n'est pas la seule enzyme à utiliser l'UDP-GlcNAc comme substrat donneur. En effet, la voie de synthèse de l'acide hyaluronique, par exemple, utilise aussi l'UDP-GlcNAc[91]. Ainsi, OGT est en compétition avec d'autres enzymes pour le même substrat permettant de moduler les voies de signalisation en fonction des changements du métabolisme cellulaire.

Étant donné l'importance d'OGT dans de nombreux processus cellulaires, sa régulation doit être finement régulée. D'ailleurs, OGT est sujette à plusieurs modifications post-traductionnelles, dont l'ubiquitination [68, 92]. Cette dernière est catalysée par l'action de LSD2, qui jusqu'à tout récemment, n'avait pas d'activité ubiquitine ligase connue. En fait, une étude récente a permis de démontrer que LSD2 catalyse l'ajout de chaîne poly-ubiquitine K48 sur OGT, ce qui résulte en sa dégradation subséquente par le protéasome [92]. De manière

intéressante, LSD2 s'est montré capable d'inhiber la croissance de cellules tumorales via cette activité, de sorte que dans ce contexte, OGT agit comme oncogène et LSD2 comme suppresseur de tumeurs[92]. Cette activité oncogénique d'OGT a été démontrée dans des cellules HEK293T traitées avec des ARN interférents contre LSD2 où l'activité d'OGT s'accroît et où les cellules prolifèrent en colonie de façon similaire à une tumeur[92].

D'autre part, comme mentionné précédemment, OGT interagit indirectement avec le complexe BAP1 par son interaction avec HCF-1. Il a été montré que BAP1 déubiquitine OGT, ce qui a pour effet de stabiliser les niveaux protéiques d'OGT dans le noyau [46]. Puisque LSD2 se trouve aussi dans le complexe BAP1, ceci suggère que la stabilité d'OGT est dynamiquement régulée par ubiquitination et déubiquitination. L'activité suppresseur de tumeurs de BAP1 provient peut-être de sa régulation des signaux pro-prolifératives d'OGT et de HCF-1 via une dynamique de modifications post-traductionnelles de ces sous-unités.

1.2.2 Phosphorylation

Comme pour l'ubiquitination, la phosphorylation est une modification post-traductionnelle intégrée et essentielle dans d'importantes cascades de signalisation et permet, entre-autre, la modulation de l'activité protéique. Brièvement, cette modification consiste en l'ajout d'un groupement phosphate aux sérines, thréonines et tyrosines d'un substrat par des protéines kinases [93]. La phosphorylation de résidus non-communs tels l'histidine, l'aspartate, les cystéines, les lysines et les arginines sont plus rares, mais quelques exemples bien précis ont été étudiés chez les procaryotes et chez les eucaryotes [94-99]. La phosphorylation est réversible via l'action de phosphatases, ce qui permet une régulation dynamique par phospho- et déphospho-rylation des protéines afin de contrôler leurs fonctions. À cet égard, la phosphorylation peut agir comme interrupteur entre l'état « actif » et « non-actif » d'une protéine, ce qui est un mécanisme à la base de nombreuses cascades de signalisation cellulaire telle que la voie RAS/MAPK par exemple [100-103]. Il existe aussi d'importants réseaux de phosphorylation et de recrutement de diverses protéines lors de la réponse aux dommages à l'ADN. Enfin, dans le contexte du complexe BAP1, plusieurs

partenaires sont hautement régulées par phosphorylation, démontrant l'importance de cette MPT dans la régulation de la fonction de ce complexe.

1.2.2.1 Phosphorylation de BAP1

Comme mentionné précédemment, lors de dommages à l'ADN, de nombreuses protéines sont phosphorylées. Très brièvement, lors de la reconnaissance d'un bris double brin d'ADN (DSB), une série de cascades de signalisation mènent à l'activation de plusieurs kinases critiques dont l'*Ataxia Telangiectasia Mutated* (ATM) [104, 105]. Cette dernière phosphoryle ensuite des centaines de substrats et provoque le recrutement de RNF8 et RNF168 qui médient l'ubiquitination de H2A par l'ajout de chaînes K63 sur les résidus K13 et K15. Ces événements d'ubiquitination permettent le recrutement de la machinerie de réparation de l'ADN. Aussi, tout un système de déubiquitination existe afin de contrôler cette réponse, d'empêcher son amplification exagérée et surtout de médier son arrêt [24, 25, 37, 105-109]. En fait, plusieurs déubiquitinases ont été impliquées dans le contrôle de la réponse aux dommages à l'ADN. Par exemple, la déubiquitinase BRCC36 joue un rôle double en antagonisant la poly-ubiquitination de H2A par l'ajout de chaînes K63 médiées par RNF8/RNF168 et en modulant la réparation par recombinaison homologue (HR) par l'inhibition du recrutement de FANCG à l'ADN [25, 107, 110].

De façon importante, BAP1 a récemment été impliquée dans les cascades de signalisation causées par des DSB, particulièrement celles en réponse aux rayonnements ionisants (RI) [111]. D'ailleurs, des études génomiques ont révélé que plusieurs mutations de BAP1 associées au cancer mènent à une sensibilité accrue aux dommages à l'ADN médiés par les RI [111, 112]. Ceci prend d'autant plus d'importance sachant que BAP1 est partiellement haploinsuffisant, ce qui, en d'autres termes, indique que la présence d'un seul allèle fonctionnel, et donc l'autre allèle muté, est suffisant pour provoquer un syndrôme de prédisposition au cancer [50, 60, 79]. Dans le même ordre d'idées, des études sur la survie cellulaire en réponse aux dommages à l'ADN induits par les RI ont démontré que des cellules $BAP1^{+/-}$ survivent aux traitements, mais contiennent une quantité non-négligeables d'aberrations chromosomiques.

Donc, non seulement BAP1 est impliquée dans la réponse aux DSB, mais sa fonction lors de cette réponse est fortement modulée par une impressionnante dynamique de phosphorylation. Des analyses par spectrométrie de masse et protéomiques ont permis l'identification de plusieurs sites de phosphorylation sur BAP1, à savoir S493, S583, S592, S595, S596 et S597 [104, 113-115]. En fait, ces résidus se retrouvent principalement dans la région flexible de BAP1, c'est-à-dire dans la région qui la distingue parmi les autre DUBs de la famille des UCHs (Figure 7).

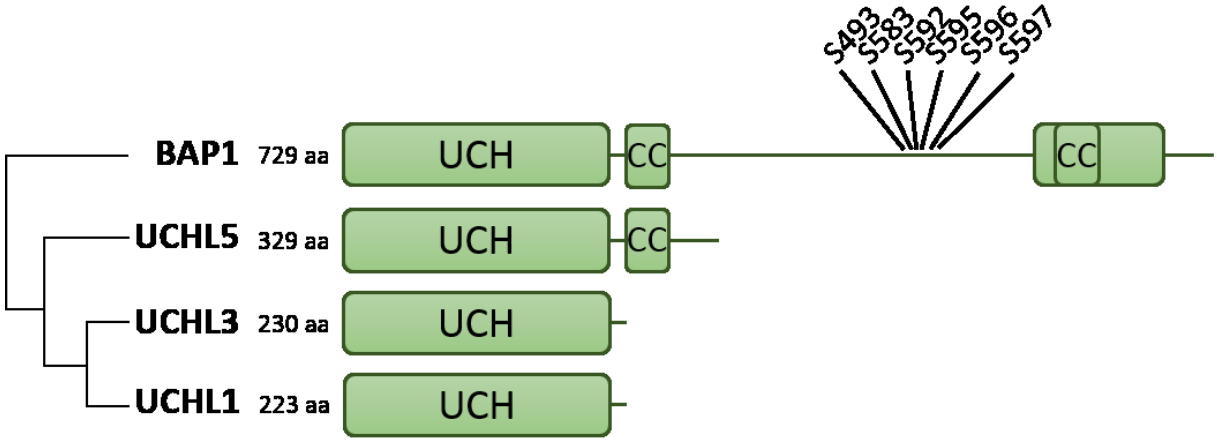

Figure 7. Hiérarchie des déubiquitinases de la famille UCH démontrant les sites de phosphorylation de BAP1. Le domaine UCH des quatres membres de la famille des UCHs est très conservé. Toutefois, BAP1 a évolué et diverge fortement des autres UCHs. Elle possède maintenant une extension en C-terminal contenant des sites de phosphorylation qui sont à la fois constitutifs (T493) et d'autres qui sont modulés en fonction de différents stimuli comme la réponse aux UV. Aa; acides aminés, UCH; Ubiquitin C-terminal Hydrolase, CC; Coiled-coil.

Parmi ces différents sites, non seulement la phosphorylation de S592 en phase S suite aux dommages UV est la plus étudiée, mais l'environnement biochimique et la séquence en acides aminé autour de cette sérine conforme au site consensus de phosphorylation par ATM connu sous le nom de motif SQ [62]. La phosphorylation de ce site cause la dissociation de BAP1 de la chromatine, cependant, seulement une petite portion du BAP1 total est phosphorylé sur ce site lors de la réponse. Les auteurs suggèrent que, via ce processus, BAP1 pourrait être dissociée de certains promoteurs de gènes impliqués dans la réparation [62]. D'autre part, puisque BAP1 est déjà connue pour activer la transcription, sa séquestration au niveau de certains loci d'ADN autre que le site de dommage pourrait aussi servir à entraver la transcription durant la réparation [60, 61]. Récemment, il a été montré que la mutation des

sites SQ de BAP1 inhibe son recrutement aux sites de dommages à l'ADN [60]. Malgré cette discordance dans le rôle de la phosphorylation de BAP1 quant à son recrutement à l'ADN, le présent modèle implique que la phosphorylation des sites SQ de BAP1 incluant S592 par ATM permet de déloger BAP1 de certains promoteurs importants tout en la recrutant spécifiquement aux sites de dommages à l'ADN. Néanmoins, ces sites ne sont pas nécessaires à la viabilité cellulaire suite aux dommages à l'ADN, ce qui pourrait vraisemblablement être dû au faible pourcentage de BAP1 qui est sujette à cette modification [62]. De toute évidence, le mécanisme d'action de BAP1 durant la réponse dommages à l'ADN est encore à approfondir.

D'autres sites de phosphorylation induits par RI ne correspondant pas aux motifs SQ sont aussi importants à la fonction de BAP1. La mutation de tous les sites de phosphorylation induits par RI a révélé une augmentation de la sensibilité à ces derniers. En fait, ces mutants de BAP1 démontrent très peu de recrutement à la chromatine, peu de déubiquitination de H2AK119Ub et peu d'effet sur l'arrêt de la réponse aux DSB. De plus, des cellules H226 (carcionome de poumons $BAP1^{-/-}$) reconstituées avec ce mutant de phosphorylation sont caractérisées par une sensibilité aigüe aux RI [60, 62].

De plus, quant à la fonction de BAP1 aux sites de dommages, des études biochimiques plus approfondies ont démontré que cette DUB joue un rôle important dans la transcription des gènes codant pour des protéines reliées à la réponse aux DSB [49, 51]. De plus, des expériences d'immunoprécipitation de chromatine (ChIP) ont fortement suggéré qu'au niveau du site de dommage, BAP1 est recrutée spécifiquement pour déubiquitiner H2AK119Ub et moduler la réponse assurée par BRCA1 et RAD51 [60]. Cependant, la fonction précise de cette déubiquitination reste inconnue, mais elle pourrait participer à la relaxation de la chromatine au site de dommage pour faciliter la réparation.

1.2.2.2 Phosphorylation de l'OGT

OGT est aussi finement régulée par phosphorylation, particulièrement au niveau de son domaine catalytique [116, 117]. En effet, vu le nombre important de kinases et de phosphatases cellulaires, la phosphorylation des sites d'OGT suggère que différentes cascades

de signalisation peuvent réguler la fonction de cette dernière. Par exemple, la voie de l'insuline est connue pour induire une forte phosphorylation d'OGT. Plus précisément, une fois activé, le récepteur à l'insuline recrute OGT à la membrane cellulaire, induit la phosphorylation de cette dernière pour ainsi augmenté son activité enzymatique [118-123]. OGT peut ensuite modifier des protéines impliquées dans la signalisation de l'insuline, incluant *Signal Transducer and Activator of Transcription* 3 (STAT3) [124]. Par ailleurs, des études récentes ont démontré que cette activation d'OGT par la phosphorylation de ses tyrosines atténue la signalisation à l'insuline via une boucle de rétroaction négative [122, 123]. Plus précisément, OGT O-GlcNAcyle les résidus S984, S985, S1011 et d'autres résidus entre 1025 et 1045 de *Insulin Receptor Substrate 1* (IRS-1) [125]. Ces sites d'O-GlcNAcylation se trouvent en C-terminal, où ce dernier lie plusieurs effecteurs de la cascade de signalisation à l'insuline, ce qui induit un effet d'encombrement stérique [125]. De plus, une augmentation de l'O-GlcNAcylation de IRS-1 corrèle avec une augmentation de la phosphorylation d'IRS-1 sur les résidus S307, S632 et S635, des marques associées avec l'atténuation de la voie de l'insuline [125]. Cependant, les sites de phosphorylation d'OGT en lien avec la voie d'insuline n'ont pas été identifiés. Néanmoins, il est évident que la dynamique de phosphorylation d'OGT pendant ce processus est critique à la coordination de la signalisation en réponse à l'insuline. Surtout, un dysfonctionnement dans sa phosphorylation et son recrutement à la membrane cellulaire aurait d'importantes conséquences sur la régulation du métabolisme cellulaire et la tolérance à l'insuline.

Il existe aussi un important *cross-talk* entre la phosphorylation d'OGT par *AMP-Activated Protein* Kinase *(AMPK*) et l'O-GlcNAcylation d'AMPK [126]. Comme OGT, AMPK est une protéine critique pour la régulation de l'homéostasie du métabolisme de la cellule [127, 128]. En effet, plusieurs évènements cellulaires impliquant le métabolisme sont co-régulés par AMPK et OGT. D'importants changements métaboliques se produisent lors de la différenciation de myoblastes en myotubes, incluant une répartition plutôt uniforme d'OGT entre le cytoplasme et le noyau [126]. Ce changement de localisation contraste très fortement avec sa localisation majoritairement nucléaire dans les cellules prolifératives. Il est à noter que des études récentes ont démontré que l'activation d'AMPK induit la phosphorylation d'OGT

sur le résidu T444 qui se trouve dans l'avant dernière répétition tétratricopeptide (TPR) et près du NLS d'OGT [126]. De ce fait, cette phosphorylation engendre un changement de conformation de ce domaine ce qui cause la translocation d'OGT vers le noyau dans les cellules différenciées, où OGT est majoritairement cytoplasmique [126]. Par contre, dans toutes les lignés cellulaires testées, prolifératives ou post-mitotiques, cette phosphorylation engendre un changement de spécificité des substrats d'OGT [126]. Cette différence de localisation d'OGT dans les cellules différenciées corrobore avec plusieurs études démontrant qu'OGT régule des processus cytoplasmiques dans les cellules post-mitotiques [126, 129]. Il est clair que la phosphorylation d'OGT joue un rôle essentiel dans la coordination de ses fonctions. De plus, sa séquestration au cytoplasme permet à OGT d'échapper à la dynamique de régulation de sa stabilité protéique médiée par l'ubiquitination via LSD2/BAP1. OGT peut alors réguler différentes cascades de signalisation du métabolisme cellulaire. Néanmoins, bien qu'aucune étude n'ait investigué la localisation de LSD2 lors de la différenciation terminale, il est possible que la translocation de BAP1 au cytoplasme lors de ce même processus serve à rétablir cette dynamique de stabilisation d'OGT afin de réguler le métabolisme des cellules post-mitotiques [9].

1.2.2.3 Phosphorylation de YY1

Bien que le facteur de transcription YY1 soit une protéine sous-stœchiométrique dans le complexe BAP1, son rôle dans la régulation de la transcription dans le contexte de ce complexe n'en ait pas moins important. Notre groupe a récemment démontré que YY1, BAP1 et HCF-1 forme un complexe ternaire capable d'activer la transcription d'une pléthore de gènes incluant le gène mitochondrial *Cytochrome C Oxidase subunit 7C* (COX7c) [61]. De plus, YY1 a une fonction anti-apoptotique et pro-prolifération indiquant que son rôle potentiellement oncogénique doit être soumis à une régulation contrôlée. De ce fait, il n'est pas étonnant que plusieurs des fonctions de YY1 soient hautement régulées par phosphorylation [130-133].

YY1 est un facteur de transcription critique pour de nombreux processus biologiques tels que le développement, l'apoptose et la différenciation. Par ailleurs, ce dernier est phosphorylé sur plusieurs sites de façon différentielle selon la phase du cycle cellulaire [134-136] (Figure 8). Par exemple, le résidu T39 qui se trouve dans sa région acide/activatrice en N-terminal est ciblé par la kinase *Polo-Like Kinase 1* (Plk1) et ce, spécifiquement pendant la transition G_2/M [137].

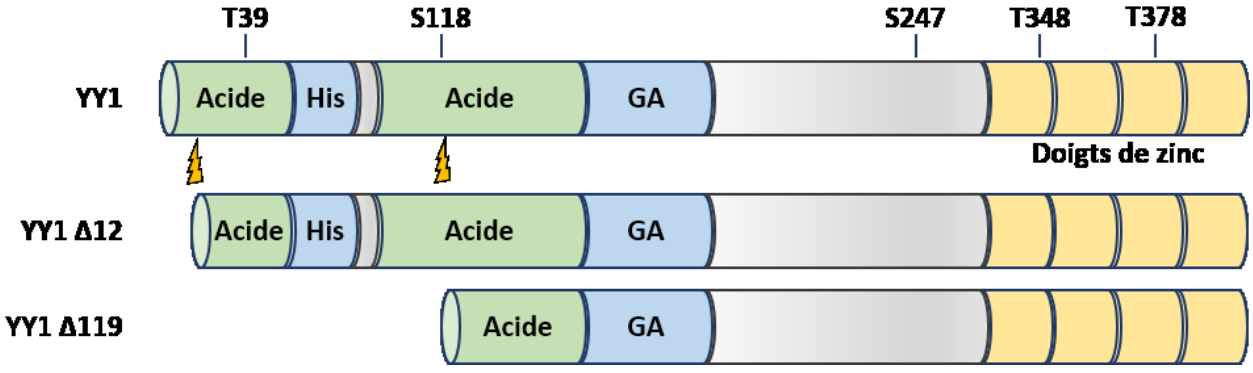

Figure 8. Structure de YY1 avec les sites de phosphorylation et de clivages identifiés. Le site T39 est spécifique à Plk1 en G2/M mais sa fonction demeure encore inconnue. Le site S118 est spécifique à CK2 et est constitutivement phosphorylé pour inhiber le clivage D119-G120 via la caspase 7 sauf durant l'apoptose quand YY1 se fait cliver à ce site pour produire le fragment YY1Δ119. Un autre site de clivage D12-G13 n'est pas protégé via phosphorylation mais la forme tronquée YY1Δ12 est toujours fonctionnelle. La phosphorylation du site S247 est constitutif avec une fonction inconnue. Les sites S348 et T378 se trouvent dans les régions entre les doigts de zinc de sorte que leur phosphorylation, spécifique en mitose, inhibe la structure des doigts de zinc et inhibe la liaison de YY1 à l'ADN. Acide; domaine de transactivation acide, His; région riche en histidine, GA; région riche en glycine et alanine.

La forte phosphorylation de YY1 lors de la transition G_2/M corrèle avec une activité transcriptionnelle importante [138]. Il est à noter que durant cette transition et jusqu'en phase G_1, les niveaux protéiques de Plk1 atteignent leur maximum [137, 139, 140]. De ce fait, bien que les niveaux de Plk1 soient encore élevés pendant la mitose et l'entrée en G_1, la phosphorylation de YY1 en G_2/M est éliminée très rapidement, ce qui suggère une fonction bien précise de cette modification bien qu'elle soit à déterminer [137].

D'autres sites de phosphorylation de YY1 sont connus. Comme indiqué à la figure 8, plusieurs sites de phosphorylation ont été répertoriés dans ou à proximité du domaine de liaison à l'ADN, soit aux résidus S247, S348 et S378. La phosphorylation de S247 est retrouvée de façon constitutive et n'a pas d'effet marquant sur l'activité de YY1, mais les sites S348 et

S378 sont phosphorylés dès l'entrée en mitose [133]. Il est intéressant de noter que S348 et S378 se trouvent dans des régions flexibles, entre les doigts de zinc, connues pour maintenir la structure et l'alignement des doigts de zinc [141-143]. De ce fait, la phosphorylation de ces sites provoque un changement de conformation dans le domaine de liaison à l'ADN ce qui inhibe ce domaine, et résulte en l'incapacité de YY1 à lier l'ADN en mitose [133].

D'autre part, YY1 est aussi connu pour son rôle anti-apoptotique. En effet, il a été reporté que le déclenchement de l'apoptose cellulaire est associé à une dégradation de YY1 [144-147]. Dans ce contexte, deux sites de clivage ont été identifiés entre les acides aminés D12-G13 et entre D119-G120 [132]. La phosphorylation constitutive de YY1 sur le résidu S118 par la kinase CK2 inhibe le clivage de D119-G120 [132]. Dès le déclenchement de l'apoptose, une phosphatase n'ayant pas été identifiée, déphosphoryle cette marque laissant place au clivage de YY1 via l'action des caspases produisant ainsi une forme non-fonctionnelle de ce dernier. En resumé, YY1, une composante du complexe BAP1 qui permet le recrutement du complexe à la chromatine pour réguler la transcription génique, est sujet à de nombreux évenements de phosphorylation et déphosphorylation permettant de contrôler sa stabilité, fonction et localisation.

1.2.3 O-GlcNAcylation et le métabolisme

Certains membres du complexe BAP1 sont aussi la cible d'OGT qui les modifie par O-GlcNAcylation, ce qui semble être critique pour réguler le lien entre le complexe BAP1 et le métabolisme cellulaire. OGT O-GlcNAcyle des substrats variés en fonction de la disponibilité de l'UDP-GlcNAc pour réguler leurs fonctions en rapport avec l'état métabolique de la cellule. Un exemple important de la collaboration entre OGT et le complexe BAP1 dans le métabolisme cellulaire a été souligné par Ruan et al. (2013) [58] qui ont démontré que par l'intermédiaire de l'O-GlcNAcylation du co-activateur transcriptionnel PGC-1α, OGT contrôle la gluconéogenèse en recrutant le complexe BAP1 qui stabilise PGC-1α par déubiquitination[58]. Il est à noter que la dérégulation de la dynamique d'O-GlcNAcylation intracellulaire est associée à plusieurs pathologies humaines, y compris le cancer et le diabète, ce qui révèle l'importance d'OGT et du complexe BAP1 pour l'homéostasie cellulaire. De plus,

l'O-GlcNAcylation des membres mêmes du complexe BAP1 s'avère être critique pour plusieurs processus cellulaires.

1.2.3.1 La O-GlcNAcylation et maturation de HCF-1

La maturation de HCF-1 est un évènement crucial pour la progression du cycle cellulaire pour lequel le mécanisme moléculaire n'a été identifié que très récemment par l'étude de ses niveaux d'O-GlcNAcylation. HCF-1 comporte plusieurs sites d'O-GlcNAcylation et, comme illustré à la figure 9, ces sites forment deux groupes distincts. La fonction des sites d'O-GlcNAcylation dans le domaine N-terminal n'a pas encore été bien caractérisée. Cependant, ce domaine est important pour le recrutement de plusieurs cofacteurs par HCF-1 et l'assemblage de complexes protéiques [148-150]. Vu l'importance de ce domaine, il est possible que l'O-GlcNAcylation de ce dernier permette de réguler l'interaction entre HCF-1 et ses partenaires [148, 150].

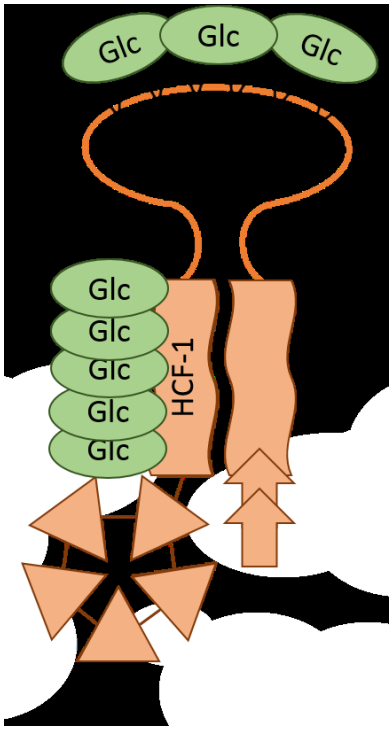

Figure 9. HCF-1 est O-GlcNAcylée sur plusieurs sites en N-terminal et l'O-GlcNAcylation joue un rôle critique dans sa maturation. Plusieurs sites d'O-GlcNacylation ont été identifiés en N-terminal de HCF-1. Puisque cette région joue un rôle dans son interaction avec d'autres protéines, il se peut que ces O-GlcNAclations régulent la formation de complexes. Aussi, des études récentes ont démontré que l'O-GlcNAcylation des répétitions PPD est un déterminant fondamental au clivage/maturation de HCF-1 par OGT. PPD : Domaine de clivage protéolytique FN3; *Fibronectlin-like type III, Glc; groupement O-GlcNAc.*

D'autre part, l'O-GlcNAcylation des sites du deuxième groupe a une fonction bien particulière pour la maturation de HCF-1 [68, 69, 72]. En effet, cette région contient six répétitions importantes pour la maturation de cette dernière. Bien que plusieurs études aient démontré que l'O-GlcNAcylation est nécessaire à la maturation de HCF-1, l'enzyme responsable du clivage est resté inconnu jusqu'à des études récentes de cristallographie qui ont cherché à décortiquer ce mécanisme. Ces études ont permis d'établir que trois résidus d'OGT sont critiques pour cette fonction, soit K842, H498 et H558. Toutefois, c'est seulement K842, qui participe à l'activation de l'UDP-GlcNAc et qui est nécessaire pour le clivage de HCF-

1 [68, 69, 72, 151-154]. Ceci démontre que l'activité d'O-GlcNAcylation elle-même est critique pour le clivage. Aussi, cette même étude sugère que contrairement à l'O-GlcNAcylation typique qui cible les thréonines ou sérines, le mécanisme de clivage de HCF-1 débute avec l'O-GlcNAcylation d'un glutamate dans les répétitions HCF-1 [72]. Comme illustré à la figure 10, l'étude propose un mécanisme par lequel c'est cette O-GlcNAcylation qui rend susceptible le glutamate de HCF-1 à un mécanisme d'auto-clivage.

À

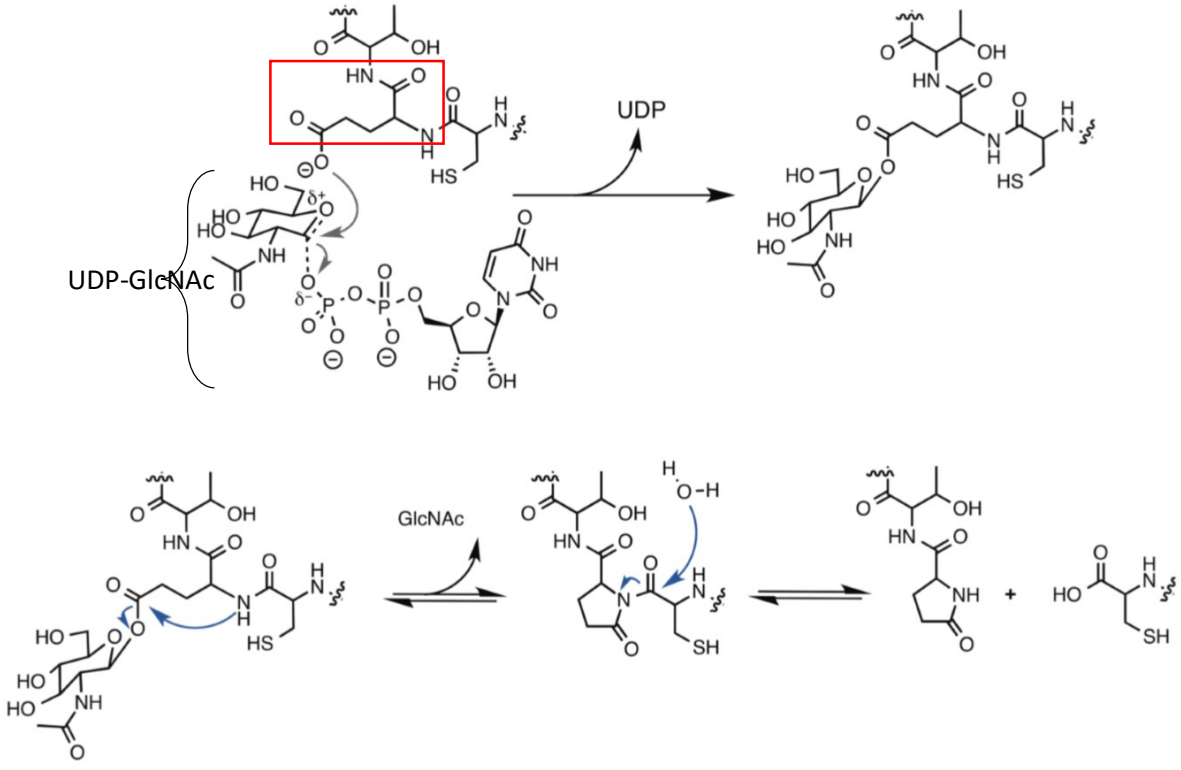

Figure 10. Modèle proposé pour le mécanisme moléculaire du clivage de HCF-1 par OGT via l'UDP-GlcNAc. Les études de cristallographie ont démontré que contrairement à l'O-GlcNAcylation typique des sérines et thréonines par OGT, HCF-1 est O-GlcNAcylé sur un glutamate, rendant ainsi le groupement acide propice à une attaque nucléophile par l'azote du lien peptidique de l'acide aminé subséquent. Les résultats ont démontré que la cystéine en position +1 du glutamate n'est pas essentielle au clivage. La possibilité qu'OGT puisse cliver d'autres protéines via un système d'auto-clivage n'est pas à exclure. L'encadré rouge démontre le glutamate de HCF-1 qui se fait O-GlcNAcylé. Tiré de [72].

et la structure de HCF-1, plaçant ainsi le glutamate dans une orientation favorable pour être sujet à l'O-GlcNacylation. Ces études ont ainsi suggéré que le site actif d'OGT peut remplir deux fonctions, soit de catalyser l'ajout de l'O-GlcNAc ou de catalyser le clivage de certains

substrats [72]. Cependant, malgré les évidences actuelles, il est difficile d'exclure la possibilité qu'une autre enzyme soit responsable du clivage une fois que HCF-1 est O-GlcNAcylé puisque la réaction d'O-GlcNAcylation est très transitoire [155]. Compte tenu de ce qui précède, il est tout de même évident qu'OGT joue un rôle primordial dans la régulation de la fonction HCF-1. D'autre part, notre groupe a déjà démontré que bien qu'OGT soit nuclecytoplasmique, le clivage de HCF-1 se produit presqu'exclusivement dans le noyau, là où se trouve BAP1 [70]. Par conséquent, dans le contexte du complexe BAP1, le complexe nucléaire BAP1-HCF1-OGT pourrait être important pour la stabilisation d'OGT via déubiquitination afin de promouvoir la maturation de HCF-1 via O-GlcNAcylation. En d'autres termes, une dynamique de déubiquitination et d'O-GlcNAcylation entre les partenaires de BAP1 serait importante pour la modulation du cycle cellulaire et probablement d'autres processus biologiques.

1.2.3.2 O-GlcNAcylation of YY1

Plusieurs facteurs de transcription sont O-GlcNAcylés en réponse à des stimuli, ce qui permet de réguler leurs fonctions à différents niveaux, entre autres en fonction du type cellulaire [156-159]. YY1 est impliqué dans plusieurs processus cellulaires et peut agir en tant qu'activateur ou répresseur de la transcription dépendamment des gènes ciblés et du contexte[136]. En phase G1 et G_1/S, une région en C-terminale de la protéine *Retinoblastoma* (Rb) interagit avec le domaine de liaison à l'ADN de YY1 de manière à inhiber sa liaison aux régions régulatrices dans les promoteurs des gènes [160]. Des études récentes ont déterminé que YY1 est O-GlcNAcylé sur plusieurs sites par OGT, mais que contrairement à la phosphorylation de son domaine de liaison à l'ADN, cet O-GlcNAcylation ne module pas l'affinité de YY1 pour l'ADN [131]. En fait, elle permettrait d'inhiber l'interaction entre Rb et YY1, libérant ainsi YY1 afin qu'il module la transcription par sa liaison à l'ADN. Puisque Rb participe à la régulation de l'entrée en phase S, ces études ont prédit que l'interaction inhibitrice de Rb sur YY1 servirait à restreindre la transcription de gènes importants à la transition G_1/S. De cette façon, en condition favorable à la prolifération ou lorsqu'il y a suffisamment de nutriments, OGT O-GlcNAcyle YY1 afin de permettre l'entrée en G_1/S. Par contre, en condition de privation de nutriment, YY1 non-O-GlcNAcylé, demeure inhibé par Rb et de ce fait la cellule n'entre pas dans le cycle cellulaire. Par ailleurs, une liste des sites d'O-

GlcNAcylation n'a pas été documentée. De plus, des études préliminaires indiquent qu'il existe une hétérogénéité de l'O-GlcNAcylation entre chaque molécule de YY1 [131, 160].

D'ailleurs, bien que l'O-GlcNAcylation de YY1 n'affecte pas directement sa liaison à l'ADN comme le fait sa phosphorylation, des études ont démontré que son activité en tant que répresseur/activateur change en fonction de son O-GlcNAcylation [161]. Par exemple, lorsque YY1 est fortement O-GlcNAcylé, il devient un puissant répresseur de l'expression de l'actine en liant le promoteur de ce dernier et en déplaçant le facteur *Serum Response Factor* (SRF), qui est aussi O-GlcNAcylé. Comme YY1, les sites d'O-GlcNAcylation de SRF ne se trouvent pas dans son domaine de liaison à l'ADN, dans son domaine de dimérisation ou dans des domaines connus pour être impliqués dans des interactions protéines-protéines [162]. Ainsi, le mécanisme qui confère à YY1 la capacité de déplacer ou d'exclure SRF de la chromatine une fois O-GlcNAcylé demeure inconnu.

Bref, différentes dynamiques de modifications post-traductionnelles dans le complexe BAP1 sont des déterminants majeurs dans la fonction et l'autorégulation de ce dernier. L'inter-régulation des composantes dans ce complexes intègre le métabolisme et le niveau énergétique cellulaire, et ce dans le but d'apporter une régulation fine de l'activité de ce complexe suppresseur de tumeurs. Cependant, les deux facteurs de transcription FOXK1 et FOXK2, bien qu'ils soient relativement peu étudiés, régissent eux aussi, différents aspects du métabolisme cellulaire.

1.3 Les facteurs de transcription FOXK

FOXK1 et FOXK2 sont deux facteurs de transcription associés à BAP1 qui sont très peu étudiés. Ils font partie de la famille de facteurs de transcription FOX, composée de plus de 40 membres dont plusieurs ont été impliqués dans une vaste gamme de processus cellulaires, incluant la différenciation, la prolifération cellulaire, le métabolisme, l'embryogenèse, etc. [163-169]. FOXK1/2 sont les seuls membres appartenant à la sous-catégorie « K » des facteurs FOX. Cette famille est caractérisée par la présence d'un domaine caractéristique de liaison à l'ADN *Forkhead* (FH) et d'un domaine de liaison aux phospho-thréonine *Forkhead Associated*

(FHA), faisant d'eux les seuls facteurs FOX capables de lier des protéines phosphorylées ainsi que l'ADN.

1.3.1 Structure et domaines des FOXK

Le domaine FH correspond à une série de quatre hélices et d'une aile formant un domaine de liaison ressemblant à celui de l'histone H1. Ce domaine est capable de lier l'ADN sous forme de monomère (figure 11) [164, 170-172]. Par ailleurs, certains membres tel que FOXA ont même une activité pionnière c'est-à-dire qu'ils ont la capacité de lier l'hétérochromatine, même en absence des complexes typiques de remodelages de la chromatine comme SWI/SNF et/ou TIP60 [170]. Le domaine FH est très conservé entre les protéines FOX et permet de lier une séquence d'ADN d'environ 16 paires de base où la troisième hélice du domaine interagit avec le sillon majeur de l'ADN et où l'aile interagit avec le sillon mineur sur le même côté de l'ADN. Le site consensus de base de liaison du FH a été déterminé comme étant 5'-TAAACA-3'.

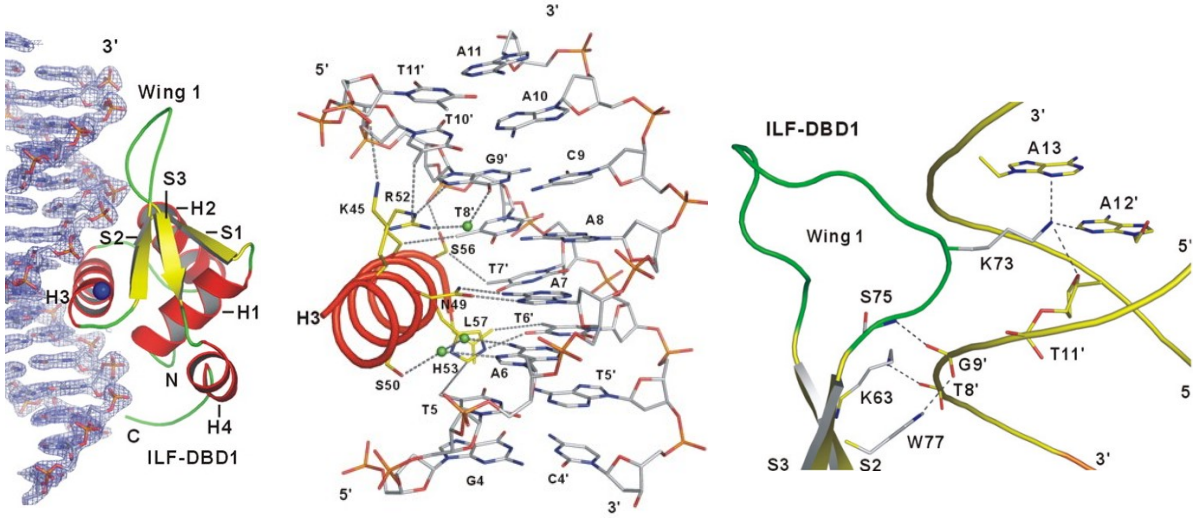

Figure 11. Structure cristalline du domaine FH de FOXK1 démontrant l'importance de l'hélice 3 et de l'aile de FOXK1 pour l'interaction avec l'ADN. À gauche, la structure cristalline de FOXK1 lié à l'ADN. Au milieu, les interactions entre l'hélice 3 et le sillon majeur de l'ADN. Les sphères vertes représentent des molécules d'eau. À droite, les interactions entre les résidus importants de l'aile de FOXK1 et le sillon mineur de l'ADN. Notez le résidu lysine K73 qui participe à trois interactions sur les deux brins d'ADN (bleu et rouge). Image tirée [172].

Le domaine FHA, quant à lui, a été identifié dans plus de 200 protéines dans différentes espèces et est hautement conservé des procaryotes aux eucaryotes supérieurs. Ce domaine est surtout observé dans des protéines ayant une certaine implication dans le contrôle du cycle cellulaire et la réponse aux dommages à l'ADN [173]. Comme mentionné précédemment, différentes études ont montré que le domaine FHA a une spécificité très étroite pour les phospho-thréonines (pT) (figure 12) [174]. Ces études ont aussi montré que non seulement le pT du substrat est critique pour l'interaction, mais aussi que le résidu à la position pT+3 est un déterminant majeur de l'interaction (figure 12). Le site consensus de liaison du FHA a donc été déterminé comme étant « pT-X-X-D/I/L » où les «X» indiquent qu'il n'y a aucune préférence pour les acides aminés en position pT+1 et pT+2[173-175]. D'autres

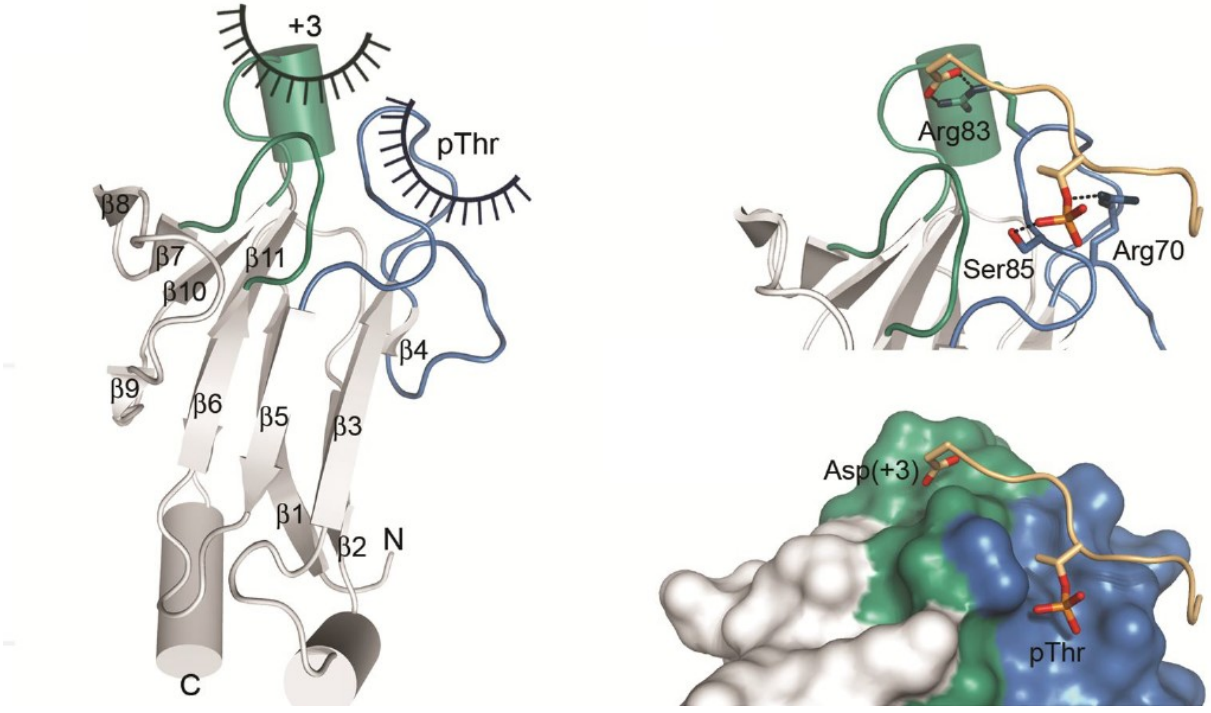

Figure 12. Structure cristalline du domaine FHA de RAD53 démontre que le résidu pT+3 confère la spécificité de l'interaction. À gauche, la structure des feuillets béta démontre l'emplacement des régions non-structurées qui participent à la reconnaissance du substrat. À droite, les résidus importants de ces régions flexibles et la représentation de la densité électronique montrent la cavité acceptrice du groupement méthyle de la thréonine. Image tirée de [173].

études ont révélé que la spécificité du domaine FHA pour son substrat est conféré par ce résidu en position pT+3 [174]. Par exemple, alors que les domaines FHA de RAD53 et CHK2 lient les pTs de leur substrat avec des affinités similaires, RAD53 a une préférence pour des

acides aspartiques en position pT+3 tandis que CHK2 en a une pour l'isoleucine [173]. L'absence total d'interaction avec des phospho-sérines s'explique par des interactions intramoléculaires dans la FHA qui favorisent la présence du groupement γ-méthyle sur la chaîne latérale de la thréonine [176, 177].

1.3.2 FOXK1

Bien que très peu d'études se soit concentrées sur la fonction des facteurs FOXK, plusieurs études ont permis de déterminer le rôle important que joue FOXK1 dans la régulation de la différenciation du tissu musculaire.

1.3.2.1 Réseau de régulation de FOXK1 dans la myogenèse

Le muscle squelettique est un organe avec une capacité de régénération impressionnante principalement grâce à une population de cellules quiescentes appelées cellules satélittes ou cellules progénitrices myogéniques (MPC) qui se trouve entre les fibres musculaires. En fait, cette population de cellules peut entrer en prolifération et se différencier afin de réparer une blessure touchant plus de 90 % de l'architecture musculaire en aussi peu que 3 semaines [178]. Des analyses transcriptomiques ont révélé que CD29, C-Met, intégrine, alpha7, M-cadhérine, Pax3, Pax7, syndécan3/4 et FOXK1 sont importantes pour la fonction de ces cellules [179, 180]. Des études ultérieures ont démontré que des souris déficientes $FOXK1^{-/-}$ ont des défauts de régénération musculaire [180-182]. Cette anomalie est due à une déficience au niveau du nombre et du potentiel d'activation des cellules MPC causée par une forte expression de p21 causant un défaut dans la cinétique du cycle cellulaire [181]. Aussi, les souris $FOXK1^{+/-}$ démontrent un phénotype d'haploinsuffisance ressemblant à celui du syndrome de dystrophie musculaire de Duchenne [180, 181]. À cet effet, l'étude de FOXK1 dans le muscle est un domaine de recherche actif visant à développer de nouvelles thérapies pour le traitement de la dystrophie musculaire.

1.3.2.1.1 Régulation de la transcription de FOXK1

En raison de l'implication majeure de FOXK1 dans la régénération musculaire et la régulation de la population MPC, il est important de comprendre comment l'expression et l'activité de FOXK1 sont régulées. Au niveau transcriptionnelle, le promoteur du gène de FOXK1 contient plusieurs séquences *Sox Binding* Element (SBE), un motif hautement conservé chez les mammifères [183]. Les protéines SOX15 et SOX8 sont connues pour être exprimées dans la population des cellules satellites. Dans le cas des MPC, seul SOX15 lie les SBE et active la transcription de FOXK1 [184]. De plus, la perte de la région SBE dans le promoteur de FOXK1 atténue de façon sévère l'expression de FOXK1 [183].

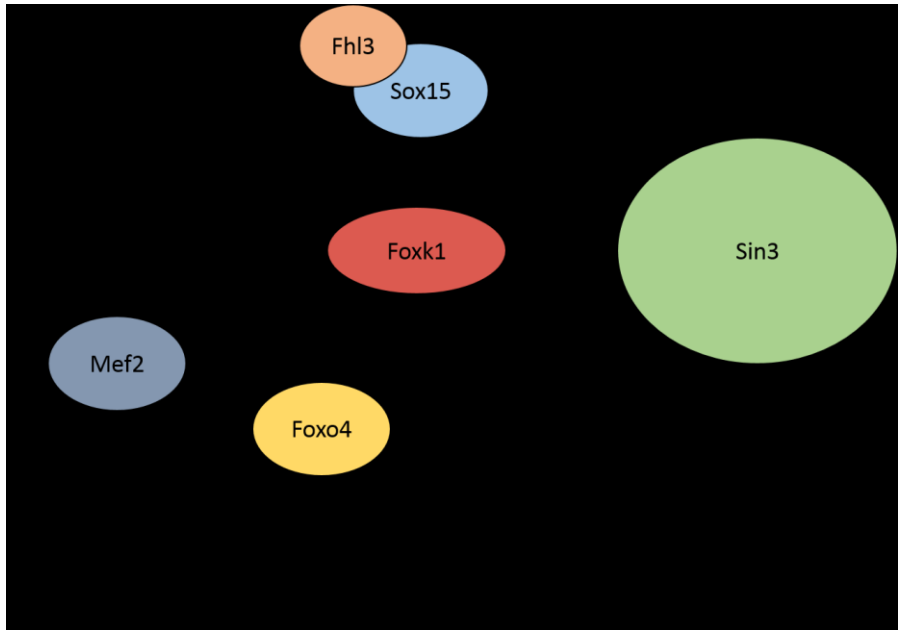

Figure 13. Schéma du réseau de signalisation de Foxk1 dans les MPC. Foxk1 joue à plusieurs niveaux dans la différenciation musculaire. En activant Sin3 et en le recrutant à la chromatine, il bloque l'expression des gènes inhibiteurs du cycle cellulaire tels que p21, p27 et p57. Foxk1 inhibe aussi directement l'action de Foxo4, un gène qui active p21 et Mef2. Ce dernier est un gène critique pour l'induction du programme de différenciation.

Des travaux récents ont permis de determiné que SOX15 n'agit pas seul et que la protéine *Four and a Half Lim Domain 3* (Fhl3), une protéine de la famille des LIM connue pour médier des interactions protéine-protéine, participe avec SOX15 pour activer la transcription de FOXK1 [185]. Les domaines d'interactions impliqués dans cette association sont une région en C-terminal de SOX15 et la totalité des quatre et demi domaines LIM de FHL3, rendant cette interaction atypique puisque les protéines Sox en général interagissent avec d'autres

protéines via leur domaine HMG [186, 187]. L'activité transcriptionnelle du complexe FHL3-SOX15 est entièrement dépendante de leur interaction [183, 188]. En effet, c'est probablement via FHL3 que SOX15 recrute la machinerie de remodelage de la chromatine pour activer la transcription de FOXK1, mais aucune étude n'a exploré cette possibilité [183]. Plus encore, les souris SOX15$^{-/-}$ démontrent un défaut de régénération musculaire suite à une lésion [183]. Ce phénotype est fort probablement dû à un défaut d'expression de FOXK1 et à une forte expression de p21.

1.3.2.1.2 Activité de FOXK1 durant la transcription

La répression de la transcription peut être médiée via l'action de plusieurs complexes de remodelage de la chromatine. Les marques d'activation telles que H3K4me3 ou H3K27ac peuvent être enlevées ou des marques répressives peuvent y être ajoutées telles que H3K9me3 ou H3K27me3 [189-195]. Un des complexes pouvant remodeler la structure de la chromatine est le complexe de répression SIN3-HDAC qui est composé de neuf partenaires d'interaction : *Paired Amphipathic Helix Protein Sin3a (*SIN3a), *Paired Amphipathic Helix Protein Sin3b (*SIN3b), les *Histone Deacetylase 1 and 2 (*HDAC1 et HDAC2), les *Retinoblastoma-Binding Protein 4 and 7* (RBBP4 et RBBP7), *Sin3 Associated Protein 18 and 30* (SAP18 et SAP30) et la *Sin3 Histone Deacetylase Corepressor Complex Component SDS3 (*SDS3)[196]. De manière importante, les deux sous-unités HDAC1 et HDAC2 sont des déacetylases d'histones qui permettent d'inhiber la transcription [196, 197]. Une étude a permis de démontrer que FOXK1 interagit avec différents membres de ce complexe afin de les recruter à la chromatine et d'inhiber la transcription de différents gènes critiques pour la différenciation musculaire. À l'aide de son domaine FHA, FOXK1 interagit de façon non-canonique avec la T49 de SDS3 [196]. Cette interaction est non-canonique car le résidu pT+3 de T49 est une alanine, contrairement au site consensus des domaines FHA qui cible les leucines, isoleucines ou acide aspartiques [174]. De plus, la région N-terminal de FOXK1, ou plus précisément les premiers quarante acides aminés, interagit avec le domaine *Paired Amphipathic Helix 2 (*PAH2) des sous-unités d'échafaudage SIN3 (SIN3a et SIN3b), permettant ainsi l'inhibition de l'expression de p21, p27 et p57, tous des inhibiteurs du cycle cellulaire (figure 13) [197]. De cette manière, FOXK1

inhibe l'arrêt du cycle cellulaire et maintient les cellules en prolifération en inhibant l'expression des inhibiteurs de ce dernier.

1.3.2.1.2 Effet de FOXK1 sur la fonction protéique

Plusieurs facteurs de transcription sont importants pour l'induction du programme de différenciation musculaire, entre autres, FOXO4 et MEF2 [198-201]. En effet, des souris transgéniques surexprimant FOXO4 ont révélé des phénotypes semblables à ceux des souris Foxk1$^{-/-}$, soit une déficience dans la régénération musculaire. D'autres études ont démontré que les protéines FOXO peuvent interagir avec les facteurs de transcription *Mothers Against Decapentaplegic 3/4* (SMAD3/4) afin de co-activer l'expression de p21 dans les MPC et de maintenir leur quiescence [202, 203]. Quant à FOXK1, il a été reporté que ce dernier peut lier le domaine de liaison à l'ADN de différents membres des FOXO incluant FOXO3a et FOXO1, mais plus particulièrement FOXO4 à l'aide de ses domaines FH et FHA pour ainsi inhiber leur capacité à lier l'ADN et de à moduler la transcription [179]. Bref, FOXK1 se lie et inhibe l'activité transcriptionnelle des protéines FOXO, bloquant ainsi l'activation de p21, p27 et p57 en plus de recruter le complexe SIN3 au promoteur de ces mêmes gènes pour inhiber leur expression dans le but de maintenir l'état prolifératif des MPC.

Dans le cadre du programme de différenciation, les souris surexprimant Foxk1 démontrent une faible activation des gènes en aval de Mef2 telles que la *Troponine 1 Type C* (Tnnc1), la chaîne légère de la Myosine 2 (Myl2), Mef2 lui-même ainsi que d'autres gènes important pour le programme de différenciation musculaire [204]. Ainsi, en plus de maintenir l'état prolifératif des MPC, FOXK1 retarde le programme de différenciation musculaire. Pour ce faire, FOXK1 lie le domaine MADS-box de Mef2 in vivo à l'aide de ses domaines FHA et FH, un domaine impliqué dans la liaison de Mef2 à l'ADN et dans ses interactions protéine-protéine [179]. Bref, FOXK1 agit à plusieurs niveaux lors du processus de différenciation musculaire afin de maintenir l'état prolifératif des cellules MPC, soit par l'entremise de l'inhibition transcriptionnelle via Sin3-HDAC et de l'inhibition de l'activité d'autres protéines telles que FOXO4 et MEF2 (figure 13). Néanmoins, le mécanisme d'inhibition de la fonction de

FOXK1 nécessaire afin d'enclencher la différenciation de cette population de cellules MPC à un moment précis n'est pas encore bien compris.

1.3.2.2 Régulation de FOXK1 par mTOR et le métabolisme

Récemment, FOXK1 a aussi été impliqué dans la réponse autophagique qui est un processus intimement lié avec le métabolisme cellulaire. Plusieurs facteurs de transcription sont activement régulés suite à l'induction de l'autophagie. Par exemple, FOXO3 est rapidement transporté dans le noyau afin d'activer la transcription des gènes nécessaires à ce processus, tandis qu'il demeure cytoplasmique et donc non-fonctionnel à des niveaux métaboliques normaux [205]. Des études très récentes ont permis de démontrer que le rôle répresseur de FOXK1 impliquant SIN3-HDAC affecte aussi des gènes cibles de FOXO3 impliqués dans la régulation autophagique, où FOXK1 et SIN3 co-localisent aux promoteurs de 79 de ces gènes tels que FBXO32, ULK1, AMBRA1 et ATG13 [206]. Cette étude a aussi révélé plusieurs sites de phosphorylation de FOXK1 ciblés par mTOR qui sont critiques à sa translocation dans le noyau, soit S225, S229, T231, S427 et S431 chez la souris [206]. Par contre, en condition de déprivation nutritionnelle, FOXK1 est phosphorylé sur d'autres sites par une ou plusieurs kinases inconnue(s) causant sont exclusion du noyau [206]. Il y a donc une importante dynamique de phosphorylation de FOXK1 en fonction de l'état métabolique de la cellule. Dans le modèle proposé par cette étude, en conditions normales, le complexe mTOR est actif et peut phosphoryler FOXK1 sur plusieurs sites. Ceci cause sa translocation au noyau où il peut recruter le complexe Sin3 afin de réprimer les gènes cibles de FOXO3 et d'inhiber l'autophagie. Par contre, en conditions de déprivation nutritionnelle, mTOR est inhibé et d'autres kinases peuvent alors phosphorylées d'autres sites sur FOXK1 résultant en sa séquestration cytoplasmique et/ou l'exclusion du noyau. À ce moment, FOXO3 peut être transloqué dans le noyau et activer la transcription des gènes d'autophagie.

1.3.3 FOXK2

Des études récentes ont démontré plusieurs fonctions de la protéine FOXK2 en rapport avec BAP1 et le contrôle du cycle cellulaire. Bien que FOXK2 soit beaucoup moins étudié que FOXK1, ses modifications post-traductionnelles ont d'importants impacts sur la régulation de différents processus cellulaires.

1.3.3.1 Recrutement de BAP1 à la chromatine

FOXK1 et FOXK2 forment des complexes avec le suppresseur de tumeur BAP1. Cependant, les mécanismes par lesquels BAP1 est spécifiquement recrutée à certains gènes en fonction du contexte cellulaire ne sont toujours pas bien compris. Des études de la fonction de YY1 ont démontré que le complexe BAP1/YY1/HCF-1 agit en tant que complexe activateur de la transcription en permettant le recrutement de BAP1 à la chromatine par un mécanisme classique de liaison directe à un facteur de transcription [51]. Néanmoins, le rôle que pouvaient jouer FOXK1 et FOXK2 dans le recrutement de BAP1 à différents promoteurs n'était pas connu jusqu'à tout récemment. Une récente étude indique que les FOXK interagissent avec BAP1 à l'aide de leur domaine FHA en liant le résidu T493 de BAP1, un résidu se trouvant dans le domaine flexible de BAP1 (figure 14) [115, 207]. D'autres études sur la fonction du complexe BAP1/FOXK2 dans les cellules H226 ont permis de déterminer qu'une fois recrutée aux gènes cibles de FOXK2 tels que MCM3, CDC14A et CDKN1B, BAP1 réprimerait leur transcription via la déubiquitination de H2AK119Ub à ces promoteurs [115]. Donc, contrairement à YY1 qui recrute BAP1 pour activer la transcription, FOXK2 recrute BAP1 pour l'inhiber et ce de manière dépendante de l'activité déubiquitinase de BAP1 [115, 207]. Cependant, bien que les gènes cibles communs de

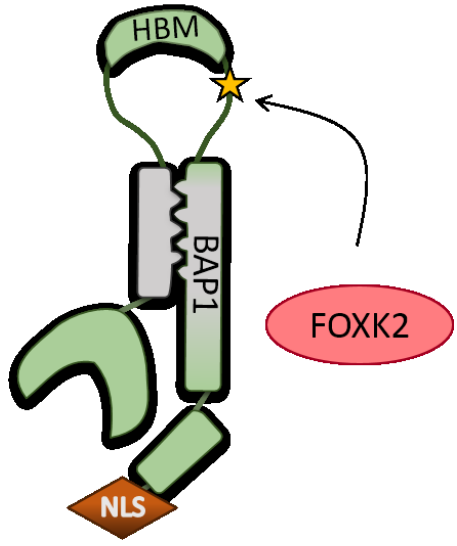

Figure 14. Le domaine FHA de FOXK2 interagit avec le T493 phosphorylé de BAP1. FOXK2 interagit avec cette région de façon constitutive et les études démontrent aussi que c'est le même résidu pour FOXK1 de sorte qu'ils risquent d'être mutuellement exclusifs dans le complexe BAP1. Astérisque démontre T493.

FOXK1/BAP1 n'aient pas été identifiés, FOXK1 interagit de la même façon que FOXK2 avec BAP1. Il reste à déterminer si les deux opèrent de façon redondante ou opposée.

1.3.3.1 Implication de FOXK2 dans la prolifération cellulaire

Comme mentionné précédemment pour YY1, beaucoup de facteurs de transcription sont modulés par modifications post-traductionnelles lors du cycle cellulaire. Parmis ces facteurs, une étude a démontré le lien étroit qu'il existe entre l'activité des kinases CDK, le cycle cellulaire et la phosphorylation de FOXK2. Comme cela est le cas pour de nombreuses protéines, les niveaux de FOXK2 fluctuent pendant le cycle cellulaire. Cependant, il a été observé que les niveaux de phosphorylation de ce dernier atteignent un maximum à l'entrée de la phase G_1 et diminuent durant la phase G_1 jusqu'à ce qu'ils atteignent un minimum en phase G_1/S, ce qui coincide avec une déstabilisation presque complète des niveaux protéiques de FOXK2 [208]. Par la suite, les niveaux protéiques et la phosphorylation de ce dernier reprennent pendant la phase G_2 jusqu'en mitose [208]. Par ailleurs, FOXK2 est hyperphosphorylé sur deux sérines critiques S368 et S423, via l'action de CDK1 et CDK2 pendant la transition G_2/M, ce qui a été décris comme causant le détachement de FOXK2 de la chromatine durant la mitose [208]. Après la cytocinèse, FOXK2 est rapidement déphosphorylé pour permettre à nouveau son interaction avec l'ADN. Cette phosphorylation dynamique de FOXK2 est critique pour la survie cellulaire puisque les mutants des sites en question entraînent rapidement l'apoptose. Cependant, étant donné qu'une grande majorité des protéines associées à la chromatine sont aussi la cible des CDK, il est difficile de déterminer à partir de ces travaux si la phosphorylation de FOXK2 est nécessaire à une étape de la mitose ou si cela est plutôt un mécanisme général afin d'éviter les abbérations chromosomales ou autres défauts de réplication.

D'autres liens entre FOXK2 et le cycle cellulaire ont été déterminés dont une étude récente démontrant l'importance de l'interaction entre FOXK2, BARD1, BRCA1 et le récepteur à l'estrogène (Erα). Selon cette étude, cette interaction permettrait la formation d'un pont entre BRCA1/BARD1 et ERα de façon à promouvoir l'ubiquitination et la dégradation du récepteur [209]. Ceci aurait pour conséquence de ralentir la prolifération cellulaire. De plus,

une augmentation de la prolifération a été observée suite à des traitements par ARNi contre FOXK2 [209]. En contradiction avec l'étude précédentes, d'autres travaux suggèrent que FOXK2 est plutôt nécessaire à la survie et à la prolifération cellulaire puisque ces travaux ont observés de l'apoptose suite au même traitement. Cette divergence entre les résultats pourrait être expliquée par l'utilisation de différents types cellulaires puisque FOXK2 pourrait ne pas avoir des fonctions redondantes d'un tissu à un autre. Aussi, elle pourrait être attribuée à l'utilisation de différentes séquences de siARN entre les études, certaines pouvant générer des effets non ciblés «*off target»* ou des effets différents en fonction du dosage (différence de pourcentage de déplétion de la cible entre les siARN). Tout de même, il est évident que FOXK2 joue un rôle critique dans la régulation du cycle cellulaire et que des dynamiques de modifications post-traductionnelles gouvernent sa fonction.

1.3.4. La redondance entre FOXK1 et FOXK2

Bien que la majorité des études démontrent des rôles différentiels de FOXK1 et de FOXK2 par rapport à différents processus cellulaires, quelques études ont aussi identifié des fonctions redondantes. Comme décrit précédemment, FOXK1 et FOXK2 contiennent des domaines très conservés. Il est donc possible que des fonctions protéiques médiées par ses domaines puissent être régulées par ces deux facteurs. Ceci semble être le cas pour la signalisation Wnt/β-caténine qui est une cascade très importante pour la prolifération cellulaire, le renouvellement des cellules souches, la différenciation, l'homéostasie cellulaire et le développement embryonnaire [210-213]. Une des étapes critiques de l'activation de cette cascade est la phosphorylation d'une protéine *Dishevelled* (DVL) qui participe à deux volets de cette cascade. D'une part, DVL mène à la stabilisation de β-caténine qui peut ensuite être transloqué au noyau et moduler l'expression de gènes [210-216]. D'autre part, DVL participe à la formation des complexes de transcription avec β-caténine dans le noyau [210-216]. Une étude récente a identifié les protéines FOXKs comme des protéines critiques à la translocation de DVL dans le noyau via leur intéraction avec cette dernière. De plus, les cancers colorectaux démontrant des surexpressions de FOXKs ont une plus forte capacité tumorale due à une augmentation de la proportion de DVL dans le noyau [217].

Une autre étude a démontré l'implication des FOXKs dans la réponse antivirale. Un des aspects caractéristiques de l'immunité innée est l'induction forte et rapide de l'expression de gènes tel que celui de l'interféron β suite à la reconnaissance d'ADN/ARN viral [218]. De récentes découvertes ont mené à l'identification de la nucléoporine Nup98 dans ce processus, via un mécanisme non-canonique. En fait, suite à une infection virale, FOXK1 et FOXK2 sont transloqués au noyau et participent avec Nup98 à la modulation de l'expression de gènes importants pour la réponse antivirale comme RIG-1, ISG54 et IFI17, permettant ainsi d'agir contre différents types de virus tels que SINV, SeV, RVFV et DCV [219]. En somme, FOXKs ont un rôle antiviral qui est conservé des insectes aux mammifères [219].

1.4 Mise en contexte du projet de recherche

Les MPTs telles que la méthylation, l'acétylation, la phosphorylation, la sumoylation, l'ubiquitination, l'O-GlcNAcylation joue des rôles primordiaux dans la coordination de la fonction, de la localisation et de l'activité protéique ainsi que dans la transcription génique. Parmi celles-ci, l'ubiquitination joue un rôle primordial dans presque tous les processus cellulaires. BAP1, qui est la déubiquitinase la plus mutée du génome humain, est capable d'hydrolyser la mono-ubiquitination de H2AK119Ub, une marque critique pour la structure et fonction de la chromatine. BAP1 forme un complexe multi-protéique contenant plusieurs protéines polycombes ainsi que plusieurs régulateurs transcriptionnels, incluant les facteurs de transcription FOXK1 et FOXK2 qui sont co-régulés via une panoplie de MPTs. FOXK1 est principalement connu pour son rôle déterminant dans la myogenèse, l'autophagie cellulaire, la signalisation Wnt/β-caténine et la réponse antivirale. De son côté, FOXK2 est connu pour recruter le complexe BAP1 à la chromatine afin d'inhiber l'expression des gènes. Il est aussi critique pour la survie cellulaire. Cependant, comment ces facteurs régulent la fonction de BAP1 et comment leurs MPTs affectent cette dynamique n'est pas bien compris.

1.5 Hypothèse

Sachant que le complexe BAP1 est en fait une plateforme regroupant de nombreuses enzymes modificatrices, cela nous a conduit à formuler l'hypothèse qu'à même le complexe BAP1,

FOXK1 et FOXK2 sont sujets à des modifications post-traductionnelles ayant un effet important sur leur régulation et leur rôle dans ce complexe. Nos objectifs sont :

1) Valider l'interaction identifiée par analyses de spectrométrie de masse entre BAP1 et les protéines FOXK par des essais dans des cellules par immunoprécipitation et in vitro par GST-pulldown. De plus, puisque les protéines FOXK ont des domaines très conservés, déterminer si les protéines sont mutuellement exclusives pour leur interaction avec BAP1.

2) Identifier les domaines d'interactions critiques pour l'interaction entre BAP1 et les protéines FOXK en utilisant des constructions mutantes des différentes protéines. Nous allons produire des constructions déficientes des domaines FHA et FH des FOXK et des constructions de délétions des différents domaines de BAP1 afin de les exprimer dans des cellules pour réaliser des essais de co-immunoprécipiations ou de les exprimer dans des bactéries pour effectuer des essais de GST-pulldown.

3) Si les FOXK s'avèrent être mutuellement exclusive pour BAP1, déterminer la fonction des complexes FOXK1-BAP1 et FOXK2-BAP1. Notre groupe a déjà démontré que le facteur de transcription YY1 recrute BAP1 à la chromatine dans le but d'activer la transcription. Les protéines FOXK ont possiblement une fonction distincte.

3) Identifier quelles MPTs spécifiques aux FOXKs pourraient avoir un effet sur la fonction du complexe BAP1 et sur son rôle suppresseur de tumeurs. Nous allons réaliser des analyses de spectrométrie de masse pour identifier les MPTs des FOXK. De plus, dû à la présence de l'E3 ligase LSD2, de la déubiquitinase BAP1 et de la O-GlcNAc transférase OGT dans le complexe BAP1, nous allons vérifier si les FOXK sont modifiées par ubiquitination et/ou O-GlcNAcylation.

L'étude des MPTs de ces facteurs de transcription mènera à une meilleure compréhension de processus tel que le remodelage de la chromatine et pourra contribuer à mieux comprendre comment le complexe BAP1 agit en tant que suppresseur de tumeur.

Chapitre 2

2. Article en préparation

FOXK1 Transcription Factor is Regulated by O-GlcNAcylation and is Required for Adipogenesis

Nicholas VG Iannantuono[1,†], Jessica Gagnon[1,†], Haithem Barbour[1], Eric Bonneil[2], Pierre Thibault[2] and El Bachir Affar[1,#]

[1]Maisonneuve-Rosemont Hospital Research Center and Department of Medicine, University of Montréal, Montréal H3C 3J7, Québec, Canada

[2]Institute for Research in Immunology and Cancer, University of Montréal, Montréal H3C 3J7, Québec, Canada

[†]Equal contribution

Conflict of interest

The authors declare no conflict of interest

Running title: FOXK1 is O-GlcNAcylated and Required for Adipogenesis

Key words: FOXK1, FOXK2, OGT, O-GlcNAcylation, BAP1, Adipogenesis, post-translational modification, starvation, differentiation, FHA

Abbreviation: Forkhead box Associated protein 1 and 2 (FOXK1 and FOXK2), Forkhead box Associated domain (FHA), O-Linked N-acetylglucosamine transferase (OGT), Host Cell Factor-1 (HCF-1), serine (Ser), threonine (Thr), post-translational modifications (MPTs), Hexosamine Biosynthetic Pathway (HBP), HCF-1 Binding Motif (HBM), Ubiquitin Carboxyl Hydrolase (UCH), C-terminal domain (CTD), Coiled-Coil1 and 2 (CC1 and CC2)

2.1 Contribution de chaque auteur

Contribution actuelle :

Je déclare que Jessica Gagnon et moi nous sommes co-premier auteur car elle a fait une contribution majeure à cette œuvre par rapport aux hypothèses testés, participation aux discussions et design d'expérience (environ 45%) par contre, bien que nous avons également contribué à ce projet, je déclare que j'ai produit plus de figures qui sont physiquement dans l'article. Jessica et moi nous avons écrit le manuscrit et préparer les figures pour publication.

Plus précisément, j'ai réalisé les expériences menant à la figure 15, 16, 17B, 18A et B et 19E. Jessica a réalisé les expériences 17A, 18C et D et 19A, B, C et D mais aussi beaucoup d'expériences sur des hypothèses que nous avions mais qui n'ont pas mené à des figures des l'article comme par exemple des essais de compétition des FOXK pour BAP1. Haithem Barbour à aussi réaliser des répétitions des expériences 19A, B, C et D.

Contribution prévisible :

Les expériences et hypothèses qui restent à tester seront faites par Jessica Gagnon et moi et nous allons modifier le manuscrit et les figures en conséquence.

2.2 Abstract

O-GlcNAcylation, catalyzed by OGT, is an extensively studied modification which consists in the addition of an O-GlcNAc moiety to serine and threonine residues of targeted proteins. OGT is known to be a core partner of BRCA1 Associated Protein 1 (BAP1) which is an important tumor suppressor complex mainly composed of transcriptional regulators whose main function is the deubiquitination of histone H2A. Furthermore, the BAP1 complex is subjected to a plethora of post-translational modifications that were shown to be crucial for the regulation of its function including O-GlcNAcylation. Among the different partners of BAP1, the transcription factors of the K subfamily of Forkhead Box protein (FOXK1 and FOXK2) have recently emerged as important regulators of BAP1-mediated deubiquitination of specific gene promoters. These factors are uniquely characterized by the presence of both, a Forkhead box Associated domain (FHA) which binds phosphothreonine residues and a DNA-binding Forkhead box domain (FH). Recent studies have demonstrated the importance of the phosphorylation of BAP1 for the binding of the FOXKs. However, why both FOXK1 and FOXK2 interact with the BAP1 complex and whether they are differentially regulated is still unclear. In this study, we report that FOXK1, but not FOXK2 is a novel target for O-GlcNAcylation and that FOXK1's interaction with BAP1 is greatly compromised in response to cellular starvation. Our data also demonstrates that FOXK1 O-GlcNAcylation is modulated during the entry of cell cycle as well as during differentiation. Using the 3T3L1 adipocyte differentiation model, we also provide new evidence that FOXK1 is critical for adipogenesis

2.3 Introduction

Networks of post-translational modifications (MPTs) in eukaryotic cells participate in the regulation of a wide variety of signaling cascades whose main output is modulation of gene transcription [1, 3, 6, 41, 93, 220-228]. Such collaboration between modifying enzymes results in a highly complex crosstalk of marks crucial for cell fate determination [229-232]. Such networks can be observed within chromatin modifying complexes that interpret multiple signaling cascades to trigger different cellular outcomes. For instance, the BRCA1 Associated Protein 1 (BAP1) forms a large protein complex containing several transcription regulators and factors.[56, 57, 61] O-GlcNAcylation and ubiquitination are MPTs that have been shown to be critical for the function of several of the BAP1 complex subunits [9, 60, 68, 72, 92, 131]. Indeed, recent studies have shown that Lysine-Specific Demethylase 1B (LSD2/KDM1B) ubiquitinates the O-linked-β-N-acetylglucosamine transferase (OGT) in order to trigger its degradation [92]. This is counteracted by deubiquitination via BAP1 so as to protect OGT for it to O-GlcNAcylate other components of the BAP1 complex to regulate their function [68].

O-GlcNAcylation is of great interest as its addition onto serine and threonine residues has been shown to compete with phosphorylation. In this way, O-GlcNAcylation may protect specific sites from kinase activity thus interfering with phosphorylation-dependent events whereby O-GlcNAcylation may have broad cellular repercussions [233, 234]. Furthermore, O-GlcNAcylation is emerging as a direct and critical mediator of metabolic signaling as the synthesis of its donor substrate is derived from the hexosamine biosynthetic pathway (HBP), resulting in dynamic O-GlcNAcylation in response to fluctuations in the major metabolic pathways, including the metabolism of nucleotides, free fatty acids, amino acids and glucose [121, 235-237]. Hence, the dynamic competition with phosphorylation would also be sensitive to metabolic fluctuations. The ternary complex of OGT/HCF1/BAP1 has also been shown to regulate gluconeogenesis via O-GlcNAcylation and deubiquitination of PGC-1α, thereby solidifying the BAP1 complex's implication in metabolic regulation [58]. Other components of the BAP1 complex have also been shown to be O-GlcNAcylated such as Yin Yang 1 (YY1) and

HCF-1, attesting to the importance of O-GlcNAcylation in the regulation of this complex [68, 69, 72].

Two other factors in the BAP1 complex are the Forkhead Box Proteins 1 and 2 (FOXK1 and FOXK2) whose functions remain poorly understood. FOXK1 and FOXK2 are two ubiquitously expressed FOX transcription factors. The FOX factors are known to bind DNA with a highly conserved FH domain but the FOXK subfamily is unique in that FOXK1 and FOXK2 also contain an FHA phosphor threonine-binding domain. Both FOXK1 and FOXK2 are present in the BAP1 complex, are highly similar in structure, but they have been reported to have very different functions. FOXK2 has been shown to recruit the BAP1 complex to chromatin in order to modulate PRC1-mediated gene expression [115, 207]. It has also been shown to act in concert with AP-1 signaling and to bind G/T mismatches [238, 239]. Further, it has been shown to mediate cell survival and most recently was shown to suppress tumour growth of ERα-positive breast cancers [209]. FOXK1, on the other hand, has been shown to be a critical regulator of myogenesis through both cell cycle control and direct protein inhibition of the differentiation program [179, 183, 196, 197, 240, 241]. Recently it has been shown that mTOR phosphorylates FOXK1, promoting its nuclear accumulation, in order to inhibit autophagy gene expression through the recruitment of the Sin3 repressive complex in normal growth conditions [206]. Importantly, both FOXK1 and FOXK2 have been shown to be regulated by phosphorylation and have been implicated in Wnt Signaling through the nuclear transport of DVL proteins [217], and the antiviral response via Nup98 [219]. However the link between metabolic regulation, OGT and the FOXK proteins has not been thoroughly explored. Here we show that, unlike FOXK2, FOXK1 is specifically O-GlcNAcylated and that this modification is modulated during various cellular processes including adipogenesis where we show that FOXK1 is critical for this process.

2.4 Material and methods

2.4.1 Bacterial induction, purification and GST-Pulldown

Gluthatione-S-Transferase (GST) Pulldown was performed as previously described [61]. Briefly, proteins were induced for 6 hours with 400 µM of Isopropyl β-D-1-thiogalactopyranoside (IPTG) and then purified from *E. Coli* bacteria with Glutathione-agarose resin (Sigma). As for His-tagged proteins, they were induced in the same manner as the GST-tagged proteins except they were purified with Ni-NTA Agarose resin (Life Technologies). For GST-Pulldown, 2 µg of proteins immobilized on beads were incubated overnight at 4°C with the indicated recombinant His-tagged protein in a GST-pulldown binding buffer (50 mM Tris-HCl, pH 7.5, 50 mM NaCl, 0.02% Tween 20, 1 mM Phenylmethanesulfonyl fluoride (PMSF) and 500 µM Dithiothreitol (DTT)). Next day, beads were washed 8 times with GST-pulldown wash buffer (50mM Tris pH 7.5, 150 mM NaCl, 1 mM EDTA, 0.1% Tween 20, 1 mM PMSF, 200 µM DTT). Proteins were then eluted with 2X Laemmli buffer and protein interaction were analyzed by western blotting.

2.4.2 Cell culture and G_0 synchronization

Human embryonic kindney (HEK293T), human osteosarcoma (U2OS), HeLa S3, and human lung carcinoma (H226) were cultured according to standard procedures in DMEM supplemented with 5% Foetal Bovine Serum (FBS), 1% Glutamine and 1% Penicillin/Streptomycin except for murin adipocyte progenitors (3T3L1) and human fibroblast (LL) which were cultured with 10% FBS. Human chronic myelogenous leukemia K562 and K562-ASXL2 suspension cells were maintained in RPMI medium supplemented with 5% FBS, 1% Glutamine and 1% Penicillin/Streptomycin. Cell cycle synchronizations in G_0 were done as previously described [242]. Briefly, cells were left to grow to confluence, media was changed and cells were left for 24 hours at confluence in media lacking serum. Cells were then refed serum-containing media and harvested at indicated time points. Cell cycle analysis was done using FACScan flow cytometer fitted with CellQuestPro software (BD Biosciences) as previously described [138] and figures were made using FlowJo software.

2.4.3 Plasmids, transfections and siRNA treatments

GST-, FLAG- and MYC-tagged constructs were generated using the recombination technology of the Gateway system from Life Technologies. siRNA-resistant cDNA coding for FOXK1 and FOXK2 were synthesized from Biobasic Int directly into Bluescript plasmid. His-YY1 was previously described [145]. pOZN, pOZN-FLAG-HA-BAP1 WT and pOZN-FLAG-HA-BAP1ΔHBM were previously generated [61]. Both MYC-OGT, FLAG-OGT WT and catalytic dead mutants were produced as described [152]. and GST-tagged deletion mutants of BAP1 were previously generated [9]. Plasmids transfections were done in HEK293T with mammalian expression vectors using polyethylenimine (PEI) (Sigma-Aldrich). Three days post-transfection cells were harvested in PBS or in lysis buffer (25 mM Tris-HCl pH 7.5) for subsequent analysis by immuneprecipitation or western blotting.

U2OS double siRNA transfections were done in serum-free DMEM medium for 16h with Lipofectamine 2000 (Life Technologies) as previously described [243]. 3T3L1 double siRNA transfection were done in serum-free DMEM medium for 16h with RNAi Max Lipofectamine (Life Technologies) using 200 pmol of either ON-TARGET plus Non-targeting pool (D-001810-10-50) (Thermo Scientific, Dharmacon) or siFoxk1 (SASI_Mm01_00032593) (SASI_Mm01_00032594) (SASI_Mm01_00032595) (SASI_Mm01_00032596) (SASI_Mm02_00351347) (SASI_Mm02_00351348) (SASI_Mm01_00160371) (SASI_Mm01_00160372) or siFoxk2 (SASI_Mm02_00294023) (SASI_Mm02_00294024) (SASI_Mm02_00294025) (SASI_Mm02_00294026). Then, medium was changed for complete DMEM supplemented with 10% FBS, 1% Glutamine and 1% Streptomycin and a second siRNA transfection was done 72h following the first siRNA transfection so as to start 3T3L1 differentiation.

2.4.4 Immunoprecipitation and complex purification

For native immunoprecipitations, cells were harvested in PBS and pellets were lysed for 30 min on ice in EB150 buffer (50 mM Tris pH 7.5, 150 mM NaCl, 5 mM EDTA, 1% Triton, 1 mM DTT, 1 mM PMSF, 2 µM PUGNAc, 10 mM BGP, 1 mM Na_3VO_4, 50 mM NaF,1X anti-protease

cocktail (Sigma)). Lysates were then spun for 20 min at 14 000 rpm at 4°C to pellet insoluble material and supernatants were incubated overnight with rotation at 4°C with either anti-FLAG resin (Sigma) or anti-Protein G Sepharose and 4 µg of the appropriate antibody. The following day, beads were washed with EB150. Bound proteins were eluted with 2X Laemmli buffer and subjected to Western Blotting. As for the stable cell line complex purifications, 1L of HeLa S3 pOZN, pOZN-FLAG-HA-BAP1 or pOZN-FLAG-HA-BAP1ΔHBM were grown to ~1x10^6 cells/ml and then cells were harvested and pelleted. Pellets were lysed on ice for 30 minutes in EB150 (50mM Tris pH 7.5, 150mM NaCl, 1mM EDTA, 0.5% Triton, 1mM DTT, 1mM PMSF, 2µM PUGNAc, 10mM BGP, 1mM Na_3VO_4, 50mM NaF, 1X anti-protease cocktail (Sigma)). Lysates were then spun at 20 000 rpm for 20 min at 4°C. Supernatant was then filtered through a 0.45 µm filter onto anti-FLAG resin (Sigma) for overnight rotation at 4ºC. The following day, beads were washed and bound proteins were eluted with 150 µg/ml of FLAG peptide and subjected to Western Blotting. For denaturing immunoprecipitations, cells were first harvested in a lysis buffer (25 mM Tris-HCl pH 7.5 and 1% SDS). Samples were boiled for 10 min, sonicated and samples were diluted with 9 volumes of EB150. Immunoprecipitations was performed as previously described for native immunoprecipitations.

2.4.5 Site-directed mutagenesis

Site-Directed Mutagenesis was performed using overlapping primers and Q5 High-Fidelity DNA Polymerase from New England Biolabs and all mutants were sequenced. Primers used for site-directed mutagenesis are as follows: FOXK1 R127A primer_F: ACGATAGGGGCGAATAGCAGCCAAGGGAGCGT, FOXK1 R127A primer_R: TGCTATTCGCCCCTATCGTCACCGACGGTTGC, BAP1 T493A primer_F: ACCCCCAGCAATGAGAGTGCAGACAC, BAP1 T493A primer_R: GATCTCAGAGGCCGTGTCTGCACT

2.4.6 Differentiation and starvation

3T3L1 differentiation assays were performed as previously described [9] in parallel with siRNA treatment. Briefly, 3T3L1 cells were plated at the same density and transfected with siRNA using Lipofectamine RNAi Max as described above. Cells were then grown to

confluence and left at confluency for 48h. The cells were then transfected with siRNA a second time but in differentiation media (DMEM supplemented with 10% foetal bovine serum, 1% Glutamine, 1% penicillin/streptomycin, 1 µM dexamethasone, 1 µg/ml insulin and 500 µM isobutylmethylxanthine (IBMX) (Sigma)). Two days post-induction, media was changed for DMEM medium supplemented with 10 % FBS, 1% Glutamine, 1% penicillin/streptomycin and 1 µg/ml insulin. Media was changed every 48h and cells were harvested at indicated time points. For LL and K562 stably expressing FLAG-HA-tagged ASXL2, cells were starved according to Bowman et al. [206] with Hank's Balanced Salt Solution (HBSS) supplemented with 10 mM HEPES pH 7.5 and 1% Penicillin-Streptomycin for the indicated time. When indicated, cells were replenished for 2h by feeding back the cells with growth medium. Cells were then harvested for subsequent immunoprecipitation and biochemical analysis by western blotting.

2.4.7 Oil Red O staining

Prior to Oil Red O staining, scans of media colour were rapidly taken using a HP Scanjet 8300. 3T3L1 cells were fixed in 10% formalin for 10 min at room temperature (RT). Cells were then washed with PBS, Milli-Q H2O and incubated with 60% isopropanol for 5 min at RT. Cells were completely dried at RT and then incubated in Oil Red O working solution composed of a filtered 60% solution of Oil Red O stain (Sigma #O0625-25G) for 10 min. Cells were then rapidly washed 4 times with Milli-Q H2O and images were taken using an inverted microscope Olympus BX53F.

2.4.8 Immunoblotting and antibodies.

Cells were harvested either in PBS for subsequent immunoprecipitation or in a lysis buffer composed of 25 mM Tris-HCl pH 7.3 and 1% SDS. Total cell lysates harvested in lysis buffer were boiled at 95°C for 10 min and sonicated. Protein quantification was done by bicinchoninic acid (BCA) assay. For western blotting, samples were diluted in 2X or 4X Laemmli buffer and SDS-PAGE and immunoblotting were performed following standard procedure. The band signals were acquired with a LAS-3000 LCD camera coupled to MultiGauge software (Fuji, Stamford, CT, USA).

Mouse monoclonal anti-BAP1 (C4, sc-28383), rabbit polyclonal anti-FOXK1 (H140, sc-134550), rabbit polyclonal anti-YY1 (H414, sc-1703), rabbit polyclonal anti-OGT (H300, sc-32921), mouse monoclonal anti-tubulin (B-5-1-2, sc-23948) and mouse monoclonal anti-CDC6 (180.2 sc-9964) were from Santa Cruz. We generated the rabbit polyclonal anti-FOXK2. Rabbit polyclonal anti-HCF-1 (A301-400A) was from Bethyl Laboratories. Mouse monoclonal anti-Flag (M2) was from Sigma-Aldrich. Mouse monoclonal anti-MYC (9E10) was from Covance. Monoclonal anti-O-Linked N-acetylglucosamine (RL2, ab2739), rabbit polyclonal anti-H3 (ab1791) were from Abcam. Mouse monoclonal anti-β-Actin (MAB1501, clone C4) was from Millipore. Rabbit monoclonal anti-perillipin (D1D8, #9341) was from Cell Signaling. Rabbit polyclonal anti-FABP4 (#10004944) was from Cayman Chemical.

2.5 Results

2.5.1 BAP1 structural conformation and Thr493 residue, but neither HCF-1 nor OGT, are important for FHA-dependant FOXKs binding to BAP1.

Several studies have mapped the potential binding domain between the FOXKs transcription factors and BAP1 identifying the FHA domain of FOXKs as the main domain responsible for the interaction with BAP1. However, it is still unclear if this interaction is mediated via BAP1 phosphorylation of its threonine 493, and/or also through its structural conformation [115, 207]. Thus, we sought to investigate the phosphorylation dependency of the interaction between BAP1 and FOXK proteins. To do so, we used GST-tagged constructs of FOXK1 and FOXK2 to perform GST-pulldowns using recombinant proteins. GST-YY1 was used as a positive control, as previous studies have demonstrated its direct interaction with BAP1 [61]. As shown in Figure 15A, despite significant degradation products from the bait proteins, both GST-FOXK1 and GST-FOXK2 strongly enrich recombinant BAP1 suggesting that its phosphorylation is not necessary for the interaction. Therefore, we sought to better characterise the interacting region of BAP1 with the FOXKs. Since the FHA and FH domains of FOXK1 and FOXK2 are highly conserved and that Okino et al. [115] showed that FOXK1 and

FOXK2 interact with the same region of BAP1, we sought to validate that the FOXKs interact with BAP1 in a mutually exclusive manner. As such, HeLa nuclear extracts were prepared and native immunoprecipitations of endogenous FOXK1 and FOXK2 were performed. Our data clearly show that FOXK2 does not co-immunoprecipitate with FOXK1 and vice versa suggesting that they are indeed mutually exclusive since the levels of FOXK1 visible in the FOXK2 IP are comparative to background binding (Figure 15B). Therefore, further mapping experiments with BAP1 were performed using GST-FOXK1 only. As shown in figure 15C (Right), we generated several BAP1 deletion constructs in order to validate previous identified binding region of BAP1[9].Despite important GST-protein degradation, our results demonstrate that FOXK1 interacts with the full length form of BAP1 as well as with the ΔUCH fragment, indicating that the NORS and the CTD of BAP1 are either completely or partially important for proper binding of BAP1 with FOXK1. However, the BAP1-Thr493A mutant reported by Okino et al.[115] completely abolished FOXKs binding as shown by the FLAG co-immunoprecipitation (Figure 15D and 15E). Reciprocally, we produced the FOXK1-Arg127A mutant, known to be critical for FHA function as it recognizes the phosphate moiety and as reported, co-immunoprecipitation of BAP1 is significantly reduced with FOXK1-Arg127A mutant (Figure 15E). Altogether, these contradictory data suggest that the Thr493 residue as well as the structural conformation of BAP1 are both important for the binding of BAP1 by the FHA domain of FOXK1. Also, due to the proximity of Thr493 to the HCF-1 binding motif (HBM) of BAP1 and since HCF-1 is a core component of the BAP1 complex, we examined if the presence of HCF-1 could regulate the presence of the FOXKs in the BAP1 complex. We reasoned that the proximity of HCF-1 to the Thr493 residue in the flexible loop of BAP1 might create steric hindrance regulating FOXKs interaction with BAP1 as schematised in Figure 15F, therefore, ablation of the HBM might increase FOXKs binding to BAP1. To verify this hypothesis, we generated HeLa S3 cells stably expressing either FLAG-HA-BAP1 or FLAG-HA-BAP1 ΔHBM and purified these complexes by FLAG immunoprecipitation. As shown in figure 15G, FOXKs levels in the BAP1 complex are not affected by HCF-1 or OGT presence. Collectively, these data suggest that FOXK proteins bind a precise structural conformation of BAP1 as well as its Thr493 residue independently of HCF-1 and OGT presence in the complex.

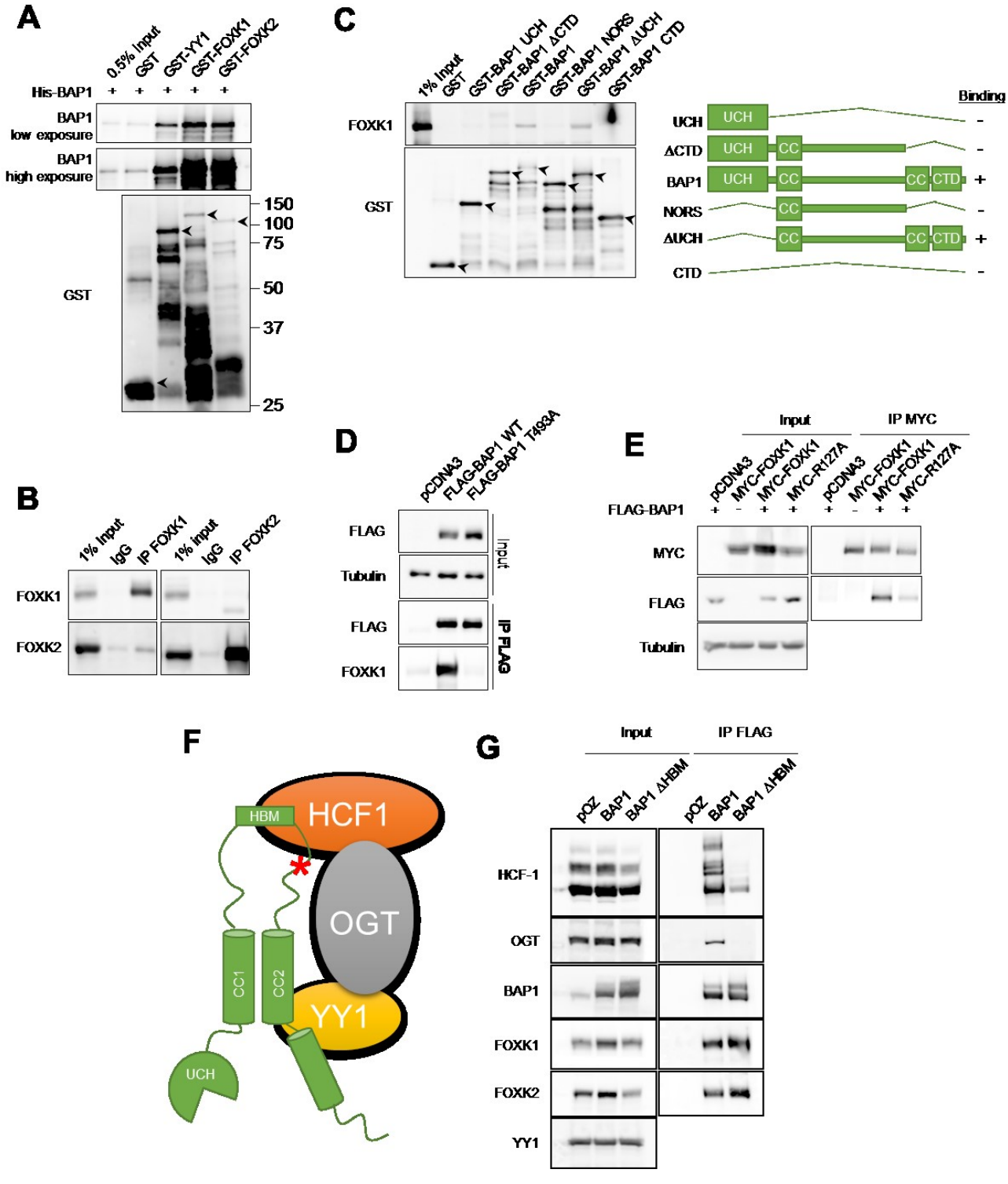
A
0.5% Input
GST
GST-YY1
GST-FOXK1
GST-FOXK2
His-BAP1 + + + + +
BAP1 low exposure
BAP1 high exposure
GST
150
100
75
50
37
25
B
1% Input
IgG
IP FOXK1
1% Input
IgG
IP FOXK2
FOXK1
FOXK2
C
1% Input
GST
GST-BAP1 UCH
GST-BAP1 ΔCTD
GST-BAP1
GST-BAP1 NORS
GST-BAP1 ΔUCH
GST-BAP1 CTD
FOXK1
GST
Binding
UCH
ΔCTD
BAP1
NORS
ΔUCH
CTD
UCH
CC
CTD
D
pCDNA3
FLAG-BAP1 WT
FLAG-BAP1 T493A
FLAG
Tubulin
FLAG
FOXK1
Input
IP FLAG
E
Input
IP MYC
pCDNA3
MYC-FOXK1
MYC-FOXK1
MYC-R127A
pCDNA3
MYC-FOXK1
MYC-FOXK1
MYC-R127A
FLAG-BAP1 + - + + + - + +
MYC
FLAG
Tubulin
F
HBM
HCF1
OGT
CC1
CC2
YY1
UCH
G
Input
IP FLAG
pOZ
BAP1
BAP1 ΔHBM
pOZ
BAP1
BAP1 ΔHBM
HCF-1
OGT
BAP1
FOXK1
FOXK2
YY1

Figure 15. BAP1 structural conformation and Thr493 residue but not HCF-1 and OGT are important for FHA-dependant FOXKs binding to BAP1. (**A**) GST-pulldown of recombinant purified His-BAP1, GST, GST-FOXK1, GST-FOXK2 and GST-YY1. His-BAP1 was used as the pray. Proteins levels were analysed by western blotting using the indicated antibodies. Arrows indicate GST-tagged proteins (**B**) HeLa nuclear extracts were lysed and native immunoprecipitations of FOXK1 and FOXK2 were performed overnight. Control IgG immunoprecipitations was performed as a negative control and proteins levels were analyzed by immunoblotting with the indicated antibodies. (**C**) (Left) GST-pulldown of recombinant BAP1 fragments with purified recombinant His-FOXK1. Arrows indicate GST-tagged BAP1 fragments. (Right) Schematics of BAP1 fragments used for the GST-pulldown. (**D**) HEK293T cells were transfected with either FLAG-BAP1 wild-type (WT) or FLAG-BAP1 Thr493A mutant. Three days post-transfection, cells were lysed and native anti-FLAG immunoprecipitation was performed. Endogenous FOXK1 co-immunoprecipitation was analyzed by western blotting. (**E**) HEK293T cells were transfected with MYC-FOXK1 WT or MYC-FOXK1 Arg127A with or without FLAG-BAP1. Three days post-transfection, cells were harvested and native anti-MYC immunoprecipitation was performed. BAP1 binding was analysed by western blotting. (**F**) BAP1 schematic illustrating the location of Thr493A with regards to the reported binding locations of HCF1/OGT/YY1 axis. Asterisk indicates the position of threonine 493 residue. (**G**) HeLa S3 cells stably expressing either pOZN, pOZN-FLAG-HA-BAP1 or pOZN-Flag-HA-BAP1 ΔHBM were grown and harvested for complex purification by overnight anti-flag immunoprecipitation. Core components of the complex were analysed by western blotting with the indicated antibodies. IP; Immunoprecipitation.

2.5.2 FOXK1 but not FOXK2 is O-GlcNAcylated by OGT

Post-translational modifications of the core proteins in the BAP1 complex have been extensively studied and characterized [9, 56, 57, 62, 92, 131]. The presence of protein post-translational modifying enzymes such as LSD2, OGT, UBE2O, HAT1 and BAP1 itself strongly advocate for the importance of MPTs in the function of this tumor suppressor complex. However, the identification and function of the various MPTs in the BAP1 complex are still largely unknown. For example, although several phosphorylation sites of FOXKs were identified, the study of the MPTs of the FOXKs transcription factors remains in its infancy [206, 208]. Therefore, we sought to identify novel MPTs of FOXKs and how they might regulate the dynamics of the BAP1 complex. Since the binding of FOXK proteins to Thr493 of BAP1 would bring them in close proximity to the O-linked N-acetylglucosamine transferase (OGT), already known to modulate the function of components of the BAP1 complex through O-GlcNAcylation, we verified if FOXK proteins may be O-GlcNAcylated in cells [56, 68, 69, 72, 131]. We co-overexpressed MYC-FOXK1 or MYC-FOXK2 with either FLAG-OGT WT or FLAG-OGT CD to perform MYC immunoprecipitations under denaturing conditions. As shown in figure 16A, a mobility shift can be observed for FOXK1 in the presence of OGT WT but not in the presence of OGT CD, indicative of a higher molecular weight for all of the ectopic FOXK1 in this condition. This modification was further confirmed to be O-GlcNAcylation as it was

detected by the highly used RL2 antibody [243]. This antibody is specific to the O-GlcNAc moiety and does not have any affinity for the protein backbone on which this modification is attached such as pTyr antibodies. Rather, this antibody simply reflects the presence of an O-GlcNAc group. Moreover, these data suggest that this O-GlcNAcylation is specific to FOXK1. To further confirm previous results on endogenous FOXK1, we harvested HEK293T to performed FOXKs immunoprecipitation under denaturing conditions in order to eliminate all interacting partners. As shown in figure 16B, immunoprecipitated FOXK1 but not FOXK2 yields an O-GlcNAcylation signal. The same result was obtain using the non-cancerous murin cell line 3T3L1 albeit FOXKs are expressed at lower levels. To verify the specificity of the detected O-GlcNAcylation signal, we depleted OGT by siRNA in U2OS cells and performed a FOXK1 immunoprecipitation under denaturing condition (Figure 16D). As expected, levels of OGT were almost completely ablated under siRNA treatment which resulted in a complete loss of the O-GlcNAcylation signal previously observed for FOXK1. Moreover, a slight decrease in BAP1 binding can be observed following depletion of OGT (Figure 16D). As O-GlcNAcylation is known to mediate certain protein functions such as localization and protein-protein interactions, we sought to determine if O-GlcNAcylation of FOXK1 could modulate its interaction with BAP1. Thus, we co-expressed OGT WT or CD in the presence of BAP1 WT or the BAP1-Thr493A mutant but observed no change in FOXK1 binding in all conditions (Figure 16E). Also, the O-GlcNAcylation of FOXK1 had no effect on the FOXK2-BAP1 interaction suggesting that FOXK1 O-GlcNAcylation does not regulate FOXKs binding to the BAP1 complex. Taken together, these results suggest that FOXK1 but not FOXK2 is specifically O-GlcNAcylated by OGT and that this modification does not regulate FOXKs presence in the complex.

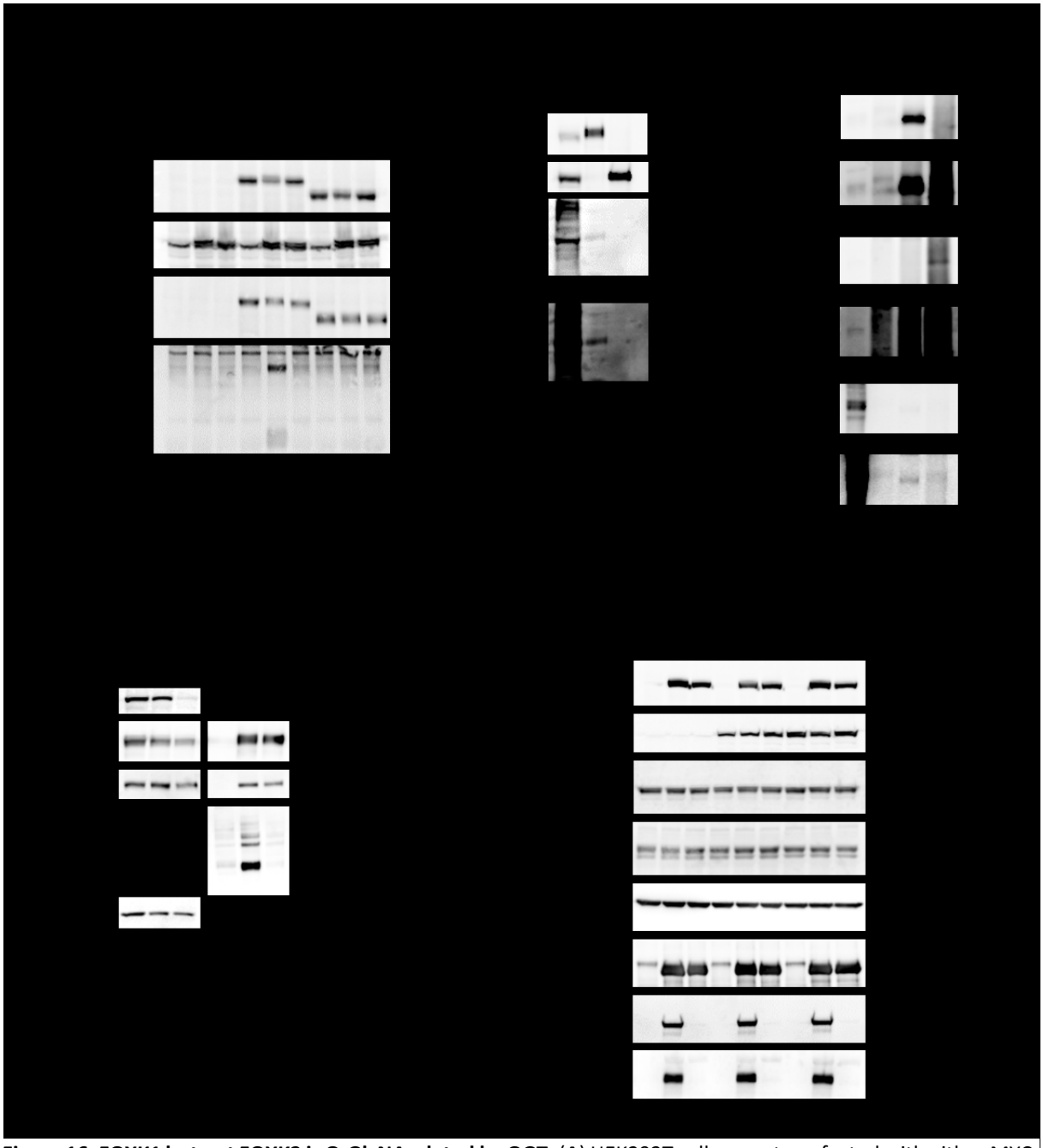

Figure 16. FOXK1 but not FOXK2 is O-GlcNAcylated by OGT. (**A**) HEK293T cells were transfected with either MYC-FOXK1 or MYC-FOXK2 and FLAG-OGT WT or catalytic dead (CD). Three days post-transfection, cells were harvested for denaturing anti-MYC immunoprecipitation and proteins levels were immunoblotted with indicated antibodies. (**B**) HEK293T cells were harvested and denaturing immunoprecipitation of endogenous FOXKs was performed. O-GlcNAcylation of FOXKs was analyzed by western blotting using RL2 antibody. (**C**) O-GlcNAcylation of endogenous Foxk1 and Foxk2 in murine 3T3L1 cell line was analysed as in (B). (**D**) U2OS cells were double treated with siRNA against OGT. Three days post-transfection, cells were harvested for native immunoprecipitation of FOXK1. Protein levels were analysed by western blotting with indicated antibodies. Control correspond to untreated U2OS cells used for the IgG immunoprecipitation. (**E**) HEK293T cells were transfected with either FLAG-BAP1 WT or FLAG-BAP1 Thr493A with either MYC-OGT WT or MYC-OGT CD. Three days post-transfection, cells were harvested for anti-FLAG immunoprecipitation and results were revealed by western blotting using indicated antibodies. IP; Immunoprecipitation. All experiments were performed three times.

2.5.3 FOXK1 O-GlcNAcylation by OGT is BAP1-independent.

OGT is a ubiquitous protein that is involved in a plethora of cellular processes and is known to interact with hundreds of substrates outside of its interaction with BAP1. Since our previous data indicates that O-GlcNAcylation does not affect FOXK1 binding with BAP1, we then wanted to verify if BAP1 is required for FOXK1 O-GlcNAcylation. We reasoned that BAP1 might serve as a bridge allowing OGT to modify FOXK1. To explore this possibility, we performed immunoprecipitation of endogenous OGT and FOXKs in H226 lung carcinoma cells, known to be devoid of BAP1 expression, as well as in an H226-BAP1 cell line in which we expressed BAP1 in order to compare the O-GlcNAcylation level of FOXK1. As shown in figure 17A, FOXK1 O-GlcNAcylation level is similar either in the presence or absence of BAP1. These data suggest that BAP1 is not required for FOXK1 O-GlcNAcylation. To further confirm that the O-GlcNAcylation of FOXK1 is independent of BAP1 and that FOXK1 may be modified by OGT outside of the BAP1 complex, we conducted a denaturing immunoprecipitation of FOXK1 from the elutions of the FLAG-BAP1 WT and FLAG-BAP1 ΔHBM purified complexes (see figure 15G). As expected, the O-GlcNAcylation levels of FOXK1 are similar regardless of the presence of HCF-1 and OGT in the BAP1 complex (figure 17B). Altogether, these data strongly suggest that FOXK1 O-GlcNAcylation is independent of BAP1.

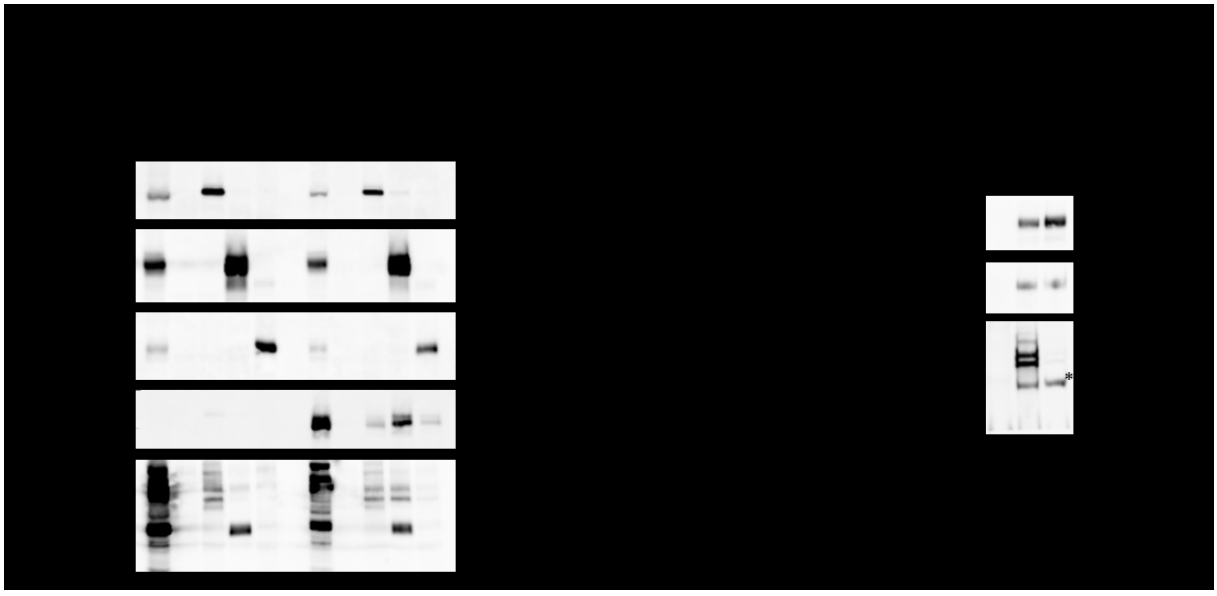

Figure 17. FOXK1 O-GlcNAcylation by OGT is BAP1-independent. (**A**) H226 cells or H226 stably expressing FLAG-HA-BAP1 were harvested for native immunoprecipitation of endogenouos OGT, FOXK1 and FOXK2. Protein levels and O-GlcNAcylation were analyzed by western blotting with indicated antibodies. (**B**) (Left) Schematic of the different steps performed to immunoprecipitate FOXK1 out of the BAP1 complexes purified in Figure 1G. (Right) O-GlcNAcylation level of FOXK1 in either BAP1 or BAP1 ΔHBM complex following denaturing immunoprecipitation of FOXK1 as indicated on the left. Immunodetection was conducted with the indicated antibodies.Asterisk indicates FOXK1 corresponding band. IP; Immunoprecipitation. Experiment A was performed two times, experiment B was performed once.

2.5.4 FOXK1 O-GlcNAcylation is modulated during cell cycle entry and in response to starvation.

We next explored if this O-GlcNAc modification of FOXK1 may be modulated during a specific cellular event. It is known that cells go through a restriction point before the decision to enter into the cell cycle is made [244, 245]. Indeed, the availability of nutrients, physical space, cell-cell communications and extracellular signaling are critical inputs to this decision. As for the availability of sufficient nutrients, OGT has been previously described as a sensor for the metabolic state of the cell [58, 126, 223]. Thus, we determined whether the O-GlcNAcylation of FOXK1 may be modulated during the entry into cell cycle. We therefore, grew U2OS osteosarcoma cells to confluence and starved them of serum for 24h in order to arrest them in G_0. We then released these cells by feeding them with 20% serum in order to provoke a flux of cells to enter into the cell cycle. As shown in figure 18A, protein levels of FOXK1 and BAP1 remain relatively stable over the course of the 12h of release. As expected, a slight

increase in CDC6 levels correlates with an entry of cells into G_1/S, as seen in the corresponding FACS analysis for the point of 12h release (Figure 18A, right panel). Interestingly, over the full course of the cell cycle entry, FOXK1 O-GlcNAcylation levels increase steadily and reach a maximum at 6h prior to the restriction point where cells begin moving towards the G_1/S boundary (Figure 18A, left panel). Then, the levels decrease slightly once cells have begun cycling. Furthermore, the interaction between BAP1 and FOXK1 increases as cells begin to cycle (Figure 18A, left panel). These data strongly suggest that FOXK1 O-GlcNAcylation is modulated during the entry of the cell cycle and that FOXK1 and BAP1 interaction may be important for the proliferative state of cells. However, it cannot be excluded that this observation may be caused by a cancer-derived process. To eliminate this possibility, the same experiment was redone using primary human fibroblasts. After maintaining cells at confluence for two days in order to trigger cell-cell contact inhibition, we further serum starved them for 24h to completely arrest cell growth. The cells were then fed 20% serum media. As expected, primary cells were able to more robustly respond to contact inhibition compared to the U2OS cancer cell line. The spike in CDC6 levels was also much more prominent. As expected, FOXK1 and BAP1 levels remain stable and the spike in CDC6 level corresponding to the entry of cells into G_1/S, albeit later than in U2OS, was observed. Again, as previously described, O-GlcNAcylation of FOXK1 is most evident at the onset of the cell cycle entry and decreases as cells are actively cycling. However, it would have been interesting to perform densitometer quantifications in order to determine if these fluctuations are statistically significant. Nevertheless, these results clearly demonstrate that FOXK1 O-GlcNAcylation is modulated during the decision to enter cell cycle.

Previous studies have demonstrated that FOXK1 phosphorylation and cellular localization are modulated in response to fluctuations in cellular metabolism through mTOR signaling [206]. Moreover, mTOR was shown to regulate OGT stability [39, 246]. Since it was reported that OGT levels decrease during starvation, we sought to determine whether FOXK1 O-GlcNAcylation is also modulated during this process. Hence, we deprived LL human fibroblasts of all nutrients and examined the differential O-GlcNAcylation of endogenous FOXK1 following denaturing immunoprecipitation. As shown in figure 18C, at the onset of

cellular starvation, the reported mobility shift of FOXK1 can be observed concording with its reported phosphorylation [206]. Also as expected, the O-GlcNAcylation levels of FOXK1 steadily decrease over the course of the starvation kinetic and this signal restabilizes itself once cells are fed complete media (Figure 18C). Since both the O-GlcNacylation of FOXK1 and its binding to BAP1 increase during the entry into cell cycle (Figure 18A and 18B) and that the O-GlcNAcylation of FOXK1 decreases during starvation (Figure 18C), we determined whether the BAP1 complex may be subjected to changes during starvation. We therefore, starved cells and co-immunoprecipitated the BAP1 complex via ASXL2 as we had K562-FLAG ASXL2 stable cell lines in culture at the time of our investigation. As shown in figure 18D, total levels of the core components of the BAP1 complex, namely, ASXL2, BAP1 and OGT decrease overtime. However the levels of both FOXKs seem unaffected. Notably however, FOXK1 and to a lesser extent FOXK2 become excluded from the BAP1 complex as cells undergo starvation, returning to the complex once cells are re-fed complete media. These data are consistent with previous studies showing that both FOXK1 and FOXK2 are shuttled out of the nucleus in response to starvation, however since FOXK1 becomes excluded much more rapidly, it is possible that the tie between FOXK1 and cellular metabolism, strictly speaking its O-GlcNAcylation may confer a sensitivity to this process.

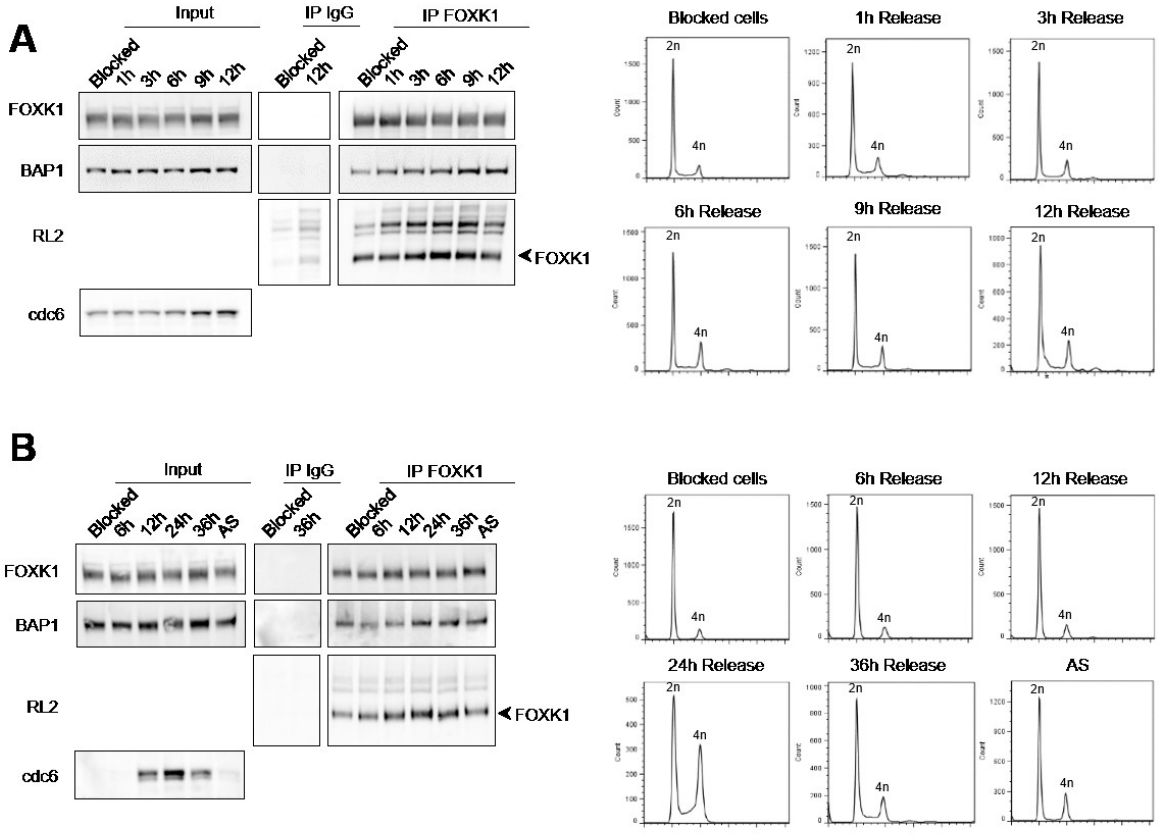
A
Input
IP IgG
IP FOXK1
Blocked
1h
3h
6h
9h
12h
FOXK1
BAP1
RL2
cdc6
FOXK1
Blocked cells
1h Release
3h Release
6h Release
9h Release
12h Release
2n
4n
B
Input
IP IgG
IP FOXK1
Blocked
6h
12h
24h
36h
AS
FOXK1
BAP1
RL2
cdc6
FOXK1
Blocked cells
6h Release
12h Release
24h Release
36h Release
AS
2n
4n
C
Input
IP FOXK1
Starvation (hrs)
0 4 8 10 R
IgG
FOXK1
RL2
β-Tubulin
D
Input
IP FLAG
Starvation (hrs)
0 6 0 2 4 6 R
0 6 0 2 4 6 R
FLAG
OGT
BAP1
FOXK1
FOXK2
β-Tubulin
K562
K562-FLAG-HA-ASXL2
K562
K562-FLAG-HA-ASXL2

Figure 18. FOXK1 O-GlcNAcylation is modulated during cell cycle entry and in response to starvation. (**A**) (Left) U2OS cells were grown to confluence and then cells were serum starved for 24h. The next day, blocked cells were harvested and remaining cells were fed with media containing 20% serum. At the indicated time points, cells were harvested for both FACS analysis and immunoprecipitation. IgG control or anti-FOXK1 native immunoprecipitation was performed overnight and western blotting was performed with indicated antibodies. (Right) FACS analysis showing very slight entry into G1/S between 9h and 12h. (**B**) (Left) Primary LL human fibroblasts were grown to confluence and left at confluence for 48h. Then, cells were serum starved for an additional 24h, replated in 20% serum containing media and finally harvested at indicated time-points for FACS analysis and immunoprecipitation as indicated in (A). (Right) FACS analysis of each time-point showing that cells began to enter the cell cycle between 12 and 24h. IP; Immunoprecipitation, AS; Asynchronous population, hrs; hours. **(C)** LL human primary fibroblasts were starved according to Bowman et al. (206) with (HBSS) supplemented with 10 mM HEPES pH 7.5 and 1% Penicillin-Streptomycin for the indicated time. When indicated, cells were replenished for 2h by feeding back the cells with growing medium. Cells were then harvested for subsequent denaturing immunoprecipitation. IgG immunoprecipitations was done as a negative control and proteins were revealed using indicated antibodies. **(D)** K562 cells stably expressing a FLAG-HA-ASXL2 construct were starved in the same manner as **(C)** and harvested at indicated time points for native FLAG immunoprecipitations. Control K562 cells were used as negative controls for the FLAG immunoprecipitations and proteins were revealed using indicated antibodies. Experiments A, B and C were performed twice. Experiment D was performed once.

2.5.5 Foxk1, but not Foxk2, is required for adipogenesis

Since our results have shown that not only FOXK1 O-GlcNAcylation but also its presence in the BAP1 complex are modulated in response to cellular starvation, we reasoned that FOXK1 itself may play a role in cellular metabolism. Furthermore, previous studies have shown that FOXK1 is a critical regulator of the differentiation of the highly metabolic C2C12 myogenic progenitor cells whereby its loss impairs muscle regeneration in KO mice.[180, 181] Therefore, we sought to determine if in fact FOXK1 regulation of differentiation could be a consequence of its regulation of metabolism rather than being specific for myogenic differentiation. 3T3L1 adipogenesis is also a highly metabolic-dependent process, thus, we investigated if FOXK1 regulation of differentiation could be extended to adipogenic tissues. Using standard 3T3L1 differentiation procedures (see material and methods) in parallel with double siRNA treatments of Foxk1, we knocked-down Foxk1 levels to study its effect on adipogenic differentiation. As shown in the upper blot of figure 19A, knockdown of Foxk1 with several different individual siRNA as well as the mix reduced Foxk1 levels by roughly 50%. Interestingly, siRNAs 2 and 4 and to a lesser extent siRNAs 1 and 3 caused a media color change (become purple) compared to the scrambled siRNA (siNT) indicative of media alkalinity (Figure 19A, lower panel). As the differentiation of 3T3L1 triggers cell cycle arrest and a flux in triglycerides and free fatty acids synthesis, normal differentiation of these cells tends to acidify

the media. Further Oil Red O staining analysis of neutral triglyceride and lipid accumulation revealed that knockdown of FOXK1 also impairs adipogenesis although to varying degrees (Figure 19B). Furthermore, the siRNA treatments that blocked differentiation the most correspond to stronger alkalinity of the media. As we identified FOXK1 as a major regulator of adipogenesis we next determine if it was also the case for FOXK2. Surprisingly, siFOXK2 showed no significant effect on differentiation compared to control siRNA albeit causing a slightly more acidic media (Figure 19C). In order to explore the molecular bases of this differentiation block and to validate that the observable effect of siFOXK1 is not an off-target effect, we differentiated 3T3L1 cells under the treatment of an additional set of FOXK1 siRNA and verified commonly used adipogenesis markers. As shown in figure 19D all siRNA treatments, except for 1 and 3, almost completely blocked differentiation as shown by Fabp4 and Perilipin levels. These results strongly suggest that Foxk1 but not Foxk2 is critical for 3T3L1 differentiation.

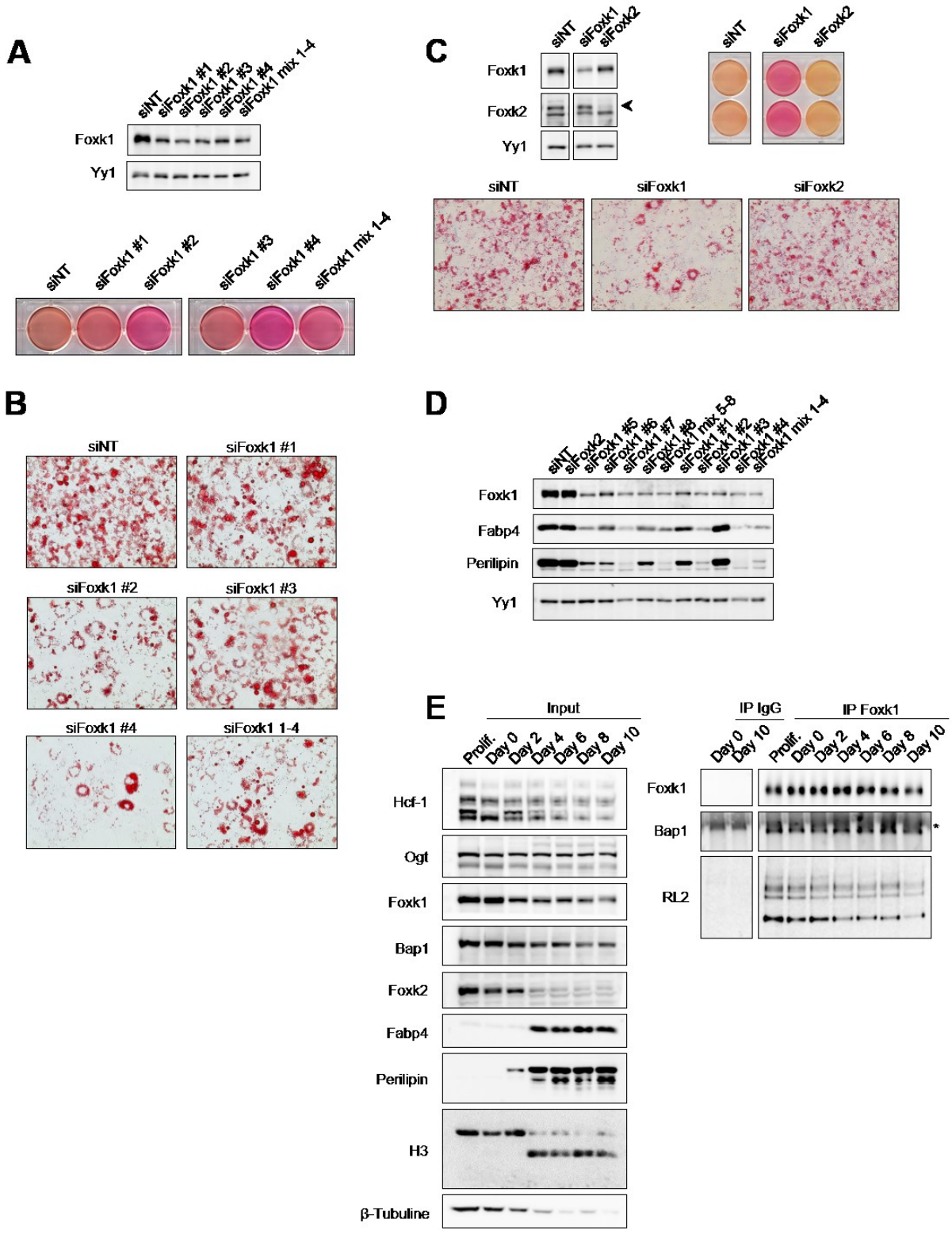
A
siNT
siFoxk1 #1
siFoxk1 #2
siFoxk1 #3
siFoxk1 #4
siFoxk1 mix 1-4
Foxk1
Yy1
B
siNT
siFoxk1 #1
siFoxk1 #2
siFoxk1 #3
siFoxk1 #4
siFoxk1 1-4
C
siNT
siFoxk1
siFoxk2
Foxk1
Foxk2
Yy1
D
siNT
siFoxk2
siFoxk1 #5
siFoxk1 #6
siFoxk1 #7
siFoxk1 #8
siFoxk1 mix 5-8
siFoxk1 #1
siFoxk1 #2
siFoxk1 #3
siFoxk1 #4
siFoxk1 mix 1-4
Foxk1
Fabp4
Perilipin
Yy1
E
Input
IP IgG
IP Foxk1
Prolif.
Day 0
Day 2
Day 4
Day 6
Day 8
Day 10
Hcf-1
Ogt
Foxk1
Bap1
Foxk2
Fabp4
Perilipin
H3
β-Tubuline
RL2

Figure 19. Foxk1 but not Foxk2 is required for adipogenesis. (**A**) (Top) 3T3L1 cells were differentiated under siRNA treatment against Foxk1 as described in material and methods. Scrambled siRNA was used as a negative control. Indicated protein levels were analyzed by western blotting. YY1 was used as a loading control. (Bottom) Differential media colour following siRNA treatments from top panel. (**B**) Oil Red O staining of differentiated 3T3L1 from (A). (**C**) (Top left) 3T3L1 cells were differentiated under siRNA treatment against Foxk1 and Foxk2 as in (A). (Top right) Differential media colour following siRNA treatments. (Bottom) Oil Red O staining corresponding to siFoxk1 and siFoxk2 treatment previously described. (**D**) 3T3L1 cells were differentiated under a more extensive panel of siRNA against Foxk1 as described in (A). Scrambled and Foxk2 siRNA were used as negative controls. Indicated protein levels were analyzed by western blotting. YY1 was used as a loading control. (**E**) 3T3L1 cells were either harvested while proliferating or differentiated according to standard procedures (see material and methods). Cells were harvested for native immunoprecipitation at indicated time-points. IgG control or anti-FOXK1 native immunoprecipitation was performed overnight and western blotting was conducted with indicated antibodies. IP; Immunoprecipitation, Prolif; Proliferating. Experiments A, B, C and D were conducted more than three times. E was performed once.

As our group already demonstrated the importance of the BAP1 complex in adipogenesis via the UBE2O-BAP1 axis, we explored its kinetics as well as the O-GlcNAcylation state of FOXK1 during this process [9]. As expected, as cells drastically modify their cytoskeleton in order to accumulate stores of lipid dropelets, tubulin expression decreases. Also, H3 clivage during differenciation has been previously described but the summation of the cleaved and full form denote equal loading between conditions [247]. Interestingly, components of the BAP1 complex change quite drastically over the course of the differentiation process (Figure 19E). Moreover, many of the protein levels of the components of the BAP1 complex differentially decrease during differentiation but most strikingly at the onset of the production of adipogenic markers at day 4, except for OGT, whose levels remain stable (Figure 19E). Finally, normalized native immunoprecipitations of Foxk1 suggest that its interaction with Bap1 does not change in a significant way over the course of the differentiation. However, FOXK1 O-GlcNAcylation is almost completely ablated near terminal differentiation, and this, despite identical levels of OGT in cells. Taken together, our results suggest that not only is FOXK1 critical for 3T3L1 differentiation, but its O-GlcNAcylation is modulated during this process.

2.6 Discussion

In this study, we show that the transcription factors FOXK1 and FOXK2 form mutually exclusive complexes with BAP1, whereby their FHA-dependant binding to BAP1 is mediated by a specific structural folding of BAP1 as well as its Thr493 residue in the NORS domain. Most

interestingly, here we show that FOXK1 is specifically O-GlcNAcylated compared to FOXK2 but also that this modification is modulated during various metabolic events such as cell cycle entry, starvation and adipogenesis. Moreover, we show that FOXK1 but not FOXK2 is critical for adipogenic differentiation.

Our study suggests that FOXK1 and FOXK2 may bind BAP1 through conformational changes that expose the residue Thr493 of BAP1, however further mutational studies are needed to pinpoint the biochemistry behind this assertion. A previous study using similar techniques, showed that deletion of either the N or C-terminal domains of BAP1 greatly hindered binding to FOXK1[207]. However, another study by Okino et al.[115] showed that deletion of the N and C-terminal of BAP1 had no effect on binding of FOXK1 in cells. Although our study does confirm that the deletion of the C-terminal domain eliminated binding between FOXK1 and BAP1, we were unable to confirm loss of binding upon the deletion of the UCH domain of BAP1.[207] Interestingly, not all of our constructs containing the reported critical Thr493 residue could bind FOXK1 in our pulldowns [207]. We have previously shown that BAP1 engages in intramolecular binding between the CC1 (amino acids 236-265) of the NORS region and the CC2 (amino acids 631-660) of the CTD [9]. Only our constructs able to perform these interactions could bind FOXK1. However, our in cell data also confirm that the Thr493 residue reported to be important for binding between the FHA domain of FOXK1 or FOXK2 and BAP1 is indeed critical for binding [115, 207]. Nonetheless, the use of recombinant proteins to perform the pulldowns indicates that phosphorylation of Thr493 might not be necessary to allow the binding although it might greatly amplify it. In fact, FHA domains are known to bind not only the phosphate group on the threonine itself but also to have stabilizing interactions with the methyl group of the threonine as well as interactions with the pT+3 residue. Furthermore non canonical phospho-independent interactions between FHA domains and substrates have been described [248, 249]. It is possible that our GST-pulldowns were successful due to these secondary interactions. Also, it is possible that the difference in protein concentration between our GST-pulldowns and our in cell immunoprecipitations could explain the difference in binding that we observe as using high concentrations of proteins can induce binding. It would be interesting to stably express the deletion constructs in cells as well

as a set of the same deletion constucts having Thr493 mutated to alanine and compare binding with FOXK proteins. It would also be interesting to purify different Thr493 phosphorylated BAP1 constructs from cells and compare binding to FOXK proteins before and after treatment with alkalin phosphatase so as to compare the importance of the phosphate group. We reason that in fact, in the context of the full length of BAP1, a concert of intramolecular binding events are necessary to properly expose BAP1 Thr493 to be bound by the FHA of FOXK proteins.

The BAP1 tumour suppressor complex contains a plethora of different transcription regulators and factors that attest to its importance in gene expression regulation.[56, 57, 61, 115] MPTs have been shown to be of great importance in the regulation of the function of several of BAP1's partners as well as BAP1 itself[9, 56, 60, 62, 68, 72, 131] Among identified MPTs, our group and others have already demonstrated the importance of OGT in regulating the function of the main partner of BAP1, namely HCF-1, as well as the Yin Yang 1 (YY1) transcription factor. This study identified the BAP1 partner FOXK1 but not FOXK2 as a novel substrate for O-GlcNAcylation. However, it would have been interesting to perform in vitro O-GlcNAcylation assays in order to determine if FOXK2 can be forcibly O-GlcNAcylated, signifying that in cells, this mechanism is repressed. If not, this would further demonstrate the difference in O-GlcNacylation potential between FOXK1 and FOXK2. Moreover, performing mass spectrometry analysis for O-GlcNAcylation of the FOXK1 and FOXK2 proteins isolated in various cellular contexts would help to determine not only the exact sites of modification but also whether FOXK2 can be O-GlcNAcylated but at a level too insignificant to be detected by western blotting but that might still have a physiological relevance. It is still unclear if FOXK1 and FOXK2 share similar or antagonist function since they were both reported to be regulated in similar context but also shown to act as a repressor and activator respectively [206, 217]. The presence of both factors in the BAP1 complex however hint at them having different functions. In fact, the identification of FOXK1 but not FOXK2 as a major substrate of OGT sheds light on the potential differential modulation of these factors through MPTs. We observed that FOXK1 interaction with the BAP1 complex is much more affected by starvation compared to FOXK2, which hints at its transcriptional function being important in the metabolic sensing

response. This could be explained by the fact that the reported mTOR-mediated phosphorylation sites of FOXK1 have been shown to be implicated in the nuclear translocation of FOXK1 whereby starvation-induced mTOR deactivation would trigger the cytoplasmic relocation of FOXK1. This relocation was also shown to be triggered by other phosphorylation sites. Further, OGT stability has been shown to be regulated by mTOR signaling. Consequently, during cellular starvation, mTOR is deactivated and the nuclear-transport phosphorylation sites of FOXK1 would remain unmodified, thus hindering its nuclear transport and retention. Moreover, destabilized OGT levels would reduce O-GlcNAcylation levels of FOXK1. As it is known that phosphorylation and O-GlcNAcylation can modify the same residues, it is possible that under normal cell growth O-GlcNAcylation might protect certain serine and threonine residues from phosphorylation but starvation induced accessibility to these sites via OGT destabilization would trigger their phosphorylation and the cytoplasmic retention, examples of which have been described [250-252]. In other words, two groups of phosphorylation sites would exist on FOXK1, a group critical for nuclear import and a second group critical for export. Under normal conditions however, the nuclear export sites would be protected from phosphorylation via OGT-mediated O-GlcNAcylation but these sites would be replaced by phosphorylation as cells undergo starvation. Therefore, crosstalk between phosphorylation and O-GlcNAcylation would allow a very fine tuning of FOXK1 function in response to starvation.

Finally, previous studies on the function of FOXK1 have revealed its critical importance in the differentiation of C2C12 myoblasts. On the other hand, our data clearly demonstrate an important role of FOXK1 in adipogenesis. As both adipogenic and myogenic tissues are derived from the mesoderm, it is possible that FOXK1 may in fact play a role in the regulation of earlier progenitor cells in these lineages. Indeed, the reported function of FOXK1 in myogenesis is in fact to impede differentiation of satellite cells by promoting sufficient clonal expansion prior to differentiation. This is accomplished through inhibition of p21 signaling whereby insufficient FOXK1 activity leads to inefficient muscle repair. Adipogenesis also triggers a clonal expansion event. In fact, a previous study showed that while this expansion was not necessary for the differentiation program to occur, its inhibition generated less Oil Red O staining

reminiscent of our siFOXK1 data [253-255]. In line with this, although significantly less cells differentiate under siFOXK1 treatments, the few that do differentiation often appear normal. It is possible that in adipogenesis, FOXK1 acts during the clonal expansion event, as it does in myogenesis, in order to increase the number of cells that will later differentiate. Importantly, as both FOXK1 and FOXK2 have been shown to mediate Wnt signaling through DVL nuclear translocation, and that Wnt signaling is known to inhibit adipogenesis, our data show that indeed FOXKs expression decreases at the onset of the differentiation program, although this observation requires further quantification in order to determine its statistical significance. Taken together, FOXK1 is O-GlcNAcylated by OGT, presumably as an output for the metabolic regulation of its function, and its activity is required for efficient differentiation of mesoderm-derived tissues, however the link between this mark and its activity remains to be elucidated.

In summary, our study provides new evidence for the regulation of adipogenesis through the transcription factor FOXK1 and demonstrates a differential regulation from its paralog FOXK2 via O-GlcNAcylation. These findings will help decipher complex post-translation modification networks in the BAP1 complex and deepen our understanding of the molecular basis of this tumour suppressor complex

2.7 Acknowledgements

We thank all the members of Dr. El Bachir Affar's laboratory for technical assistance. This work was supported by grants from the Canadian Institutes of Health Research (CIHR) (MOP-115132) and the Natural Sciences and Engineering Research Council of Canada (NSERC) (355814-2010) to E.B.A. E.B.A. is a scholar of the Fonds de la Recherche du Québec - Santé (FRQ-S) and the CIHR. J.G. has a M.Sc. scholarship from the FRQ-S. The Proteomics facility at The Institute for Research in Immunology and Cancer (IRIC) receives infrastructure support from IRICoR, the Canadian Foundation for Innovation, and the Fonds de Recherche du Québec-Santé (FRQS).

Chapitre 3

3. Discussion

3.1 Résumé des travaux de recherches

Les modifications post-traductionnelles des protéines sont critiques pour la régulation de leurs fonctions, localisation, activités et interactions avec d'autres protéines. Quant au complexe BAP1, la présence d'une multitude de protéines « modificatrices » suggère qu'il y a une importante inter-régulation de ces composantes. Lors de nos travaux sur les facteurs de transcription FOXK1 et FOXK2, nous avons pu confirmer et approfondir des données déjà publiées au sujet du domaine d'interaction entre FOXK et BAP1. Nos données révèlent plutôt que l'interaction n'est pas uniquement dépendant de la phosphorylation, mais de déterminants supplémentaires comme la structure de BAP1. Nous avons aussi démontré que FOXK1 est un nouveau substrat d'OGT et que cette O-GlcNAcylation est modulée durant plusieurs processus cellulaires, entre autre lors de la sortie du cycle cellulaire durant la différenciation adipocytaire. Enfin, nos données révèlent aussi que FOXK1, mais pas FOXK2 est critique pour l'adipogenèse.

3.2 Un concert d'interactions protéiques médient l'association entre les facteurs FOXK et BAP1.

Des études récentes ont caractérisé le domaine d'interaction de FOXK1/2 avec BAP1. En effet, le domaine FHA, capable de lier les thréonines phosphorylées est nécessaire pour l'interaction avec le résidu T493 phosphorylé de BAP1, démontrant encore l'importance des modifications post-traductionnelle dans ce complexe. Par contre, comme indiqué à la figure 12, la spécificité du domaine FHA est déterminée par des interactions protéines-protéines entre le FHA et le résidu pT ainsi que le résidu pT+3 du substrat. Suite à des essais in vitro avec des protéines recombinantes, nos travaux suggèrent que l'interaction entre FOXK1/2 et BAP1 est directe, mais que dans ces conditions, elle ne nécessite pas la phosphorylation de BAP1. Paradoxalement, nous avons effectué des essais de GST-pulldown in vitro et de co-immunoprécipitation in vivo et nous avons aussi confirmé que le résidu T493 est important pour l'interaction, mais que dans le contexte de la structure de la séquence complète de BAP1, cette région pourrait être masquée. En effet, notre groupe a précédemment déterminé que BAP1 contient deux domaines *Coiled-Coil* qui permettent un repliement intra-moléculaire permettant le rapprochement du domaine catalytique et du domaine C-terminal de BAP1

(figure 14). De plus, nos résultats suggèrent que ce repliement permet de bien exposé le T493 et/ou le résidu pT+3. Afin de confirmer ce concept, il serait intéressant d'utiliser des constructions déficientes en ce repliement intra-moléculaire et de vérifier in vivo par immunoprécipitation si l'interaction a encore lieu entre les FOXK et BAP1 mutés. Aussi, le site de T493 de BAP1 ne correspond pas au site « consensus » du domaine FHA soit pT-X-X-D/I/L , ce qui suggère que d'autres éléments de spécificités d'intéraction puissent médier l'interaction des FOXKs avec leur protéines cibles [173-175, 248, 249, 256, 257]. À cet effet, il serait intéressant de déterminer l'importance du résidu pT+3 de BAP1, soit le résidu A495, dans l'interaction avec les facteurs FOXKs. Il serait aussi interessant de purifier les différents constructions de BAP1 de la figure 15 dans des cellules et de comparer l'interaction entre BNAP1 et les protéines FOXKs avant et après un traitement de phosphatase. Il est possible que les FOXKs puissent interagir avec BAP1 sans cette phosphorylation mais à des niveaux négligeables qui sont rendus visibles dans nos expériences de GST-pulldown parce que nous utilisons des concentrations de protéines élevés. Il se peut que la phosphorylation de BAP1 augmente de façon aiguë cette interaction. Il est donc primordial de bien décortiquer cette interaction dans le contexte de la phosphorylation et du repliement de BAP1.

Par ailleurs, HCF-1 est une des protéines les plus stœchiométriques du complexe BAP1. En effet, notre groupe a déterminé que toutes les molécules de BAP1 sont associées à HCF-1. Aussi, c'est HCF-1 qui fait le pont entre OGT et BAP1, une interaction indirecte qui semble importante pour la fonction du complexe bien que sa fonction n'ait pas encore été investiguée. De plus, des études récentes ont montré que FOXK1/2 peuvent interagir avec le complexe BAP1-HCF-1, et que surtout via des expériences de *ligation par proximité* (PLA), FOXK1/2 et HCF-1 colocalisent [115, 207]. Nous avons donc vérifié si la présence de HCF-1 dans le complexe BAP1 permettait de promouvoir ou d'inhiber l'association des FOXKs au complexe. Par contre, après avoir purifié des complexes BAP1 sauvages et BAP1 sans motif HBM, aucune différence quant à l'abondance des FOXK dans les complexes BAP1 n'a été observée. De ce fait, ceci suggère que les facteurs FOXK ne sont pas affectés par la présence de HCF-1 dans le complexe et sont des *bona fide* partenaires d'interactions de BAP1. Finalement, les deux FOXKs interagissent avec le même résidu de BAP1, soit le T493, il est

donc possible ces derniers compétitionnent pour ce site. Il aurait été intéressant d'immunodépléter des extraits cellulaires de BAP1 et d'examiner la proportion des FOXKs qui s'enrichit et vice versa. De cette façon nous aurions pu avoir une idée sur i) la proportion de BAP1 qui est en complexe avec FOXK1 comparé à FOXK2 ainsi que ii) la proportion de la quantité totale de chaque FOXK qui est en complexe avec BAP1. Cependant, il est clair que BAP1 forme simultanément des complexes mutuellement exclusifs avec FOXK1 ou FOXK2, ce qui pourrait procurer au complexe des fonctions différentes (figure 20).

3.3 FOXK1 est régulé par O-GlcNAcylation.

FOXK1 et FOXK2 sont donc mutuellement exclusif au complexe BAP1. Par rapport aux autres sous-unités du complexe, nous n'avons pas détecté de différences entre FOXK1-BAP1

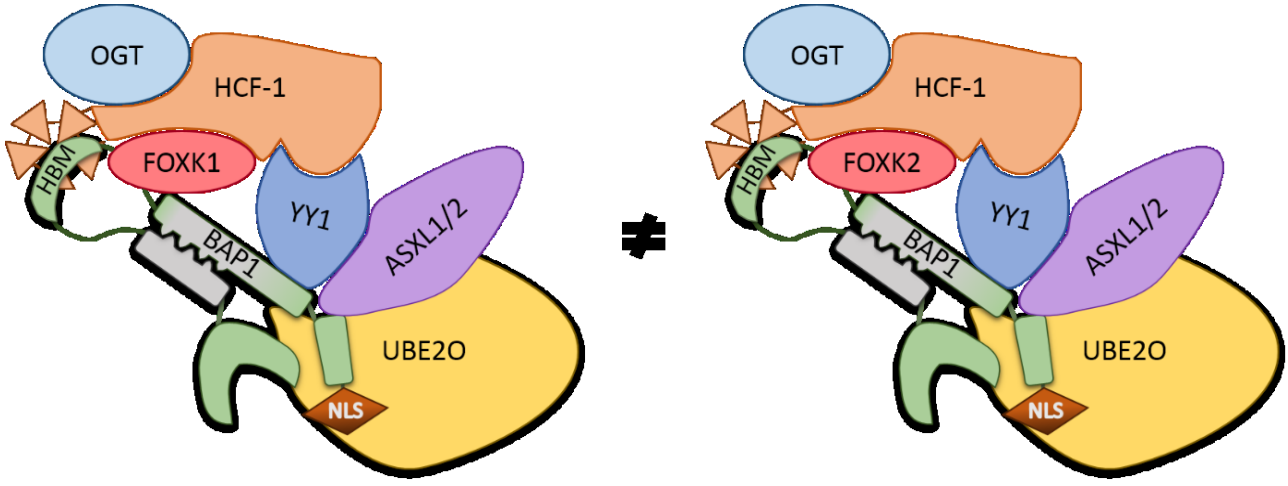

Figure 20. FOXK1 et FOXK2 forment deux complexes distincts avec BAP1 qui ont probablement des fonctions différentes. Notre caractérisation de l'interaction entre les FOXKs et BAP1 ont permis de confirmer les résultats d'autres études qui impliquent le résidu T493 de BAP1. Les deux FOXKs interagissent avec le même résidu de BAP1 et de co-immunoprécipitent pas l'un avec l'autre. De ce fait, ceci suggère qu'ils forment des complexes mutuellement exclusifs.

et FOXK2-BAP1 en ce qui concerne la présence de HCF-1/OGT. Il est probable que HCF-1 et OGT interagissent avec BAP1 en un complexe stable et que c'est un autre aspect du complexe qui est modulé en fonction de la présence d'un ou l'autre des FOXK. De plus, vu la présence importante d'OGT et la régulation des membres du complexe par O-GlcNAcylation, entre autres YY1 et HCF-1, nous avons vérifié si les FOXKs sont des substrats d'OGT [68, 69, 72, 131]. En effet, bien que les deux facteurs de transcription FOXK1 et FOXK2 se retrouvent à proximité

d'OGT dans leur complexe respectif, seul FOXK1 est modifié par O-GlcNAcylation (figure 16). Étant donné que FOXK1 joue un rôle important dans le contrôle du cycle cellulaire des myoblastes pendant la différenciation via son inhibition de p21, p27 et p57, nous avons vérifié si l'O-GlcNAcylation de FOXK1 fluctuait en fonction du cycle cellulaire [169, 179, 183, 196, 197, 240, 241]. Nous avons déterminé que cette O-GlcNAcylation augmente lors de l'entrée et diminue lors de la sortie du cycle cellulaire (figure 18-19). L'O-GlcNAcylation est une des modifications les plus répandue dans les différentes cascades de signalisation, affectant des centaines, même des milliers de différentes protéines, au même titre que la phosphorylation. C'est une modification hautement dynamique qui fluctue en fonction de l'état énergétique de la cellule et qui sert de modulateur de la fonction protéique. De ce fait, nous avons vérifié si l'O-GlcNAcylation de FOXK1 avait un rôle dans la régulation du complexe BAP1. Comme attendue, l'O-GlcNAcylation de FOXK1 diminue pendant la privation de nutriments. De manière intéressante, cette diminution corrèle fortement avec la présence de FOXK1 dans le complexe. Bien que FOXK2 soit aussi exclu du complexe, FOXK1 est davantage sensible à ce processus. Il est à noter qu'une étude récente a démontré que FOXK1, via son recrutement du complexe SIN3-HDAC répressif, inhibe l'expression des gènes de l'autophagie, et ce en fonction de sa localisation nucléaire qui est dépendante du complexe mTOR [206]. De ce fait, lorsque mTOR n'est pas fonctionnelle, comme lors d'un jeûne, FOXK1 est séquestré au cytoplasme et ne peut pas réguler le recrutement du complexe Sin3. Aussi, des travaux récents ont fait le lien entre FOXK1/2, le complexe BAP1 et la répression de la transcription [115, 207]. Il est possible que les protéines FOXK recrutent de façon redondante, soit SIN3, soit BAP1 dans le but de réprimer la transcription. Il serait très interessant de vérifier le recrutement du complexe BAP1 aux gènes d'autophagie et aussi de vérifier si ce recrutement est dépendant des FOXKs. Tout de même, la sensibilité accrue de FOXK1 à cette exclusion du noyau/complexe en condition de privation nutritionnelle démontre qu'il y a une importante différence entre les FOXKs par rapport à, soit leur activité nucléaire (interactions protéiques, inhibition transcriptionnelle, etc), soit leur recrutement à la chromatine. À ce sujet, il est possible de croire que FOXK1 régulerait le complexe BAP1 dans des voies de signalisation métabolique, alors que FOXK2 régulerait ce dernier dans des voies à caractères prolifératifs. Dans ce cas, il

serait critique de rapidement moduler le métabolisme, ce qui concorde avec l'effondrement rapide du complexe FOXK1-BAP1, tandis que la prolifération cellulaire, régulée par le complexe FOXK2-BAP1 pourrait persister un certain temps avant d'être régulée en conséquence. La corrélation entre la dissolution du complexe FOXK1-BAP1 et la perte de l'O-GlcNAcylation de FOXK1 suggère que cette modification pourrait jouer un rôle d'interrupteur dans la formation de ce complexe.

3.4 L'importance de la dynamique phosphorylation/O-GlcNAcylation de FOXK1

L'O-GlcNAcylation et la phosphorylation sont connues pour affecter les mêmes résidus. En excluant la phosphorylation des tyrosines et des résidus rares comme l'aspartate [94, 96, 99], des exemples d'O-GlcNAcylation dites « protectrices » envers des sites de phosphorylation ont été documentés [86, 122, 123, 125, 234]. D'autres travaux ont démontré que suite à l'induction de l'autophagie, FOXK1 est fortement phosphorylé afin de le séquestrer au cytoplasme (figure 21) [206]. De plus, nous avons observé que les niveaux d'O-GlcNAcylation de ce dernier sont inversément proportionnels au retard de migration détecté (figure 18C) et identifié ce groupe comme étant de la phosphorylation. Cependant, bien que nous n'ayons pas confirmé cette phosphorylation, nous croyons que différents sites d'O-GlcNAcylation permettent d'inhiber ces phosphorylations « d'exclusions » sur FOXK1. Il serait intéressant d'identifier ces sites de phosphorylations/O-GlcNAcylation par analyses de

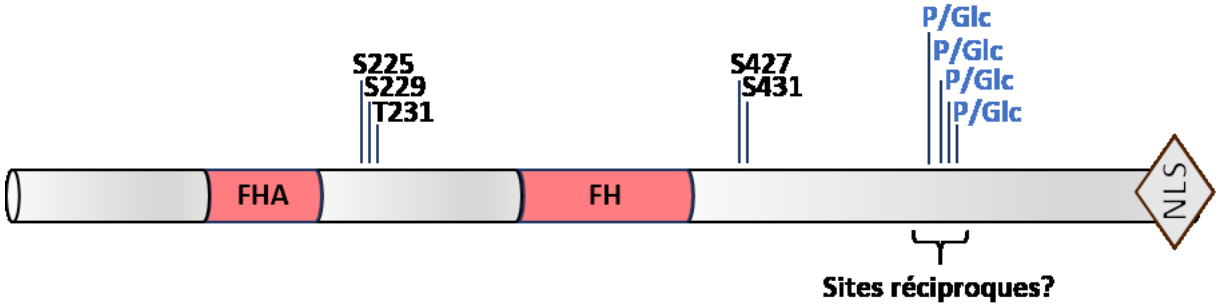

Figure 21. Modèles des différents groupes de modifications post-traductionnelles sur FOXK1 et leurs fonctions respectives. En bleu, les sites de phosphorylation déjà démontrés comme étant critiques à la localisation nucléaire de FOXK1. Ces sites sont dépendants de l'activité de mTOR et donc ils sont phosphorylés en condition de nutriments. En vert, les sites de phosphorylation qui sont spécifiques à la réponse à l'autophagie par des kinases inconnues, soit ces sites affectent l'activité du NLS en C-terminal ou induisent le changement de localisation de FOXK1 via un différent mécanisme. Ces sites, en condition favorable de croissance, serait O-GlcNAcylé par OGT afin de maintenir FOXK1 dans le noyau.

spectrométrie de masse afin de déterminer si la mutation de ces sites cause des phénotypes de gain et/ou de perte de fonction et de déterminer s'ils sont importants pour la localisation de FOXK1. Par exemple, il serait possible de muter les sites d'O-GlcNAcylation détectés, soit en alanine afin de déterminer leur importance dans la fonction de FOXK1 et sa localisation cellulaire, soit en acide aspartique afin de mimer la phosphorylation des sites d'exclusions pour déterminer si FOXK1 serait séquestré au cytoplasmique et ne pourrait pas être transloqueé au noyau malgré l'activité de mTOR.

En effet, comme schématisé à la figure 22, nos résultats nous permettent de proposer un modèle où FOXK1 nouvellement synthétisé dans le cytoplasme serait (figure 22.1) phosphorylé sur différents sites par mTOR lors de condition favorable à la prolifération cellulaire. Après translocation dans le noyau, FOXK1 serait ciblé par OGT complexé ou non à BAP1 et serait modifié par O-GlcNAcylation sur plusieurs sites (figure 17A et 21). Cette O-GlcNAcylation protègerait contre sa phosphorylation qui mènerait à son exclusion du noyau. Cependant, en condition de privation de nutriments où mTOR est désactivé (figure 22.2), FOXK1 cytoplasmique serait retenu dans le cytoplasme et étant donné qu'OGT est déstabilisé pendant ce processus, les niveaux d'O-GlcNAcylation de FOXK1 nucléaire seraient diminués, permettant sa phosphorylation subséquente et son exclusion du noyau. Il y a aussi la possibilité qu'OGA soit transloqué dans le noyau pour hydrolyser l'O-GlcNAc des substrats en fonction du manque de nutriments, mais des études d'immunofluorescence et de purification de différentes fractions cellulaires sont nécessaires afin de considérer ce mécanisme.

3.5 FOXK1 dans l'adipogenèse et la myogenèse

Bien que nous ayons démontré une dynamique d'O-GlcNAcylation et de phosphorylation de FOXK1 pendant différents processus et que FOXK1 et le complexe BAP1 était modulés en réponse au métabolisme cellulaire, nous avons voulu vérifier si FOXK1 pouvait réguler un aspect du métabolisme cellulaire. Certains tissus sont très sensibles au métabolisme, entre autres le tissu gras et le tissu musculaire. Étant donné l'implication importante de FOXK1 dans la myogenèse, il était important de déterminer si cette activité inhibitrice de la différenciation musculaire déjà observée était une conséquence de son lien

avec le métabolisme. En fait, nos donnés suggèrent fortement que FOXK1 joue un rôle dans la régulation du métabolisme puique suite à la déplétion de FOXK1 par siARN nous avons observé 1) un changement de pH du milieu de culture qui devient plus alkalin et 2) une inhibition de la différenciation adipocytaire (figure 19A, B et D). Cependant, étant donné que la différenciation adipocytaire implique une forte synthèse d'acide gras, il est donc possible que ce changement de couleur puisse être causé par le défaut de différenciation. Il est a noté que FOXK2 n'a pas cet effet, ni sur la différenciation ni sur le pH du milieu de culture (figure 19C). Par ailleurs, notre groupe a déjà démontré l'implication du complexe BAP1 dans la différenciation adipocytaire via la dynamique d'ubiquitination de BAP1 par UBE2O [9]. Il se peut que le complexe BAP1-FOXK1-OGT intègre une dynamique métabolique via l'O-GlcNAcylation dans ce même processus.

Par ailleurs, les lignées cellulaires adipocytaires et myogéniques sont dérivées du mésoderme. Il est possible que FOXK1 joue un rôle plus général aux niveaux des progéniteurs du mésoderme plutôt. Dans les myoblastes, FOXK1 inhibe principalement p21, p27 et p57 afin de promouvoir l'expansion clonale des MPC. Quant à la différenciation adipocytaire, il existe aussi un évenement d'expansion clonale avant la différenciation, mais il existe une contreverse quant à son importance pour la différenciation [253-255, 258]. D'un côté, des études démontrent une différenciation adipocytaire normal en bloquant le cycle cellulaire et de l'autre, l'inhibition de la réplication de l'ADN et du cycle cellulaire inhibe la différenciation [253, 254, 258-263]. Il est possible que les particularités et effets secondaires de chaques inhibiteurs utilisés dans ces études puissent jouer un rôle dans cette différence. Néanmoins, comme dit précédemment, FOXK1 est déjà connu pour induire l'expansion clonal dans les myoblastes. Nos résultats indiquent que le peu d'adipocytes qui se différencient semblent le faire de façon normale, car il n'y a pas de différence majeure dans la quantité de vésicules lipidiques dans les cellules (figure 19). Il est donc très possible que FOXK1 joue dans l'expansion clonale des adipocytes, ce qui expliquerait pourquoi la coloration à *l'Oil Red O* produit un plus faible signal. De plus, vu l'importance du complexe BAP1 et de FOXK1 dans ce processus, nous avons vérifié l'état du complexe pendant la différenciation adipocytaire. De manière intéressante, nous avons observé des changements important dans la composition

du complexe au fil de la différenciation. Les niveaux protéiques de FOXK1 demeurent stables pendant l'expansion clonale (jour 0 à jour 2, figure 19E) pour ensuite chuter d'environ 75%. L'expression de FOXK2 est presqu'abolit dès l'induction des marqueurs de différenciation ce qui concorde avec le fait que FOXK2 n'affecte pas la différenciation, mais qu'il est plutôt impliqué dans la replication cellulaire. Ceci concorde avec le patron d'expression de HCF-1, aussi impliquée dans la replication. Ces résultats corroborent avec des données récentes qui montrent que FOXK1 et FOXK2 sont critiques à la voie Wnt/β-caténine, une voie connue pour inhiber la différenciation terminale [210, 211, 213, 217, 264]. Aussi, il aurait été interessant de réaliser des quantifications de l'intensité de nos bandes d'immunobuvardage, afin de vérifier si les changements que nous observons sont significatifs. Nos données suggèrent que l'expression des FOXKs doit donc cesser après l'expansion clonale afin d'inhiber la voie Wnt et de permettre la différenciation.

Quant à l'O-GlcNacylation de FOXK1, elle diminue de façon significative dès l'entrée dans la phase de différenciation (figure 19E Jours 4-10) bien que les niveaux d'OGT restent stables pendant toute la cinétique. Il existe plusieurs raisons pour expliquer ce phénomène. Premièrement, suivant le modèle proposé précédemment, il est possible que les sites d'O-GlcNAcylation de FOXK1 doivent être éliminés afin de permettre leur phosphorylation et l'exclusion de FOXK1 du noyau lors de la différenciation adipocytaire (figure 20). Dans ce cas, il serait intéressant d'utiliser des mutants de ces sites d'O-GlcNAcylation pour en déterminer l'importance dans le contexte de la différenciation adipocytaire. Deuxièmement, OGT est connue pour être transloquée à la membrane cytoplasmique suite à une stimulation à l'insuline afin de réguler cette voie. Il est aussi connu qu'OGT est transloquée au cytoplasme lors de la différenciation terminale des myotubes [121-123, 126]. Le milieu de différenciation contient une concentration saturante d'insuline, il est donc possible que la diminution progressive d'O-GlcNAcylation de FOXK1 soit due à une séparation physique entre OGT et son substrat FOXK1. Dans ce cas, il serait important de vérifier la localisation des différents partenaires d'interaction de BAP1 pendant cette différenciation. Par contre, le patron plutôt stable d'O-GlcNAcylation des fragments de HCF-1 comparé à celui de FOXK1 lors de la différenciation adipocytaire (figure 20E) suggère que comme dans le cas de la privation

nutrionnelle, FOXK1 a une sensibilité accrue à ce processus. Il est alors possible de proposer que c'est plutôt, OGT et BAP1 qui changent de localisation, ce qui aurait un effet indirect sur l'O-GlcNAcylation de FOXK1. Bien que nous n'ayons pas déterminé la demi-vie de FOXK1, il se peut que les nouvelles protéines traduites ne puissent plus être maintenues dans le noyau via l'action d'OGT puisqu'elles sont séquestrés progressivement dans le cytoplasme durant la différenciation. D'ailleurs, pendant la différenciation adipocytaire, le NLS de BAP1 est ubiquitiné par UBE2O de sorte que BAP1 est séquestré dans le cytoplasme [9]. Puisque nos résultats démontrent que l'interaction entre FOXK1 et BAP1 ne change pas pendant la différenciation, il se peut donc que les nouvelles protéines de FOXK1 se trouvent séquestrées dans le cytoplasme, mais peuvent toujours interagir avec BAP1. Enfin, il est possible que tous ces processus soient liés pour former une boucle de rétroaction négative. Le traitement de l'insuline induit une forte activation de mTOR ce qui induit une forte accumulation de FOXK1 dans le noyau où il participe à l'expansion clonale. Cependant, lorsque la différenciation est enclenchée, BAP1 et OGT sont progressivement séquestrées dans le cytoplasme, ce qui élimine la protection de FOXK1 pour demeurer dans le noyau. Puisque les protéines FOXK1 nouvellement synthétisées s'accumulent dans le cytoplasme, elles ne pourraient ni activer la voie Wnt, ni inhiber l'arrêt du cycle cellulaire, ce qui résulterait en la progression de la différenciation. Il est donc primordial d'observer la localisation protéique de BAP1, OGT et de FOXK1 pendant la différenciation adipocytaire afin de déterminer la cause de ce changement d'O-GlcNAcylation et de comprendre la dynamique de cette modification post-traductionnelle.

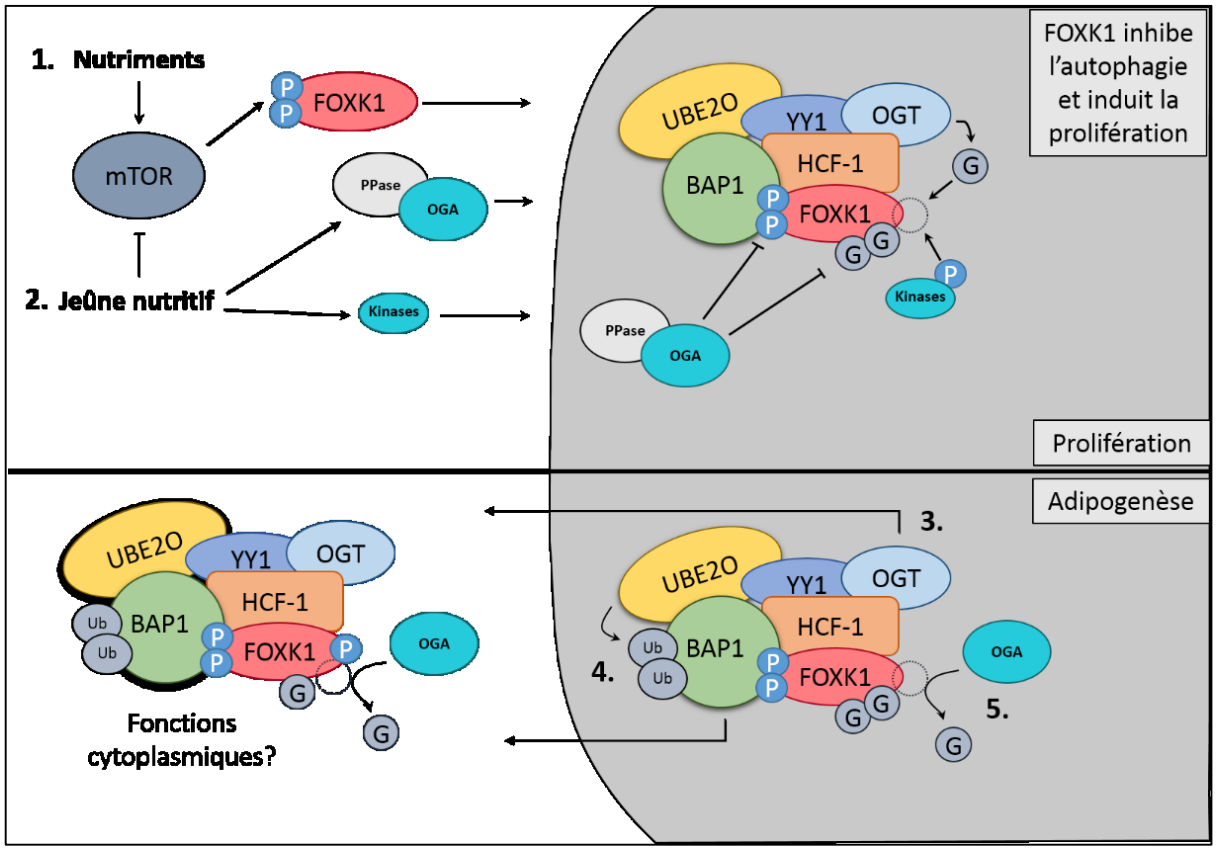

Figure 22. Modèle spéculé de la fonction de la dynamique de phosphorylation et O-GlcNAcylation de FOXK1. 1. En condition d'activation du complexe mTOR, FOXK1 est phosphorylé, peut entrer dans le noyau, interagir ou pas avec le complexe BAP1 et réguler les gènes de l'autophagie et le cycle cellulaire. Dans le noyau, OGT O-GlcNAcyle des sérines/thréonines spécifiques de FOXK1 qui les protège de la phosphorylation, une marque qui pourrait engendrer sa séquestration cytoplasmique. 2. En condition de jeûne, mTOR est non-fonctionnelle, ce qui inhibe la voie (1). OGT est donc déstabilisée résultant en une baisse des niveaux d'O-GlcNAcylation globaux. Par ailleurs, il existe peut-être des voies de signalisation qui promeuvent l'accumulation d'OGA dans le noyau et/ou activent des protéines phosphatases (PPase) pour enlever les marques d'entrée au noyau et protectrices de FOXK1 respectivement. Ensuite, des kinases encore inconnues, phosphorylent les sites de FOXK1 pour le séquestrer dans le cytoplasme. 3. Pendant la différenciation, OGT est exclue du noyau. Ceci pourrait affecter l'O-GlcNAcylation de ses substrats nucléaires comme FOXK1. Aussi, UBE2O ubiquitine BAP1 sur son NLS pour l'exclure du noyau. Il est possible que ce changement de localisation de BAP1 et d'OGT facilite l'enlèvement de l'O-GlcNAcylation de FOXK1 via OGA par un mécanisme inconnu ou que la séquestration d'OGT dans le cytoplasme provoque une accumulation de FOXK1 nouvellement synthétisé dans le cytoplasme. Le complexe FOXK1-BAP1-OGT a peut-être une fonction cytoplasmique dans les cellules post-mitotiques.

Avec tous ces résultats, dans le contexte spécifique de l'adipogenèse, il est possible de spéculer que la régulation de FOXK1 se rapproche du modèle schématisé en figure 22 : où la stimulation à l'insuline promouvoit l'accumulation de FOXK1 nucléaire mais aussi une forte translocation d'OGT (figure 22.3) à la membrane cytoplasmique. Ce manque d'OGT nucléaire pourrait affecter l'O-GlcNAcylation de FOXK1 directe- ou indirecte-ment, ainsi diminuer la protection de ses sites d'exclusion. Pendant la différenciation, l'ubiquitination du NLS de BAP1

via l'action de UBE2O permet la séquestration de BAP1 dans cytoplasme. Ensuite, après avoir participé dans l'expansion clonale, il y aurait une accumulation de FOXK1 dans le cytoplasme (via déprotection ou nouvelle synthèse piégée dans le cytoplasme) où il peut intéragir avec BAP1. Il existe peut-être aussi une voie de signalisation permettant la translocation d'OGA au noyau (figure 22.5) et ceci pourrait accélérer le processus de séquestration de FOXK1 dans le cytoplasme mais plus d'expériences seront nécessaires afin d'explorer cette hypothèse. Enfin, dans un tel modèle, il y aurait peut-être une fonction pour le complexe BAP1/FOXK1 cytoplasmique mais plus d'expériences seront nécessaires afin de le déterminer.

4. Conclusion

Ces travaux de recherches ont mis en évidence une nouvelle dynamique de modification post-traductionnelle d'un des partenaires d'interaction de BAP1, le facteur de transcription FOXK1. En effet, l'O-GlcNAcylation de FOXK1 présente un nouvel axe de régulation de l'activité suppresseur de tumeurs du complexe BAP1 en fonction du métabolisme cellulaire.

En somme, il reste encore beaucoup à apprendre sur la biochimie de la régulation des dynamiques de modifications post-traductionnelles telles que la phosphorylation, l'ubiquitination et l'O-GlcNAcylation dans ce complexe. Comment cette dynamique régule la transcription des gènes, la déubiquitination de H2AK119Ub et d'autres fonctions cellulaires restent encore un mystère. Cependant, puisque BAP1 est considérablement mutée dans le cancer, l'étude de sa régulation et des répercussions contextuelles de sa spécificité d'action pourra aider à développer de nouvelles thérapies pour traiter des cancers où aider au diagnostic et prognostic des patients qui démontrent des défauts de ce complexe suppresseur de tumeurs.

5. Listes des références

1. Brown, J.S. and S.P. Jackson, *Ubiquitylation, neddylation and the DNA damage response.* Open Biol, 2015. **5**(4).
2. Cao, R., Y.-i. Tsukada, and Y. Zhang, *Role of Bmi-1 and Ring1A in H2A Ubiquitylation and Hox Gene Silencing.* Molecular Cell, 2005. **20**(6): p. 845-854.
3. Davis, M.E. and M.U. Gack, *Ubiquitination in the antiviral immune response.* Virology, 2015. **479-480c**: p. 52-65.
4. Hoeller, D. and I. Dikic, *Review Article Targeting the ubiquitin system in cancer therapy.* Nature, 2009. **458**: p. 438-444.
5. Husnjak, K. and I. Dikic, *Ubiquitin-binding proteins: decoders of ubiquitin-mediated cellular functions.* Annu Rev Biochem, 2012. **81**: p. 291-322.
6. Kerscher, O., R. Felberbaum, and M. Hochstrasser, *Modification of Proteins by Ubiquitin and Ubiquitin-Like Proteins.* Annual Review of Cell and Developmental Biology, 2006. **22**(1): p. 159-180.
7. Komander, D. and M. Rape, *The ubiquitin code.* Annu Rev Biochem, 2012. **81**: p. 203-29.
8. David, Y., et al., *E3 ligases determine ubiquitination site and conjugate type by enforcing specificity on E2 enzymes.* J Biol Chem, 2011. **286**(51): p. 44104-15.
9. Mashtalir, N., et al., *Autodeubiquitination protects the tumor suppressor BAP1 from cytoplasmic sequestration mediated by the atypical ubiquitin ligase UBE2O.* Mol Cell, 2014. **54**(3): p. 392-406.
10. Tai, H.-C. and E.M. Schuman, *Ubiquitin, the proteasome and protein degradation in neuronal function and dysfunction.* Nat Rev Neurosci, 2008. **9**(11): p. 826-838.
11. Huang, J. and J.H. Brumell, *Bacteria-autophagy interplay: a battle for survival.* Nat Rev Microbiol, 2014. **12**(2): p. 101-14.
12. Rytkonen, A. and D.W. Holden, *Bacterial interference of ubiquitination and deubiquitination.* Cell Host Microbe, 2007. **1**(1): p. 13-22.
13. Jiang, X. and Z.J. Chen, *The role of ubiquitylation in immune defence and pathogen evasion.* Nat Rev Immunol, 2012. **12**(1): p. 35-48.
14. Fan, J.-B., et al., *Identification and characterization of a novel ISG15-ubiquitin mixed chain and its role in regulating protein homeostasis.* Sci. Rep., 2015. **5**.
15. Ohtake, F., et al., *Ubiquitin acetylation inhibits polyubiquitin chain elongation.* EMBO Rep, 2015. **16**(2): p. 192-201.
16. Wauer, T., et al., *Mechanism of phospho-ubiquitin-induced PARKIN activation.* Nature, 2015.
17. Koyano, F., et al., *Ubiquitin is phosphorylated by PINK1 to activate parkin.* Nature, 2014. **510**(7503): p. 162-6.
18. Komander, D., M.J. Clague, and S. Urbe, *Breaking the chains: structure and function of the deubiquitinases.* Nat Rev Mol Cell Biol, 2009. **10**(8): p. 550-63.
19. Wei, R., et al., *Deubiquitinases in cancer.* Oncotarget, 2015. **6**(15): p. 12872-12889.
20. Iyer, L.M., E.V. Koonin, and L. Aravind, *Novel predicted peptidases with a potential role in the ubiquitin signaling pathway.* Cell Cycle, 2004. **3**(11): p. 1440-50.
21. Kim, Y., H. Jo, and C.J. Lim, *Deubiquitinating activity of Sdu1, a putative member of the PPPDE peptidase family, in Schizosaccharomyces pombe.* Can J Microbiol, 2013. **59**(12): p. 789-96.
22. Nijman, S.M., et al., *A genomic and functional inventory of deubiquitinating enzymes.* Cell, 2005. **123**(5): p. 773-86.
23. Li, M., et al., *Deubiquitination of p53 by HAUSP is an important pathway for p53 stabilization.* Nature, 2002. **416**(6881): p. 648-53.

24. Butler, L.R., et al., *The proteasomal de-ubiquitinating enzyme POH1 promotes the double-strand DNA break response.* Embo j, 2012. **31**(19): p. 3918-34.
25. Cooper, E.M., et al., *K63-specific deubiquitination by two JAMM/MPN+ complexes: BRISC-associated Brcc36 and proteasomal Poh1.* Embo j, 2009. **28**(6): p. 621-31.
26. Matyskiela, M.E., G.C. Lander, and A. Martin, *Conformational switching of the 26S proteasome enables substrate degradation.* Nat Struct Mol Biol, 2013. **20**(7): p. 781-788.
27. Biggs, P.J., et al., *The cylindromatosis gene (cyld1) on chromosome 16q may be the only tumour suppressor gene involved in the development of cylindromas.* Oncogene, 1996. **12**(6): p. 1375-7.
28. Biggs, P.J., et al., *Familial cylindromatosis (turban tumour syndrome) gene localised to chromosome 16q12-q13: evidence for its role as a tumour suppressor gene.* Nat Genet, 1995. **11**(4): p. 441-3.
29. Brummelkamp, T.R., et al., *Loss of the cylindromatosis tumour suppressor inhibits apoptosis by activating NF-kappaB.* Nature, 2003. **424**(6950): p. 797-801.
30. Hu, G., et al., *A novel missense mutation in CYLD in a family with Brooke-Spiegler syndrome.* J Invest Dermatol, 2003. **121**(4): p. 732-4.
31. Lian, F. and C.J. Cockerell, *Cutaneous appendage tumors: familial cylindromatosis and associated tumors update.* Adv Dermatol, 2005. **21**: p. 217-34.
32. Trompouki, E., et al., *CYLD is a deubiquitinating enzyme that negatively regulates NF-kappaB activation by TNFR family members.* Nature, 2003. **424**(6950): p. 793-6.
33. Eletr, Z.M. and K.D. Wilkinson, *Regulation of proteolysis by human deubiquitinating enzymes.* Biochim Biophys Acta, 2014. **1843**(1): p. 114-28.
34. Hamazaki, J., et al., *A novel proteasome interacting protein recruits the deubiquitinating enzyme UCH37 to 26S proteasomes.* EMBO J, 2006. **25**(19): p. 4524-36.
35. Hammond-Martel, I., H. Yu, and B. Affar el, *Roles of ubiquitin signaling in transcription regulation.* Cell Signal, 2012. **24**(2): p. 410-21.
36. MacGurn, J.A., P.C. Hsu, and S.D. Emr, *Ubiquitin and membrane protein turnover: from cradle to grave.* Annu Rev Biochem, 2012. **81**: p. 231-59.
37. Nakada, S., et al., *Non-canonical inhibition of DNA damage-dependent ubiquitination by OTUB1.* Nature, 2010. **466**(7309): p. 941-6.
38. Nakayama, K.I. and K. Nakayama, *Ubiquitin ligases: cell-cycle control and cancer.* Nat Rev Cancer, 2006. **6**(5): p. 369-81.
39. Park, S., et al., *Inhibition of mTOR affects protein stability of OGT.* Biochem Biophys Res Commun, 2014. **453**(2): p. 208-12.
40. Sahtoe, D.D., et al., *Mechanism of UCH-L5 activation and inhibition by DEUBAD domains in RPN13 and INO80G.* Mol Cell, 2015. **57**(5): p. 887-900.
41. Zhimin, L. and H. Tony, *Degradation of Activated Protein Kinases by Ubiquitination.* Annual Review of Biochemistry, 2009. **78**(1): p. 435-475.
42. Abdel-Wahab, O. and A. Dey, *The ASXL-BAP1 axis: new factors in myelopoiesis, cancer and epigenetics.* Leukemia, 2013. **27**(1): p. 10-15.
43. Jensen, D.E., et al., *BAP1: a novel ubiquitin hydrolase which binds to the BRCA1 RING finger and enhances BRCA1-mediated cell growth suppression.* Oncogene, 1998. **16**(9): p. 1097-112.
44. Abdel-Rahman, M.H., et al., *Germline BAP1 mutation predisposes to uveal melanoma, lung adenocarcinoma, meningioma, and other cancers.* J Med Genet, 2011.
45. Abdel-Wahab, O., et al., *ASXL1 mutations promote myeloid transformation through loss of PRC2-mediated gene repression.* Cancer Cell, 2012. **22**(2): p. 180-93.

46. Dey, A., et al., *Loss of the tumor suppressor BAP1 causes myeloid transformation.* Science, 2012. **337**(6101): p. 1541-6.
47. Carbone, M., et al., *BAP1 and cancer.* Nat Rev Cancer, 2013. **13**(3): p. 153-9.
48. Murali, R., T. Wiesner, and R.A. Scolyer, *Tumours associated with BAP1 mutations.* Pathology, 2013. **45**(2): p. 116-26.
49. Bott, M., et al., *The nuclear deubiquitinase BAP1 is commonly inactivated by somatic mutations and 3p21.1 losses in malignant pleural mesothelioma.* Nat Genet, 2011. **43**(7): p. 668-72.
50. Testa, J.R., et al., *Germline BAP1 mutations predispose to malignant mesothelioma.* Nat Genet, 2011. **43**(10): p. 1022-5.
51. Yu, H., et al., *The ubiquitin carboxyl hydrolase BAP1 forms a ternary complex with YY1 and HCF-1 and is a critical regulator of gene expression.* Mol Cell Biol, 2010. **30**(21): p. 5071-85.
52. Scheuermann, J.C., et al., *Histone H2A deubiquitinase activity of the Polycomb repressive complex PR-DUB.* Nature, 2010. **465**(7295): p. 243-7.
53. Eletr, Z.M. and K.D. Wilkinson, *An emerging model for BAP1's role in regulating cell cycle progression.* Cell Biochem Biophys, 2011. **60**(1-2): p. 3-11.
54. Ismail, I.H., et al., *Germ-line Mutations in BAP1 Impair its Function in DNA Double-Strand break Repair.* Cancer Res, 2014.
55. Lee, H.S., et al., *Stabilization and targeting of INO80 to replication forks by BAP1 during normal DNA synthesis.* Nat Commun, 2014. **5**: p. 5128.
56. Machida, Y.J., et al., *The deubiquitinating enzyme BAP1 regulates cell growth via interaction with HCF-1.* J Biol Chem, 2009. **284**(49): p. 34179-88.
57. Misaghi, S., et al., *Association of C-terminal ubiquitin hydrolase BRCA1-associated protein 1 with cell cycle regulator host cell factor 1.* Mol Cell Biol, 2009. **29**(8): p. 2181-92.
58. Ruan, H.B., et al., *O-GlcNAc transferase/host cell factor C1 complex regulates gluconeogenesis by modulating PGC-1alpha stability.* Cell Metab, 2012. **16**(2): p. 226-37.
59. Yu, H., et al., *BAP1 Promotes Homologous Recombination Repair.* PNAS, 2013. **In Press**.
60. Yu, H., et al., *Tumor suppressor and deubiquitinase BAP1 promotes DNA double-strand break repair.* Proc Natl Acad Sci U S A, 2014. **111**(1): p. 285-90.
61. Yu, H., et al., *The Ubiquitin carboxyl hydrolase BAP1 forms a ternary complex with YY1 and HCF-1 and is a critical regulator of gene expression.* Mol Cell Biol, 2010. **30**(21): p. 5071-5085.
62. Eletr, Z.M., L. Yin, and K.D. Wilkinson, *BAP1 is phosphorylated at serine 592 in S-phase following DNA damage.* FEBS Lett, 2013. **587**(24): p. 3906-11.
63. Sirbu, B.M., et al., *Identification of proteins at active, stalled, and collapsed replication forks using isolation of proteins on nascent DNA (iPOND) coupled with mass spectrometry.* J Biol Chem, 2013. **288**(44): p. 31458-67.
64. Chambers, A.L. and J.A. Downs, *The RSC and INO80 chromatin-remodeling complexes in DNA double-strand break repair.* Prog Mol Biol Transl Sci, 2012. **110**: p. 229-61.
65. Falbo, K.B. and X. Shen, *Function of the INO80 chromatin remodeling complex in DNA replication.* Front Biosci (Landmark Ed), 2012. **17**: p. 970-5.
66. Gerhold, C.B. and S.M. Gasser, *INO80 and SWR complexes: relating structure to function in chromatin remodeling.* Trends Cell Biol, 2014.
67. Bargaje, R., et al., *Proximity of H2A.Z containing nucleosome to the transcription start site influences gene expression levels in the mammalian liver and brain.* Nucleic Acids Res, 2012. **40**(18): p. 8965-78.
68. Daou, S., et al., *Crosstalk between O-GlcNAcylation and proteolytic cleavage regulates the host cell factor-1 maturation pathway.* Proc Natl Acad Sci U S A, 2011. **108**(7): p. 2747-52.

69. Capotosti, F., et al., *O-GlcNAc transferase catalyzes site-specific proteolysis of HCF-1.* Cell, 2011. **144**(3): p. 376-88.
70. Daou, S., et al., *Crosstalk between O-GlcNAcylation and proteolytic cleavage regulates the host cell factor-1 maturation pathway.* Proc Natl Acad Sci U S A, 2011.
71. Goto, H., et al., *A single-point mutation in HCF causes temperature-sensitive cell-cycle arrest and disrupts VP16 function.* Genes Dev, 1997. **11**(6): p. 726-37.
72. Lazarus, M.B., et al., *HCF-1 is cleaved in the active site of O-GlcNAc transferase.* Science, 2013. **342**(6163): p. 1235-9.
73. Zargar, Z. and S. Tyagi, *Role of host cell factor-1 in cell cycle regulation.* Transcription, 2012. **3**(4): p. 187-92.
74. Julien, E. and W. Herr, *A switch in mitotic histone H4 lysine 20 methylation status is linked to M phase defects upon loss of HCF-1.* Mol Cell, 2004. **14**(6): p. 713-25.
75. Tyagi, S., et al., *E2F activation of S phase promoters via association with HCF-1 and the MLL family of histone H3K4 methyltransferases.* Mol Cell, 2007. **27**(1): p. 107-19.
76. Tyagi, S. and W. Herr, *E2F1 mediates DNA damage and apoptosis through HCF-1 and the MLL family of histone methyltransferases.* EMBO J, 2009. **28**(20): p. 3185-95.
77. Pena-Llopis, S., et al., *BAP1 loss defines a new class of renal cell carcinoma.* Nat Genet, 2012. **44**(7): p. 751-9.
78. Wiesner, T., et al., *Germline mutations in BAP1 predispose to melanocytic tumors.* Nat Genet, 2011. **43**(10): p. 1018-21.
79. Xu, J., et al., *Germline mutation of Bap1 accelerates development of asbestos-induced malignant mesothelioma.* Cancer Res, 2014. **74**(16): p. 4388-97.
80. Lubas, W.A. and J.A. Hanover, *Functional expression of O-linked GlcNAc transferase. Domain structure and substrate specificity.* J Biol Chem, 2000. **275**(15): p. 10983-8.
81. O'Donnell, N., et al., *Ogt-dependent X-chromosome-linked protein glycosylation is a requisite modification in somatic cell function and embryo viability.* Mol Cell Biol, 2004. **24**(4): p. 1680-90.
82. Shafi, R., et al., *The O-GlcNAc transferase gene resides on the X chromosome and is essential for embryonic stem cell viability and mouse ontogeny.* Proc Natl Acad Sci U S A, 2000. **97**(11): p. 5735-9.
83. Chu, C.S., et al., *O-GlcNAcylation regulates EZH2 protein stability and function.* Proc Natl Acad Sci U S A, 2014. **111**(4): p. 1355-60.
84. Gambetta, M.C. and J. Muller, *O-GlcNAcylation prevents aggregation of the Polycomb group repressor polyhomeotic.* Dev Cell, 2014. **31**(5): p. 629-39.
85. Diernfellner, A.C. and M. Brunner, *O-GlcNAcylation of a circadian clock protein: dPER taking its sweet time.* Genes Dev, 2012. **26**(5): p. 415-6.
86. Kaasik, K., et al., *Glucose sensor O-GlcNAcylation coordinates with phosphorylation to regulate circadian clock.* Cell Metab, 2013. **17**(2): p. 291-302.
87. Kim, E.Y., et al., *A role for O-GlcNAcylation in setting circadian clock speed.* Genes Dev, 2012. **26**(5): p. 490-502.
88. Li, M.D., et al., *O-GlcNAc signaling entrains the circadian clock by inhibiting BMAL1/CLOCK ubiquitination.* Cell Metab, 2013. **17**(2): p. 303-10.
89. Hanover, J.A., M.W. Krause, and D.C. Love, *Bittersweet memories: linking metabolism to epigenetics through O-GlcNAcylation.* Nat Rev Mol Cell Biol, 2012. **13**(5): p. 312-321.
90. Bond, M.R. and J.A. Hanover, *A little sugar goes a long way: the cell biology of O-GlcNAc.* J Cell Biol, 2015. **208**(7): p. 869-80.

91. Weigel, P.H., et al., *Hyaluronan synthase assembles chitin oligomers with -GlcNAc(alpha1-->)UDP at the reducing end.* Glycobiology, 2015. **25**(6): p. 632-43.
92. Yang, Y., et al., *Histone Demethylase LSD2 Acts as an E3 Ubiquitin Ligase and Inhibits Cancer Cell Growth through Promoting Proteasomal Degradation of OGT.* Mol Cell, 2015. **58**(1): p. 47-59.
93. Tarrant, M.K. and P.A. Cole, *The Chemical Biology of Protein Phosphorylation.* Annual Review of Biochemistry, 2009. **78**(1): p. 797-825.
94. Feng, J., et al., *Phosphoproteome analysis of isoflurane-protected heart mitochondria: phosphorylation of adenine nucleotide translocator-1 on Tyr194 regulates mitochondrial function.* Cardiovasc Res, 2008. **80**(1): p. 20-9.
95. Seyda, A. and B.H. Robinson, *Functional expression of four PDH-E(1)alpha recombinant histidine mutants in a human fibroblast cell line with zero endogenous PDH complex activity.* Biochem Biophys Res Commun, 2000. **270**(3): p. 1068-73.
96. Wagner, P.D. and N.D. Vu, *Histidine to aspartate phosphotransferase activity of nm23 proteins: phosphorylation of aldolase C on Asp-319.* Biochem J, 2000. **346 Pt 3**: p. 623-30.
97. Guan, K.L. and J.E. Dixon, *Evidence for protein-tyrosine-phosphatase catalysis proceeding via a cysteine-phosphate intermediate.* J Biol Chem, 1991. **266**(26): p. 17026-30.
98. Pannifer, A.D., et al., *Visualization of the cysteinyl-phosphate intermediate of a protein-tyrosine phosphatase by x-ray crystallography.* J Biol Chem, 1998. **273**(17): p. 10454-62.
99. Matthews, H.R., *Protein kinases and phosphatases that act on histidine, lysine, or arginine residues in eukaryotic proteins: a possible regulator of the mitogen-activated protein kinase cascade.* Pharmacol Ther, 1995. **67**(3): p. 323-50.
100. Heidenreich, O., et al., *MAPKAP kinase 2 phosphorylates serum response factor in vitro and in vivo.* J Biol Chem, 1999. **274**(20): p. 14434-43.
101. Mor, A. and M.R. Philips, *COMPARTMENTALIZED RAS/MAPK SIGNALING.* Annual Review of Immunology, 2006. **24**(1): p. 771-800.
102. Vanhaesebroeck, B., et al., *SYNTHESIS AND FUNCTION OF 3-PHOSPHORYLATED INOSITOL LIPIDS.* Annual Review of Biochemistry, 2001. **70**(1): p. 535-602.
103. Greenblatt, M.B., J.-H. Shim, and L.H. Glimcher, *Mitogen-Activated Protein Kinase Pathways in Osteoblasts.* Annual Review of Cell and Developmental Biology, 2013. **29**(1): p. 63-79.
104. Matsuoka, S., et al., *ATM and ATR substrate analysis reveals extensive protein networks responsive to DNA damage.* Science, 2007. **316**(5828): p. 1160-1166.
105. Shanbhag, N.M., et al., *ATM-dependent chromatin changes silence transcription in cis to DNA double-strand breaks.* Cell, 2010. **141**(6): p. 970-81.
106. Nicassio, F., et al., *Human USP3 is a chromatin modifier required for S phase progression and genome stability.* Curr Biol, 2007. **17**(22): p. 1972-7.
107. Shao, G., et al., *The Rap80-BRCC36 de-ubiquitinating enzyme complex antagonizes RNF8-Ubc13-dependent ubiquitination events at DNA double strand breaks.* Proc Natl Acad Sci U S A, 2009. **106**(9): p. 3166-71.
108. Chagraoui, J., et al., *An anticlastogenic function for the Polycomb Group gene Bmi1.* Proc Natl Acad Sci U S A, 2011. **108**(13): p. 5284-9.
109. Zhou, W., X. Wang, and M.G. Rosenfeld, *Histone H2A ubiquitination in transcriptional regulation and DNA damage repair.* Int J Biochem Cell Biol, 2009. **41**(1): p. 12-5.
110. Zhu, B., et al., *K63-linked ubiquitination of FANCG is required for its association with the Rap80-BRCA1 complex to modulate homologous recombination repair of DNA interstand crosslinks.* Oncogene, 2014.

111. Pena-Llopis, S., et al., *BAP1 loss defines a new class of renal cell carcinoma.* Nat Genet, 2012. **44**(7): p. 751-759.
112. Nishikawa, H., et al., *BRCA1-associated protein 1 interferes with BRCA1/BARD1 RING heterodimer activity.* Cancer Res, 2009. **69**(1): p. 111-9.
113. Hornbeck, P.V., et al., *PhosphoSitePlus: a comprehensive resource for investigating the structure and function of experimentally determined post-translational modifications in man and mouse.* Nucleic acids research, 2011: p. gkr1122.
114. Stokes, M.P., et al., *Profiling of UV-induced ATM/ATR signaling pathways.* Proceedings of the National Academy of Sciences, 2007. **104**(50): p. 19855-19860.
115. Okino, Y., et al., *BRCA1-associated protein 1 (BAP1) deubiquitinase antagonizes the ubiquitin-mediated activation of FoxK2 target genes.* J Biol Chem, 2015. **290**(3): p. 1580-91.
116. Kreppel, L.K., M.A. Blomberg, and G.W. Hart, *Dynamic glycosylation of nuclear and cytosolic proteins. Cloning and characterization of a unique O-GlcNAc transferase with multiple tetratricopeptide repeats.* J Biol Chem, 1997. **272**(14): p. 9308-15.
117. Kreppel, L.K. and G.W. Hart, *Regulation of a cytosolic and nuclear O-GlcNAc transferase. Role of the tetratricopeptide repeats.* J Biol Chem, 1999. **274**(45): p. 32015-22.
118. Hanover, J.A., M.W. Krause, and D.C. Love, *The hexosamine signaling pathway: O-GlcNAc cycling in feast or famine.* Biochim Biophys Acta, 2010. **1800**(2): p. 80-95.
119. Perez-Cervera, Y., et al., *Insulin signaling controls the expression of O-GlcNAc transferase and its interaction with lipid microdomains.* Faseb j, 2013. **27**(9): p. 3478-86.
120. Schleicher, E.D. and C. Weigert, *Role of the hexosamine biosynthetic pathway in diabetic nephropathy.* Kidney Int Suppl, 2000. **77**: p. S13-8.
121. Wells, L., K. Vosseller, and G.W. Hart, *A role for N-acetylglucosamine as a nutrient sensor and mediator of insulin resistance.* Cell Mol Life Sci, 2003. **60**(2): p. 222-8.
122. Whelan, S.A., et al., *Regulation of insulin receptor substrate 1 (IRS-1)/AKT kinase-mediated insulin signaling by O-Linked beta-N-acetylglucosamine in 3T3-L1 adipocytes.* J Biol Chem, 2010. **285**(8): p. 5204-11.
123. Whelan, S.A., M.D. Lane, and G.W. Hart, *Regulation of the O-linked beta-N-acetylglucosamine transferase by insulin signaling.* J Biol Chem, 2008. **283**(31): p. 21411-7.
124. Cernkovich, E.R., et al., *Adipose-specific disruption of signal transducer and activator of transcription 3 increases body weight and adiposity.* Endocrinology, 2008. **149**(4): p. 1581-90.
125. Zeidan, Q. and G.W. Hart, *The intersections between O-GlcNAcylation and phosphorylation: implications for multiple signaling pathways.* J Cell Sci, 2010. **123**(Pt 1): p. 13-22.
126. Bullen, J.W., et al., *Cross-talk between two essential nutrient-sensitive enzymes: O-GlcNAc transferase (OGT) and AMP-activated protein kinase (AMPK).* J Biol Chem, 2014. **289**(15): p. 10592-606.
127. Carling, D. and B. Viollet, *Beyond energy homeostasis: the expanding role of AMP-activated protein kinase in regulating metabolism.* Cell Metab, 2015. **21**(6): p. 799-804.
128. Qi, D. and L.H. Young, *AMPK: energy sensor and survival mechanism in the ischemic heart.* Trends Endocrinol Metab, 2015. **26**(8): p. 422-9.
129. Ramirez-Correa, G.A., et al., *O-linked GlcNAc modification of cardiac myofilament proteins: a novel regulator of myocardial contractile function.* Circ Res, 2008. **103**(12): p. 1354-8.
130. Stovall, D.B. and G. Sui, *The Function of YY1 and Its Oncogenic Role in Prostate Cancer*. Advances in Prostate Cancer. 2013.
131. Hiromura, M., et al., *YY1 is regulated by O-linked N-acetylglucosaminylation (O-glcNAcylation).* J Biol Chem, 2003. **278**(16): p. 14046-52.

132. Riman, S., et al., *Phosphorylation of the transcription factor YY1 by CK2alpha prevents cleavage by caspase 7 during apoptosis.* Mol Cell Biol, 2012. **32**(4): p. 797-807.
133. Rizkallah, R. and M.M. Hurt, *Regulation of the transcription factor YY1 in mitosis through phosphorylation of its DNA-binding domain.* Mol Biol Cell, 2009. **20**(22): p. 4766-76.
134. Shi, Y., J.S. Lee, and K.M. Galvin, *Everything you have ever wanted to know about Yin Yang 1.* Biochim Biophys Acta, 1997. **1332**(2): p. F49-66.
135. Donohoe, M.E., et al., *Targeted disruption of mouse Yin Yang 1 transcription factor results in peri-implantation lethality.* Mol Cell Biol, 1999. **19**(10): p. 7237-44.
136. Gordon, S., et al., *Transcription factor YY1: structure, function, and therapeutic implications in cancer biology.* Oncogene, 2006. **25**(8): p. 1125-42.
137. Rizkallah, R., et al., *The transcription factor YY1 is a substrate for Polo-like kinase 1 at the G2/M transition of the cell cycle.* PLoS One, 2011. **6**(1): p. e15928.
138. Affar el, B., et al., *Essential dosage-dependent functions of the transcription factor yin yang 1 in late embryonic development and cell cycle progression.* Mol Cell Biol, 2006. **26**(9): p. 3565-81.
139. Whitfield, M.L., et al., *Identification of genes periodically expressed in the human cell cycle and their expression in tumors.* Mol Biol Cell, 2002. **13**(6): p. 1977-2000.
140. Palko, L., et al., *The Yin Yang-1 (YY1) protein undergoes a DNA-replication-associated switch in localization from the cytoplasm to the nucleus at the onset of S phase.* J Cell Sci, 2004. **117**(Pt 3): p. 465-76.
141. Choo, Y. and A. Klug, *A role in DNA binding for the linker sequences of the first three zinc fingers of TFIIIA.* Nucleic Acids Res, 1993. **21**(15): p. 3341-6.
142. Wuttke, D.S., et al., *Solution structure of the first three zinc fingers of TFIIIA bound to the cognate DNA sequence: determinants of affinity and sequence specificity1.* Journal of Molecular Biology, 1997. **273**(1): p. 183-206.
143. Laity, J.H., H.J. Dyson, and P.E. Wright, *DNA-induced α-helix capping in conserved linker sequences is a determinant of binding affinity in Cys2-His2 zinc fingers1.* Journal of Molecular Biology, 2000. **295**(4): p. 719-727.
144. Garban, H.J. and B. Bonavida, *Nitric oxide inhibits the transcription repressor Yin-Yang 1 binding activity at the silencer region of the Fas promoter: a pivotal role for nitric oxide in the up-regulation of Fas gene expression in human tumor cells.* J Immunol, 2001. **167**(1): p. 75-81.
145. Sui, G., et al., *Yin Yang 1 is a negative regulator of p53.* Cell, 2004. **117**(7): p. 859-72.
146. Gronroos, E., et al., *YY1 inhibits the activation of the p53 tumor suppressor in response to genotoxic stress.* Proc Natl Acad Sci U S A, 2004. **101**(33): p. 12165-70.
147. Hongo, F., et al., *Inhibition of the transcription factor Yin Yang 1 activity by S-nitrosation.* Biochem Biophys Res Commun, 2005. **336**(2): p. 692-701.
148. Knez, J., et al., *Host cell factor-1 and E2F4 interact via multiple determinants in each protein.* Mol Cell Biochem, 2006. **288**(1-2): p. 79-90.
149. Mangone, M., M.P. Myers, and W. Herr, *Role of the HCF-1 basic region in sustaining cell proliferation.* PLoS One, 2010. **5**(2): p. e9020.
150. Wysocka, J., et al., *Human Sin3 deacetylase and trithorax-related Set1/Ash2 histone H3-K4 methyltransferase are tethered together selectively by the cell-proliferation factor HCF-1.* Genes & Development, 2003. **17**(7): p. 896-911.
151. Schimpl, M., et al., *O-GlcNAc transferase invokes nucleotide sugar pyrophosphate participation in catalysis.* Nat Chem Biol, 2012. **8**(12): p. 969-74.

152. Clarke, A.J., et al., *Structural insights into mechanism and specificity of O-GlcNAc transferase.* Embo j, 2008. **27**(20): p. 2780-8.
153. Martinez-Fleites, C., et al., *Structure of an O-GlcNAc transferase homolog provides insight into intracellular glycosylation.* Nat Struct Mol Biol, 2008. **15**(7): p. 764-5.
154. Lazarus, M.B., et al., *Structure of human O-GlcNAc transferase and its complex with a peptide substrate.* Nature, 2011. **469**(7331): p. 564-7.
155. Kearse, K.P. and G.W. Hart, *Lymphocyte activation induces rapid changes in nuclear and cytoplasmic glycoproteins.* Proceedings of the National Academy of Sciences of the United States of America, 1991. **88**(5): p. 1701-1705.
156. Comer, F.I., et al., *Characterization of a mouse monoclonal antibody specific for O-linked N-acetylglucosamine.* Anal Biochem, 2001. **293**(2): p. 169-77.
157. Jackson, S.P. and R. Tjian, *O-glycosylation of eukaryotic transcription factors: implications for mechanisms of transcriptional regulation.* Cell, 1988. **55**(1): p. 125-33.
158. Hanover, J.A., *Glycan-dependent signaling: O-linked N-acetylglucosamine.* Faseb j, 2001. **15**(11): p. 1865-76.
159. Wells, L., K. Vosseller, and G.W. Hart, *Glycosylation of nucleocytoplasmic proteins: signal transduction and O-GlcNAc.* Science, 2001. **291**(5512): p. 2376-8.
160. Petkova, V., et al., *Interaction between YY1 and the retinoblastoma protein. Regulation of cell cycle progression in differentiated cells.* J Biol Chem, 2001. **276**(11): p. 7932-6.
161. Natesan, S. and M. Gilman, *YY1 facilitates the association of serum response factor with the c-fos serum response element.* Mol Cell Biol, 1995. **15**(11): p. 5975-82.
162. Reason, A.J., et al., *Localization of O-GlcNAc modification on the serum response transcription factor.* J Biol Chem, 1992. **267**(24): p. 16911-21.
163. Greer, E.L. and A. Brunet, *FOXO transcription factors in ageing and cancer.* Acta Physiol (Oxf), 2008. **192**(1): p. 19-28.
164. Hannenhalli, S. and K.H. Kaestner, *The evolution of Fox genes and their role in development and disease.* Nat Rev Genet, 2009. **10**(4): p. 233-40.
165. Katoh, M., et al., *Cancer genetics and genomics of human FOX family genes.* Cancer Lett, 2013. **328**(2): p. 198-206.
166. Leung, T.W., et al., *Over-expression of FoxM1 stimulates cyclin B1 expression.* FEBS Lett, 2001. **507**(1): p. 59-66.
167. Munekata, K. and K. Sakamoto, *Forkhead transcription factor Foxo1 is essential for adipocyte differentiation.* In Vitro Cell Dev Biol Anim, 2009. **45**(10): p. 642-51.
168. Myatt, S.S. and E.W. Lam, *The emerging roles of forkhead box (Fox) proteins in cancer.* Nat Rev Cancer, 2007. **7**(11): p. 847-59.
169. Sel, S., et al., *The Transcription factor Foxk1 is expressed in developping and adult neuroretina.* Gene Expression Patterns, 2013. **13**: p. 280-286.
170. Cirillo, L.A., et al., *Opening of compacted chromatin by early developmental transcription factors HNF3 (FoxA) and GATA-4.* Mol Cell, 2002. **9**(2): p. 279-89.
171. Clark, K.L., et al., *Co-crystal structure of the HNF-3/fork head DNA-recognition motif resembles histone H5.* Nature, 1993. **364**(6436): p. 412-20.
172. Tsai, K.L., et al., *Crystal structure of the human FOXK1a-DNA complex and its implications on the diverse binding specificity of winged helix/forkhead proteins.* J Biol Chem, 2006. **281**(25): p. 17400-9.
173. Durocher, D. and S.P. Jackson, *The FHA domain.* FEBS Lett, 2002. **513**(1): p. 58-66.
174. Durocher, D., et al., *The FHA Domain Is a Modular Phosphopeptide Recognition Motif.* Molecular Cell, 1999. **4**(3): p. 387-394.

175. Matthews, L.A. and A. Guarne, *Extending the Interaction Repertoire of FHA and BRCT Domains*. The Mechanisms of DNA Replication, ed. C. BY. 2013: InTech.
176. Zhou, M.-M., *Phosphothreonine recognition comes into focus.* Nat Struct Mol Biol, 2000. **7**(12): p. 1085-1087.
177. Yaffe, M.B. and S.J. Smerdon, *PhosphoSerine/Threonine Binding Domains: You Can't pSERious?* Structure, 2001. **9**(3): p. R33-R38.
178. Mauro, A., *Satellite cell of skeletal muscle fibers.* J Biophys Biochem Cytol, 1961. **9**: p. 493-5.
179. Shi, X., et al., *Foxk1 promotes cell proliferation and represses myogenic differenciation by regulating Foxo4 and Mef2.* Journal of Cell Science, 2012. **125**: p. 5329-5337.
180. Garry, D.J., et al., *Persistent expression of MNF identifies myogenic stem cells in postnatal muscles.* Dev Biol, 1997. **188**(2): p. 280-94.
181. Garry, D.J., et al., *Myogenic stem cell function is impaired in mice lacking the forkhead/winged helix protein MNF.* Proc Natl Acad Sci U S A, 2000. **97**(10): p. 5416-21.
182. Yang, Q., et al., *The winged-helix/forkhead protein myocyte nuclear factor beta (MNF-beta) forms a co-repressor complex with mammalian sin3B.* Biochem J, 2000. **345 Pt 2**: p. 335-43.
183. Meeson, A.P., et al., *Sox15 and Fhl3 transcriptionally coactivate Foxk1 and regulate myogenic progenitor cells.* EMBO J, 2007. **26**(7): p. 1902-12.
184. Schmidt, K., et al., *Sox8 is a specific marker for muscle satellite cells and inhibits myogenesis.* J Biol Chem, 2003. **278**(32): p. 29769-75.
185. Matthews, J.M., et al., *Competition between LIM-binding domains.* Biochem Soc Trans, 2008. **36**(Pt 6): p. 1393-7.
186. Muller, J.M., et al., *The transcriptional coactivator FHL2 transmits Rho signals from the cell membrane into the nucleus.* Embo j, 2002. **21**(4): p. 736-48.
187. Turner, J., et al., *The LIM protein FHL3 binds basic Kruppel-like factor/Kruppel-like factor 3 and its co-repressor C-terminal-binding protein 2.* J Biol Chem, 2003. **278**(15): p. 12786-95.
188. Lee, H.J., et al., *Sox15 is required for skeletal muscle regeneration.* Mol Cell Biol, 2004. **24**(19): p. 8428-36.
189. Allan, R.S. and S.L. Nutt, *Deciphering the epigenetic code of T lymphocytes.* Immunol Rev, 2014. **261**(1): p. 50-61.
190. Barski, A., et al., *High-Resolution Profiling of Histone Methylations in the Human Genome.* Cell, 2007. **129**(4): p. 823-837.
191. Fischle, W., H.D. Mootz, and D. Schwarzer, *Synthetic histone code.* Curr Opin Chem Biol, 2015. **28**: p. 131-140.
192. Ng, M.K. and P. Cheung, *A brief histone in time: understanding the combinatorial functions of histone PTMs in the nucleosome context.* Biochem Cell Biol, 2015: p. 1-10.
193. Nickel, B.E. and J.R. Davie, *Structure of polyubiquitinated histone H2A.* Biochemistry, 1989. **28**(3): p. 964-8.
194. Rothbart, S.B. and B.D. Strahl, *Interpreting the language of histone and DNA modifications.* Biochim Biophys Acta, 2014. **1839**(8): p. 627-43.
195. Steffen, P.A. and L. Ringrose, *What are memories made of? How Polycomb and Trithorax proteins mediate epigenetic memory.* Nat Rev Mol Cell Biol, 2014. **15**(5): p. 340-56.
196. Shi, X., D.C. Seldin, and D.J. Garry, *Foxk1 recruits the Sds3 complex and represses gene expression in myogenic progenitors.* Biochem J, 2012. **446**(3): p. 349-57.
197. Shi, X. and D.J. Garry, *Sin3 interacts with Foxk1 and regulates myogenic progenitors.* Mol Cell Biochem, 2012. **366**(1-2): p. 251-8.
198. Wu, Z., et al., *p38 and extracellular signal-regulated kinases regulate the myogenic program at multiple steps.* Mol Cell Biol, 2000. **20**(11): p. 3951-64.

199. Li, Y., et al., *Myogenic differentiation requires signalling through both phosphatidylinositol 3-kinase and p38 MAP kinase.* Cell Signal, 2000. **12**(11-12): p. 751-7.
200. Keren, A., Y. Tamir, and E. Bengal, *The p38 MAPK signaling pathway: a major regulator of skeletal muscle development.* Mol Cell Endocrinol, 2006. **252**(1-2): p. 224-30.
201. Sanchez, A.M., R.B. Candau, and H. Bernardi, *FoxO transcription factors: their roles in the maintenance of skeletal muscle homeostasis.* Cell Mol Life Sci, 2014. **71**(9): p. 1657-71.
202. Tothova, Z., et al., *FoxOs are critical mediators of hematopoietic stem cell resistance to physiologic oxidative stress.* Cell, 2007. **128**(2): p. 325-39.
203. Seoane, J., et al., *Integration of Smad and forkhead pathways in the control of neuroepithelial and glioblastoma cell proliferation.* Cell, 2004. **117**(2): p. 211-23.
204. Black, B.L. and E.N. Olson, *Transcriptional control of muscle development by myocyte enhancer factor-2 (MEF2) proteins.* Annu Rev Cell Dev Biol, 1998. **14**: p. 167-96.
205. Zhao, J., et al., *FoxO3 coordinately activates protein degradation by the autophagic/lysosomal and proteasomal pathways in atrophying muscle cells.* Cell Metab, 2007. **6**(6): p. 472-83.
206. Bowman, C.J., D.E. Ayer, and B.D. Dynlacht, *Foxk proteins repress the initiation of starvation-induced atrophy and autophagy programs.* Nat Cell Biol, 2014. **16**(12): p. 1202-14.
207. Ji, Z., et al., *The forkhead transcription factor FOXK2 acts as a chromatin targeting factor for the BAP1-containing histone deubiquitinase complex.* Nucleic Acids Res, 2014. **42**(10): p. 6232-42.
208. Marais, A., et al., *Cell cycle-dependent regulation of the forkhead transcription factor FOXK2 by CDK.cyclin complexes.* J Biol Chem, 2010. **285**(46): p. 35728-39.
209. Liu, Y., et al., *FOXK2 transcription factor suppresses ERalpha-positive breast cancer cell growth through down-regulating the stability of ERalpha via mechanism involving BRCA1/BARD1.* Sci Rep, 2015. **5**: p. 8796.
210. Clevers, H., *Wnt/β-Catenin Signaling in Development and Disease.* Cell, 2006. **127**(3): p. 469-480.
211. Huang, H. and X. He, *Wnt/β-catenin signaling: new (and old) players and new insights.* Current Opinion in Cell Biology, 2008. **20**(2): p. 119-125.
212. Nusse, R., *Wnt signaling and stem cell control.* Cell Res, 2008. **18**(5): p. 523-527.
213. Clevers, H. and R. Nusse, *Wnt/β-Catenin Signaling and Disease.* Cell, 2012. **149**(6): p. 1192-1205.
214. Chiurillo, M.A., *Role of the Wnt/beta-catenin pathway in gastric cancer: An in-depth literature review.* World J Exp Med, 2015. **5**(2): p. 84-102.
215. Kobayashi, Y., et al., *The regulation of osteoclast differentiation by Wnt signals.* Bonekey Rep, 2015. **4**: p. 713.
216. Li, C., et al., *Noncanonical WNT Signaling in the Lung.* J Biochem, 2015.
217. Wang, W., et al., *FOXKs Promote Wnt/beta-Catenin Signaling by Translocating DVL into the Nucleus.* Dev Cell, 2015. **32**(6): p. 707-18.
218. Gonzales-van Horn, S.R. and J.D. Farrar, *Interferon at the crossroads of allergy and viral infections.* J Leukoc Biol, 2015. **98**(2): p. 185-94.
219. Panda, D., et al., *The Transcription Factor FoxK Participates with Nup98 To Regulate Antiviral Gene Expression.* MBio, 2015. **6**(2).
220. Gajjala, P.R., et al., *Emerging role of post-translational modifications in chronic kidney disease and cardiovascular disease.* Nephrol Dial Transplant, 2015.
221. Zhu, Y., et al., *The Emerging Link Between O-GlcNAc and Alzheimer's Disease.* J Biol Chem, 2014.

222. Hart, G.W., M.P. Housley, and C. Slawson, *Cycling of O-linked beta-N-acetylglucosamine on nucleocytoplasmic proteins.* Nature, 2007. **446**(7139): p. 1017-22.
223. Ruan, H.B., et al., *Cracking the O-GlcNAc code in metabolism.* Trends Endocrinol Metab, 2013. **24**(6): p. 301-9.
224. Cooper, J.A., T. Kaneko, and S.S. Li, *Cell Regulation by Phosphotyrosine-Targeted Ubiquitin Ligases.* Mol Cell Biol, 2015. **35**(11): p. 1886-1897.
225. Bogachek, M.V., J.P. De Andrade, and R.J. Weigel, *Regulation of epithelial-mesenchymal transition through SUMOylation of transcription factors.* Cancer Res, 2015. **75**(1): p. 11-5.
226. Hart, G.W., *Three Decades of Research on O-GlcNAcylation - A Major Nutrient Sensor That Regulates Signaling, Transcription and Cellular Metabolism.* Front Endocrinol (Lausanne), 2014. **5**: p. 183.
227. Tasaki, T., et al., *The N-End Rule Pathway.* Annual Review of Biochemistry, 2012. **81**(1): p. 261-289.
228. Joerger, A.C. and A.R. Fersht, *Structural Biology of the Tumor Suppressor p53.* Annual Review of Biochemistry, 2008. **77**(1): p. 557-582.
229. Hottiger, M.O., *Nuclear ADP-Ribosylation and Its Role in Chromatin Plasticity, Cell Differentiation, and Epigenetics.* Annual Review of Biochemistry, 2015. **84**(1): p. null.
230. Tang, Q.Q. and M.D. Lane, *Adipogenesis: From Stem Cell to Adipocyte.* Annual Review of Biochemistry, 2012. **81**(1): p. 715-736.
231. Kurosaki, T., H. Shinohara, and Y. Baba, *B Cell Signaling and Fate Decision.* Annual Review of Immunology, 2010. **28**(1): p. 21-55.
232. Tajbakhsh, S., P. Rocheteau, and I. Le Roux, *Asymmetric Cell Divisions and Asymmetric Cell Fates.* Annual Review of Cell and Developmental Biology, 2009. **25**(1): p. 671-699.
233. Hu, P., S. Shimoji, and G.W. Hart, *Site-specific interplay between O-GlcNAcylation and phosphorylation in cellular regulation.* FEBS Letters, 2010. **584**(12): p. 2526-2538.
234. Hardiville, S., et al., *O-GlcNAcylation/phosphorylation cycling at Ser10 controls both transcriptional activity and stability of delta-lactoferrin.* J Biol Chem, 2010. **285**(25): p. 19205-18.
235. Bond, M.R. and J.A. Hanover, *O-GlcNAc Cycling: A Link Between Metabolism and Chronic Disease.* Annual Review of Nutrition, 2013. **33**(1): p. 205-229.
236. Benhamed, F., et al., *O-GlcNAcylation Links ChREBP and FXR to Glucose-Sensing.* Front Endocrinol (Lausanne), 2014. **5**: p. 230.
237. Slawson, C., R.J. Copeland, and G.W. Hart, *O-GlcNAc signaling: a metabolic link between diabetes and cancer?* Trends Biochem Sci, 2010. **35**(10): p. 547-55.
238. Ji, Z., et al., *The forkhead transcription factor FOXK2 promotes AP-1-mediated transcriptional regulation.* Mol Cell Biol, 2012. **32**(2): p. 385-98.
239. Fujii, Y. and M. Nakamura, *FOXK2 transcription factor is a novel G/T-mismatch DNA binding protein.* Journal of Biochemistry, 2010. **147**(5): p. 706-709.
240. Shi, X., K.M. Bowlin, and D.J. Garry, *Fhl2 interacts with Foxk1 and corepresses Foxo4 activity in myogenic progenitors.* Stem Cells, 2010. **28**(3): p. 462-9.
241. Freddie, C., et al., *Functional interactions between the Forkhead transcription factor FOXK1 and the MADS-box protein SRF.* Nucleic Acids Research, 2007. **35**(15): p. 5203-5212.
242. Hammond-Martel, I., et al., *PI 3 kinase related kinases-independent proteolysis of BRCA1 regulates Rad51 recruitment during genotoxic stress in human cells.* PLoS One, 2010. **5**(11): p. e14027.
243. Gagnon, J., et al., *Undetectable histone O-GlcNAcylation in mammalian cells.* Epigenetics, 2015. **10**(8): p. 677-91.

244. Lea, N.C., et al., *Commitment point during G0-->G1 that controls entry into the cell cycle.* Mol Cell Biol, 2003. **23**(7): p. 2351-61.
245. Dong, P., et al., *Division of labour between Myc and G1 cyclins in cell cycle commitment and pace control.* Nat Commun, 2014. **5**: p. 4750.
246. Sodi, V.L., et al., *mTOR/MYC Axis Regulates O-GlcNAc Transferase Expression and O-GlcNAcylation in Breast Cancer.* Mol Cancer Res, 2015.
247. Duncan, E.M., et al., *Cathepsin L proteolytically processes histone H3 during mouse embryonic stem cell differentiation.* Cell, 2008. **135**(2): p. 284-94.
248. Matthews, L.A., et al., *A novel non-canonical forkhead-associated (FHA) domain-binding interface mediates the interaction between Rad53 and Dbf4 proteins.* J Biol Chem, 2014. **289**(5): p. 2589-99.
249. Nott, T.J., et al., *An intramolecular switch regulates phosphoindependent FHA domain interactions in Mycobacterium tuberculosis.* Sci Signal, 2009. **2**(63): p. ra12.
250. Zhao, B., et al., *A coordinated phosphorylation by Lats and CK1 regulates YAP stability through SCF(beta-TRCP).* Genes Dev, 2010. **24**(1): p. 72-85.
251. Jiao, W., et al., *Nucleocytoplasmic shuttling of the retinoblastoma tumor suppressor protein via Cdk phosphorylation-dependent nuclear export.* J Biol Chem, 2006. **281**(49): p. 38098-108.
252. Elrick, L.J. and K. Docherty, *Phosphorylation-dependent nucleocytoplasmic shuttling of pancreatic duodenal homeobox-1.* Diabetes, 2001. **50**(10): p. 2244-52.
253. Hallenborg, P., et al., *PPARgamma ligand production is tightly linked to clonal expansion during initiation of adipocyte differentiation.* J Lipid Res, 2014. **55**(12): p. 2491-500.
254. Qiu, Z., et al., *DNA synthesis and mitotic clonal expansion is not a required step for 3T3-L1 preadipocyte differentiation into adipocytes.* J Biol Chem, 2001. **276**(15): p. 11988-95.
255. Patel, Y.M. and M.D. Lane, *Mitotic clonal expansion during preadipocyte differentiation: calpain-mediated turnover of p27.* J Biol Chem, 2000. **275**(23): p. 17653-60.
256. Durocher, D., et al., *The Molecular Basis of FHA Domain:Phosphopeptide Binding Specificity and Implications for Phospho-Dependent Signaling Mechanisms.* Molecular Cell, 2000. **6**(5): p. 1169-1182.
257. Mahajan, A., et al., *FHA domain-ligand interactions: importance of integrating chemical and biological approaches.* J Am Chem Soc, 2005. **127**(42): p. 14572-3.
258. Guo, L., X. Li, and Q.Q. Tang, *Transcriptional regulation of adipocyte differentiation: a central role for CCAAT/enhancer-binding protein (C/EBP) beta.* J Biol Chem, 2015. **290**(2): p. 755-61.
259. Yeh, W.C., B.E. Bierer, and S.L. McKnight, *Rapamycin inhibits clonal expansion and adipogenic differentiation of 3T3-L1 cells.* Proc Natl Acad Sci U S A, 1995. **92**(24): p. 11086-90.
260. Lee, Y. and E.J. Bae, *Inhibition of mitotic clonal expansion mediates fisetin-exerted prevention of adipocyte differentiation in 3T3-L1 cells.* Arch Pharm Res, 2013. **36**(11): p. 1377-84.
261. Li, X., et al., *Role of cdk2 in the sequential phosphorylation/activation of C/EBPbeta during adipocyte differentiation.* Proc Natl Acad Sci U S A, 2007. **104**(28): p. 11597-602.
262. Rosen, E.D., et al., *C/EBPalpha induces adipogenesis through PPARgamma: a unified pathway.* Genes Dev, 2002. **16**(1): p. 22-6.
263. Tang, Q.Q., T.C. Otto, and M.D. Lane, *Mitotic clonal expansion: a synchronous process required for adipogenesis.* Proc Natl Acad Sci U S A, 2003. **100**(1): p. 44-9.
264. Tang, Q.Q. and M.D. Lane, *Adipogenesis: from stem cell to adipocyte.* Annu Rev Biochem, 2012. **81**: p. 715-36.
265. Lewis, B.A. and J.A. Hanover, *O-GlcNAc and the Epigenetic Regulation of Gene Expression.* J Biol Chem, 2014.

266. Janetzko, J. and S. Walker, *The Making of a Sweet Modification: Structure and Function of O-GlcNAc Transferase.* J Biol Chem, 2014.
267. Nagel, A.K. and L.E. Ball, *O-GlcNAc transferase and O-GlcNAcase: achieving target substrate specificity.* Amino Acids, 2014. **46**(10): p. 2305-16.
268. Vocadlo, D.J., *O-GlcNAc processing enzymes: catalytic mechanisms, substrate specificity, and enzyme regulation.* Curr Opin Chem Biol, 2012. **16**(5-6): p. 488-97.
269. Hanover, J.A., M.W. Krause, and D.C. Love, *Bittersweet memories: linking metabolism to epigenetics through O-GlcNAcylation.* Nat Rev Mol Cell Biol, 2012. **13**(5): p. 312-21.
270. Harwood, K.R. and J.A. Hanover, *Nutrient-driven O-GlcNAc cycling - think globally but act locally.* J Cell Sci, 2014. **127**(Pt 9): p. 1857-67.
271. Caldwell, S.A., et al., *Nutrient sensor O-GlcNAc transferase regulates breast cancer tumorigenesis through targeting of the oncogenic transcription factor FoxM1.* Oncogene, 2010. **29**(19): p. 2831-42.
272. Fardini, Y., et al., *O-GlcNAcylation: A New Cancer Hallmark?* Front Endocrinol (Lausanne), 2013. **4**: p. 99.
273. Zhang, S., et al., *Modification of histones by sugar beta-N-acetylglucosamine (GlcNAc) occurs on multiple residues, including histone H3 serine 10, and is cell cycle-regulated.* J Biol Chem, 2011. **286**(43): p. 37483-95.
274. Fong, J.J., et al., *beta-N-Acetylglucosamine (O-GlcNAc) is a novel regulator of mitosis-specific phosphorylations on histone H3.* J Biol Chem, 2012. **287**(15): p. 12195-203.
275. Lazarus, B.D., D.C. Love, and J.A. Hanover, *O-GlcNAc cycling: implications for neurodegenerative disorders.* Int J Biochem Cell Biol, 2009. **41**(11): p. 2134-46.
276. Jozwiak, P., et al., *O-GlcNAcylation and Metabolic Reprograming in Cancer.* Front Endocrinol (Lausanne), 2014. **5**: p. 145.
277. Forma, E., et al., *The potential role of O-GlcNAc modification in cancer epigenetics.* Cell Mol Biol Lett, 2014. **19**(3): p. 438-60.
278. Issad, T. and P. Pagesy, *[Protein O-GlcNAcylation and regulation of cell signalling: involvement in pathophysiology].* Biol Aujourdhui, 2014. **208**(2): p. 109-17.
279. Dehennaut, V., D. Leprince, and T. Lefebvre, *O-GlcNAcylation, an Epigenetic Mark. Focus on the Histone Code, TET Family Proteins, and Polycomb Group Proteins.* Front Endocrinol (Lausanne), 2014. **5**: p. 155.
280. Deng, R.P., et al., *Global identification of O-GlcNAc transferase (OGT) interactors by a human proteome microarray and the construction of an OGT interactome.* Proteomics, 2014. **14**(9): p. 1020-30.
281. Ozcan, S., S.S. Andrali, and J.E. Cantrell, *Modulation of transcription factor function by O-GlcNAc modification.* Biochim Biophys Acta, 2010. **1799**(5-6): p. 353-64.
282. Zhang, Q., et al., *Differential regulation of the ten-eleven translocation (TET) family of dioxygenases by O-linked beta-N-acetylglucosamine transferase (OGT).* J Biol Chem, 2014. **289**(9): p. 5986-96.
283. Yang, X., F. Zhang, and J.E. Kudlow, *Recruitment of O-GlcNAc transferase to promoters by corepressor mSin3A: coupling protein O-GlcNAcylation to transcriptional repression.* Cell, 2002. **110**(1): p. 69-80.
284. Hanover, J.A., *Epigenetics gets sweeter: O-GlcNAc joins the "histone code".* Chem Biol, 2010. **17**(12): p. 1272-4.
285. Sakabe, K., Z. Wang, and G.W. Hart, *Beta-N-acetylglucosamine (O-GlcNAc) is part of the histone code.* Proc Natl Acad Sci U S A, 2010. **107**(46): p. 19915-20.

286. Arnaudo, A.M. and B.A. Garcia, *Proteomic characterization of novel histone post-translational modifications.* Epigenetics Chromatin, 2013. **6**(1): p. 24.
287. Chen, Q., et al., *TET2 promotes histone O-GlcNAcylation during gene transcription.* Nature, 2013. **493**(7433): p. 561-4.
288. Fujiki, R., et al., *GlcNAcylation of histone H2B facilitates its monoubiquitination.* Nature, 2011. **480**(7378): p. 557-60.
289. Xu, Q., et al., *AMPK regulates histone H2B O-GlcNAcylation.* Nucleic Acids Res, 2014. **42**(9): p. 5594-604.
290. Ito, R., et al., *TET3-OGT interaction increases the stability and the presence of OGT in chromatin.* Genes Cells, 2014. **19**(1): p. 52-65.
291. Vella, P., et al., *Tet proteins connect the O-linked N-acetylglucosamine transferase Ogt to chromatin in embryonic stem cells.* Mol Cell, 2013. **49**(4): p. 645-56.
292. Isono, T., *O-GlcNAc-specific antibody CTD110.6 cross-reacts with N-GlcNAc2-modified proteins induced under glucose deprivation.* PLoS One, 2011. **6**(4): p. e18959.
293. Ogawa, M., et al., *GTDC2 modifies O-mannosylated alpha-dystroglycan in the endoplasmic reticulum to generate N-acetyl glucosamine epitopes reactive with CTD110.6 antibody.* Biochem Biophys Res Commun, 2013. **440**(1): p. 88-93.
294. Zhang, B.B., G. Zhou, and C. Li, *AMPK: an emerging drug target for diabetes and the metabolic syndrome.* Cell Metab, 2009. **9**(5): p. 407-16.
295. Vassilev, L.T., et al., *Selective small-molecule inhibitor reveals critical mitotic functions of human CDK1.* Proc Natl Acad Sci U S A, 2006. **103**(28): p. 10660-5.
296. Hart, C., et al., *Metabolic labeling and click chemistry detection of glycoprotein markers of mesenchymal stem cell differentiation.* Methods Mol Biol, 2011. **698**: p. 459-84.
297. Haynes, P.A. and R. Aebersold, *Simultaneous detection and identification of O-GlcNAc-modified glycoproteins using liquid chromatography-tandem mass spectrometry.* Anal Chem, 2000. **72**(21): p. 5402-10.
298. Vester-Christensen, M.B., et al., *Mining the O-mannose glycoproteome reveals cadherins as major O-mannosylated glycoproteins.* Proc Natl Acad Sci U S A, 2013. **110**(52): p. 21018-23.
299. Alfaro, J.F., et al., *Tandem mass spectrometry identifies many mouse brain O-GlcNAcylated proteins including EGF domain-specific O-GlcNAc transferase targets.* Proc Natl Acad Sci U S A, 2012. **109**(19): p. 7280-5.
300. Myers, S.A., B. Panning, and A.L. Burlingame, *Polycomb repressive complex 2 is necessary for the normal site-specific O-GlcNAc distribution in mouse embryonic stem cells.* Proc Natl Acad Sci U S A, 2011. **108**(23): p. 9490-5.
301. Vosseller, K., et al., *O-linked N-acetylglucosamine proteomics of postsynaptic density preparations using lectin weak affinity chromatography and mass spectrometry.* Mol Cell Proteomics, 2006. **5**(5): p. 923-34.
302. Trinidad, J.C., et al., *Global identification and characterization of both O-GlcNAcylation and phosphorylation at the murine synapse.* Mol Cell Proteomics, 2012. **11**(8): p. 215-29.
303. Myers, S.A., et al., *Electron transfer dissociation (ETD): the mass spectrometric breakthrough essential for O-GlcNAc protein site assignments-a study of the O-GlcNAcylated protein host cell factor C1.* Proteomics, 2013. **13**(6): p. 982-91.
304. Wysocka, J., et al., *Human Sin3 deacetylase and trithorax-related Set1/Ash2 histone H3-K4 methyltransferase are tethered together selectively by the cell-proliferation factor HCF-1.* Genes Dev, 2003. **17**(7): p. 896-911.
305. Wilson, A.C., et al., *The VP16 accessory protein HCF is a family of polypeptides processed from a large precursor protein.* Cell, 1993. **74**(1): p. 115-25.

306. Wilson, A.C., et al., *HCF-1 amino- and carboxy-terminal subunit association through two separate sets of interaction modules: involvement of fibronectin type 3 repeats.* Mol Cell Biol, 2000. **20**(18): p. 6721-30.
307. Minsky, N. and M. Oren, *The RING domain of Mdm2 mediates histone ubiquitylation and transcriptional repression.* Mol Cell, 2004. **16**(4): p. 631-9.
308. Stoscheck, C.M., *Quantitation of protein.* Methods Enzymol, 1990. **182**: p. 50-68.
309. Jackson, S.P. and D. Durocher, *Regulation of DNA damage responses by ubiquitin and SUMO.* Mol Cell, 2013. **49**(5): p. 795-807.
310. Metzger, M.B., V.A. Hristova, and A.M. Weissman, *HECT and RING finger families of E3 ubiquitin ligases at a glance.* J Cell Sci, 2012. **125**(Pt 3): p. 531-7.
311. Reyes-Turcu, F.E., K.H. Ventii, and K.D. Wilkinson, *Regulation and cellular roles of ubiquitin-specific deubiquitinating enzymes.* Annu Rev Biochem, 2009. **78**: p. 363-97.
312. Harbour, J.W., et al., *Frequent mutation of BAP1 in metastasizing uveal melanomas.* Science, 2010. **330**(6009): p. 1410-3.
313. Goldstein, A.M., *Germline BAP1 mutations and tumor susceptibility.* Nat Genet, 2011. **43**(10): p. 925-6.
314. Ventii, K.H., et al., *BRCA1-associated protein-1 is a tumor suppressor that requires deubiquitinating activity and nuclear localization.* Cancer Res, 2008. **68**(17): p. 6953-62.
315. Machida, Y.J., et al., *The deubiquitinating enzyme BAP1 regulates cell growth via interaction with HCF-1.* J Biol Chem, 2009.
316. Sowa, M.E., et al., *Defining the human deubiquitinating enzyme interaction landscape.* Cell, 2009. **138**(2): p. 389-403.
317. Yu, H., et al., *The Ubiquitin Carboxyl Hydrolase BAP1 Forms a Ternary Complex with YY1 and HCF-1 and is a Critical Regulator of Gene Expression.* Mol Cell Biol, 2010.
318. Pan, H., et al., *BAP1 regulates cell cycle progression through E2F1 target genes and mediates transcriptional silencing via H2A monoubiquitination in uveal melanoma cells.* Int J Biochem Cell Biol, 2015. **60C**: p. 176-184.
319. Wang, H., et al., *Role of histone H2A ubiquitination in Polycomb silencing.* Nature, 2004. **431**(7010): p. 873-8.
320. Milne, T.A., D.A. Sinclair, and H.W. Brock, *The Additional sex combs gene of Drosophila is required for activation and repression of homeotic loci, and interacts specifically with Polycomb and super sex combs.* Mol Gen Genet, 1999. **261**(4-5): p. 753-61.
321. Gildea, J.J., R. Lopez, and A. Shearn, *A screen for new trithorax group genes identified little imaginal discs, the Drosophila melanogaster homologue of human retinoblastoma binding protein 2.* Genetics, 2000. **156**(2): p. 645-63.
322. Cho, Y.S., et al., *Additional sex comb-like 1 (ASXL1), in cooperation with SRC-1, acts as a ligand-dependent coactivator for retinoic acid receptor.* J Biol Chem, 2006. **281**(26): p. 17588-98.
323. Lee, S.W., et al., *ASXL1 represses retinoic acid receptor-mediated transcription through associating with HP1 and LSD1.* J Biol Chem, 2010. **285**(1): p. 18-29.
324. Park, U.H., et al., *Additional sex comb-like (ASXL) proteins 1 and 2 play opposite roles in adipogenesis via reciprocal regulation of peroxisome proliferator-activated receptor {gamma}.* J Biol Chem, 2011. **286**(2): p. 1354-63.
325. Katoh, M., *Functional and cancer genomics of ASXL family members.* Br J Cancer, 2013.
326. Fisher, C.L., et al., *Characterization of Asxl1, a murine homolog of Additional sex combs, and analysis of the Asx-like gene family.* Gene, 2006. **369**: p. 109-18.

327. Yao, T., et al., *Proteasome recruitment and activation of the Uch37 deubiquitinating enzyme by Adrm1.* Nat Cell Biol, 2006.
328. Qiu, X.B., et al., *hRpn13/ADRM1/GP110 is a novel proteasome subunit that binds the deubiquitinating enzyme, UCH37.* EMBO J, 2006. **25**(24): p. 5742-53.
329. Sanchez-Pulido, L., L. Kong, and C.P. Ponting, *A common ancestry for BAP1 and Uch37 regulators.* Bioinformatics, 2012. **28**(15): p. 1953-6.
330. Morrow, M.E., et al., *Stabilization of an unusual salt bridge in ubiquitin by the extra C-terminal domain of the proteasome-associated deubiquitinase UCH37 as a mechanism of its exo specificity.* Biochemistry, 2013. **52**(20): p. 3564-78.
331. Chen, X. and K.J. Walters, *Structural plasticity allows UCH37 to be primed by RPN13 or locked down by INO80G.* Mol Cell, 2015. **57**(5): p. 767-8.
332. VanderLinden, R.T., et al., *Structural basis for the activation and inhibition of the UCH37 deubiquitylase.* Mol Cell, 2015. **57**(5): p. 901-11.
333. Belle, J.I. and A. Nijnik, *H2A-DUBbing the mammalian epigenome: expanding frontiers for histone H2A deubiquitinating enzymes in cell biology and physiology.* Int J Biochem Cell Biol, 2014. **50**: p. 161-74.
334. Jacobs, J.J., et al., *The oncogene and Polycomb-group gene bmi-1 regulates cell proliferation and senescence through the ink4a locus.* Nature, 1999. **397**(6715): p. 164-8.
335. Dietrich, N., et al., *Bypass of senescence by the polycomb group protein CBX8 through direct binding to the INK4A-ARF locus.* EMBO J, 2007. **26**(6): p. 1637-48.
336. Luis, N.M., et al., *Regulation of human epidermal stem cell proliferation and senescence requires polycomb- dependent and -independent functions of Cbx4.* Cell Stem Cell, 2011. **9**(3): p. 233-46.
337. Leung, C., et al., *Bmi1 is essential for cerebellar development and is overexpressed in human medulloblastomas.* Nature, 2004. **428**(6980): p. 337-41.
338. Xu, F., et al., *Overexpression of the EZH2, RING1 and BMI1 genes is common in myelodysplastic syndromes: relation to adverse epigenetic alteration and poor prognostic scoring.* Ann Hematol, 2011. **90**(6): p. 643-53.
339. Bosch, A., et al., *The Polycomb group protein RING1B is overexpressed in ductal breast carcinoma and is required to sustain FAK steady state levels in breast cancer epithelial cells.* Oncotarget, 2014. **5**(8): p. 2065-76.

Chapitre 4

4. Articles en annexes

4.1 Article 1 : Undetectable Histone O-GlcNAcylation in Mammalian Cells

Jessica Gagnon[1,†], Salima Daou[1,†], Natalia Zamorano[1], Nicholas VG Iannantuono[1], Ian Hammond-Martel[1], Nazar Mashtalir[1], Eric Bonneil[2], Hugo Wurtele[1], Pierre Thibault[2] and El Bachir Affar[1,#]

[1]Maisonneuve-Rosemont Hospital Research Center and Department of Medicine, University of Montréal, Montréal H3C 3J7, Québec, Canada

[2]Institute for Research in Immunology and Cancer, University of Montréal, Montréal H3C 3J7, Québec, Canada

[†]Equal contribution

[#]Correspondence

Conflict of interest

The authors declare no conflict of interest

Running title: Undetectable Histones O-GlcNAcylation

Key words: Histone, OGT, O-GlcNAc, O-GlcNAcylation, Chromatin, Epigenetics, Polycomb, post-translational modification, HCF-1, TET2.

Abbreviation: O-Linked N-acetylglucosamine (O-GlcNAc), O-Linked N-acetylglucosamine transferase (OGT), O-GlcNAcase (OGA), Host Cell Factor-1 (HCF-1), Ten-Eleven Translocation protein 2 (TET2), serine (Ser), threonine (Thr), Uridine Diphosphate *N*-Acetylglucosamine (UDP-GlcNAc), Wheat Germ Agglutinin (WGA), Histone H2B serine 112 O-GlcNAc (H2B Ser112 O-GlcNAc), Histone H2B lysine 120 monoubiquitination (H2Bub Lys120), O-(2-acetamido-2-deoxyglucopyranosylidene) amino N-phenylcarbamate (PUGNAc)

Abstract

O-GlcNAcylation is a post-translational modification catalyzed by the O-Linked *N*-acetylglucosamine (O-GlcNAc) transferase (OGT) and reversed by O-GlcNAcase (OGA). Numerous transcriptional regulators including chromatin modifying enzymes, transcription factors and co-factors are targeted by O-GlcNAcylation indicating that this modification is central for chromatin-associated processes. Recently, OGT-mediated O-GlcNAcylation was reported to be a novel histone modification, suggesting a potential role in directly coordinating chromatin structure and function. In contrast, using multiple biochemical approaches, we report here that histone O-GlcNAcylation is undetectable in mammalian cells. Conversely, O-GlcNAcylation of the transcription regulators Host Cell Factor-1 (HCF-1) and the Ten-Eleven Translocation protein 2 (TET2) could be readily observed. Our study raises questions on the occurrence and abundance of O-GlcNAcylation as a histone modification in mammalian cells and reveals technical complications regarding the detection of genuine protein O-GlcNAcylation. Therefore, the identification of the specific contexts in which histone O-GlcNAcylation might occur is still to be established.

Introduction

O-GlcNAcylation is a widespread post-translational modification corresponding to the addition of a single O-Linked *N*-acetylglucosamine (O-GlcNAc) moiety to nuclear and cytosolic proteins [222, 265, 266]. Similar to other post-translational modifications, O-GlcNAcylation regulates protein function by influencing protein-protein interactions, enzymatic activity and sub-cellular localization [223, 226]. In mammals, this modification is coordinated by two enzymes, the O-Linked β-*N*-acetylglucosamine transferase (OGT) which catalyzes the attachment of the O-GlcNAc moiety on serine and threonine residues of target proteins, while the O-GlcNAcase (OGA) ensures its removal through hydrolysis [267, 268]. O-GlcNAcylation signaling is dependent on the availability of the donor substrate, Uridine Diphosphate *N*-Acetylglucosamine (UDP-GlcNAc), which is produced via the Hexosamine Biosynthetic Pathway [118]. O-GlcNAcylation is a highly dynamic modification, being regulated by a plethora of intracellular and extracellular cues, including growth factor signaling, fluctuation of nutrient levels, as well as stress responses [126, 269, 270]. Indeed, O-GlcNAcylation signaling acts as a metabolic sensor that links changes in the cellular metabolism to downstream regulation of numerous cellular pathways [223, 271, 272]. Moreover, recent studies have shown that direct competition between phosphorylation and O-GlcNAcylation can occur for the same amino acid residue, thus adding another layer of complexity to the outcome and regulation of this post-translational modification [273, 274]. The physiological importance of O-GlcNAcylation is further emphasized by the fact that defects in its regulation have been associated with human pathologies such as diabetes, neurodegenerative diseases and cancer [237, 275-278].

O-GlcNAcylation signaling was proposed to play important roles in regulating the epigenome [265, 279]. Indeed, several transcriptional regulators and chromatin-modifying enzymes are modified by O-GlcNAcylation, thus impacting their recruitment to chromatin, assembly into functional transcription regulatory complexes, stability and activity [280-283]. For instance, we and others have identified a non-canonical mechanism of OGT-mediated transcriptional regulation which involves the O-GlcNAcylation of the Host Cell Factor 1 (HCF-1) transcriptional regulator inducing its proteolytic maturation [68, 69, 72].

Recent studies have also reported that histones are modified by O-GlcNAcylation, suggesting an interesting possibility of crosstalk with other well-established histone marks [284-286]. Moreover, it was suggested that the methylcytosine dioxygenase Ten Eleven Translocation 2 (TET2) enzyme directly interacts with OGT to stimulate histone H2B S112 O-GlcNAcylation (H2B S112 O-GlcNAc) and gene expression [287]. Several methods were used to detect histone O-GlcNAcylation, including mass spectrometry, immunodetection with O-GlcNAc-specific antibodies and affinity binding to Wheat Germ Agglutinin lectin (WGA) [273, 285, 288]. However, discrepancies regarding the occurrence and the identity of the histones being modified were also reported. For instance, some studies suggested that histones H2A and H2B might be the principal targets for O-GlcNAcylation while others have shown that histone H3 would be the main substrate [273, 274, 286, 288]. Upon further characterization, it was reported that histone H2B S112 O-GlcNAcylation promotes H2B monoubiquitination on lysine 120 (H2B K120ub), an event associated with transcriptional activation [288, 289]. On the other hand, histone H3 serine 10 was also reported to be O-GlcNAcylated, and this appears to compete with the phosphorylation of this site as well as modulate the transcriptional state of chromatin [273, 274]. Other O-GlcNAcylation sites were reported within the globular domains of histones suggesting that they may function in maintaining higher-order chromatin structure [286]. Strikingly, during our investigation on the role of OGT in chromatin function; we were unable to reproduce the previous findings regarding histone O-GlcNAcylation in mammalian cells, whereas modification of other known OGT substrates was readily detected. Our results raise questions about the occurrence of histone O-GlcNAcylation and its proposed function in chromatin regulation.

Results & discussion

Undetectable Histone O-GlcNAcylation using various extraction techniques

OGT interacts with the TET family of methylcytosine dioxygenase enzymes, notably TET2, which appear to be required for the chromatin association of OGT and this was suggested to promote histone O-GlcNAcylation [287, 290]. To further investigate the potential biological significance of histone O-GlcNAcylation, we initially sought to reproduce previously published results on the modification of histones H2B and H2A [273, 285, 287-289]. We co-expressed Flag-H2B or Flag-H2A with either Myc-OGT or the D925A catalytic inactive mutant (Myc-

OGT CD) [152]. Coexpression of Myc-TET2 with Myc-OGT was also included since their association was expected to significantly increase OGT-mediated histone O-GlcNAcylation.[287, 291] We conducted an immunoprecipitation of Flag-H2B or Flag-H2A under denaturing conditions to determine their potential O-GlcNAcylation levels by using the widely employed anti-O-GlcNAc antibodies RL2 and CTD110.6 (Figure 12 and Figure 2.S1).

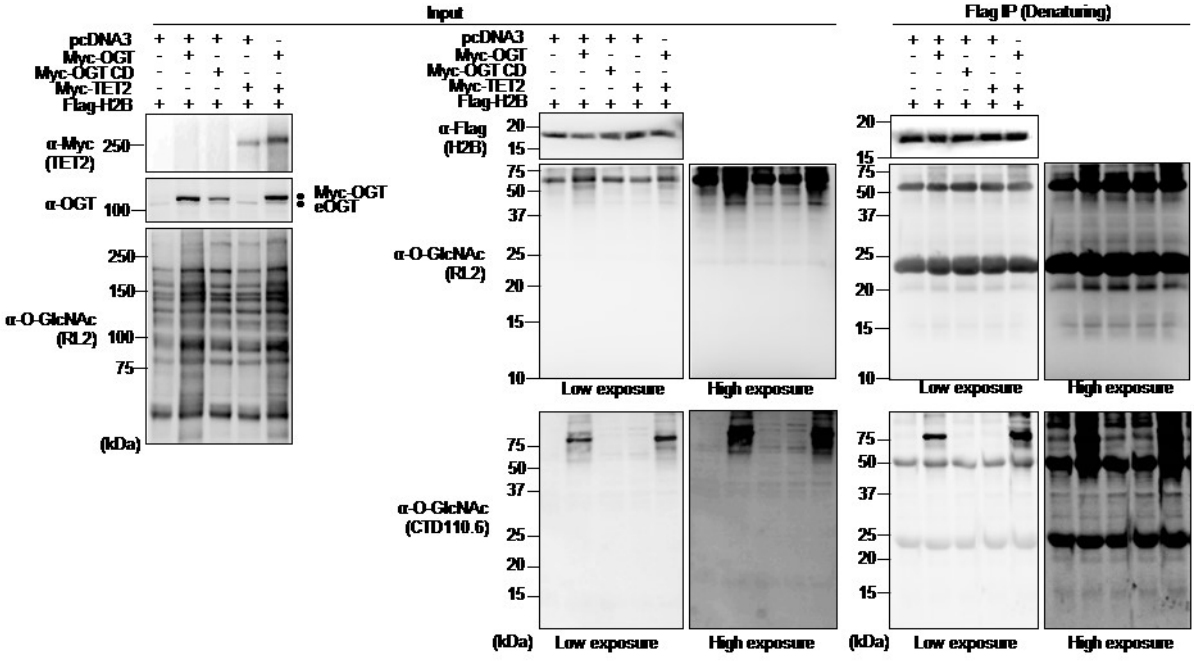

Figure 12. Undetectable Histone O-GlcNAcylation following OGT and TET2 overexpression. (A) HEK293T cells were transfected with Flag-H2B along with either pcDNA3 empty vector, Myc-OGT or Myc-OGT catalytic dead (CD), as well as Myc-TET2 alone or in combination with Myc-OGT. Three days post-transfection, cells pellets were harvested and immunoprecipitation (Flag-IP) following protein denaturation was conducted to obtain purified Flag-H2B. The immuno-purified histones were subjected to western blotting analysis using the indicated antibodies. Dots indicate Myc-OGT and endogenous OGT (eOGT). (B) HEK293T cells were transfected with either GFP-OGT or GFP-OGT catalytic dead (CD) in the presence of HA-HCF-1 full length (FL) or Myc-TET2 expression vectors. Three days post-transfection, cells were harvested and total cell lysates were subjected to immunoprecipitation (IP), following sample denaturation, using anti-Myc or anti-HA antibodies to purify TET2 and HCF-1 respectively. Total cell lysates (Input fractions) as well as immunopurifications were subjected to western blotting analysis using the indicated antibodies. Arrow indicates the full length (precursor) form of HCF-1 and brace indicates the cleaved forms of HCF-1. Dots indicate GFP-OGT and endogenous OGT (eOGT). kDa; Molecular weight marker in Kilodalton.

We did not detect a specific signal at the molecular weight region corresponding to histones Flag-H2B or Flag-H2A using the two anti-O-GlcNAc antibodies. However, using similar conditions, we were able to detect HCF-1 and TET2 O-GlcNAcylation, two known substrates of OGT (Figure 2.S1) [68, 282]. Of note, as expected, OGT-mediated HCF-1 proteolytic cleavage also confirmed the activity of OGT in our co-transfection conditions (Figure 2.S1)

[68, 69, 72]. Next, using the same transfection conditions indicated above, we performed several established extraction methods in order to enrich endogenous histones for O-GlcNAcylation detection. Chromatin and Histones were isolated using both high salt/detergent (300 mM NaCl, 1% NP-40) extraction (Figure 13A and Figure 2.S3A) and acid extraction (0.2 N HCl) (Figure 13B and Figure 2.S3B) methods, respectively. First, immunoblotting with RL2 or CTD110.6 antibodies was conducted on the soluble fractions to detect global O-GlcNAcylation levels (Figure 13 and Figure 2.S3, Left panels). As expected, we observed an increase of cellular O-GlcNAcylation levels following OGT overexpression. However, chromatin fractions revealed faint signals between 10 and 20 kDa when the blots probed with RL2 antibody were overexposed. The CTD110.6 antibody occasionally produced more pronounced signals at the levels of histones (Figure 13 and Figure 2.S3, Right panels). Overall, we did not observe increasing signals following overexpression of OGT or TET2, regardless of the O-GlcNAc antibody used, the quantity of proteins loaded or the method of extraction performed (Figure 13 and Figure 2.S3). On the other hand, upon OGT overexpression, we detected increased O-GlcNAcylation of certain chromatin-associated proteins corresponding to bands $\geq$ 37 kDa. Based on these results, we concluded that the faint and inconsistent signals produced between 10 and 20 kDa by the RL2 or CTD110.6 antibodies are not indicative of histone O-GlcNAcylation.

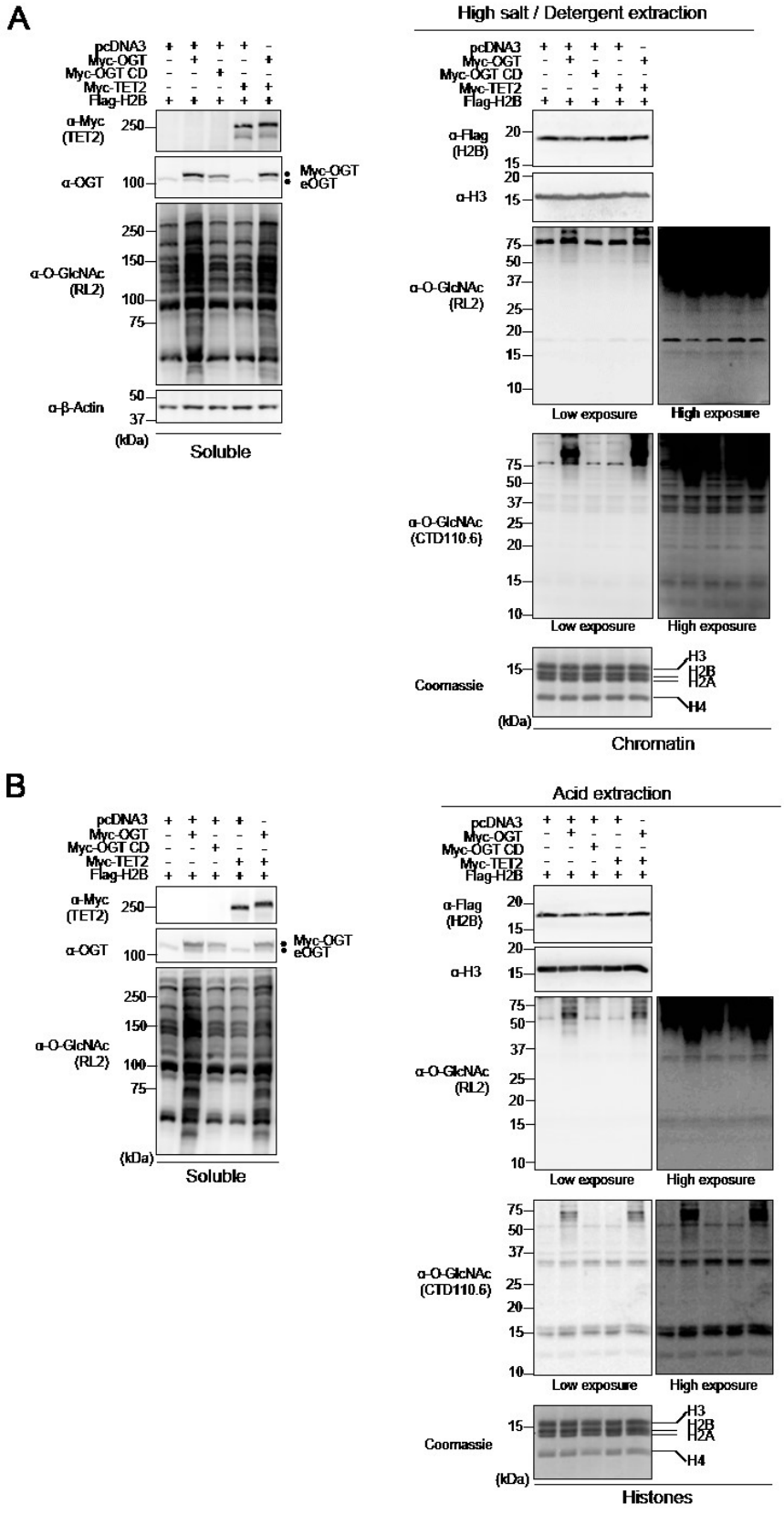
A
pcDNA3
Myc-OGT
Myc-OGT CD
Myc-TET2
Flag-H2B
α-Myc (TET2)
α-OGT
Myc-OGT
eOGT
α-O-GlcNAc (RL2)
α-β-Actin
(kDa)
Soluble
High salt / Detergent extraction
α-Flag (H2B)
α-H3
α-O-GlcNAc (CTD110.6)
Low exposure
High exposure
Coomassie
H3
H2B
H2A
H4
Chromatin
B
Acid extraction
Histones

Figure 13. Undetectable histone O-GlcNAcylation following various extraction procedures. (**A**) HEK293T cells were transfected with Flag-H2B along with either pcDNA3 empty vector, Myc-OGT, Myc-OGT catalytic dead (CD) or Myc-TET2, as well as the combination of Myc-OGT with Myc-TET2. Three days post-transfection, cells pellets were collected for subsequent high salt/detergent extraction and cellular extracts were then analysed by western blotting with the indicated antibodies. (Left panel) Soluble fraction showing global increase of O-GlcNAcylation following OGT overexpression. (Right panel) Immunodetection of histone O-GlcNAcylation by RL2 and CTD110.6 antibodies on chromatin fraction. β-Actin and histone H3 were used as loading controls. (**B**) HEK293T cells were transfected as in (**A**). Three days post-transfection, cells were harvested and histones were extracted. The samples were analysed by western blotting with the indicated antibodies. (Left panel) Soluble fraction showing global O-GlcNAcylation levels. (Right panel) Histones fraction detected with both RL2 and CTD110.6 anti-O-GlcNAc antibodies. Coomassie Brilliant Blue staining indicates abundance of histones loaded. Histone H3 was use as a loading control. Dots indicate Myc-OGT and endogenous OGT (eOGT). kDa; Molecular weight marker in Kilodalton.

Modulation of O-GlcNAc levels does not result in the detection of specific histone O-GlcNAcylation

We reasoned that if the signals detected by RL2 or CTD110.6 around 10-20 kDa correspond to histone O-GlcNAcylation, then it might be possible to modulate these signals by depleting endogenous OGT. Thus, we conducted siRNA knockdown of OGT in U2OS cells and performed cellular fractionation to separate the soluble and histone-containing chromatin fractions. As shown in figure 14A (Right panel), the signals detected with RL2 or CTD110.6 antibodies around 10-20 kDa, did not decrease following OGT depletion suggesting that these signals are unspecific. In contrast, using both antibodies, we detected a significant decrease in global O-GlcNAcylation in the soluble fraction upon siRNA treatment (Figure 14A, Left panel). Again, we noted that while the signal obtained with RL2 antibody in the 10-20 KDa region can be seen only upon overexposure of the membrane, the CTD110.6 antibody produced a much more readily detectable signal in this region. As RL2 and CTD110.6 are respectively IgG and IgM isotypes, we sought to determine if the signal detected at the level of histones with CTD110.6 could be due to the peroxidase-coupled secondary anti-IgM antibody. This is particularly relevant as high quantities of histones were probed with anti-O-GlcNAc antibodies. Thus, we incubated the blots with a non-relevant anti-rhodamine IgM antibody prior to incubation with the same anti-IgM HRP-conjugated antibody or with this secondary antibody alone (Figure 14A, Right panel). Interestingly, both combinations displayed a similar signal pattern as that obtained using the CTD110.6, suggesting that the non-specific signal originates from the combination of secondary anti-IgM antibody and high protein density of histone bands. In addition, probing the membranes with a non-relevant anti-BAP1 antibody also resulted in background signals at molecular weights corresponding to histone bands (Figure 14A, Right

panel). These data indicate that the high abundance of histones present on membranes renders the detection of O-GlcNAcylation amenable to false-positive immunoblotting signals. Of note, previous studies questioned the specificity of CTD110.6 towards O-GlcNAc and revealed cross-reactivity with N-GlcNAc$_2$-modified glycoprotein and GlcNAcylated O-mannose modified proteins [292, 293]. Consequently, we used the RL2 antibody to continue our investigation since it was not shown to cross react with other GlcNAc modifications. Nonetheless, our data suggested that the faint signal obtained with RL2 corresponds to a non-specific background caused by high amounts of histones. To further support our data, we extracted endogenous histones from HeLa cells for comparison with purified yeast H2B (yH2B) and recombinant human H2B (hH2B) produced in bacteria. We reasoned that if the faint signal produced by RL2 corresponds to histone O-GlcNAcylation, then this signal should not be detected for histones purified from yeast or bacteria which are not O-GlcNAcylated. We observed that the RL2 antibody produced low signals following overexposure of the blot, and these signals increased proportionally with the amount of histones loaded, irrespective of the species from which the histones were isolated (Figure 2.S4, panels A, B). Next, we conducted competition assays and found that, as expected, *N*-Acetylglucosamine (GlcNAc) inhibited RL2 binding to high molecular weight O-GlcNAcylated proteins present in the soluble fraction or associated with the chromatin fraction (Figure 2.S4C). However, GlcNAc also strongly reduced the signal produced by RL2, in the region of histone bands, for both mammalian chromatin and recombinant human H2B (Figure S4C). These results are not surprising as a non-specific and low affinity binding of the RL2 antibody to histone fraction could also be potentially blocked by GlcNAc. Thus, these results further suggest that the RL2 antibody recognizes non-specifically antigenic determinants on histones through its paratope.

To further investigate potential histone O-GlcNAcylation, we sought to determine if inhibiting O-GlcNAcase (OGA), the enzyme responsible for O-GlcNAc removal, with O-(2-acetamido-2-deoxyglucopyranosylidene) amino N-phenylcarbamate (PUGNAc) would increase the signal of histone O-GlcNAcylation above background levels. Treatment of HeLa and HEK293T cells with PUGNAc promoted the accumulation of O-GlcNAcylated proteins but not of the background signal at the level of histones (Figure 14B, Left and Right panel). We also conducted a nutrient starvation in C2C12 myoblasts, and analysed global protein and

potential histone O-GlcNAcylation. As expected, AMPK phosphorylation progressively increased and decreased with starvation and medium replenishment (R) respectively (Figure 14C, Left panel) [294]. We observed that while chromatin-associated high molecular weight protein O-GlcNAcylation was reduced upon starvation, only weak and inconsistent background signals were detected for histones (Figure 14C, Right panel).

Taken altogether, our results indicate that the immunoblot signal detected by RL2 in the region corresponding to histones, is a non-specific O-GlcNAcylation-independent background signal.

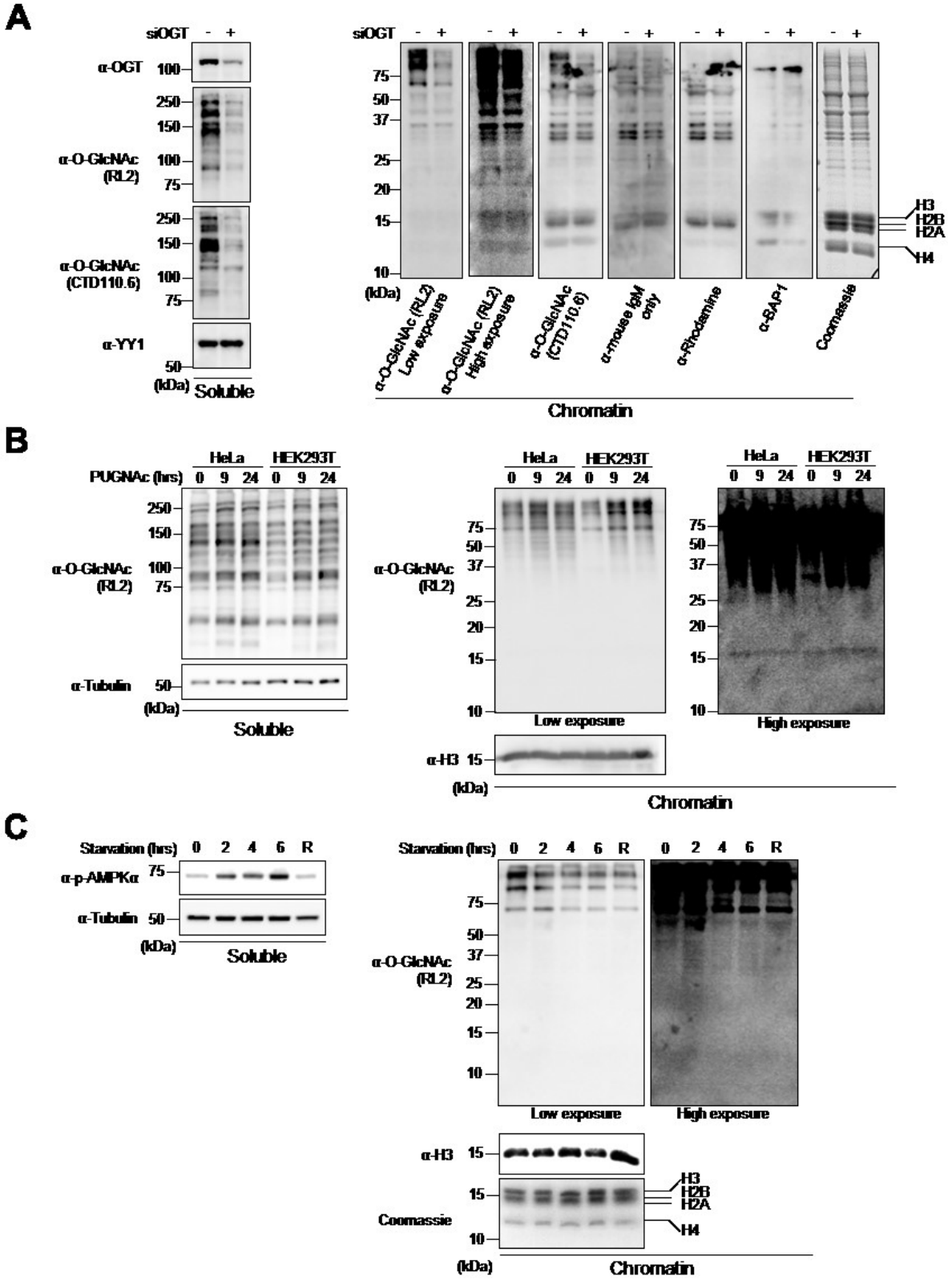
A
siOGT - +
α-OGT
100
250
150
α-O-GlcNAc (RL2)
100
75
250
150
α-O-GlcNAc (CTD110.6)
100
75
α-YY1
50
(kDa)
Soluble
siOGT - + - + - + - + - + - + - +
75
50
37
25
20
15
10
(kDa)
α-O-GlcNAc (RL2) Low exposure
α-O-GlcNAc (RL2) High exposure
α-O-GlcNAc (CTD110.6)
α-mouse IgM only
α-Rhodamine
α-SAP-1
Coomassie
H3
H2B
H2A
H4
Chromatin
B
HeLa HEK293T
PUGNAc (hrs) 0 9 24 0 9 24
250
150
α-O-GlcNAc (RL2)
100
75
α-Tubulin
50
(kDa)
Soluble
HeLa HEK293T
0 9 24 0 9 24
75
50
37
25
20
15
10
α-O-GlcNAc (RL2)
Low exposure
α-H3
15
(kDa)
Chromatin
HeLa HEK293T
0 9 24 0 9 24
75
50
37
25
20
15
10
High exposure
C
Starvation (hrs) 0 2 4 6 R
α-p-AMPKα
75
α-Tubulin
50
(kDa)
Soluble
Starvation (hrs) 0 2 4 6 R 0 2 4 6 R
75
50
37
25
20
15
10
α-O-GlcNAc (RL2)
Low exposure
High exposure
α-H3
15
15
Coomassie
10
H3
H2B
H2A
H4
(kDa)
Chromatin

Figure 14. Modulation of O-GlcNAcylation does not result in detectable histone O-GlcNAcylation. (**A**) U2OS cells were transfected twice with OGT siRNA and three days post-transfection, cells were harvested. Chromatin fraction was isolated and protein levels were analysed by western blotting with the indicated antibodies. (Left) U2OS soluble fraction showing OGT depletion and decrease of global O-GlcNAcylation levels. YY1 was used as a loading control. (Right) Chromatin fraction showing O-GlcNAcylation background detection of histones using various antibodies. (**B**) HeLa and HEK293T cells that were treated with 100 μM PUGNAc for 0, 9 and 24 hours. The soluble and chromatin fractions were blotted with RL2 antibody. Histone H3 and Tubulin were used as loading controls. (**C**) C2C12 mouse myoblast cell line were starved by incubation in HBSS buffer, and harvested at the indicated times for cellular fractionation. R; 4 hours of starvation followed by 2 hours of replenishment with complete culture medium. (Left) Western blot analysis of the soluble fraction showing increasing levels of phosphorylated AMPKα (α-p-AMPKα) as a control of the starvation treatment. Tubulin was used as a loading control. (Right) The chromatin fraction was analysed by western blotting using the indicated antibodies. Histone H3 was used as a loading control and Coomassie Brilliant Blue staining indicates the abundance of histones loaded. kDa; Molecular weight marker in Kilodalton.

Undetectable histone O-GlcNAcylation in different cell lines and during cell cycle progression

Although our data did not reveal constitutive histone O-GlcNAcylation, we could not exclude that this post-translational modification might occur on histones in specific cell types. Thus, we investigated potential histone O-GlcNAcylation in a variety of previously used cell lines including mouse Embryonic Fibroblast (MEF) as well as mouse Embryonic Stem Cells (mESCs) [287, 289, 291]. We also included the mouse pre-adipocyte 3T3-L1 cell line often used in differentiation studies as well as several multiple myeloma cell lines, RPMI-8226, JJN-3, NCI-H292 cells, that we had in culture at the time of our investigation. We find that this cell line panel is representative of multiple tissue-origins as well as primary and cancer cells. When immunoblotting the insoluble chromatin fraction for O-GlcNAcylation, we detected a very faint signal at the level of histones (Figure 15A, Top panel). This signal, obtained only following extended exposure of the blot, does not correlate with the cell-specific levels of endogenous O-GlcNAcylation detected for high molecular weight proteins. Instead, by probing total H2A levels, it can be noticed that the RL2 signal follows the trend of histones abundance (Figure 4A, Bottom blot).

To further determine whether histone O-GlcNAcylation might be enriched in a specific phase of the cell cycle, U2OS cells were synchronized at the G1/S boundary with a double thymidine block and released to progress through the cell cycle [242]. These cells were also treated with the CDK1 inhibitor (RO-3306) to enrich for late G2 cells (Figure 15B, Top panel) [295]. The chromatin fraction was isolated from cells at different phases of the cell cycle and histone O-GlcNAcylation was monitored by western blotting using the RL2 antibody. We

noticed the expected faint signal at the level of histones and that this signal did not change during cell cycle progression. However, high molecular weight chromatin-associated proteins show significantly increased O-GlcNAcylation at G1/S transition. Therefore, we concluded that fluctuating histone O-GlcNAcylation could not be observed during cell cycle. Moreover, along with our previous data, these results strengthen the notion that the signal detected by RL2 at the level of histones following blot overexposure corresponds to background.

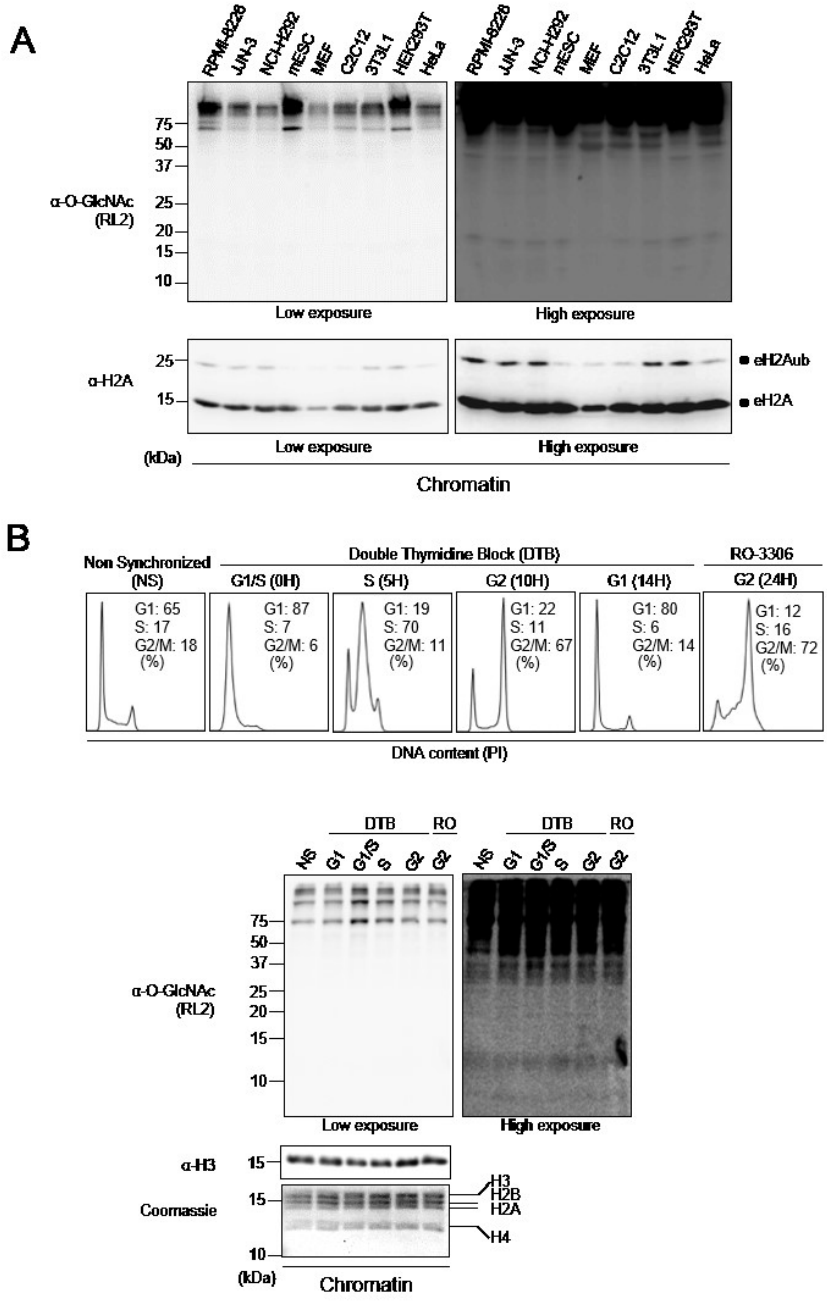

Figure 15. Unspecific signal detected at the level of histones in various cell lines and during cell cycle progression. (A) Various cell lines were cultured and harvested to perform chromatin extraction. The chromatin fraction was analysed by western blotting with the indicated antibodies. Total histone H2A was used as a loading control. Dots indicate endogenous H2A ubiquitination (eH2Aub) and total H2A (eH2A). (B) Histones O-GlcNAcylation analysis of synchronized U2OS cells. Cells were blocked in G1/S boundary by double thymidine block (DTB) and then released to progress through the cell cycle. U2OS cells were also treated with the CDK1 inhibitor, RO-3306, for 24 hours to block cells in late G2. Cells were harvested at the indicated times for FACS analysis (Upper panel) and for chromatin extraction (Bottom panel). The chromatin fraction was analysed by western blotting with the indicated antibodies and by Coomassie Brilliant Blue staining. Histone H3 was used as a loading control. NS; Non-Synchronized, DTB; Double Thymidine Block. kDa; Molecular weight marker in Kilodalton.

Lack of evidence supporting H2B Ser112 O-GlcNAcylation and its link with H2B Lys120 monoubiquitination

It was reported that H2B S112 is O-GlcNAcylated (H2B S112 O-GlcNAc), an event that appears to promote the monoubiquitination of H2B Lys120 (H2B K120ub) thus coordinating gene expression [288]. It was also described that AMPK-mediated OGT Thr444 phosphorylation hindered its ability to associate with chromatin, and this was shown to reduce the reported H2B S112 O-GlcNAc signal [126]. In turn, this effect was proposed to inhibit monoubiquitination of H2B K120, thus repressing gene expression in MEF cells [289]. As an anti-O-GlcNAcylated H2B S112 is commercially available [289], we first inquired about the specificity of this antibody. Since H2B S112 O-GlcNAc was shown to decrease dramatically following knockdown of OGT by RNAi, we used a similar approach to deplete OGT by siRNA in HeLa cells (Figure 16A) [288, 289]. As expected, OGT knockdown resulted in the accumulation of the precursor form of HCF-1, as its proteolytic maturation is O-GlcNAcylation-dependent (Figure 16A, Left panel) [68, 69, 72]. However, neither the signal generated by the anti-H2B S112 O-GlcNAc nor that for anti-H2B K120ub changed following OGT depletion (Figure 16A, Right panel). In addition, we expressed Flag-H2B WT and Flag-H2B S112A mutant in HEK293T cells and conducted anti-Flag immunoprecipitation under denaturing conditions (Figure 16B). Unexpectedly, the anti-H2B S112 O-GlcNAc signal decreases by only ~3-fold in the H2B S112A mutant, instead of completely disappearing. In addition, we observed no change in H2B K120ub levels. Our results could not validate the reported link between H2B S112 O-GlcNAc and H2B K120ub and moreover further suggest that the anti-H2B S112O-GlcNAc antibody might not confer specific detection for H2B O-GlcNAcylation. Next, we sought to further investigate the anti-H2B S112 O-GlcNAc antibody specificity by producing recombinant human histones H2B (His-hH2B) and H2B S112A (his-

hH2B S112A) purified from bacteria (Figure 16C). We also used a GST-H2A construct as a negative control. Following relative quantification of recombinant histones shown by Coomassie Brilliant Blue staining (Figure 16C, Top panel), we subsequently probed increasing quantities of these proteins by immunoblotting using the anti-H2B S112O-GlcNAc antibody. We found that purified recombinant proteins are detectable using this antibody and that this signal decreased by about two to three folds when the serine was mutated to alanine (His-hH2B S112A) (Figure 16C, Middle panel). Moreover, the H2B S112O-GlcNAc signal detected for the recombinant His-hH2B protein is comparable to that detected for a similar amount of mammalian endogenous H2B in the chromatin fraction (Figure 16C, Bottom panel). Thus, these results indicate that this antibody recognizes the H2B backbone itself rather than O-GlcNAc moiety and that unmodified S112 is a major determinant in epitope recognition by this antibody.

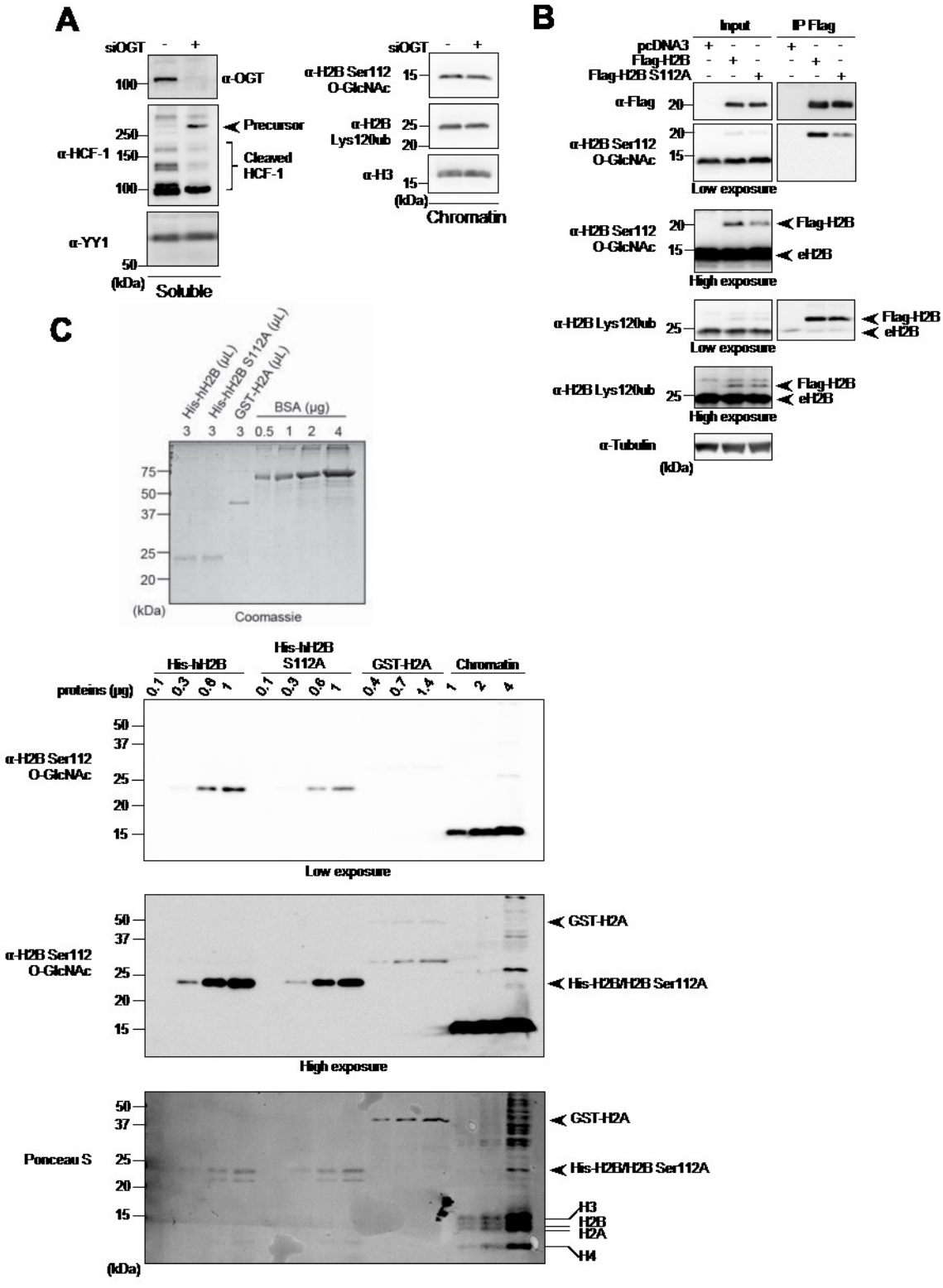
A
siOGT - +
α-OGT
100
Precursor
250
α-HCF-1 150
Cleaved HCF-1
100
α-YY1
50
(kDa)
Soluble
siOGT - +
α-H2B Ser112 O-GlcNAc 15
α-H2B Lys120ub 25 20
α-H3 15
(kDa)
Chromatin
B
Input
IP Flag
pcDNA3 + - - + - -
Flag-H2B - + - - + -
Flag-H2B S112A - - + - - +
α-Flag 20
α-H2B Ser112 O-GlcNAc 20 15
Low exposure
α-H2B Ser112 O-GlcNAc 20 15
Flag-H2B
eH2B
High exposure
α-H2B Lys120ub 25
Flag-H2B
eH2B
Low exposure
α-H2B Lys120ub 25
Flag-H2B
eH2B
High exposure
α-Tubulin
(kDa)
C
His-hH2B (μL)
His-hH2B S112A (μL)
GST-H2A (μL)
BSA (μg)
3 3 3 0.5 1 2 4
75
50
37
25
20
(kDa)
Coomassie
His-hH2B
His-hH2B S112A
GST-H2A
Chromatin
proteins (μg)
0.1 0.3 0.6 1 0.1 0.3 0.6 1 0.4 0.7 1.4 1 2 4
α-H2B Ser112 O-GlcNAc
50 37 25 20 15
Low exposure
α-H2B Ser112 O-GlcNAc
50 37 25 20 15
GST-H2A
His-H2B/H2B Ser112A
High exposure
Ponceau S
50 37 25 20 15
GST-H2A
His-H2B/H2B Ser112A
H3
H2B
H2A
H4
(kDa)

Figure 16. H2B Ser112 O-GlcNAc antibody is not specific and Ser112 O-GlcNAcylation is not linked to H2B K120 monoubiquitination. (A) HeLa cells were transfected twice with OGT siRNA and three days post-transfection, cells were harvested to perform cellular fractionation. Protein levels were analysed by western blotting with the indicated antibodies. HeLa soluble fraction was analysed for HCF-1 proteolytic cleavage. YY1 was used as a loading control (left panel). Chromatin fraction was analysed for H2B Ser112 O-GlcNAc and H2B Lys120ub levels (Right panel). (B) HEK293T cells were transfected with Flag-H2B or Flag-H2B Ser112A. Three days post-transfection, cells were harvested and total cell lysates were subjected to protein denaturation and immunoprecipitation (IP) using α-Flag antibody. Input as well as IP fractions were subjected to immunoblotting analysis using the indicated antibodies. Arrows indicate Flag-H2B and endogenous H2B (eH2B). Tubulin was used as a loading control for the input fraction. (C) Relative quantification of eluted purified recombinant histones detected by Coomassie Brilliant Blue staining. Known amounts of BSA protein were used as standards for relative quantification (top panel). Increasing amounts of recombinant His-hH2B, His-hH2B Ser112A mutant, GST-H2A as well as chromatin extract from HEK293T cells were analysed by western blot using the indicated antibodies. Red Ponceau S staining of the membrane used for subsequent western blotting showing the loading of purified proteins (bottom panel). Arrows and lines indicate the position of recombinant and endogenous histones respectively. kDa; Molecular weight marker in Kilodalton.

Undetectable binding of mammalian histones to the Wheat Germ Agglutinin (WGA) lectin

It was previously reported that HeLa cell nucleosomes obtained by micrococcal digestion can be enriched with a WGA lectin resin which is known to strongly bind O-GlcNAcylated proteins [288]. However, the extraction procedure does not preclude histone binding to the WGA column as a consequence of interaction of histones with O-GlcNAcylated proteins associated with nucleosomes. Thus, we sought to use an acid extraction procedure to separate the soluble histones from all other proteins that remain in the insoluble fraction. Moreover, acid treatment ensures denaturation of proteins, thereby preventing potential interactions of histones with O-GlcNAcylated proteins associated with chromatin. We cultured HEK293T cells with PUGNAc for 24 hours and also included this inhibitor during the extraction steps to exclude the possibility of losing protein O-GlcNAc modification [273]. Moreover, to ensure that acid treatment does not influence detection of O-GlcNAc modification, we also analyzed the ability of chromatin-associated-proteins in the acid extraction mixture to bind the WGA column (Figure 17). Importantly, HCF-1 and several chromatin-associated proteins were enriched approximately 5 to 10 times compared to the input signal, thus confirming that the WGA resin strongly and efficiently binds O-GlcNAcylated proteins (Figure 17, Left panel). This result also indicates that acid treatment did not covalently modify or disrupt the O-GlcNAc moiety. In contrast, immunoblotting with RL2, anti-H2B S112 O-GlcNAc or anti-H2A revealed that histones were found only in the input and the flow through

fractions (Figure 17, Right panel). Consistently, staining of histones with Coomassie Brilliant Blue did not reveal histones binding to WGA-agarose. Note that the background signal produced by the RL2 antibody at the level of histones was observed in the input and the flow through fractions. To further exclude the possibility that only a small fraction of histones are modified in proliferating human cells, and that such limited amounts of modified histones are below immunoblotting detection thresholds, we carried out a WGA pull-down experiment in conditions that would allow for the total depletion of HCF-1 from the cell lysate (Figure 2.S5, Left panel). Even in these conditions, histones were again only detected in the inputs and the flow through fractions by immunodetection and silver staining (Figure 2.S5, Right panels). Altogether, these data support our findings that histone O-GlcNAcylation is undetectable in mammalian cells.

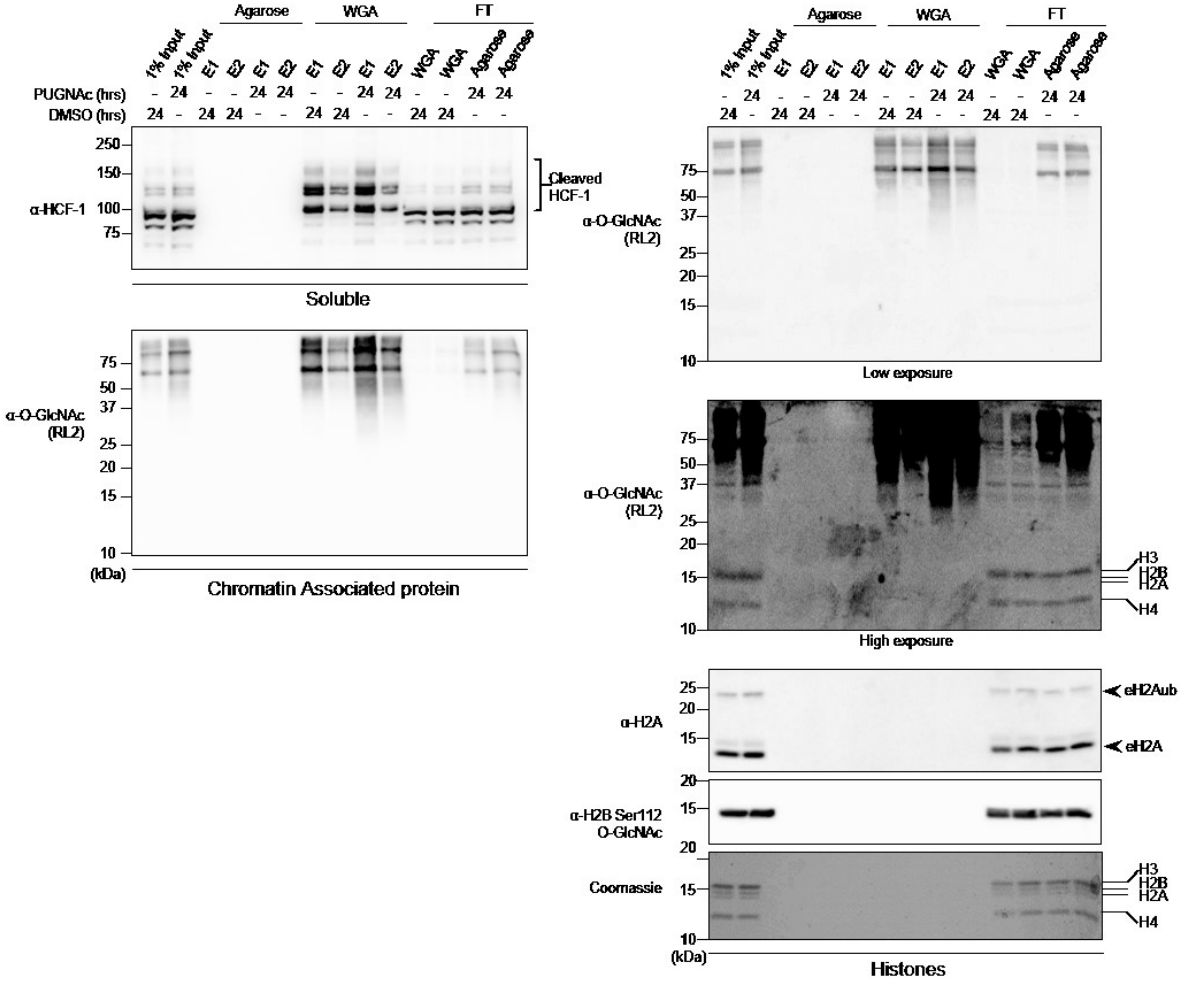

Figure 17. HCF-1 and several chromatin-associated proteins but not histones bind to WGA lectin. HEK293T cells were treated with 100 µM PUGNAc or equal volume of DMSO for 24 hours as indicated and harvested to perform acid extraction of histones. The indicated soluble and chromatin-associated-proteins fractions (Left panels), and histone fraction (Right panels) were incubated for 2 hours with agarose bound WGA lectin or with agarose resin to control for non-specific binding. Two elutions (E1 and E2) of agarose and WGA bound proteins as well as the flow through (FT) fractions were analysed by western blot using the indicated antibodies. The Coomassie Brilliant Blue staining and the anti-H2A antibody indicate that histones are found in the input and the FT fractions. Arrows indicate endogenous H2A ubiquitination (eH2Aub) and total H2A (eH2A). kDa; Molecular weight marker in Kilodalton.

Histone O-GlcNAcylation is not detected by *Click-it* biotin-alkyl chemistry, mass spectrometry or following *in vitro* O-GlcNAcylation reactions

To further corroborate our observations, we sought to use other methods for O-GlcNAcylation detection. We first used the commercially available *in vitro Click-it* chemistry system. This procedure consists in modifying O-GlcNAcylated proteins with an azido sugar (GalNAz), which can then react with biotin-alkyne thus becoming detectable via streptavidin-conjugated HRP [296]. This approach is highly sensitive since it allows for the detection of the O-GlcNAcylation of α-crystallin, a lens protein that was reported to be O-GlcNAcylated at a very low stoichiometric ratio [296, 297]. Thus, we performed the *Click-it* chemistry reaction on histones extracted from HeLa cells, as well as on α-crystallin, used as the positive control. As shown in Figure 7A, although similar amount of both purified histones and α-crystallin were used (Figure 18A, Right panel), we could only detect O-GlcNAcylation of α-crystallin in these conditions (Figure 18A, Left panel). Moreover, O-GlcNAcylation of co-purified high molecular weight proteins could be readily observed, thus demonstrating the efficiency of GalNAz labeling in the same reaction conditions as histones.

Next, we sought to determine, by performing ETD-MS/MS analysis, if we could recapitulate the reported histone O-GlcNAcylation sites using acid extracted histones from HeLa cells. We also purified HCF-1 from HEK293T cells and included it as a positive control. Mass spectrometry analysis by HCD and ETD for proper glycan localization was conducted [298]. As shown in Figure 2.S6 and Supplemental Table 1, in addition to several novel sites, we were able to identify 6 of the reported HCF-1 O-GlcNAcylation sites [68, 69, 299-303]. However, we were unable to detect O-GlcNAcylation of the core histones. Indeed, even though the MS analysis revealed the presence of histone peptides that were reported to be modified (e.g., H2B S112, H2A T101, H3 S10 and H4 S47), we did not detect their corresponding O-GlcNAcylated forms (Figures 2.S7 and 2.S8).

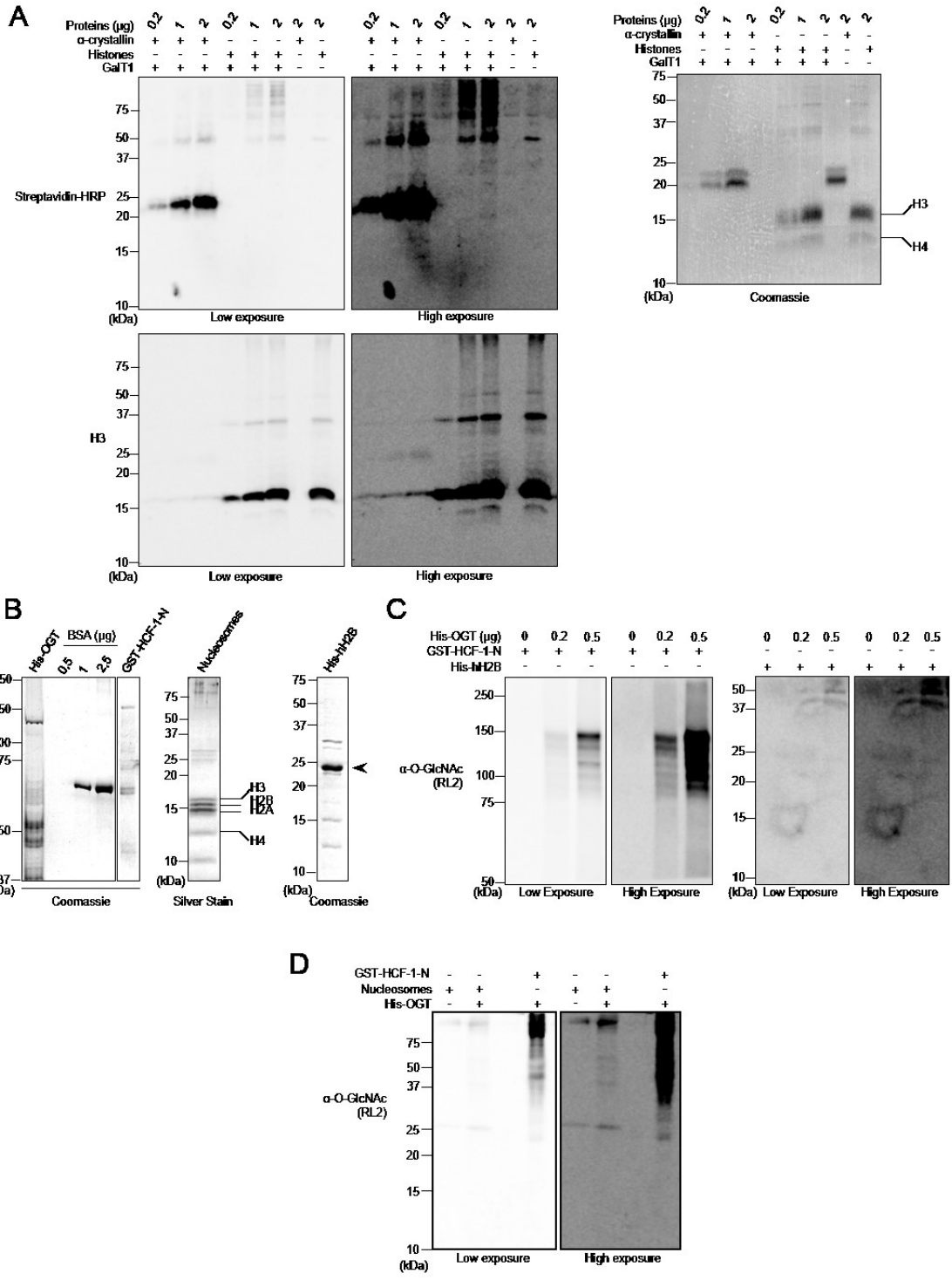
A
Proteins (µg)
α-crystallin
Histones
GalT1
Streptavidin-HRP
H3
Low exposure
High exposure
Coomassie
H4
(kDa)
B
His-OGT
BSA (µg)
GST-HCF-1-N
Nucleosomes
His-hH2B
Coomassie
Silver Stain
H2B
H2A
C
His-OGT (µg)
GST-HCF-1-N
His-hH2B
α-O-GlcNAc
(RL2)
Low Exposure
High Exposure
D
Nucleosomes
His-OGT
Low exposure
High exposure

Figure 18. Histones are not modified by Click-it biotin-alkyl chemistry or by *in vitro* OGT-mediated O-GlcNAcylation. (A) The poorly O-GlcNAcylated α-crystallin is detected with the click-it biotin-alkyl chemistry but not histones. HeLa cells were harvested and acid extraction followed by acetone precipitation was performed to purify histones. The GalNAz labeling reaction was carried out for a minimum of 16 hours and the biotin-alkyl reaction was performed in the presence or absence of the GalT1 enzyme. (Left panel) O-GlcNAcylation was analysed by blotting with streptavidin-HRP. (Right panel) Coomassie Brilliant Blue staining shows the indicated amounts of used purified proteins. (B-D) Histones are not O-GlcNAcylated *in vitro* by OGT. (B) Purified proteins analysed by Coomassie Brilliant Blue or silver staining as indicated. (Left panel) Relative quantification of purified recombinant His-OGT and GST-HCF-1-N to known amounts of BSA. (Middle and Right panels) Integrity of Flag-H2A-purified mammalian nucleosomes and recombinant His-hH2B. (C) *In vitro* O-GlcNAcylation reaction of the purified recombinant His-hH2B. GST-HCF-1-N and recombinant His-hH2B were incubated with increasing amounts of recombinant His-OGT for 4 hours. O-GlcNAcylation was detected by western blotting using the anti-O-GlcNAc antibody (RL2). (D) *In vitro* O-GlcNAcylation reaction of the purified mammalian nucleosomes by OGT. GST-HCF-1-N and nucleosomes were incubated in the absence or presence of His-OGT for 11 hours. The O-GlcNAcylation was detected as in (C). kDa; Molecular weight marker in Kilodalton.

Previous studies reported that histones can be modified by OGT *in vitro* [288]. Thus, we performed *in vitro* O-GlcNAcylation reactions using purified recombinant human His-hH2B and purified mammalian nucleosomes. As a positive control, we also used purified recombinant GST-HCF-1N (for N-Terminal HCF-1) [304] as this domain is a well-established substrate of OGT [68, 69, 304]. The relative quantity and integrity of the purified proteins were assessed by Coomassie Brilliant Blue staining or silver staining as indicated (Figure 18B). As shown in Figures 18C and 18D, we detected a strong O-GlcNAcylation of HCF-1-N, but not of the recombinant His-hH2B (Figure 18C) or nucleosomal histones (Figure 18D).

In summary, using various approaches, we were unable to detect histone O-GlcNAcylation. Thus, our study provides strong evidence that histone O-GlcNAcylation, if occurring, must be present at levels below detection limits of commonly available tools, while O-GlcNAcylation of other known proteins including HCF-1 and TET2 can be observed. We emphasize that histones are hundreds- to thousands-folds more abundant than the majority of cellular proteins and their modifications, even in relatively low abundance, are in general easily monitored. On the other hand, detection of histone modifications can be prone to false-positive signals, especially when analyzing a large amount of proteins by immunoblotting.

Acknowledgements

We thank Haider Dar and Diana Adjaoud for technical assistance. This work was supported by grants from the Canadian Institutes of Health Research (CIHR) (MOP-115132) and the Natural Sciences and Engineering Research Council of Canada (NSERC) (355814-2010) to E.B.A and (435636-2013) to H.W.. E.B.A. is a scholar of the Fonds de la Recherche

du Québec - Santé (FRQ-S) and the CIHR. H.W is a scholar of the FRQ-S, J.G. has a M.Sc. scholarship from the FRQ-S. The Proteomics facility at The Institute for Research in Immunology and Cancer (IRIC) receives infrastructure support from IRICoR, the Canadian Foundation for Innovation, and the Fonds de Recherche du Québec- Santé (FRQS).

Material & Methods

Plasmids and mutagenesis

Plasmids and mutagenesis

The cDNA of human of OGT and TET2 were cloned from HeLa total RNA by reverse transcription and inserted into pENTR D-Topo plasmid (Life Technologies). Expression construct of Myc-TET2 was generated by recombination using LR clonase kit (Life Technologies) into pDEST-Myc construct. pCGN-HCF-1 FL was previously described [305, 306]. Myc-OGT, Myc- OGT D925A catalytic inactive mutant (Myc-OGT CD) were also previously described [68] GFP-OGT and GFP-OGT CD were generated by recombination into pDEST-GFP expression construct. pcDNA3-Flag-H2A and pcDNA3-Flag-H2B were obtained from Dr. Moshe Oren [307]. H2B and H2A were generated using gene synthesis (BioBasic) and then subcloned into modified pENTR D-Topo plasmid. H2B S112A construct was generated by site direct mutagenesis using Q5 High-Fidelity DNA Polymerase. The Primers used are: Forward primer: CACGCCGTG**G**CGGAGGGCACCAAGGCCGTCA; Reverse primer: TGCCCTCCG**C**CACGGCGTGCTTGGCCAGCTC. HCF-1N was amplified from pCGN-HCF-1 FL and inserted into pENTR D-Topo plasmid. The T antigen NLS coding sequence was added in the primers. His-OGT was generated by subcloning the OGT cDNA into pET30a+ vector. Expression constructs of H2B and H2B S112A were generated by recombination using LR clonase kit into pDEST-Flag or pDEST-6xHis constructs. Expression constructs of H2B and HCF-1N were generated by recombination into pDEST-Flag or pDEST-GST constructs. All DNA constructs were sequenced.

Immunoblotting and antibodies.

Total cell lysates were prepared by harvesting cells with buffer containing 25 mM Tris-HCl pH 7.3 and 1% sodium dodecyl sulfate (SDS). Cell extracts were boiled at 95°C for 10 min

and sonicated. Quantification of total proteins was conducted using the bicinchoninic acid (BCA) assay [308]. Total cell extracts as well as chromatin fractions and immunoprecipitation samples were diluted in 2X or 4X Laemmli buffer**.** SDS-PAGE and immunoblotting were conducted according to standard procedures. The band signals were acquired with a LAS-3000 LCD camera coupled to MultiGauge software (Fuji, Stamford, CT, USA).

Mouse monoclonal anti-BAP1 (C4, sc-28383), rabbit polyclonal anti-YY1 (H414, sc-1703), rabbit polyclonal anti-OGT (H300, sc-32921), mouse monoclonal anti-Tubulin (B-5-1-2, sc-SC-23948), were from Santa Cruz. Rabbit polyclonal anti-HCF-1 (A301-400A) was from Bethyl Laboratories. Mouse monoclonal anti-Flag (M2) was from Sigma-Aldrich. Mouse monoclonal anti-MYC (9E10) was from Covance. Rabbit polyclonal anti-H2B K120ub (D11 XP) was from Cell Signaling. Rabbit polyclonal anti-H2B S112 O-GlcNAc (ab130951), rabbit polyclonal anti-H2A (ab18255) Rabbit polyclonal anti-H3 (ab1791) and mouse monoclonal anti-O-Linked *N*-acetylglucosamine (RL2, ab2739) were from Abcam. The mouse monoclonal anti-O-Linked *N*-acetylglucosamine (CTD110.6) was kindly provided by Dr. Gerald Hart [156]. Mouse monoclonal anti-β-Actin (MAB1501, clone C4) was from Millipore. Anti-rhodamine (IgM) was a generous gift from Dr. Li-Huei Tsai. Peroxidase Affini-Pure Goat anti-mouse IgM μ chain specific secondary antibody was from Jackson Laboratories.

Cell culture and cell transfection

U2OS osteosarcoma, HeLa, human embryonic kidney HEK293T, 3T3-L1 mouse preadipocytes, C2C12 mouse myoblasts, mouse embryonic fibroblasts (MEF) cell lines were grown in Dulbecco's modified Eagle's medium (DMEM) supplemented with 10 % of foetal bovine serum (FBS), L-glutamine and penicillin/streptomycin. Multiple myeloma cell lines (JJN-3, RPMI-8226, NCI-H292) were cultured in RPMI-1640 medium supplemented with 10 % of foetal bovine serum (FBS), L-glutamine and penicillin/streptomycin. Mouse embryonic stem cells (mESCs) were maintained in DMEM medium supplemented with 15% of embryonic stem cells qualified FBS (Gibco), L-glutamine, penicillin/streptomycin, 0.1 mM β-mercaptoethanol, 0.1 mM MEM (Non-essential amino acids), 1 mM sodium pyruvate and 1,000 U/ml of leukemia inhibitory factor (LIF) (Life technologies).

HeLa or HEK293T cells were treated with 100 µM of PUGNAc or equal volume of DMSO for 0, 9 and 24 hours and were subjected to sub-cellular fractionation (soluble and chromatin) or histone extraction. HEK293T cells were transfected with mammalian expressing vectors using polyethylenimine (PEI) (Sigma-Aldrich). Three days post-transfection, cells were harvested for immunoblotting using total cell extracts or following cellular fractionation and histones extraction. Prior to immunoblotting, histones were also immunoprecipitated using anti-Flag antibody following denaturation of cell extracts. HeLa or U2OS cells were transfected using Lipofectamine 2000 (Life technologies) with 200 pmol of either ON-TARGET plus Non-targeting pool (D-001810-10-50) or ON-TARGET plus SMARTpool OGT (L-019111-00-0050) (Thermo Scientific, Dharmacon). Cells were transfected in a serum-free DMEM medium for 16 hours, then changed with DMEM complemented with 5 % FBS, 1 % Glutamine and 1 % Penicillin-Streptomycin and 8 hours later, cells were transfected again as described above. Three days following the first transfection, cells were harvested in PBS and soluble and chromatin extractions were conducted and used for immunoblotting.

Histone and chromatin extraction

For histone extraction, HEK293T cells were transfected with Flag-H2A or Flag-H2B with or without Myc-OGT, Myc-OGT CD, Myc-TET2 or with the combination of Myc-OGT and Myc-TET2 and harvested three days post-transfection. For high salt/detergent chromatin extraction, cells were lysed in 300 mM NaCl, 1% NP-40, 2 µM PUGNAc, 1 mM PMSF and 1 X protease inhibitors (Sigma). Samples were kept on ice for 15 min and then centrifuged at 6,000 rpm for 10 min. The supernatant was kept as the soluble fraction for western blotting analysis. The pellet was washed 2 times with the previous buffer and resuspended in 1% SDS for protein quantification. For the histones acid extraction, cells were lysed in 50 mM Tris-HCl pH 7.4, 300 mM NaCl, 2 mM EDTA and 2 µM PUGNAc. The lysate was centrifuged at 6,000 rpm for 10 min and the supernatant was kept as the soluble fraction. The pellet was washed 2 times with the same buffer and treated with 0.2 N HCl (1 volume of buffer for 1 volume 0.4 HCl) for 1 hour on ice. After centrifugation at 14,000 rpm for 5 min, the supernatant containing histones was neutralized by adding equal volume of 100 mM Tris-HCl pH 8.8. The pellet was also resuspended in 1% SDS. To quantify proteins, part of the histones fraction was precipitated using 100% acetone at -20°C for 2 hours, centrifuged at 14,000 rpm for 10 min and resuspended

in 1% SDS. Proteins were then quantified using the BCA assay. For chromatin extraction, the cell pellet was resuspended in 50 mM Tris-HCl pH 7.3, 300 mM NaCl, 5 mM EDTA, 1% Triton, 2 μM PUGNAc, 1X protease inhibitors (Sigma) and 1 mM PMSF and kept on ice for 30 min. The chromatin was pelleted by centrifugation at 10,000 rpm for 10 min at 4^0C, the supernatant was kept (soluble fraction) and the chromatin pellet was resuspended in 25 mM Tris-HCl pH 7.3 and 1 % SDS. Both fractions were quantified using the BCA protein quantification method.

Wheat Germ Agglutinin lectin Pull-Down

HEK293T cells were either treated with 100 μM PUGNAc or DMSO for 24 hours. Cells were then harvested in 1X PBS and the cell pellet was lysed with 0.25 M sucrose, 3 mM $CaCl_2$, 1 mM Tris-HCl pH 8.0, 0.5 % triton, 2 μM PUGNAc and 1X protease inhibitors (Sigma). The chromatin was pelleted by centrifugation at 3,900 rpm for 5 minutes at 4°C and the supernatant was kept (soluble fraction). Next, the pellet was washed with 300 mM NaCl, 5 mM $MgCl_2$, 1% Triton, 50 mM Tris-HCl pH 8.0, 5 mM DTT and 2 μM PUGNAc and centrifuged at 3,900 rpm for 5 min at 4°C. Supernatant was discarded and the pellet was very quickly resuspended in 3 volumes of acid extraction buffer containing 0.5 M HCl, 10% glycerol and 0.1 M β-mercaptoethanol and left on ice for 30 min. The sample was centrifuged at 14,000 rpm for 5 min at 4°C, the supernatant containing the histones was transferred in a new tube and 10 volumes of acetone were added to both the pellet (chromatin-associated proteins) and the supernatant (histones) fractions and were left at -20 °C overnight. The next day, protein precipitates were pelleted at 14,000 rpm for 1 hour at 4°C, resuspended in 25 mM Tris-HCl pH7.3 and 1 % SDS, sonicated and diluted in 10 volumes of EB300 Buffer containing 50 mM Tris-HCl pH7.5, 300 mM NaCl, 5 mM EDTA, 1% Triton X-100, 1X protease inhibitors (Sigma), 1 mM PMSF, 1 mM DTT and 2 μM PUGNAc. The samples were incubated for 2 hours with WGA lectin resin (Vector Laboratories, #AL-1023) or agarose beads, washed with EB300 buffer and eluted with 500 mM *N*-acetylglucosamine. Sample were then analysed by western blotting.

Immunoprecipitation

For histone immunoprecipitation following denaturation, HEK293T cells were transfected with Flag-H2A or Flag-H2B with pcDNA3 empty vector, Myc-OGT or Myc-OGt CD, Myc-TET2 or the combination of Myc-OGT with Myc-TET2 using Polyethylenimine (PEI). Three days post-transfection, cells were harvested and the cell pellets were lysed in 20 mM Tris-HCl pH 8.0, 600 mM NaCl, 0.5% NP-40, 0.5% SDS, 0.5% sodium deoxycholate, 1 mM EDTA and 2 µM PUGNAc. Samples were sonicated and centrifuged at 14,000 rpm for 10 min. The lysate was then diluted in 5 volumes of 50 mM Tris-HCl pH 7.4, 2 mM EDTA and 100 mM NaCl. For TET2 and HCF-1 immunoprecipitation, HEK293T cells were transfected with Myc-TET2 or HA-HCF-1 FL with and without GFP-OGT or GFP-OGT CD. Three days post-transfection, cells were harvested to perform denaturing immunoprecipitation. Briefly cells pellets were lysed using 300 mM NaCl containing buffer (50 mM Tris-HCl pH 7.5, 300 mM NaCl, 1% Triton, 1% SDS, 10 mM NaF, 5 mM EDTA 1 mM PMSF, 2 µM PUGNAc and 1X protease inhibitors (Sigma)). After boiling for 3 min in the lysis buffer, cell lysate was sonicated and samples were diluted 10 folds with the same buffer but without SDS prior to immunoprecititation using anti-Myc or anti-HA antibodies. For mutant histones, HEK293T cells were transfected with PEI with either FLAG-H2B or FLAG-H2B S112A. Three days post-transfection, cells were harvested for denaturing immunoprecipitation in 25 mM Tris pH 7.3 and 1.5 % SDS. Next, suspensions were diluted 10 times with dilution buffer containing 50 mM Tris-HCl pH7.5, 100 mM NaCl, 1% Triton, 1 mM EDTA, 1 mM DTT, 1 mM PMSF, 1X protease inhibitors (Sigma), 2 µM PUGNAc and 20 mM N-Ethylmaleimide (NEM, Sigma). Suspensions were mixed with anti-FLAG M2 resin (Sigma Aldrich #A2220) overnight at 4 ^{0}C. Next day, beads were washed 5 times with the dilution buffer. Proteins were then eluted from the beads by adding Laemmli Buffer 2X and analysed by western blotting.

Recombinant proteins

pDEST-6xHis-H2B, pDEST-6xHis-H2BS112A, pDEST-GST-HCF-1-N and pET30a+ OGT were transformed into RIL bacteria. Following induction with 400 µM IPTG, recombinant proteins were purified either under native or denaturing conditions. For the denaturing immunopurification, the bacterial pellets were lysed in 50 mM Tris-HCl pH 8, 8 M Urea and 3

mM DTT and left on ice for 30 min. After incubation, suspensions were sonicated and centrifuged at 16,000 rpm for 20 min. Supernatants were incubated with Ni-NTA Agarose resin (Invitrogen #R901-15) overnight at 4 ^{0}C and the resin was then washed with 50 mM Tris-HCl pH 8.0, 500 mM NaCl, 3 mM DTT and 20 mM imidazole and transferred into a Bio-Spin Disposable Chromatography columns (Bio Rad #732-6008). Proteins were eluted with 200 mM Imidazole. For the native purification of His-H2B, His-H2B S112A and His-OGT, cell pellets were lysed in 50 mM Tris pH 8, 500 mM NaCl and 3 mM DTT, 1 mM PMSF, 1X protease inhibitors (Sigma) and left on ice for 30 min. After incubation and sonication, the purified proteins were obtained as described above except for His-OGT which was kept on the Ni-NTA Agarose resin in order to use it for the *in-vitro* O-GlcNAcylation reaction. The OGT Ni-NTA Agarose resin beads were washed 6 times and kept in 50 mM Tris-HCl pH 7.5, 12.5 mM $MgCl_2$, 3 mM DTT, 10% glycerol, 1 mM PMSF, 1X protease inhibitors (Sigma). The induction of GST-H2A expression in bacteria was done in the same manner as indicated above. Pellets of cells were lysed on ice in 50 mM Tris-HCl pH 8, 150 mM NaCl, 1 mM EDTA, 1 % Triton, and 1 mM PMSF, 1 mM DTT, 1X protease inhibitors (Sigma). The lysates were sonicated, centrifuged at 16,000 rpm for 20 min and supernatants were incubated with GSH-Agarose (Sigma Aldrich #A8580) overnight at 4 ^{0}C. Then, the resin was washed with 50 mM Tris-HCl pH 7.5, 150 mM NaCl, 1 mM EDTA, 0.1% Tween20, 1 mM PMSF, 200 μM DTT and 1X protease inhibitors (Sigma)). Proteins were eluted with the same buffer containing 250 mM reduced gluthatione. GST-HCF-1-N was purified in the same manner as GST-H2A. Elutions of His-H2B, His-H2B S112A, GST-H2A and GST-HCF-1N were loaded on SDS-PAGE for Coomassie Brilliant Blue staining using BSA for relative quantification.

Purification of the nucleosomes

For mammalian nucleosomes purification, HEK293T cells were transfected with 7 μg of pCDNA-Flag-H2A using PEI in serum free media. Three days post-transfection, cells were harvested and chromatin fraction extraction and nucleosomes were purified using anti-Flag beads as previously described [60]. For yeast Flag-H2B nucleosomes purification, 2 liters of cells expressing Flag-H2B were grown under standard conditions and 4 grams of cell pellet

were used for the purification. Briefly, cells were resuspended in the SP Buffer (20 mM HEPES 7.4, 1.2 M sorbitol, 10 mM DTT) supplemented with 5 mg/ml of Zymolyase 20T. When the spheroplasting is completed, the cell pellet is washed again with the SP buffer and then resuspended in the Buffer L (20 mM HEPES 7.4, 18% Ficoll 400, 20 mM KCl, 5 mM $MgCl_2$, 1 mM EDTA, protease inhibitors (1 µg/ml leupeptin, pepstatin, aprotinin), 3 mM DTT, 1 mM PMSF) prior to the dounce homogenization. The extract was then diluted with the Buffer S (buffer L supplemented with 2.4 M sorbitol instead of Ficoll) and chromatin fraction was recovered by centrifugation at 11,000 rpm for 20 min. The chromatin pellet was washed with the IP buffer (20 mM HEPES 7.6, 150 mM KCl, 5% glycerol, 5 mM $MgCl_2$, 1 mM $CaCl_2$, 0.1% NP-40, protease inhibitors, 1 mM PMSF prior to the MNase treatment. After MNase treatment (15KU/ml for 30 min at room temperature), the reaction was stopped with 1 mM EDTA and 5 mM EGTA. Following centrifugation at 20,000g for 5 min at 4°C, the soluble chromatin fraction was incubated 1 hour at 4°C with anti-Flag M2 beads. The beads were washed four times with the IP2 buffer (same as IP buffer but with 1 mM EDTA, 1 mM EGTA and without $CaCl_2$). Bound nucleosomes were then eluted with 200 µg/ml of Flag peptides (Biobasic Inc.)

Click-it chemistry

HeLa cells were harvested and acid extraction was performed to purify histones as described for the WGA pull-down. Following acetone precipitation the histones were resuspended in 1% SDS, 20mM HEPES pH 7.9 and quantified using the BCA assay. The GalNAz labeling reaction was performed following the manufacturer's instructions using the Click-iT® GalNAz metabolic glycoprotein labeling reagent kit (Life Technologies). α-crystalline was included as a positive control. Following labeling of histones and α-crystalline, the detection was carried out with the Click-iT® Biotin Glycoprotein Detection Kit (Life Technologies) and the reaction was loaded on SDS-PAGE for blotting analysis using streptavidin-HRP (Cell Signaling #3999S) affinity detection.

In Purified GST-HCF-1-N (0.2 µg) and recombinant His-H2B (0.4 µg) were incubated with purified His-OGT (0.2 to 0.5 µg) in the presence of UDP-GlcNAc (1 mM) at 37°C overnight for 4 or 11 hours. The reaction was carried out in 50 mM Tris-HCl pH 7.5 containing 12.5 mM $MgCl_2$ and 3 mM DTT. Purified nucleosomes were also included in the O-

GlcNAcylation reaction as described above. The reaction was stopped by adding Laemmli buffer and analysed by immunoblotting.

Synchronization and cell cycle analysis

U2OS cells were synchronized at the G1/S border using the method of thymidine (2 mM) double block as previously described [242]. Cells were then released into new media to follow the progression through S and G2/M phases. U2OS cells were also arrested in late G2 by treating them with 10 μM of the CDK1 inhibitor RO-3306 for 24 hours [295]. Cell cycle analysis was carried out as described [242].

Cell starvation.

C2C12 cells were incubated for 6 hours in the Hanks Balanced Salt Solution (HBSS) medium completed with 10 mM HEPES pH 7.5 and penicillin/streptomycin. After 4 hours of treatment, a separate plate dish of cells was replenished with fresh media and released for another 2 hours. Cells pellets were harvested at the indicated times for chromatin extraction.

Mass spectrometry analysis

Reduction of histone and HCF-1 samples was performed by adding 5 mM DTT in 50 mM ammonium bicarbonate. Alkylation was performed with chloroacetamide 50 mM with ammonium bicarbonate 50 mM. The digestion with trypsin was performed for 8 h at 37°C. Samples were loaded and separated on a homemade reversed-phase column (150 μm i.d. x 150 mm) with a 106-min gradient from 0–40% acetonitrile (0.2% FA) and a 600 nl/min flow rate on an Easy nLC-1000 (Thermo Fisher Scientific) connected to an LTQ-Orbitrap Fusion (Thermo Fisher Scientific). Each full MS spectrum acquired with a 70,000 resolution was followed by 10 MS/MS spectra, where the 10 most abundant multiply charged ions were selected for MS/MS sequencing. Tandem MS experiments were performed using high-energy C-trap dissociation (HCD) and electron transfer dissociation (ETD) acquired in the Orbitrap. Peaks were identified using a Peaks 7.0 (Bioinformatics Solution Inc.) and peptide sequences were blasted against the human Uniprot database (74,530 sequences). Tolerance was set at 10 ppm for precursor and 0.01 Da for fragment ions during data processing and with

carbamidomethylation (C), oxidation (M), deamidation (NQ), and Hex-N-acylation (ST) as variable modifications.

Supplemental Figures and Tables

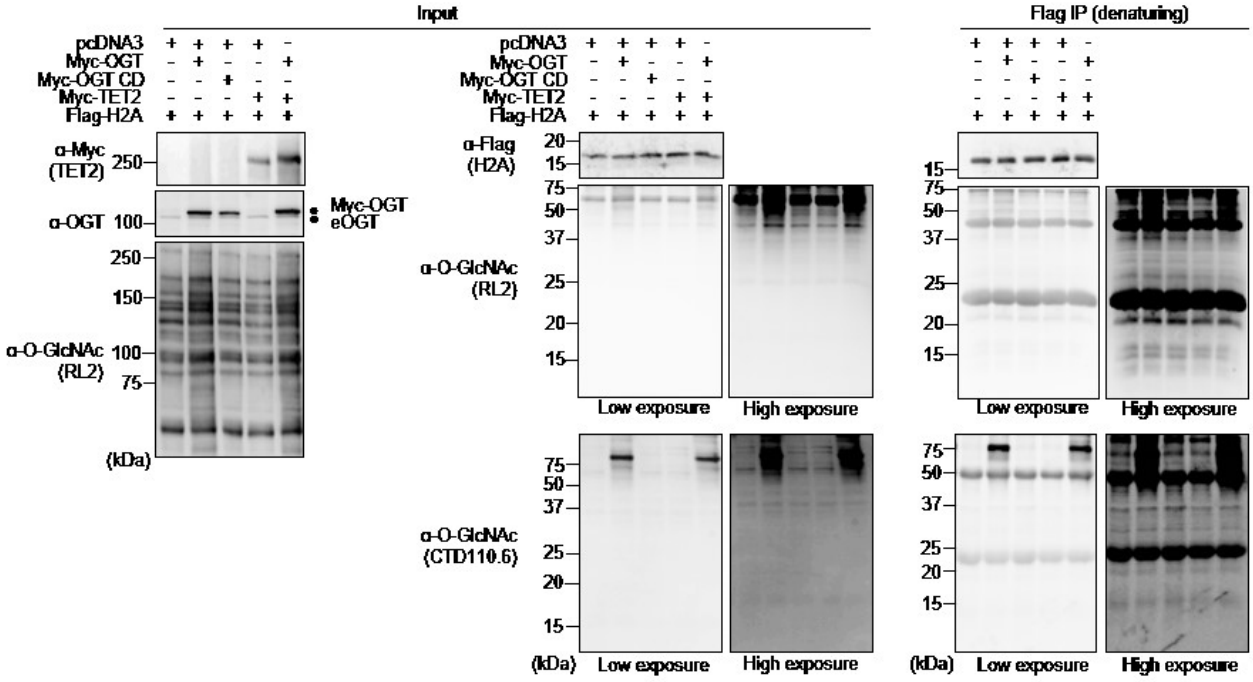

Figure 2.S1 Undetectable O-GlcNAcylation of histone H2A. HEK293T cells were transfected with Flag-H2A along with either pcDNA3 empty vector, Myc-OGT, Myc-OGT catalytic dead (MYC-OGT CD) or Myc-TET2, as well as the combination of Myc-OGT with Myc-TET2. Three days post-transfection, cells were harvested and analysed for Flag-H2A O-GlcNAcylation as conducted for Flag-H2B (see Fig.1). Flag immunoprecipitation (Flag-IP) of exogenous H2A was conducted following sample denaturation. Dots indicate Myc-OGT and endogenous OGT (eOGT). kDa; Molecular weight marker in Kilodalton.

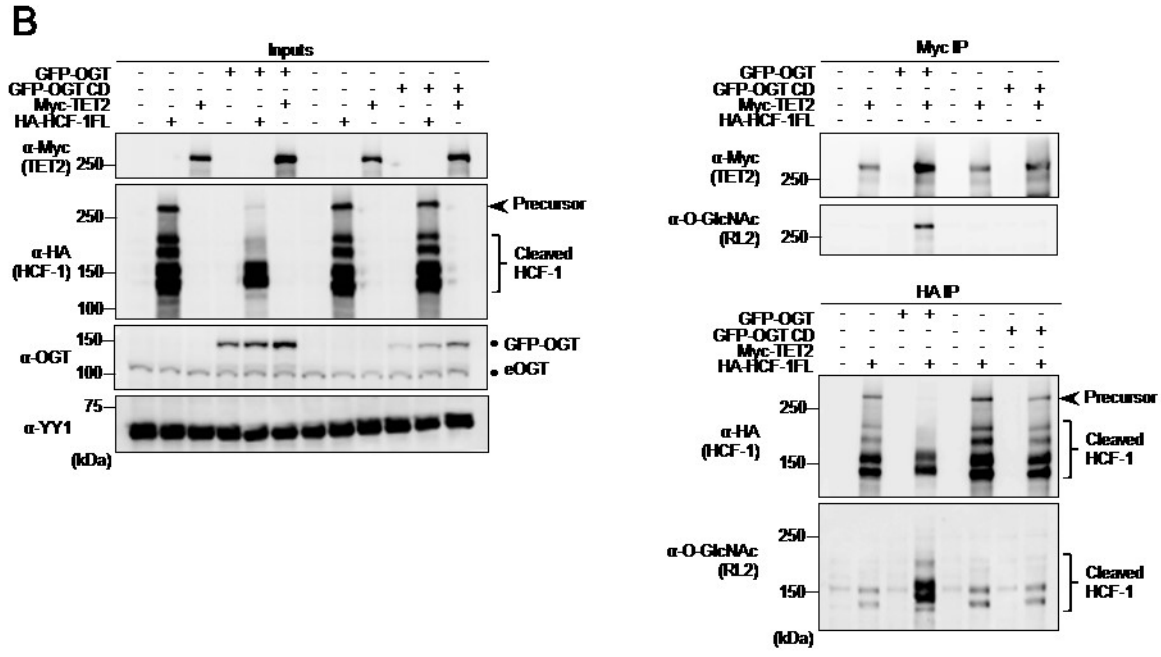

Figure 2.S2 OGT O-GlcNAcylates both TET2 and HCF-1 and Modulates HCF-1 cleavage. HEK293T cells were transfected with either GFP-OGT or GFP-OGT catalytic dead (CD) in the presence of HA-HCF-1 full length (FL) or Myc-TET2 expression vectors. Three days post-transfection, cells were harvested and total cell lysates were subjected to immunoprecipitation (IP), following sample denaturation, using anti-Myc or anti-HA antibodies to purify TET2 and HCF-1 respectively. Total cell lysates (Input fractions) as well as immunoprecipitations were subjected to western blotting analysis using the indicated antibodies. Arrow indicates the full length (precursor) form of HCF-1 and brace indicates the cleaved forms of HCF-1. Dots indicate GFP-OGT and endogenous OGT (eOGT). kDa; Molecular weight marker in Kilodalton.

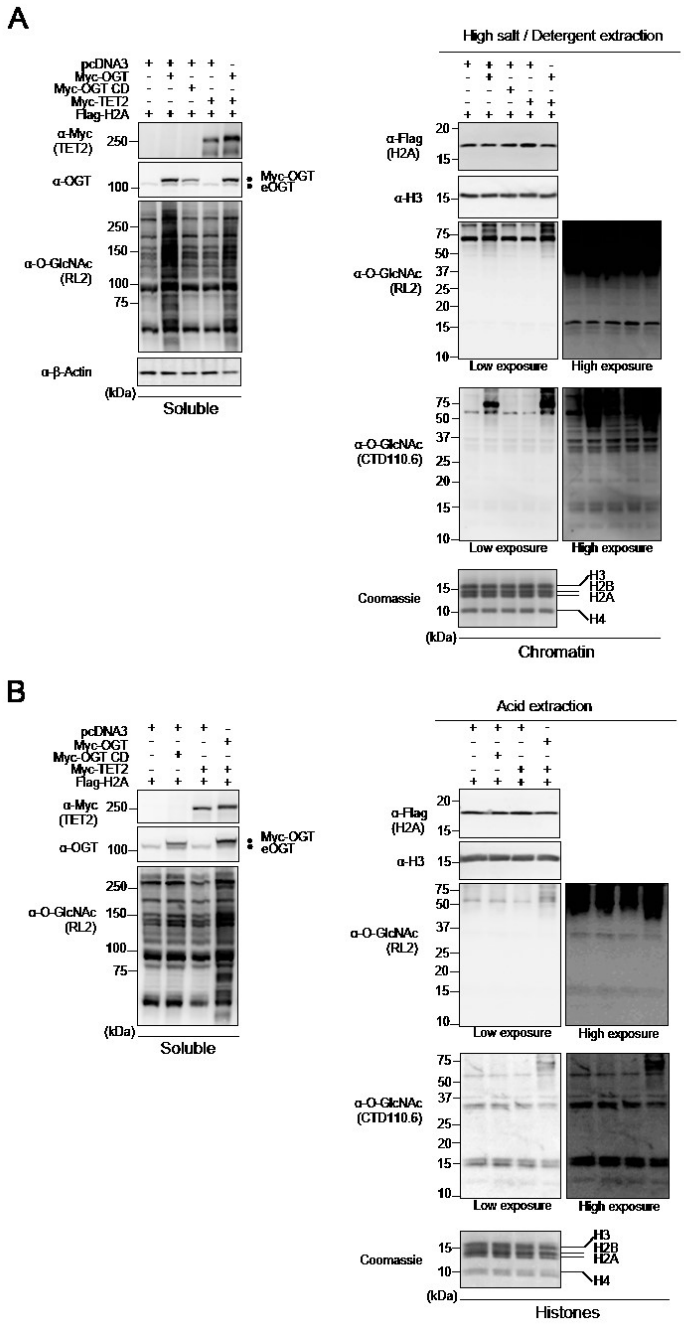

Figure 2.S3 Undetectable O-GlcNAcylation of endogenous histones. HEK293T cells were transfected as in Supplemental Fig.1. Three days post-transfection, cells pellets were collected for subsequent high salt / high detergent extraction as well as histones acid extraction and cellular extracts were analysed by western blotting with the indicated antibodies. (**A**) Chromatin high salt extraction. (Left) Soluble fraction showing global increase of O-GlcNAcylation following OGT overexpression. (Right) Detection of O-GlcNAcylation using RL2 and CTD110.6 antibodies on chromatin fraction. (**B**) Histone acid extraction showing (Left) the soluble fraction and global O-GlcNAcylation levels and (Right) the histone fraction detected with both O-GlcNAc antibodies. β-Actin and histone H3 were used as loading controls. Coomassie Brilliant Blue staining indicates abundance of histones loaded. Dots indicate Myc-OGT and endogenous OGT (eOGT). kDa; Molecular weight marker in Kilodalton.

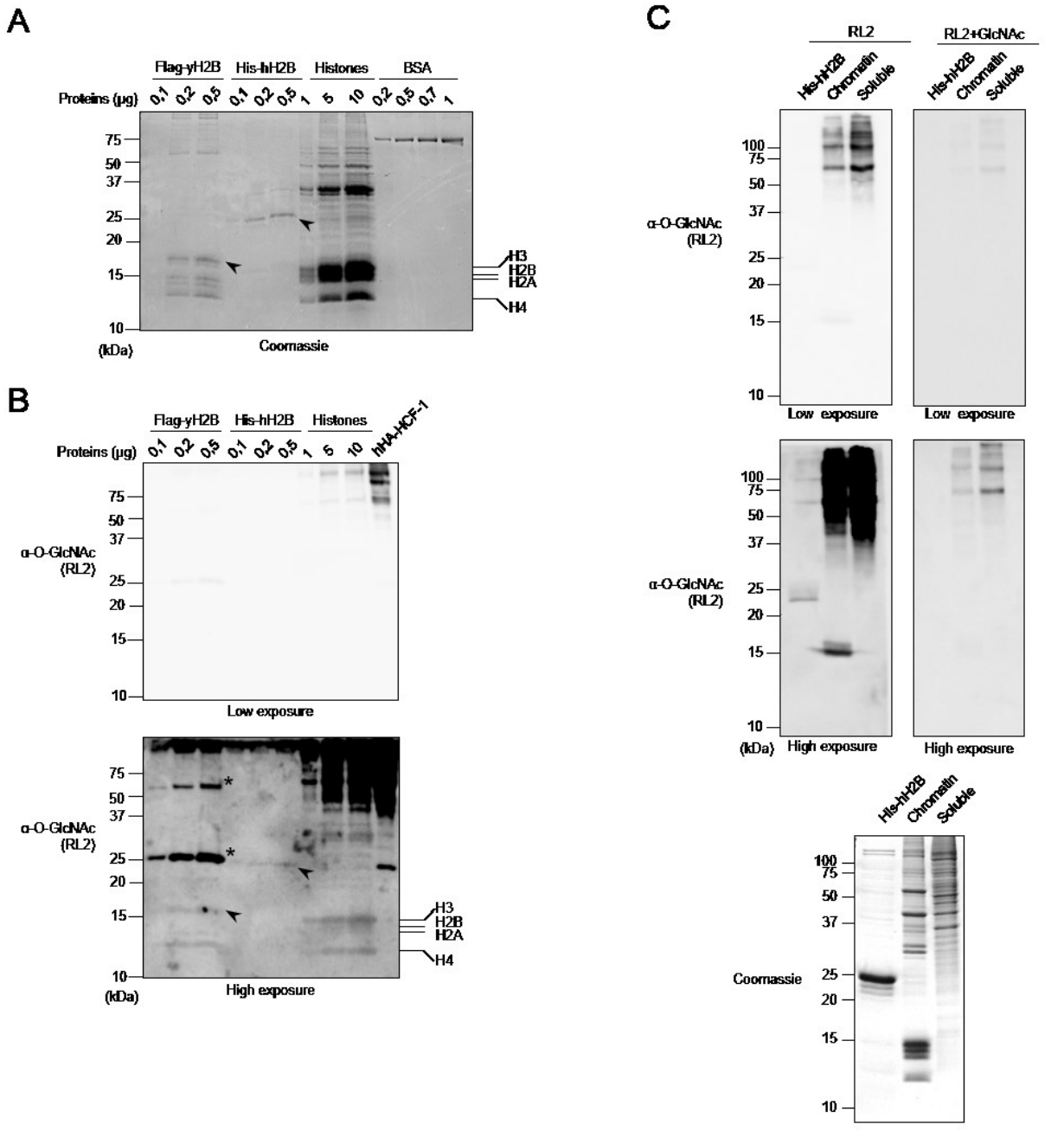

Figure 2.S4 Detection of background immunoblotting of mammalian, yeast or recombinant histones (A) Coomassie Brilliant Blue staining showing molecular weight and relative quantification of purified recombinant yeast Flag-H2B (Flag-yH2B), human His-H2B (His-hH2B) and acid extracted histones purified from HeLa cells relative to bovine serum albumin (BSA). (B) Increasing amounts of recombinant Flag-yH2B, His-hH2B and acid extracted histones from HeLa cells quantified in (A) were analysed by western blot using α-O-GlcNAc (RL2) antibody. Purified human HCF-1(hHA-HCF-1) from HEK293T cells was used as a control for RL2 detection. Lines indicate purified endogenous histones from HeLa cells and Flag-yH2B. Arrows indicate Flag-yH2B and His-hH2B position. Asterisks indicate non-specific signal from the heavy and light chains of Flag antibody respectively. (C) N-Acetyl-D-Glucosamine competition with RL2 antibody. RL2 antibody was incubated with 1M of N-acetylglucosamine (GlcNAc) for 1 hour. Antibody mixture was then used to immunoblot recombinant human His-hH2B, chromatin and soluble fractions from U2OS cells. Coomassie Brilliant Blue staining was used as a loading control. kDa; Molecular weight marker in Kilodalton.

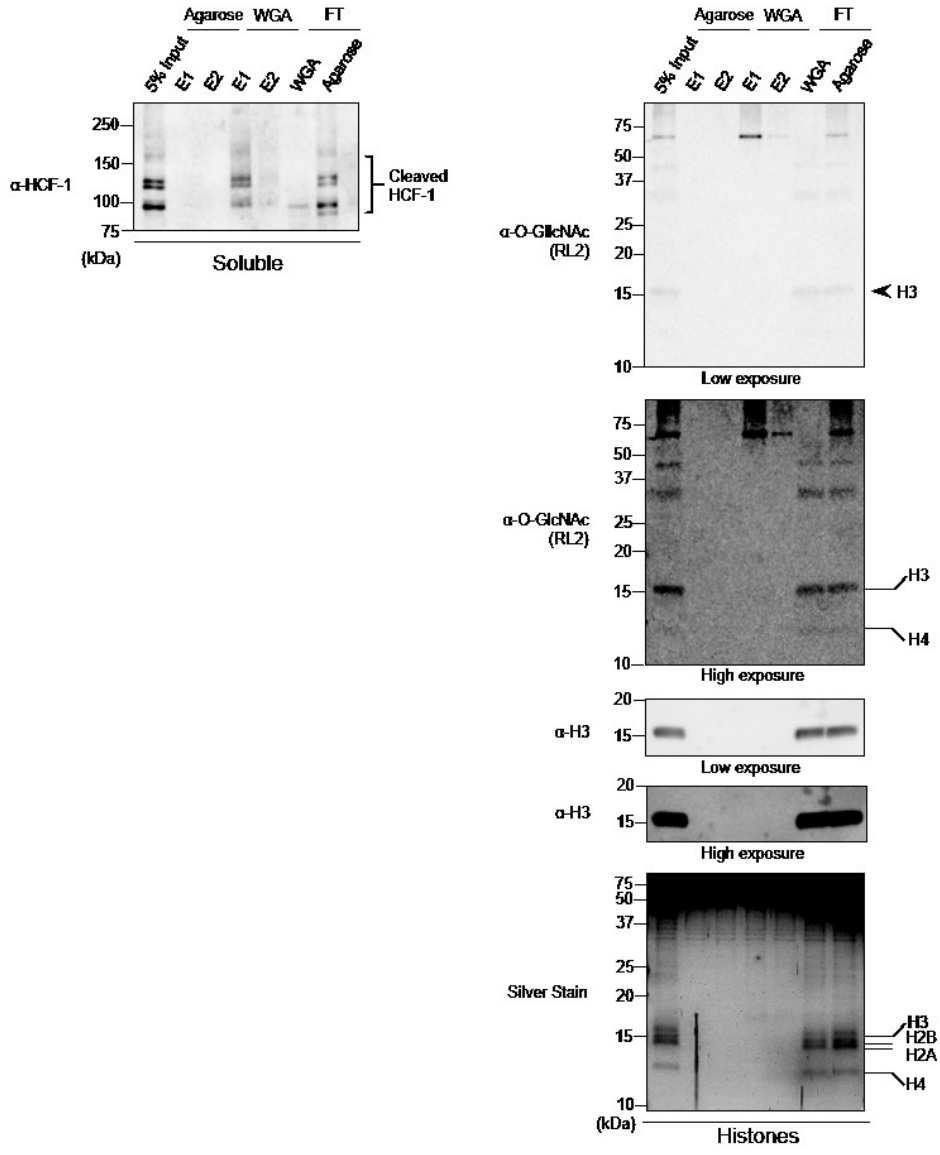

Figure 2.S5 The core histones are not enriched by WGA lectin resin in conditions that ensure complete HCF-1 depletion from extracts. HeLa cells were harvested and acid extraction of histones was performed. The indicated soluble (Left panel) and histone fractions (Right panel) were incubated overnight with the agarose bound WGA lectin resin or with the agarose resin to control for non-specific binding. The flow through (FT) was kept and the proteins were eluted from the resins (E1 and E2) with N-acetylglucosamine (GlcNAc). Soluble fraction showing depletion of HCF-1 on the WGA lectin resin (Left panel) . Western blot and silver stain analysis of the collected elutions revealed no interaction between the core histones and the WGA lectin resin (Right panel). Arrows and lines indicate histones molecular weight. kDa; Molecular marker in Kilodalton.

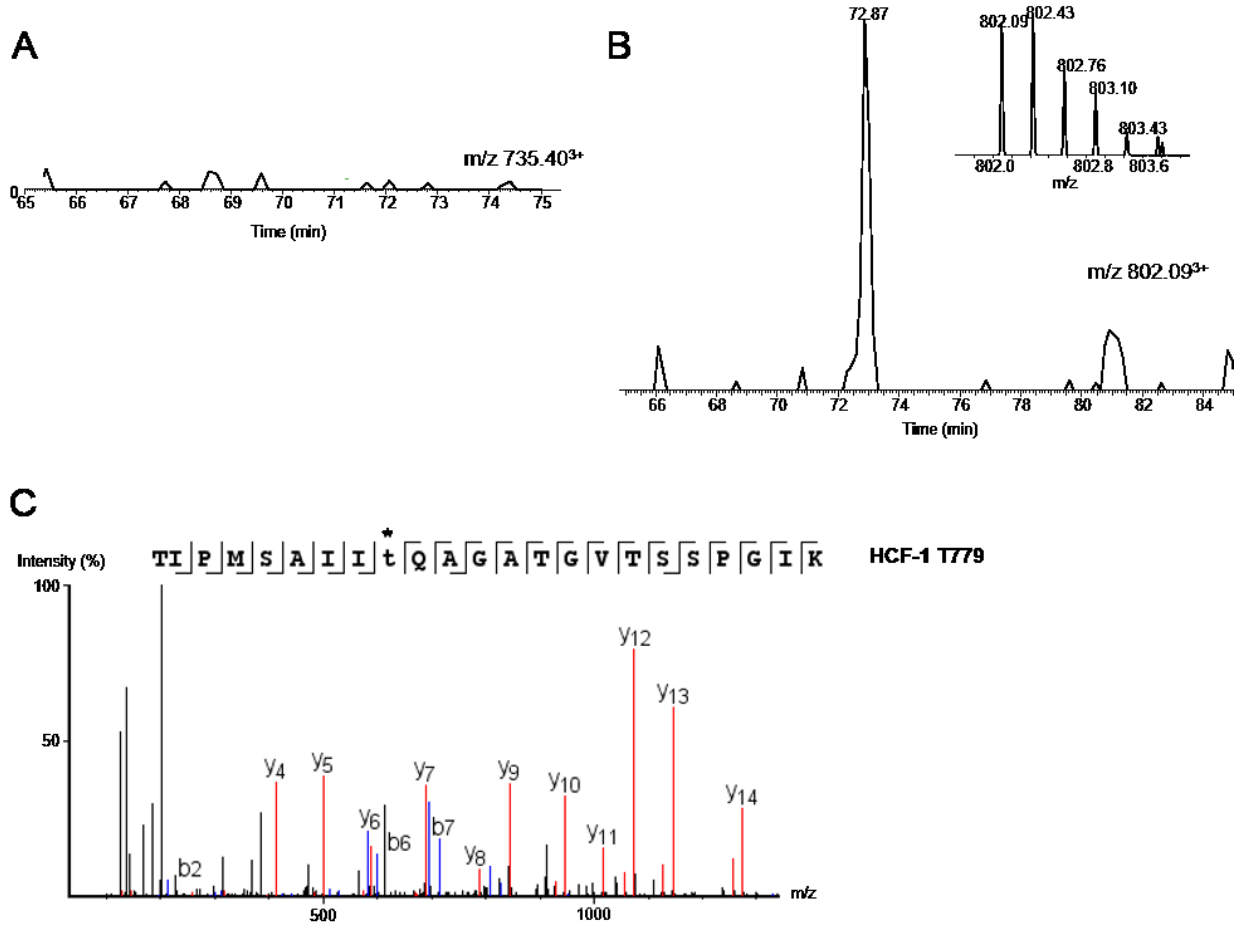

Figure 2.S6 HCD MS/MS spectra for HCF-1 O-GlcNAcylated peptide containing T779 modification site. (A) extracted ion chromatogram for the HCF-1 peptide TIPMSAIITQAGATGVTSSPGIK at m/z 735.40^{2+} showing that the peptide was not detected. (B) Extracted ion chromatogram for the HCF-1 peptide TIPMSAIIT(GlcNAc)QAGATGVTSSPGIK at m/z 802.09^{2+} with the corresponding MS spectrum at 72.87 min. (C) MS/MS spectrum showing that the Thr9 indicated with the star is modified with the GlcNAc moiety.

Table 1. Identification of O-GlcNAcylation sites on HCF-1

m/z	PTM sites of HCF-1	Peptide Sequence	References	ppm
927.77	T575	IPPSSAPTVLSVPAGTtIVKTMAVTPGTTTLPATVK	Novel	1.07
896.47	T588	TMAVTPGTTtLPATVK	Novel	-2.9
751.89	S620?/S622	TAAAQVGTsVsSATNTSTRPIITVHK	Ref. 47, 48, 50	-0.88
1,002.19	T625?/S628?	TAAAQVGTSVSSAtNTsTRPIITVHK	Ref. 51	0.12
846.12	T640?/T642	SGtVtVAQQAQVVTTVVGGVTK	Novel	0.3
778.42	T654	SGTVTVAQQAQVVtTVVGGVTK	Novel	0.67
1,084.85	T694	VMSVVQTKPVQtSAVTGQASTGPVTQIIQTKGPLPAGTILK	Novel	-1.9
847.70	T698	VMSVVQTKPVQTSAVtGQASTGPVTQIIQTKGPLPAGTILK	Novel	-2.9
1,001.94	T738?/S742	LVTSADGKPTTIITtTQAsGAGTKPTILGISSVSPSTTKPGTTTIIK	Novel	0.04
802.09	T771	tIPMSAIITQAGATGVTSSPGIK	Ref. 26, 27	1.0
1,187.97	S775?	TIPMsAIItQAGATGVTSSPGIKSPITIITTK	Novel	-3.7
802.09	T779	TIPMSAIItQAGATGVTSSPGIK	Ref. 26, 27, 47, 48, 50	0.32
1,141.36	T784	TIPMSAIItQAGAtGVTSSPGIKSPITIITTKVMTSGTGAPAK	Novel	1.2
726.40	T800	SPITIItTKVMTSGTGAPAK	Ref. 26, 27	-0.2
1,089.09	T801	SPITIITtKVMTSGTGAPAK	Ref. 47, 48, 49, 50	-0.2
742.45	T858	LVtPVTVSAVKPAVTTLVVK	Novel	0.11

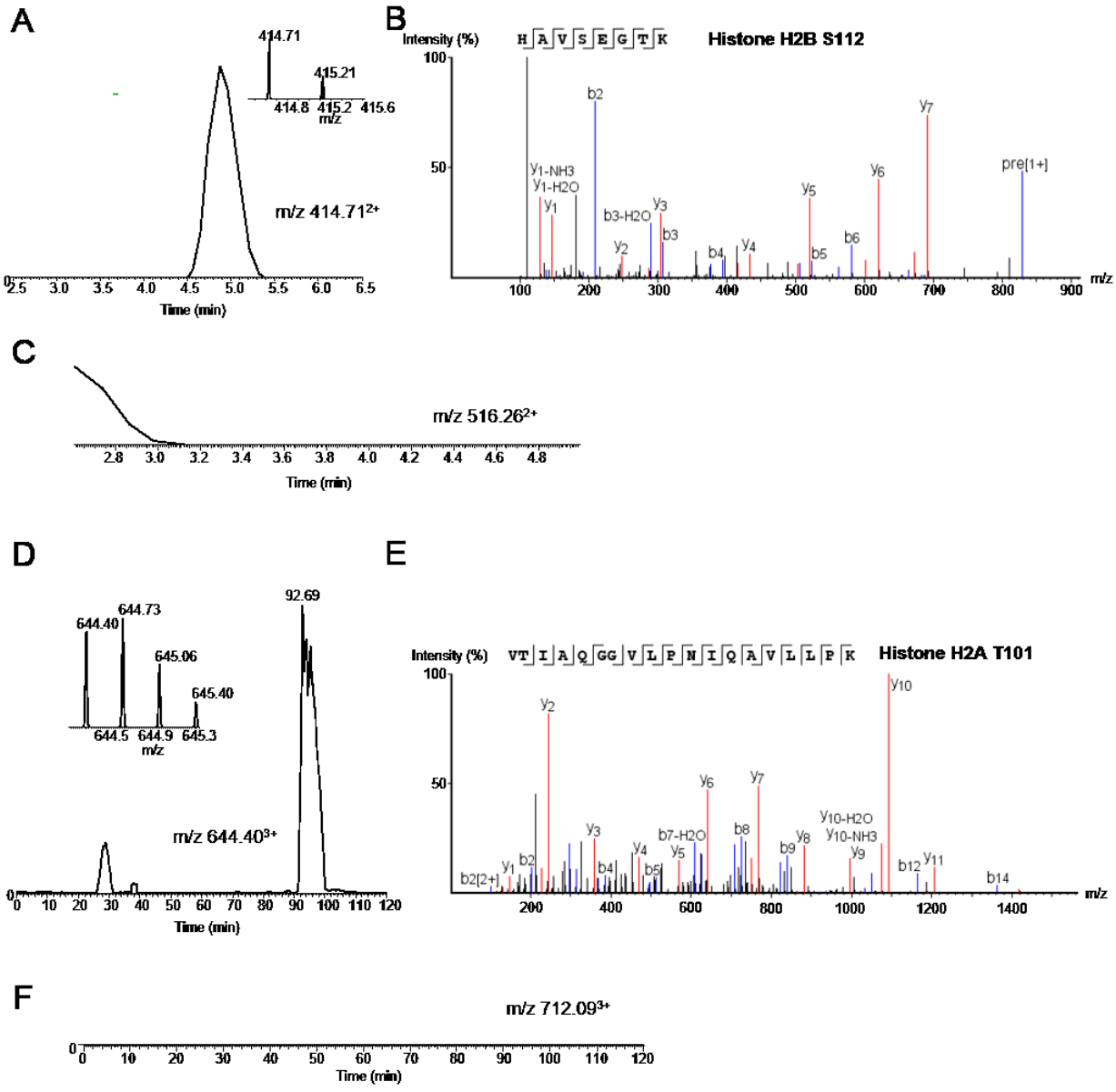

Figure 2.S1. HCD MS/MS spectra for H2B and H2A peptides containing Ser112 and Thr101 respectively.(A-C) HCD MS/MS spectra for H2B. Extracted ion chromatogram for the H2B peptide HAVSEGTK at m/z 414.712+ showing that the peptide was detected (A) along with the corresponding MS spectrum at 4.9 min and its MS/MS spectrum (B). (C) Extracted ion Chromatogram for m/z 516,262+ corresponding to the expected peptide HAVSEGTK with a GlcNAC moiety. The absence of signal at m/z 516,262+ indicates that the corresponding glycopeptide was not detected. (D-F) HCD MS/MS spectra for H2A. Extracted ion chromatogram for the H2A peptide VTIAQGGVLPNIQAVLLPK at m/z 644.403+ showing that the peptide was detected (D) along with the corresponding MS spectrum at 92.69 min and its MS/MS spectrum (E). (F) Extracted ion Chromatogram at m/z 712.093+ corresponding to the expected peptide VTIAQGGVLPNIQAVLLPK bearing a GlcNAC moiety. The absence of a signal at m/z 712.093+ indicates that the corresponding glycopeptide was not detected.

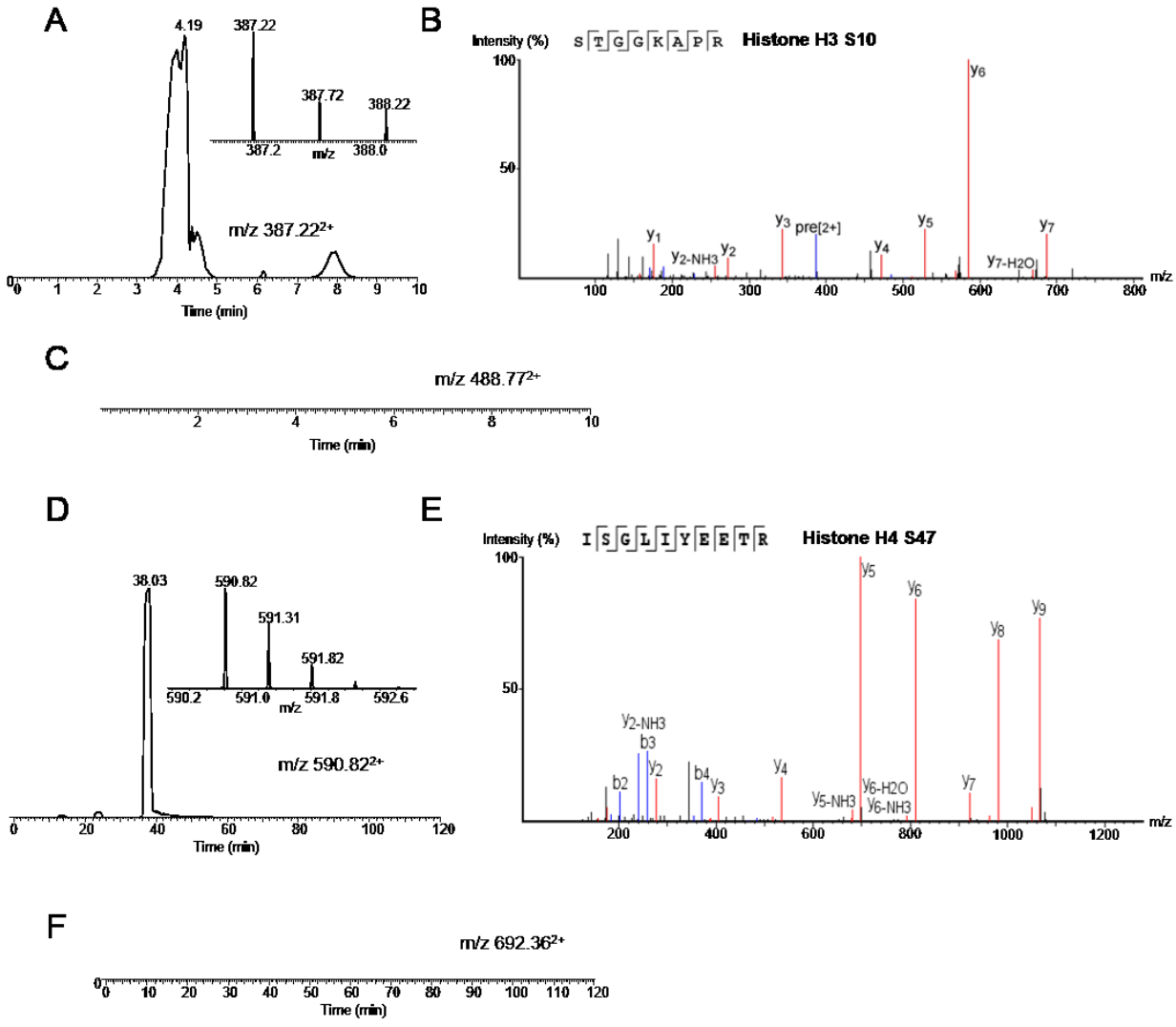

***F*igure 2.S2. HCD MS/MS spectra for H3 and H4 peptides containing Ser10 and Ser47 respectively**.(A-C) HCD MS/MS spectra for H3. Extracted ion chromatogram for the H3 peptide STGGKAPR at m/z 387.222+ showing that the peptide was detected as evidenced from its (A) corresponding MS spectrum at 4.01 min and its MS/MS spectrum (B). (C) Extracted ion Chromatogram for the expected peptide STGGKAPR bearing a GlcNAC moiety at m/z 488.773+, the absence of a signal indicates that the corresponding glycopeptide was not detected. (D-F) HCD MS/MS spectra for H4. Extracted ion chromatogram for the H4 peptide ISGLIYEETR at m/z 590.822+ showing that the peptide was detected as evidenced from the corresponding (D) MS spectrum at 39.03 min and its MS/MS spectrum (E). (F) Extracted ion Chromatogram for the expected peptide ISGLIYEETR bearing a GlcNAC moiety at m/z 692.362+, the absence of signal indicates that the corresponding glycopeptide was not detected.

4.2 Article 2 : The BAP1/ASXL2 Histone H2A Deubiquitinase Complex Regulates Cell Proliferation and is Disrupted in Cancer*

Salima Daou[1], Ian Hammond-Martel[1], Nazar Mashtalir[1], Haithem Barbour[1], Jessica Gagnon[1], Nicholas V.G. Iannantuono[1], Nadine S. Nkwe[1], Alena Motorina[1], Helen Pak[1], Helen Yu[1], Hugo Wurtele[1], Eric Milot[1], Frédérick A. Mallette[1], Michele Carbone[2] and El Bachir Affar[1]

[1]Maisonneuve-Rosemont Hospital Research Center and Department of Medicine, University of Montréal, Montréal H3C 3J7, Québec, Canada

[2]University of Hawaii Cancer Center, BSB200, 701 Ilalo Street, Honolulu, Hawaii 96813, USA.

***Running title**: Inactivation of BAP1/ASXL DUB activity in cancer.

To whom correspondence should be addressed: EL Bachir Affar, Maisonneuve-Rosemont Hospital Research Center and Department of Medicine, University of Montréal, Montréal H3C 3J7, Québec, Canada, Tel.: (1) 514 252 3400 (EXT: 3343); Fax: (1) 514 252 3430;

Keywords: Histone H2A ubiquitination; epigenetics; deubiquitylation (deubiquitination); Polycomb Group Proteins; BAP1; Calypso; ASXL; cancer biology; cell proliferation; cellular senescence

[2]The abbreviations used are: DUB, Deubiquitinase; H2Aub, H2A K119 ubiquitination; CTD, C-Terminal domain; CUBI, Composite Ubiquitin Binding Interface; UCH, Ubiquitin Carboxyl Hydrolase; CC1, Coiled Coil motif 1; CC2, Coiled Coil motif 2; ULD, C-Terminal Domain of UCH37; UBD, Ubiquitin Binding domains; PR-DUB, Polycomb Repressive-DUB, PRC1, Polycomb Repressive Complex 1; PcG, Polycomb Group Proteins; TrxG, Trithorax Group Proteins; PHD, Plant Homeo Domain.

Abstract

The deubiquitinase (DUB) and tumor suppressor BAP1 catalyzes ubiquitin removal from histone H2A K119 and coordinates cell proliferation, but how BAP1 partners modulate its function remains poorly understood. Here, we report that BAP1 forms two mutually exclusive complexes with the transcriptional regulators ASXL1 and ASXL2, which are necessary for maintaining proper protein levels of this DUB. Conversely, BAP1 is essential for maintaining ASXL2, but not ASXL1 protein stability. Notably, cancer-associated loss of BAP1 expression results in ASXL2 destabilization and hence loss of its function. ASXL1 and ASXL2 use their ASXM domains to interact with the C-terminal domain (CTD) of BAP1 and these interactions are required for ubiquitin binding and H2A deubiquitination. The deubiquitination promoting effect of ASXM requires intramolecular interactions between catalytic and non-catalytic domains of BAP1 which generate a composite ubiquitin binding interface (CUBI). Notably, the CUBI engages multiple interactions with ubiquitin involving, (i) the ubiquitin carboxyl hydrolase (UCH) catalytic domain of BAP1 which interacts with the hydrophobic patch of ubiquitin and (ii) the CTD domain which interacts with a charged patch of ubiquitin. Significantly, we identified cancer-associated mutations of *BAP1* that disrupt the CUBI, and notably an in frame deletion in the CTD that inhibits its interaction with ASXL1/2, DUB activity and deregulates cell proliferation. Moreover, we demonstrated that BAP1 interaction with ASXL2 regulates cell senescence and that *ASXL2* cancer-associated mutations disrupt BAP1 DUB activity. Thus BAP1 orchestrates tumor suppression function via a unique mechanism of deubiquitination and inactivation of BAP1/ASXL2 axis contributes to cancer development.

Introduction

Covalent attachment of ubiquitin on lysine or N-terminal residues of target proteins can influence substrate stability and function, and as such exerts major roles in diverse cellular processes including intracellular trafficking, protein quality control, cell cycle progression, transcription, DNA replication and repair [7, 35, 36, 38, 309]. Ubiquitination is catalyzed by the concerted action of E1-ubiquitin activating, E2-ubiquitin conjugating and E3-ubiquitin ligases and generally results in the attachment of one or several ubiquitin molecules, i.e. mono- or poly-ubiquitination, respectively [7, 310]. Ubiquitination events are tightly coordinated by DUBs,

which are responsible for reversing this modification [33, 311]. Proteins containing ubiquitin-binding domains (UBDs) are responsible for the specific and non-covalent recognition of free ubiquitin and of mono- or poly-ubiquitinated substrates. UBDs can be categorized into several families based on structural characteristics such as the presence of single or multiple α-helices, zinc fingers or pleckstrin-homology fold, which constitute interfaces of low affinity interaction with one or multiple molecules of ubiquitin. UBD-containing proteins are thus widely involved in the proper and timely initiation, propagation or termination of ubiquitin-mediated signaling events [5, 7].

The nuclear DUB BAP1 is a tumor suppressor deleted and mutated in an increasing number of cancers of diverse origins [47, 48]. Indeed, somatic or germinal inactivating mutations in BAP1 are found in mesothelioma, uveal melanoma, cutaneous melanocytic tumors, clear cell renal cell carcinoma, breast and lung cancers, thereby making BAP1 the most frequently and widely mutated DUB-encoding gene in cancer [43, 44, 46, 49, 50, 77, 78, 312, 313]. Previous studies indicated that BAP1 tumor suppressor function requires DUB activity and nuclear localization[314]. Consistent with its role in tumor suppression, BAP1 was shown to act as a positive or a negative regulator of cell proliferation [57, 60, 314, 315]. Moreover, genetic ablation of BAP1 in mice inhibits embryonic development, while selective inactivation of BAP1 in the hematopoietic system induces severe defects in the myeloid cell lineage, recapitulating key features of myelodysplastic syndrome [46]. At the molecular level, BAP1 acts as a chromatin-associated protein that is assembled into large multi-protein complexes containing several transcription factors and co-factors including the Host Cell Factor 1 (HCF-1), the O-linked N-acetyl-Glucosamine Transferase (OGT), the Lysine Specific Demethylase KDM1B/LSD2/AOF1, the Additional Sex Comb Like proteins ASXL1 and ASXL2 (ASXL1/2), the Forkhead transcription factors FOXK1 and FOXK2 as well as the zinc finger transcription factor Yin Yang 1 (YY1) [315-317]. BAP1 is recruited at gene promoter regions to activate transcription, and has been shown to regulate the expression of genes involved in cell proliferation [49, 317, 318]. BAP1 is also recruited to sites of DNA double strand breaks to promote repair by homologous recombination [54, 60], and is implicated in DNA replication-associated processes [55, 62]. Importantly, BAP1 functions appear to be regulated by post-translational modifications including phosphorylation and ubiquitination [9, 60, 62].

Nonetheless, the mechanism by which BAP1 function is coordinated by its partners remains poorly defined.

Calypso, the *Drosophila* ortholog of BAP1 is a Polycomb Group (PcG) protein that interacts with the transcriptional regulator ASX and assembles the Polycomb Repressive-DUB (PR-DUB) complex which deubiquitinates histone H2A K118 (H2A K119 in vertebrates, hereafter H2Aub) and promotes PcG target gene repression [52]. While the exact mechanism of repression remains unknown, it is interesting to note that the Polycomb Repressive Complex 1 (PRC1), which catalyzes H2A ubiquitination, is also required for PcG target gene repression [319]. *Drosophila* ASX protein is an atypical PcG factor, since it is involved in both transcriptional silencing and activation [320, 321]. ASXL1 and ASXL2 (hereafter ASXL1/2) are paralogs that appear to have diverged from ASX during evolution, and are reported to function with a number of co-repressors and co-activators, notably the Lysine-Specific Demethylase KDM1A/LSD1, the PcG complex PRC2 and the Trithorax Group (TrxG) epigenetic regulators [45, 322-324]. Similar to PR-DUB complex, a minimal complex containing mammalian BAP1 and the N-terminal region of ASXL1 was shown to efficiently deubiquitinate H2A *in vitro,* indicating the requirement of ASX or ASXL1 for DUB activity [52]. The DUB activity of BAP1 toward histone H2A K119 was also observed in vivo [60, 77, 115, 318]. BAP1 was also shown to deubiquitinate and stabilise some of its interacting partners including HCF-1 and OGT indicating the functional importance of its catalytic activity [46, 57, 315].

The genes encoding ASXL1/2 are involved in chromosomal translocations and are frequently truncated in various cancer types [325]. ASXL1 interaction with BAP1 was not revealed to play a role in in leukemia development [45]. However, the involvement of this interaction in other cancers remains unknown. In addition, the specific contribution of ASXL1 and ASXL2 to BAP1 function remains undefined. Here, we sought to determine how ASXL1/2 modulates the H2A DUB activity of BAP1, and the relevance of these factors for BAP1 tumor suppressor function. We mapped the interaction domains and motifs between BAP1 and ASXL1/2 and demonstrated that ASXL1/2 form two mutually exclusive complexes with BAP1, both of which are competent in deubiquitinating H2A. Furthermore, we showed that the loss of BAP1 expression in cancer is concomitant with a destabilization of ASXL2. We also found that the ASXM domain of ASXL1/2 is prerequisite for ubiquitin binding and deubiquitination by BAP1. Moreover, we found that BAP1 catalytic and non-catalytic domains form, along with the ASXM domain, a composite ubiquitin binding interface (CUBI) required for promoting BAP1 DUB activity by ASXL1/2 and coordination of cell proliferation. Finally, we identified a cancer-derived mutation of BAP1 CTD, ΔR606-H609, which results in a selective loss of interaction with ASXL1/2 and inhibition of H2A DUB activity. The ΔR606-H609 mutation also abolishes the ability of BAP1/ASXL2 axis to

regulate cell proliferation and cellular senescence, thus providing a link between BAP1 function and mechanisms of tumor suppression.

Results

ASXL1 and ASXL2 compete for their interaction with BAP1

ASXL1 and ASXL2 factors co-purified with BAP1 [316, 317], and mass spectrometry peptide counts suggest that they are associated with BAP1 at similar levels (Fig. 1A). BAP1 interaction with ASXL1/2 was not affected by the loss of HCF-1, a major subunit of the BAP1 core complexes associated through its HCF-1 binding motif (HBM). We also note that the interaction between BAP1 and OGT is strongly reduced in the context of $BAP1^{\Delta HBM}$ complexes, indicating that HCF-1 bridges OGT and BAP1. (Fig.1B). We sought to further investigate the functional relationship between these factors. Immunoprecipitation (IP) of ASXL2 from purified BAP1 complexes did not show interaction with ASXL1 (Fig. 1C), and ASXL1 and ASXL2 failed to interact with each other following overexpression (Fig. 1D). We noted that BAP1 interaction with ASXL2 was reduced following expression of ASXL1 (Fig. 1D), suggesting that ASXL1 might compete with ASXL2, thus titrating BAP1. To further confirm that ASXL1 and ASXL2 compete for interaction with BAP1, we overexpressed increasing amounts of ASXL1 with constant amounts of BAP1 and ASXL2 in 293T cells and conducted immunoprecipitation. Interestingly, although ASXL2 and BAP1 protein levels also increased following ASXL1 overexpression, we observed that ASXL2 was displaced from BAP1-containing protein complexes (Fig. 1E). Taken together, our results suggest that BAP1 assembles mutually exclusive complexes with either ASXL1 or ASXL2.

BAP1 and ASXL1/2 are co-regulated and loss of BAP1 in cancer is concomitant with ASXL2 destabilization

To further investigate the relevance of ASXL1 and ASXL2 in regulating BAP1 function, we transfected 293T cells with BAP1 and increasing amounts of Myc-tagged ASXL1/2-expressing constructs. We found that BAP1 protein levels increased with ASXL1/2 expression in a dose-dependent manner (Fig. 2A). Conversely, ASXL1/2 protein levels were also increased following overexpression of BAP1 (Fig. 2B). siRNA knockdown of either ASXL1 or ASXL2 in U2OS osteosarcoma cells or primary human fibroblasts resulted in a significant decrease of BAP1 protein levels (Fig. 2C,D), while combined knockdown of ASXL1/2 caused an even stronger decrease of BAP1 levels than depletion of individual proteins (Fig. 2C). This indicates that ASXL1/2 are necessary for maintaining proper protein levels of this DUB. We also observed that depletion of ASXL1 resulted in a noticeable decrease of ASXL2, while knockdown of ASXL2 caused an increase of ASXL1 (Fig. 2C,D). Knockdown of BAP1 strongly

reduced ASXL2 levels. This effect is independent of BAP1 DUB activity, as the decrease of ASXL2 protein in U2OS cells was prevented by re-expression of siRNA-resistant forms of BAP1, either wild type or catalytically dead mutant, $BAP1^{C91S}$ (Fig. 2E). The dependency of ASXL2 protein levels on BAP1 abundance suggests that ASXL2/BAP1 may form an obligate complex. Consistently, immunodepletion of endogenous proteins from HeLa nuclear extracts revealed that the majority of ASXL2 is associated with BAP1 (Fig. 2F). However, only about half the amount of BAP1 is in complex with ASXL2. PARP1 was used as a control which remained in the flow through fraction. Significantly, ASXL2 was downregulated in BAP1-deficient H28 mesothelioma and H226 lung carcinoma cells, and re-expression of BAP1 or $BAP1^{C91S}$ restored ASXL2 protein levels in these cells, without affecting its mRNA levels (Fig. 2G,H). These data suggest that BAP1/ASXL1/2 interactions are highly regulated and that loss of BAP1 during cancer development results in concomitant loss of ASXL2 protein and function.

The ASXM domain of ASXL1/2 is required for interaction with the CTD of BAP1

ASXL1/2 contain two uncharacterized N-terminal domains, ASXN and ASXM, and a C-terminal Plant Homeo Domain (PHD) finger [322, 326] (Fig. 3A). BAP1 was shown to interact with the N-terminal region of ASXL1 (1-337 a.a.) and this fragment promotes H2A deubiquitination by BAP1 [52]. Interestingly, the DUB activity of a BAP1 family member, UCH37, is stimulated by RPN13 (ADRM1) 19S proteasome subunit [34, 327, 328], and phylogenetic studies suggest that RPN13 and ASXL1/2 shared a conserved domain termed the DEUBiquitinase ADaptor (DEUBAD) domain highly similar to the ASXM domain [329]. This suggests that BAP1/ASXL1/2 might use a similar mechanism of DUB activation than UCH37/RPN13. Indeed, *in vitro*-translated ASXM domain (ASXM1: 253-391 a.a., ASXM2: 253-411 a.a. of ASXL1 and ASXL2 respectively) strongly interacted with GST-BAP1 in pulldown assays (Fig. 3B). To gain insights into the significance of the BAP1/ASXL1/2 interactions, we generated ASXL1/2 expression constructs lacking the BAP1-interacting domain ($ASXL1/2^{\Delta ASXM}$). As expected, protein levels of $ASXL2^{\Delta ASXM}$, but not $ASXL1^{\Delta ASXM}$, were reduced in comparison to their wild type counterparts following transfection (Fig. 3C). After adjusting the amounts of transfected plasmids to obtain comparable expression of the wild type and mutant forms of ASXL1/2, we found that the ability of ASXL1/2 mutants, lacking their respective ASXM domain, to interact with BAP1 and to form protein complexes *in vivo* was strongly reduced (Fig. 3D). BAP1 contains an Ubiquitin Carboxyl Hydrolase (UCH) catalytic domain and a Coiled-Coil motif (CC1) in the N-terminal region, as well as a C-Terminal Domain (CTD) containing a second Coiled-Coil motif (CC2) [9, 43, 57] (Fig. 3E). The

CTD is highly similar to the C-terminal domain of UCH37 (ULD) [57], a domain involved in the interaction of this DUB with the DEUBAD domain of RPN13 [40, 330-332]. However, in contrast to UCH37, BAP1 possesses a big middle region (MR), that contain the HBM and other protein interaction motifs, separating UCH/CC1 from the CTD, [43, 57, 115, 207]. Nonetheless, only GST-tagged fragments of BAP1 containing an intact CTD interacted with ASXM domains of ASXL1/2 (Fig. 3F). These results indicate that ASXL1/2 use the ASXM domain to interact with the CTD of BAP1. To provide further insights into ASXL1/2/BAP1 interactions, we constructed BAP1 mutants disrupted in the CTD region (Fig. 3G). The BAP1$^{\Delta CTD1}$ represents a deletion of CTD except for the KRKKFK putative nuclear localization signal [314] (Fig. 3G). The BAP1$^{\Delta CTD}$ and BAP1$^{\Delta CC2}$ represent a complete deletion of the CTD and CC2, respectively (Fig. 3G). Supporting our finding reported above, we noticed that disruption of CTD resulted in decreased BAP1 protein levels (Fig. 3H). We also generated HeLa cell lines stably expressing BAP1wild type or its mutant form lacking most of the CTD, BAP1$^{\Delta CTD1}$, and use them for complex purification. To enable meaningful comparisons, the eluted complexes were adjusted by immunoblotting for similar amounts of BAP1 protein prior to silver staining. This revealed that BAP1 and BAP1$^{\Delta CTD1}$ complexes were quite similar in protein composition (Fig. 3I). However, immunoblotting analysis showed that the interaction between BAP1$^{\Delta CTD1}$ and ASXL1/2 was abolished (Fig. 3I). In contrast, association of BAP1$^{\Delta CTD1}$ with HCF-1/OGT remained unchanged in comparison to the wild type variant. Altogether, these results indicate that CTD and ASXM domains are necessary and sufficient for assembly of BAP1/ASXL1/2 complexes.

BAP1 is a major DUB for H2Aub K119 and its enzymatic activity is ASXM-dependent

Several DUBs including BAP1 were reported to target H2Aub K119 in mammals [35, 333]. However, the relative contribution of each enzyme in H2A deubiquitination *in vivo* remained unknown. We conducted an siRNA screen using a library that covers the human DUB repertoire by analyzing the global increase of H2Aub using an in-cell western assay. Strikingly, depletion of BAP1 produced the most significant increase of H2Aub, indicating that this enzyme is a major DUB for this histone modification under normal growth conditions (Fig. 4A). To investigate how ASXL1/2 regulate mammalian BAP1 DUB activity *in vivo*, we conducted RNAi-mediated depletion of these factors, and found that neither ASXL1 nor ASXL2 individual knockdown induced noticeable changes in global H2Aub levels (Fig. 4B, 4C). However, combined knockdown of ASXL1 and ASXL2 resulted in significant increase of H2Aub, similar to the effect induced by BAP1 depletion (Fig. 4B). This prompted us to determine the respective contribution of ASXL1 and ASXL2 to the H2A DUB activity of BAP1. A striking BAP1-mediated deubiquitination of H2A was observed upon its co-expression with either

ASXL1 or ASXL2, and this effect was dependent on BAP1 catalytic activity (Fig. 4D). Consistent with our mapping analysis, ASXL1 and ASXL2 lacking ASXM were unable to stimulate H2A deubiquitination (Fig. 4E). In addition, we purified monoubiquitinated nucleosomal Flag-H2A, from 293T cells, that we used for *in vitro* DUB assay and found that ASXM1 or ASXM2, but not GST-CTD used as a control, are sufficient for stimulating BAP1-mediated deubiquitination of H2A (Fig. 4F). Based on these results, we concluded that the interaction between ASXL1/2 and BAP1 requires ASXM, and the latter is necessary and sufficient for promoting BAP1-mediated deubiquitination of its physiological substrate H2Aub K119.

Identifications of domains and motifs in ASXM required for promoting ubiquitin binding and DUB activity towards histone H2A of BAP1

To further dissect the mechanism of H2A deubiquitination by BAP1, we conducted ubiquitin pull down assays and found that ASXM2 strongly enhanced BAP1 binding to ubiquitin (Fig. 5A). ASXM2 alone can directly bind ubiquitin, but this interaction was weak as an enrichment of about two-folds above the background was observed (Fig. 5A). ASXM1 also promoted BAP1 binding to ubiquitin in a similar manner as ASXM2 (Fig. 5B). Since ASXM1 and ASXM2 domains acted similarly in promoting BAP1 binding to ubiquitin and DUB activity, we selected ASXM2 for further studies. Sequence alignment of ASXL proteins indicated that the ASXM domain is highly conserved (Fig. 5C). We generated several constructs encompassing several regions and highly conserved motifs of ASXM2 (Fig. 5C). We found that the 246-347 a.a. region interacted with BAP1 as efficiently as the full length ASXM2 (246-401 a.a.), while no interaction was observed for the 316-401 a.a. region (Fig. 5D). The 246-313 a.a. and 300-401 a.a. regions interacted only poorly with BAP1. These results suggest that critical interaction motifs are located within or overlapping with the 300-347 a.a. region (Fig. 5D). Only the full length ASXM2 and the 246-347 a.a. fragment, that strongly interacted with BAP1, promoted its binding to ubiquitin and DUB activity, Nonetheless, we noted that the 246-347 a.a. fragment was significantly less competent in promoting BAP1 binding to ubiquitin which could explain its weakness in promoting deubiquitination (Fig. 5D,E). Next, we generated discrete mutations of several highly conserved residues of ASXM2 (Fig. 5C), and found that ASXM2 interaction with BAP1 and ubiquitin binding are maintained for most mutants except for the LLLL303-306AAAA hydrophobic stretch mutant which essentially lost its interaction

with BAP1 (Fig. 5F,G). As expected, the LLLL303-306AAAA mutant failed to stimulate DUB activity (Fig. 5H). Interestingly, while the L286A and NN328-329AA mutants were essentially equally efficient in promoting BAP1 binding to ubiquitin, their ability to deubiquitinate H2A was significantly different (Fig. 5G,H).

Intramolecular interactions in BAP1 create an ASXM-dependent Composite Ubiquitin Binding Interface (CUBI) and enable DUB activity

The CTD of BAP1 is necessary and sufficient for the interaction between BAP1 and ASXL1/2 (Fig. 3). This domain also engages an intramolecular interaction with both the CC1 and the UCH domains in order to ensure BAP1 auto-deubiquitination and proper nuclear localization [9]. Hence, we sought to test whether this intramolecular interaction in BAP1 is necessary for ASXM stimulation of ubiquitin binding and DUB activity. Indeed, as is the case for $BAP1^{\Delta UCH}$ or $BAP1^{C91S}$, $BAP1^{\Delta CTD}$ was unable to deubiquitinate H2A following incubation with ASXM2 (Fig. 6A,B). $BAP1^{\Delta CTD}$ or $BAP1^{\Delta CC2}$ mutants were also incapable of deubiquitinating H2A in the context of BAP1 protein complexes *in vitro* (Fig. 6C), As a control, $BAP1^{\Delta HBM}$ complexes were competent in promoting DUB activity (Fig. 6D), as previously shown [77]. Consistently, $BAP1^{\Delta CTD}$ was also unable to promote BAP1 DUB activity *in vivo* when expressed with either ASXL1 or ASXL2 (Fig. 6E). In addition, while ASXM2 promoted binding to ubiquitin of both BAP1 and $BAP1^{C91S}$, this domain failed to enhance ubiquitin binding of $BAP1^{\Delta CTD}$ or $BAP1^{\Delta UCH}$ (Fig. 6F). ASXM2 only partially promoted $BAP1^{\Delta CC1}$ binding to ubiquitin, and this mutant is completely inactive in H2A deubiquitination (Fig. 6A,B,F). Thus, ASXM2 requires intramolecular interactions between multiple domains of BAP1 to promote ubiquitin binding and catalysis. In contrast to the CC1 and CTD in BAP1, the corresponding domains in UCH37, helix α7 and ULD respectively, are contiguous (Fig. 7A, left panel) [330]. Nonetheless, co-crystallization of UCH37 of the worm *Trichinella spiralis* (tsUCH37) with ubiquitin indicated an intramolecular interaction similar to the one observed in BAP1 [330]. In addition, R261 and Y262 a.a. residues of the ULD establish direct contacts with ubiquitin K48 and Q49/R72, respectively [330]. Molecular dynamics simulation suggested that E265 and N272, part of a non-crystalized extension of the ULD, might also bind R42 and D52 of ubiquitin, respectively [330]. R261, Y262, E265 and N272 are essentially conserved in BAP1 and correspond to K659, F660, D663 and N670, respectively (Fig. 7A, right panel). Thus, we were prompted to test whether the CTD is sufficient for binding ubiquitin in solution. We found that the CTD weakly interacted with ubiquitin, as a signal above the background was consistently observed (Fig. 7B). Importantly, mutation of ubiquitin R42/Q49/D52/R72 residues (we termed the RQDR charged patch),

involved in binding the tsUCH37 ULD, reduced this interaction (Fig. 7B,C). Moreover, mutation of the RQDR patch also abolished ubiquitin binding by the BAP1/ASXM2 complex (Fig. 7D). Also, ubiquitin binding by BAP1/ASXM2 is completely abrogated by mutating the VLI, Ile36 and Il44 hydrophobic patches of ubiquitin, which are involved in binding by the UCH domain [40, 330, 332] (Fig. 7C,D). These data indicate that the hydrophobic and the charged RQDR patches are necessary to ensure strong ubiquitin binding by the BAP1/ASXM2 complex. Finally, mutation of the TEK box, Phe4 patch or D58 did not affect ubiquitin binding by BAP1/ASXM2 (Fig. 7C,D). We concluded that ASXM induces the assembly of a composite ubiquitin binding interface (CUBI) that requires catalytic and non-catalytic domains of BAP1 and involves multiple patches of ubiquitin.

Cancer-derived mutations abolish BAP1 interaction with ASXL1/2, ubiquitin binding and DUB activity

BAP1 interaction with ASXL1 was not found to play an important role in Leukemia [45]. However, the role of BAP1 interaction with either ASXL1 or ASXL2 in other cancers remains unknown. We asked whether tumor-associated mutations of BAP1 result in selective loss of interaction with ASXL1/2 and ubiquitin binding and catalysis. Based on our data and tsUCH37-ubiquitin co-crystal structure [330], we analyzed the previously reported cancer mutation landscape of BAP1 (cBioPortal for Cancer Genomics and COSMIC cancer databases), notably in solid tumors (e.g. uveal melanoma and renal cell carcinoma) and selected several mutations within or near its UCH (E31K, Y33D), CC1 (L230Q, Q253K) and CTD (K656N, K658R, D663H, R666-H669) domains [77, 312] (Fig. 7A). We also included additional mutations, not found in cancer, but corresponding to highly conserved amino acids in the vicinity of these cancer mutations (F228A, N670A) (Fig. 7A). We co-expressed these BAP1 mutants with ASXL2 and found that most mutations did not significantly affect protein interactions except for the R666-H669 mutant whose interaction with ASXL2 is strongly reduced (Fig. 8A). It is worth mentioning that although BAP1 and ASXL2 are overexpressed in 293T cells, reduced protein levels of R666-H669 mutant are still observed (Fig. 8A). *In vitro* ubiquitin pull down interaction assays revealed that E31K and Y33D mutations in the UCH domain result in a reduced binding of BAP1/ASXM2 to ubiquitin (Fig. 8B). Significantly, several mutants in other domains, e.g., F228A, L230Q, K658R and R666-H669 strongly affected BAP1/ASXM2 ability to bind ubiquitin (Fig. 8B). Most BAP1 mutants were also significantly disrupted in their ability to deubiquitinate H2A (Fig. 8B). Interestingly, the D663H mutant was essentially efficient in binding ASXM2 and ubiquitin but failed to promote efficient DUB activity. Since the deletion of amino acids R666-H669 (hereafter $BAP1^{R666\text{-}H669}$) abolished interaction with ASXL2, ubiquitin binding and DUB activity, we selected this mutant for further biochemical and

functional studies. We generated HeLa cells stably expressing Flag-HA-BAP1$^{R666\text{-}H669}$ and conducted immuno-affinity purification of DUB complexes. After adjusting for similar amounts of immunopurified BAP1 we conducted silver staining of the eluted material. This indicated that R666-H669 mutation did not change the overall composition of BAP1 complexes as compared to the wild type, except for missing ASXL2 band in the purified BAP1$^{R666\text{-}H669}$ complexes (Fig. 8C, left panel). ASXL1 co-migrates with other high M.W. proteins, and could not be discerned as a distinct band. Strikingly, western blot analysis of the complexes indicated that BAP1$^{R666\text{-}H669}$ does not interact with ASXL1/2, whereas interaction with HCF-1/OGT were not affected (Fig. 8C, right panel). Moreover, the purified BAP1$^{R666\text{-}H669}$ complex was unable to deubiquitinate nucleosomal histone H2A (Fig. 8D, top panel), or to bind ubiquitin *in vitro* (Fig. 8D, bottom panel). Concordant with this data, neither full length ASXL1 nor ASXL2 are capable of stimulating DUB activity by BAP1$^{R666\text{-}H669}$ *in vivo* (Fig. 8E). To further investigate the disruption of BAP1/ASXL2 DUB activity in cancer, we selected several reported cancer-associated point mutations in ASXM2 (Fig. 5C), especially in solid tumors (e.g. breast carcinoma and colorectal adenocarcinoma), and found that these mutations did not disrupt ASXM2 interaction with BAP1 (Fig. 8F). The BAP1/ASXM2 complex with P274L mutation showed reduced binding to ubiquitin, while the ability of other mutants to bind ubiquitin was essentially unaffected (Fig. 8G). Finally, three of these mutants (P274L, E330Q, F331L) showed reduced DUB activity toward H2A indicating that ASXL2 is also targeted by mutations that inhibit the enzymatic activity of the complex (Fig. 8G). Altogether, these results indicate that several cancer-associated mechanisms target the BAP1/ASXL2 complexes inducing loss of ubiquitin binding and DUB activity.

BAP1/ASXL1/2 axis is required for proper cell cycle progression

We enquired to determine the biological significance of BAP1/ASXL1/2 interactions. Since BAP1 knockdown delays cell proliferation in multiple cell types [57, 112, 315], we sought to determine whether ASXL1/2 and BAP1 interactions influence cell cycle progression. We generated U2OS cells stably expressing comparable levels of siRNA-resistant BAP1, BAP1^{C91S} or BAP1$^{R666\text{-}H669}$ (Fig. 9A), and conducted RNAi depletion of endogenous BAP1. Cells were then synchronized in early S phase using double thymidine block and released in the cell cycle. As expected, in the empty vector cells, depletion of endogenous BAP1 delayed S phase progression. While re-expression of BAP1 rescued the defect induced by knockdown of endogenous BAP1, this was not observed with BAP1^{C91S} nor BAP1$^{R666\text{-}H669}$ (Fig. 9B). In addition, expression of BAP1^{C91S} or BAP1$^{R666\text{-}H669}$ significantly affected the ability of U2OS cells to be synchronized (Fig. 9B). Similar cell cycle defects were also observed following expression of BAP1 lacking CTD, BAP1$^{\Delta CTD}$ (Fig. 9C). The increase of H2Aub levels following knockdown of BAP1, was prevented by re-expression of wild type BAP1, but not by BAP1$^{R666\text{-}H669}$ or

BAP1^{C91S} mutants (Fig. 9A). We note that the higher levels of H2Aub in U2OS expressing BAP1^{C91S} might result from a dominant negative effect on endogenous BAP1. Next, re-introduction of BAP1, but not the BAP1$^{R666\text{-}H669}$ nor the BAP1^{C91S} in the BAP1-deficent lung carcinoma cell line H226 promoted substantial H2A deubiquitination (Fig. 9D, top panel). In addition, unlike the wild type BAP1, which strongly inhibited cell proliferation as previously observed [314], the BAP1$^{R666\text{-}H669}$ mutant only partially inhibited cell proliferation (Fig. 9D, bottom panel). Thus, physical interaction between ASXL1/2 and BAP1 and DUB activity are required for proper control of cell cycle progression.

Enforced expression of BAP1 or ASXL2 induce cellular senescence and the p53/p21 tumor suppressor pathway in CTD/ASXM-dependent manner

Cellular senescence-associated cell cycle exit is a potent tumor suppressor mechanism. Since we established that BAP1 function is coordinated with ASXL1 and ASXL2 in regulating cell cycle progression, we were prompted to determine if BAP1/ASXL1/2 might influence cellular senescence. Of note, PcG proteins, notably BMI1, are known to be involved in senescence [334-336]. Therefore, we evaluated whether enforced expression of BAP1, trigger senescence in the normal diploid human fibroblasts IMR90 cell line model. Strikingly, retroviral overexpression of BAP1 reduced cell proliferation and induced senescence-associated β-galactosidase (SA-β-gal) activity (Fig. 10A,B). Interestingly, overexpression of BAP1^{C91S} mutant also induced senescence with a more pronounced effect than the wild type form (Fig.10A,B). To probe whether this effect is due to BAP1 ability to interact with ASXL1/2, we evaluated the effect of BAP1$^{\Delta CTD}$ and BAP1$^{R666\text{-}H669}$ on cellular senescence. Indeed, these mutations significantly reduced the ability of BAP1 to induce senescence (Fig 10A,B). Similar effects were observed for the double mutants BAP1$^{C91S\text{-}\Delta CTD}$, although a complete rescue was observed for BAP1$^{C91S\text{-}R666\text{-}H669}$ (Fig. 10A,B). On the other hand, overexpression of ASXL2, but not ASXL1, also strongly induced senescence and reduced cell proliferation (Fig. 10C,D). Moreover, deletion of ASXM (ASXL2$^{\Delta ASXM}$) inhibited the senescence-inducing ability of ASXL2, indicating the importance of ASXL2-BAP1 interaction in coordinating cellular senescence. To provide further insights into the molecular mechanism that orchestrate BAP1/ASXL2-mediated senescence, we evaluated the expression levels of known proteins that induce cellular senescence upon overexpression of BAP1, BAP1^{C91S} and corresponding mutants (Fig. 10E). We found that, although the effect of BAP1 was less pronounced than the BAP1^{C91S} form, overexpression of this DUB induced the p53/p21 tumor suppressor pathway. Overexpression of BAP1$^{\Delta CTD}$, BAP1$^{R666\text{-}H669}$, BAP1$^{C91S\text{-}\Delta CTD}$ or BAP1$^{C91S\text{-}R666\text{-}H669}$ did not upregulate p53/p21 indicating the requirement for ASXL1/2 in BAP1-mediated senescence (Fig. 10E). We also observed a concomitant decrease of CDC6 and pRB following overexpression of BAP1 or BAP1^{C91S},

and these effects required interaction with ASXL1/2. In contrast, no significant changes were observed on p16INK4a cell cycle inhibitor and the p53 E3 ligase MDM2.

Altogether, these results indicate that the fine balance between ASXL1/2 complexes and their coordination of BAP1 DUB activity are required for the proper progression of cell cycle and tumor suppression.

Discussion

We provided novel insights into the mechanisms by which the DUB activity and function of the tumor suppressor BAP1 are coordinated. First, we revealed that BAP1 and ASXL1/2 protein levels are tightly regulated by each other. Notably, BAP1 protein levels are nearly completely reduced following concomitant depletion of ASXL1 and ASXL2. This regulation is highly conserved since, in drosophila, deletion of ASX also destabilized dBAP1/Calypso [52]. The fact that relatively similar protein amounts of ASXL1 and ASXL2 co-purified with mammalian BAP1 and that siRNA depletion of either ASXL1 or ASXL2 reduced BAP1 protein levels by approximately half, it is likely that BAP1/ASXL1 and BAP1/ASXL2 complexes coexist in the cells with a similar abundance. These complexes might exert distinct functions and/or compete for gene regulatory regions. We also found that depletion or loss of BAP1 destabilized ASXL2, but not ASXL1. These findings demonstrate for the first time the importance of complex assembly in maintaining proper protein levels of ASXL2, and hence its function in vivo. Thus, developmental or disease-associated inactivation or loss of expression of one component would result in a profound functional impact on the other partners. Indeed, loss of BAP1 in two tumor types of different histological origins, i.e., mesothelioma and non-small lung carcinoma, caused a severe reduction of ASXL2 protein levels. A survey of mutations in several cancers shows truncating mutations and deletions of BAP1 that would often result in the loss of the CTD and consequently ASXL1/2 interaction. Therefore, loss of ASXL2 function is a prevalent event in cancers with BAP1 mutations.

Similar to other post-translational modifications, ubiquitin recognition plays important roles in ubiquitin-dependent signaling [5]. Often, UBDs involve distinct protein domains that engage interactions with the hydrophobic patches or other surfaces of ubiquitin and act as signal readers [5]. Our study revealed that the CTD domain of BAP1 plays a central role in coordinating ubiquitin binding and catalysis by BAP1/ASXL1/2 complexes. First, the CTD is sufficient for binding a RQDR charged patch of ubiquitin and can be qualified as a bona fide UBD. Second, the CTD interacts with the CC1 and the UCH domains [9], and acts to stabilize the interaction of the ubiquitin with the catalytic domain.

Third, CTD also strongly interacts with ASXM domain, and the latter induces ubiquitin binding by the CUBI and is required for catalysis. We also found that ASXM itself weakly bind ubiquitin, and hence probably participate in ubiquitin positioning. Thus, our data support a model whereby UCH, CC1, CTD and ASXM domains cooperate in order to generate an interface for stable binding with multiple ubiquitin patches, thus facilitating recruitment and specific substrate deubiquitination (Fig. 11). In support of our findings on BAP1/ASXL1/2, recent crystallography and molecular studies characterized the mechanism of activation of UCH37 by RPN13 [40, 332]. The most remarkable similarities with BAP1 are the conserved intramolecular interaction between the DEUBAD of RPN13 and the ULD of UCH37 and the stimulatory effect of RPN13 at the level of substrate binding. Moreover, highly conserved amino acid residues in BAP1 and UCH37, are required for the interaction with the hydrophobic patch of ubiquitin. Finally, similar to ASXM, the DEBUAD of RPN13 also establishes a weak interaction with ubiquitin [40, 332]. Thus, BAP1 and UCH37 share a highly conserved mechanism of cofactor-mediated DUB activation. Interestingly, INO80 chromatin remodeling factor also possesses a DEUBAD, and through molecular mimicry, this domain associates with and inhibits UCH37 [40, 332]. Of note, BAP1 also interacts with INO80 ATPase, a component of the INO80 chromatin remodeling complex, and promotes its deubiquitination [55]. As INO80G (NFRKB) subunit of the complex inhibits UCHL5 through its DEUBAD, it will be interesting to determine whether, in specific contexts, this factor could also negatively regulate the DUB activity of BAP1.

Our protein complex purification studies indicated that deletion of BAP1 HBM domain does not interfere with BAP1 interaction with ASXL1/2. Conversely, mutation in CTD does not impact the interaction of BAP1 with HCF-1/OGT. Moreover, BAP1 complexes lacking HCF-1/OGT are competent in deubiquitinating nucleosomal histone H2A indicating that these components do not directly participate in ubiquitin binding and catalysis. Taking into account that dBAP1/Calypso does not possess the middle region which was acquired later in vertebrate evolution [52], HCF1/OGT and ASXL1/2 appear to define two functional axes of the BAP1 complexes. Notably, HCF-1 recruits chromatin modifying complexes including MLL family of histone H3K4 methyltransferases and Sin3/HDAC deacetylase complexes at gene regulatory regions [75, 304]. Thus, HCF1/OGT and ASXL1/2 exert distinct, but likely concerted, functions tethered by BAP1. Indeed, similar to HCF-1 interactions with BAP1 [315], ASXL1/2 association with this DUB also regulates cell proliferation.

To establish the significance of BAP1/ASXL1/2 complexes for tumor suppression, we conducted RNAi rescue studies, and showed that cancer-derived mutations that directly target BAP1/ASXL1/2 interaction result in a loss of DUB activity, increased H2Aub levels and deregulation of cell cycle progression. In addition, mutations that directly target the BAP1 catalytic site are frequently

found in cancer [47, 77, 312], and these mutations also result in increased H2Aub levels and deregulation of cell cycle control. These findings highlight the importance of the catalytic activity of BAP1/ASXL1/2 complexes for tumor suppression. Interestingly, overexpression of BAP1 or its catalytically dead form in primary human fibroblasts induced cellular senescence and up regulation of the p53/p21 DNA damage response in CTD-dependent manner, although more pronounced effects were observed for the catalytic inactive form of BAP1. It is currently unclear how both catalytically competent and inactive BAP1 promote cellular senescence. Nonetheless, as the catalytic dead BAP1 binds ubiquitin, it is possible that these effects are associated mostly with BAP1/ASXL1/2 binding to H2Aub rather than catalysis. Deregulation of H2Aub levels or its recognition might cause defects in transcriptional events [317], DNA double strand break repair [60] or replication fork progression [55], all of which could promote the induction of DNA damage and the p53 response and lead to genomic instability and cancer development. While further studies are needed to address these possibilities, our findings, nonetheless, suggest that the proper balance of BAP1/ASXL1/2 complexes and their coordinated binding to ubiquitinated substrates and/or DUB activity are essential for normal control of cell proliferation. Another interesting finding is that, overexpression of ASXL2, but not ASXL1, induces senescence in ASXM-dependent manner. Taking into account that ASXL2 and BAP1 form an obligate complex, our study delineates that ASXL2 plays an important role in regulating BAP1 function in cell proliferation. Moreover, a cancer-derived mutation of BAP1 that abolishes its interaction with ASXL1/2 prevents cellular senescence, further supporting the notion that the BAP1/ASXL2 signaling axis is important for tumor suppression.

Although, we cannot exclude that BAP1/ASXL1/2 target other known substrates such HCF-1 and OGT [46, 57], our study and others provide strong support for the role of this DUB in the regulation of H2Aub levels and tumor suppression. Indeed (i) BAP1 was revealed as a major DUB for H2A in mammalian cells, (ii) several cancer mutations of BAP1 and ASXL2 target the UCH/CC1/CTD/ASXM platform, which is critical for ubiquitin binding and H2A deubiquitination, (iii) BAP1 null cancer cells display high H2Aub levels that could be reduced following reintroduction of BAP1, but not ASXL1/2 interaction-deficient mutants, (iv) both PcG proteins Ring1B and BMI1, two critical components of the PRC1 complex that catalyze H2A ubiquitination, regulate cell proliferation and are overexpressed in cancer [337-339]. Thus, our study provides further insights into the involvement of H2Aub in tumorigenesis.

Acknowledgements

We thank Yang Shi for support, Haider Dar, Sarah Hadj-Mimoune, Diana Adjaoud and Marie-Anne Germain for technical assistance. *This work was supported by grants from the Canadian Institutes of Health Research (CIHR) (MOP-115132) and the Natural Sciences and Engineering Research Council of Canada (355814-2010) to E.B.A, and CIHR to F.A.M (MOP-133442). E.B.A. is a scholar of the Fonds de la Recherche du Québec - Santé (FRQ-S) and the CIHR. H.W. and F.A.M. are Scholars of the FRQ-S. S.D. had a PhD scholarship from the Islamic Bank for Development. H.Y. had a PhD scholarship from the CIHR. H.B has a PhD scholarship from the Ministry of Higher Education and from Scientific Research of Tunisia and the Cole Foundation. J.G has a M.Sc. scholarship from the FRQ-S. H.Y. had a PhD scholarship from the CIHR.

1To whom correspondence may be addressed: Maisonneuve-Rosemont Hospital Research Center and Department of Medicine, University of Montréal, Montréal H3C 3J7, Québec, Canada, Tel.: (1) 514 252 3400 (EXT: 3343); Fax: (1) 514 252 3430

Experimental Procedures

Plasmids

Retroviral constructs pOZ-N-Flag-HA-BAP1, pOZ-N-Flag-HA-BAP1 C91S (catalytic dead) and pOZ-N-Flag-HA-BAP1ΔHBM (BAP1 mutant deleted in the NHNY sequence corresponding to the HCF-1 binding motif); constructs to produce recombinant full-length GST-BAP1 and various deleted forms; pET30a+ BAP1 for production of His-tagged BAP1 were previously described [317]. pCDNA3-Flag-H2A was obtained from Moshe Oren [307]. pOZ-N-Flag-HA-BAP1 ΔCTD1 and pOZ-N-Flag-HA-BAP1 ΔCC2 were generated by PCR-based subcloning. Non-tagged pCDNA3-BAP1 and pCDNA3-BAP1-C91S were generated by subcloning the cDNAs from pOZ-N-Flag-HA-BAP1 and pOZ-N-Flag-HA-BAP1-C91S respectively. siRNA resistant constructs for BAP1, BAP1-C91S, BAP1 ΔCTD, BAP1R666-H669 were generated using gene synthesis (BioBasic) and then subcloned into modified pENTR D-Topo plasmid (Life Technologies). Expression constructs of siRNA resistant BAP1, BAP1 C91S, BAP1 ΔCTD and BAP1 ΔR666-H669 were generated by recombination using LR clonase kit (Life Technologies) into pMSCV-Flag-HA-IRES-Puro or pDEST-Myc constructs [316]. BAP1ΔUCH, BAP1ΔCC1 and BAP1ΔCTD were described [9], and were sub-cloned by PCR into pENTR. Ubiquitin constructs (Ub wild type, Ub VLI (V70A/L8A/I44A), Ub I36A, Ub I44A, Ub D58A) flanked by att-B and att-P recombination sites were generated by gene synthesis (Life technologies) directly into pMK-Rq plasmid and bacterial expression constructs were generated by recombination into pDEST-GST. Other Ubiquitin mutants constructs (Ub TEK (K6A/L11A/T12A/T14A/E34A), Ub Il36 patch (L8A/I36A/L71A/L73A), Ub IL44 patch (L8A/L44A/H68A/V70A), Ub Phe4 patch (Q2A/F4A/T14A), Ub (Q49A/R72A), Ub (R42A/Q49A/D52A/R72A)) flanked by att-B and att-P recombination sites were generated by gene synthesis (Biobasic) directly into pUC57-Kan Vector and bacterial expression constructs were generated by recombination into pDEST-GST. Human cDNA ASXL1 (NCBI: NM_015338.5) and ASXL2 (NCBI: NM_018263.4) were cloned from HeLa total RNA by reverse transcription and inserted into pENTR D-Topo plasmid. BAP1 point mutations constructs were generated by site direct mutagenesis in pENTR D-Topo BAP1 using PfuUltra High-Fidelity DNA Polymerase. Human Myc-ASXL1 ΔASXM and ASXL2 ΔASXM constructs were generated by PCR-based subcloning of 2 fragments each ligated in frame into pENTR D-Topo. Expression constructs of ASXL1, ASXL2 and corresponding vectors with deletions of ASXM were generated in pDEST-Myc and pDEST-Flag. Other expression constructs for BAP1 and corresponding mutants forms, were generated using LR clonase in pDEST-Myc, pDEST-Flag and bacterial pDEST-His. Full length ASXM1 and ASXM2 and deletions mutants forms of ASXM2 (ASXM2 246-313, ASXM2 300-401,

ASXM2 316-401, ASXM2 246-347) were sub-cloned by PCR and inserted into pENTR D-Topo plasmid. ASXM2 point mutations constructs were generated by site direct mutagenesis in pENTR D-Topo ASXM2. Bacterial expression vectors of ASXM1, ASXM2 and respective mutant forms were generated in pDEST-GST and pDEST-MBP vectors.

Cell culture and cell transfection

Primary human skin fibroblasts (LF1), BAP1-deficient human lung squamous carcinoma NCI-*H226*, BAP1-deficient human mesothelioma NCI-H28, U2OS osteosarcoma, human embryonic kidney HEK293T (293T), Cervical cancer HeLa, normal Human Lung Fibroblasts (IMR90), phoenix ampho and 293-GPG packaging cells were cultured in Dulbecco's modified Eagle's medium (DMEM) supplemented with foetal bovine serum (FBS), L-glutamine and penicillin/streptomycin. HeLa S3 cells were cultured in Minimum Essential Media (MEM) supplemented with FBS, L-glutamine and penicillin/streptomycin.

293T cells were transfected with the mammalian expressing vectors using polyethylenimine (PEI) (Sigma-Aldrich). Three days post-transfection, cells were harvested for immunoblotting, immunoprecipitation or immunostaining.

Similar numbers of H226 BAP1-null cells stably expressing BAP1, $BAP1^{C91S}$ or $BAP1^{R666\text{-}H669}$ were seeded on the plates and cultured for 5 days. The clonogenic survival assay was essentially done as described before [60].

U2OS or LF1 cells were transfected using Lipofectamine 2000 (Life technologies) with 200 pmol of either ON-TARGET plus Non-targeting pool (D-001810) or ON-TARGET plus SMARTpool BAP1 (L-005791) (Thermo Scientific, Dharmacon) or with a pool of siRNA sequences purchased from Sigma-Aldrich targeting ASXL1 (pool of 4 oligonucleotides, SASI_Hs02_00347642, SASI_Hs01_00200507, SASI_Hs01_00200508, SASI_Hs01_00200509) and ASXL2 (2 pools of 4 oligonucleotides, SASI_Hs01_00202197, SASI_Hs01_00202198, SASI_Hs01_00202199, SASI_Hs01_00202200 and SASI_Hs01_00202197, SASI_Hs01_00202200, SASI_Hs01_00202203, SASI_Hs01_00202201). Four days post-transfection, cells were harvested for immunoblotting.

siRNA DUB screen

HeLa cells were transfected with individual siRNA pool targeting DUBs (ON-TARGETplus® SMARTpool® siRNA Library-Human Deubiquitinating Enzymes) using Lipofectamine 2000 (Life Technologies). Three days post-transfection, cells were fixed and used for immunostaining with H2Aub

antibody and the fluorescence signals were detected with a Fluoroskan Ascent™ Microplate Fluorometer (Thermo Scientific), and the obtained values were used to derive the Z-scores. The screen was done in duplicate and the values of H2Aub signals were normalized to DAPI staining.

qRT-PCR analysis of mRNA expression

Total RNA was used to prepare the cDNAs as described [317]. The cDNAs were analyzed by Real time PCR using SYBR Green detection DNA quantification kit (Life technologies) to determine levels of gene mRNAs. PCR was conducted on an Applied Biosystems® 7500 Real-Time PCR Systems (Life Technologies). To ensure accurate quantification of mRNA, similar amounts of total RNA were spiked with an *in vitro* synthesized GAL4 mRNA, which was performed following the manufacturer procedure (MAXIscript Kit Procedure, Life Technologies). The transcript was synthesized from pcDNA.3-GAL4 construct with T7 promoter. The primers used are listed below. hASXL2-F: GAATCCAGGTGCGAAAAGTAC and hASXL2-R: GATGGAGACTGGAAAACGAGC and GAL4-F: CAACTGGGAGTGTCGCTACT, and GAL4-R: AATCATGTCAAGGTCTTCTCGA

Immunoblotting and antibodies-Total cell extracts were used for SDS-PAGE and immunoblotting was done according to standard procedures [317]. The band signals were acquired with a LAS-3000 LCD camera coupled to MultiGauge software (Fuji, Stamford, CT, USA). Anti-FOXK2 rabbit polyclonal antibody was previously described [9]. The rabbit polyclonal antibody anti-ASXL1 was generated using bacteria-expressed fragment (700-950 amino acids of the human protein) with Pacific Immunology. Mouse monoclonal anti-BAP1 (C4, sc-28383), rabbit polyclonal anti-BAP1 (H300, sc-28236), rabbit polyclonal anti-YY1 (H414, sc-1703), rabbit polyclonal anti-OGT (H300, sc-32921), mouse monoclonal anti-CDC6 (180.2, sc-9964), mouse monoclonal anti-MCM6, mouse monoclonal anti-tubulin (B-5-1-2, sc-SC-23948), mouse monoclonal anti-p53 (DO-1, sc-126), mouse monoclonal anti-p16 (JC8, sc-56330), mouse monoclonal anti-MDM2 (SMP14, sc-965), rabbit polyclonal anti-FOXK1 (H-140, sc-134550), and mouse monoclonal anti-PARP1 (F2, sc-8007) were from Santa Cruz. Rabbit polyclonal anti-HCF-1 (A301-400A) and rabbit polyclonal anti-ASXL2 (A302-037A) were from Bethyl Laboratories. Mouse monoclonal anti-p21 (55643) was from BD Pharmigen. Mouse monoclonal anti-Flag (M2) and rabbit polyclonal anti-GST (G7781) were from Sigma-Aldrich. Mouse monoclonal anti-MYC (9E10) was from Covance. Rabbit polyclonal anti-

H2Aub K119 (D27C4) rabbit polyclonal anti-H2Bub K120 (D11 XP), mouse monoclonal anti-RB (4H1), rabbit polyclonal anti-pRB (S807/811) and mouse monoclonal (HRP conjugated) anti-MBP (E8038) were from Cell Signaling. Mouse monoclonal anti-H2Bub antibody (NRO3) was from MEDIMABS. Mouse monoclonal anti-Phospho-H2AX (ser139) (clone JBW301, 05-636), Mouse monoclonal anti-H2Bub antibody clone 56 (05-1312), Mouse monoclonal anti-H2Aub K119 antibody clone E6C5 (05-678) and mouse monoclonal anti-β-Actin (MAB1501, clone C4) were from Millipore.

Immunodepletion and Immunoprecipitation

Immunodepletion experiments were done as described [317]. Reciprocal immunoprecipitation from the BAP1 complexes was conducted essentially as described [9]. Briefly, the purified BAP1 complexes were incubated with the indicated antibodies overnight at 4 ºC. The immuno-depleted complexes were recovered next day with protein G sepharose beads saturated with 1% BSA. Co-immunoprecipitation was conducted as described [317].

Cell lines with stable expression and protein complex purification

HeLa S3 cell lines stably expressing Flag-HA-BAP1, Flag-HA-BAP1$^{\Delta CTD1}$, or Flag-HA-BAP1$^{R666\text{-}H669}$, H28 cell lines stably expressing Flag-HA-BAP1 and Flag-HA-BAP1^{C91S}, as well as H226 cell lines stably expressing Flag-HA-BAP1, Flag-HA-BAP1^{C91S} and Flag-HA-BAP1$^{R666\text{-}H669}$ were generated following retroviral infection using pOZ-N-Flag-HA-IRES-IL2R retroviral constructs and selection using anti-IL2 magnetic beads (Life Technologies) [317]. U2OS expressing siRNA resistant Flag-HA-BAP1, Flag-HA-BAP1^{C91S}, Flag-HA-BAP1 $^{\Delta CTD}$ and Flag-HA- BAP1$^{R666\text{-}H669}$ were generated following retroviral infection using pMSCV-Flag-HA-IRES-Puro based constructs and selection with 3 μg/ml of puromycin. Around 3 X 10^9 of HeLa S3 cells were used for the immunoaffinity purification of the different BAP1 complexes. The purification was done as previously described [9]. Eluted complexes were used for silver stain, western blot analysis and *in vitro* ubiquitin pulldown and DUB assays.

In vitro interaction assays

Protein interaction pull down assays were conducted as previously described [317].

Ubiquitin pull down interaction assays

GST-ubiquitin immobilized beads and its corresponding mutant forms were purified using glutathione agarose beads. For the Ubiquitin-Agarose pull down interaction assays, His-BAP1 or the corresponding mutant forms (1.6 µg, 20 nM) were pre-incubated for 30 min to 1 hour with GST-ASXM1 or GST-ASXM2 (2 µg each, 50 nM) or GST-ASXM2 deletion mutant forms at 4 ºC in 50 mM Tris, pH 7.5; 150 mM NaCl; 1% Triton; 1 mM PMSF, protease inhibitors cocktail and 2mM DTT. The mix was incubated for 3 hours with Ubiquitin-Agarose beads (Boston Biochem) which were then washed 6 times with the same buffer. The associated proteins were eluted in Laemmli buffer and subjected to western blotting. For the GST-Ubiquitin (GST-Ub) pull down interaction assays, His-BAP1 or His-BAP1 C91S or the recombinant BAP1 deletion mutants (1.6 µg, 20 nM) were pre-incubated for 30 min to 1 hour with either MBP-ASM2 or its corresponding mutant forms (2 µg, 30 nM). The mix was then incubated overnight with either GST-Ubiquitin immobilized beads or mutant forms (3 µg, 80 nM). The beads were washed 6 times with the same buffer and the associated proteins were subjected to western blotting. For the GST-Ubiquitin (GST-Ub) pull down interaction assays using MBP-ASXM2 (2 µg, 30 nM) or MBP-CTD (3 µg, 40 nM), the purified proteins were incubated for 16 hours with GST-Ubiquitin immobilized beads (3 µg, 80 nM). The beads were washed 6 times with the same buffer and the associated proteins were subjected to western blotting.

Purification of the nucleosomes and in vitro DUB assay

Native nucleosomes were purified as described [60]. The purified nucleosomes were used for the *in vitro* DUB assay using either Flag-HA purified BAP1 complexes or bacteria-purified His-BAP1 (8 ng, 2 pM) with or without bacteria purified GST-ASXM1/2 (10 ng, 4 pM) or MBP-ASXM2 (10 ng, 2,8 pM) as described [60]. The DUB reaction was carried out in the reaction buffer (50 mM Tris-HCl, pH 7.3; 1 mM $MgCl_2$; 50 mM NaCl; 1 mM DTT) for the indicated times at 37°C. The *in vitro* reaction was stopped by adding Laemmli buffer and analyzed by immunoblotting.

Synchronization and cell cycle analysis-U2OS cells were synchronized at the G1/S border using the method of thymidine (2 mM) double block and analyzed by flow cytometry as described previously [242].

Immunofluorescence

The immunostaining procedure was carried as previously described [68].

Protein sequence analysis and structure modeling-Conservation of protein sequences was determined using Geneious 6.1.2 (Biomatters, http://www.geneious.com). The ubiquitin resolved 3D structure PDB

file (1UBQ) was downloaded from the PDB database (http://www.rcsb.org/pdb/home/home.do). We used the Chimera software (UCSF Chimera V 1.10) to visualize the 3D structure and to highlight different ubiquitin interfaces.

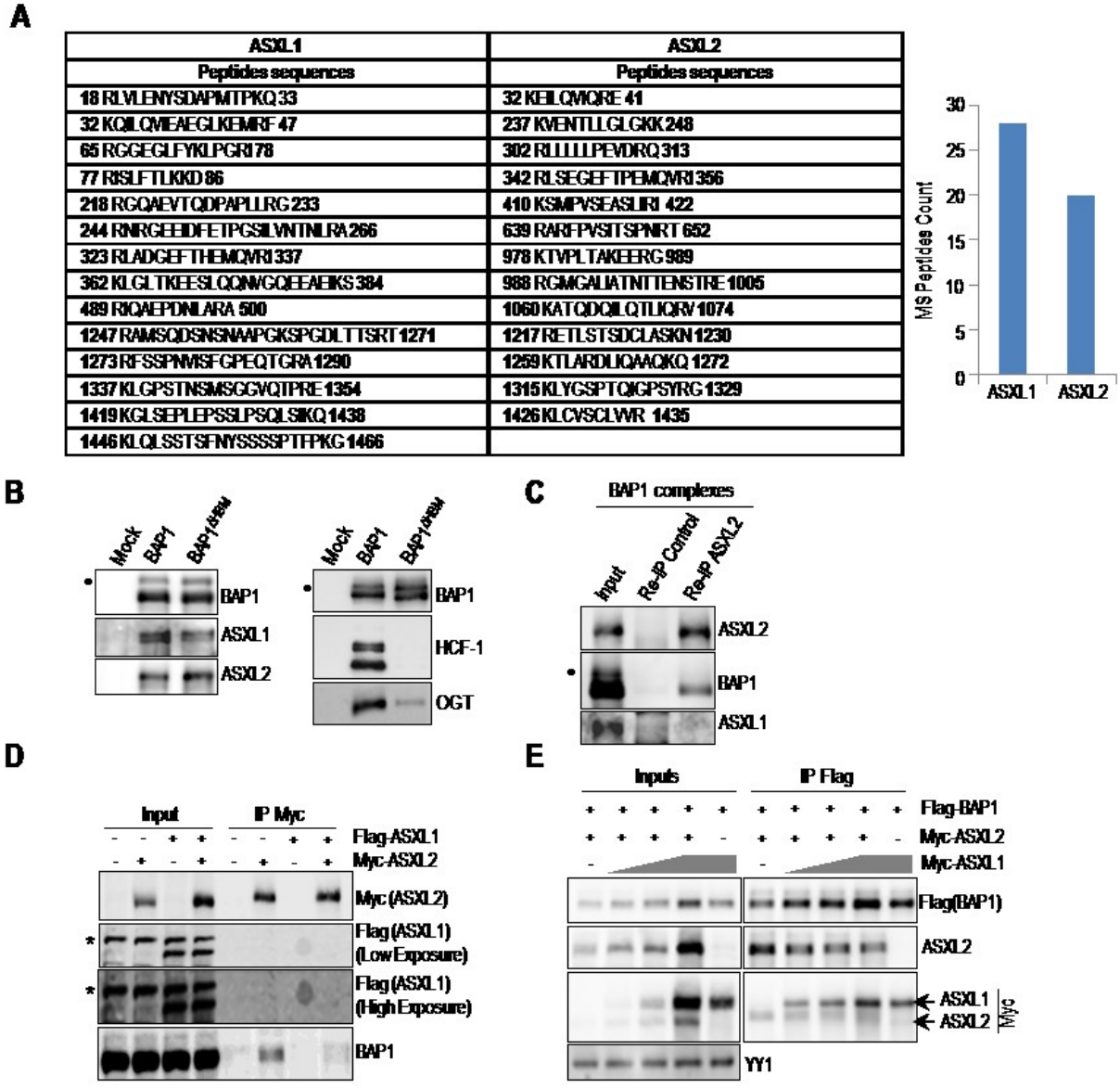

Figure 1

Figure 1. BAP1 interacts with either ASXL1 or ASXL2.A) BAP1 complexes contain relatively similar amounts of ASXL1/2 proteins. (**A**) ASXL1/2 peptides identified by mass spectrometry following the purification of BAP1 complexes from HeLa S3 cells. The amino acid positions of the peptides are indicated. (**B**) HCF-1 is not required to maintain the interaction between BAP1 and ASXL1/2. Purification of BAP1 or BAP1$^{\Delta HBM}$ (lacking the HCF-1-binding motif) complexes and detection of ASXL1/2 and BAP1 by immunoblotting (left panel). The immunopurifed proteins were also analyzed by immunoblotting to detect the two major components of the BAP1 complexes, HCF-1 and OGT (right panel). Note that OGT is greatly reduced in the BAP1$^{\Delta HBM}$ complexes due to the absence of HCF-1. (**C**) Reciprocal immunoprecipitation (Re-IP) of ASXL2 from the purified BAP1 complexes. (**D**) 293T cells were transfected with Myc-ASXL2 (6 µg) with or without Flag-ASXL1 (4 µg) expression vectors and harvested, three days later, for IP of Myc (ASXL2). (**E**) 293T cells were transfected with Flag-BAP1 (0.1 µg)

and Myc-ASXL2 (3 µg) constructs in the presence of increasing amounts of Myc-ASXL1 construct (1, 2 and 5 µg) and harvested, three days later, for IP of BAP1 using anti-Flag. Overexpressed Myc-ASXL2 was detected with anti-ASXL2 and anti-Myc antibodies. ASXL1 was detected with anti-Myc antibody. The difference in M.W. allows discrimination between ASXL1 and ASXL2 bands. YY1 is used as a loading control The dot and the star indicate a monoubiquitinated form of BAP1 [9], and non-specific bands respectively (panels **B**, **C**, **D**

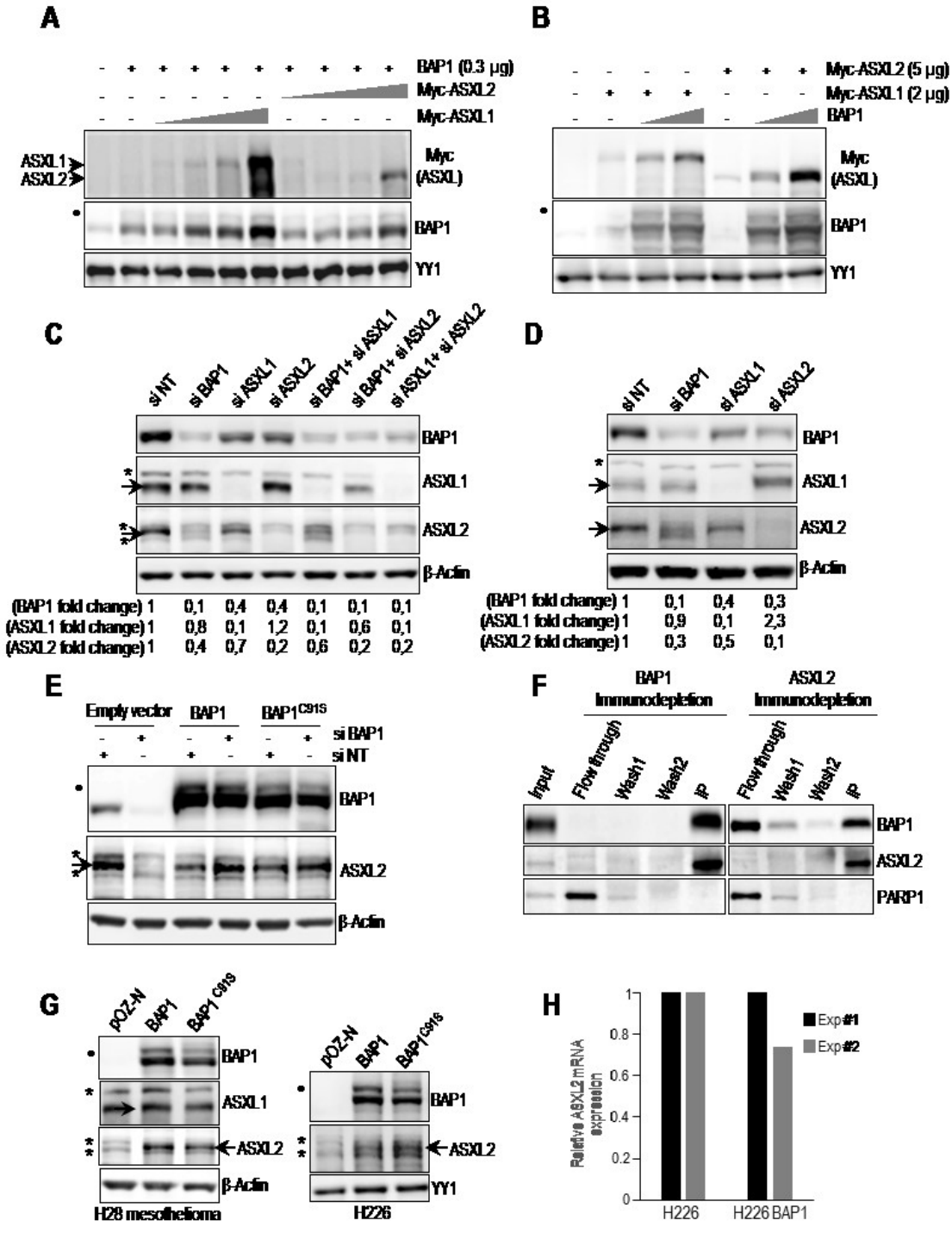
A
BAP1 (0.3 µg)
Myc-ASXL2
Myc-ASXL1
ASXL1
ASXL2
Myc (ASXL)
BAP1
YY1
B
Myc-ASXL2 (5 µg)
Myc-ASXL1 (2 µg)
BAP1
Myc (ASXL)
BAP1
YY1
C
si NT
si BAP1
si ASXL1
si ASXL2
si BAP1+ si ASXL1
si BAP1+ si ASXL2
si ASXL1+ si ASXL2
BAP1
ASXL1
ASXL2
β-Actin
(BAP1 fold change) 1 0,1 0,4 0,4 0,1 0,1 0,1
(ASXL1 fold change) 1 0,8 0,1 1,2 0,1 0,6 0,1
(ASXL2 fold change) 1 0,4 0,7 0,2 0,6 0,2 0,2
D
si NT
si BAP1
si ASXL1
si ASXL2
BAP1
ASXL1
ASXL2
β-Actin
(BAP1 fold change) 1 0,1 0,4 0,3
(ASXL1 fold change) 1 0,9 0,1 2,3
(ASXL2 fold change) 1 0,3 0,5 0,1
E
Empty vector
BAP1
BAP1C91S
si BAP1
si NT
BAP1
ASXL2
β-Actin
F
BAP1 Immunodepletion
ASXL2 Immunodepletion
Input
Flow through
Wash1
Wash2
IP
BAP1
ASXL2
PARP1
G
pOZ-N
BAP1
BAP1 C91S
BAP1
ASXL1
ASXL2
β-Actin
H28 mesothelioma
YY1
H226
H
Relative ASXL2 mRNA expression
Exp#1
Exp#2
H226
H226 BAP1

Figure 2

Figure 2. BAP1 and ASXL1/2 are co-regulated and loss of BAP1 in cancer is concomitant with ASXL2 depletion. (**A**) 293T cells were transfected with BAP1 and increasing amounts of either Myc-ASXL1 (0.5, 1, 2 and 5 μg) or Myc-ASXL2 (0.5, 1, 2 and 5 μg) expression vectors and harvested, three days later, for immunoblotting. (**B**) 293T cells were transfected with Myc-ASXL1 or Myc-ASXL2 with increasing amounts of BAP1 (0.3 and 1 μg) vectors and harvested, three days later, for immunoblotting. (**C**) Protein levels following siRNA depletion of BAP1 and/or ASXL1/2 in U2OS cells. (**D**) Protein expression following siRNA depletion of BAP1, ASXL1 and ASXL2 in LF1 human fibroblasts. Quantification of band intensity was conducted relative to the non-target siRNA control (panels **C**, **D**). (**E**) Depletion of endogenous BAP1 using siRNA in U2OS cells stably expressing empty vector, siRNA-resistant BAP1 wild-type or siRNA-resistant BAP1 catalytic dead mutant (C91S). Protein levels of BAP1 and ASXL2 were detected by immunoblotting. (**F**) Immunodepletion of BAP1 or ASXL2 from HeLa nuclear extracts. The nuclear DNA damage signaling enzyme, PARP1, was used as a control, which mostly remained in the flow through fraction. (**G**) Reconstitution by retroviral infection of H28 mesothelioma and H226 non-small lung carcinoma BAP1-deficient cells with BAP1 or $BAP1^{C91S}$. Protein levels of BAP1 and mutants were detected by immunoblotting. (**H**) mRNA of ASXL2 in reconstituted H226 cells was quantified by qPCR. The data represent two independent experiments. β-Actin or YY1 are used as protein loading controls.The dot and stars indicate a monoubiquitinated form of BAP1 [9], and non-specific bands respectively (panels, **A**, **B**, **C**, **D**, **E**, **G**).

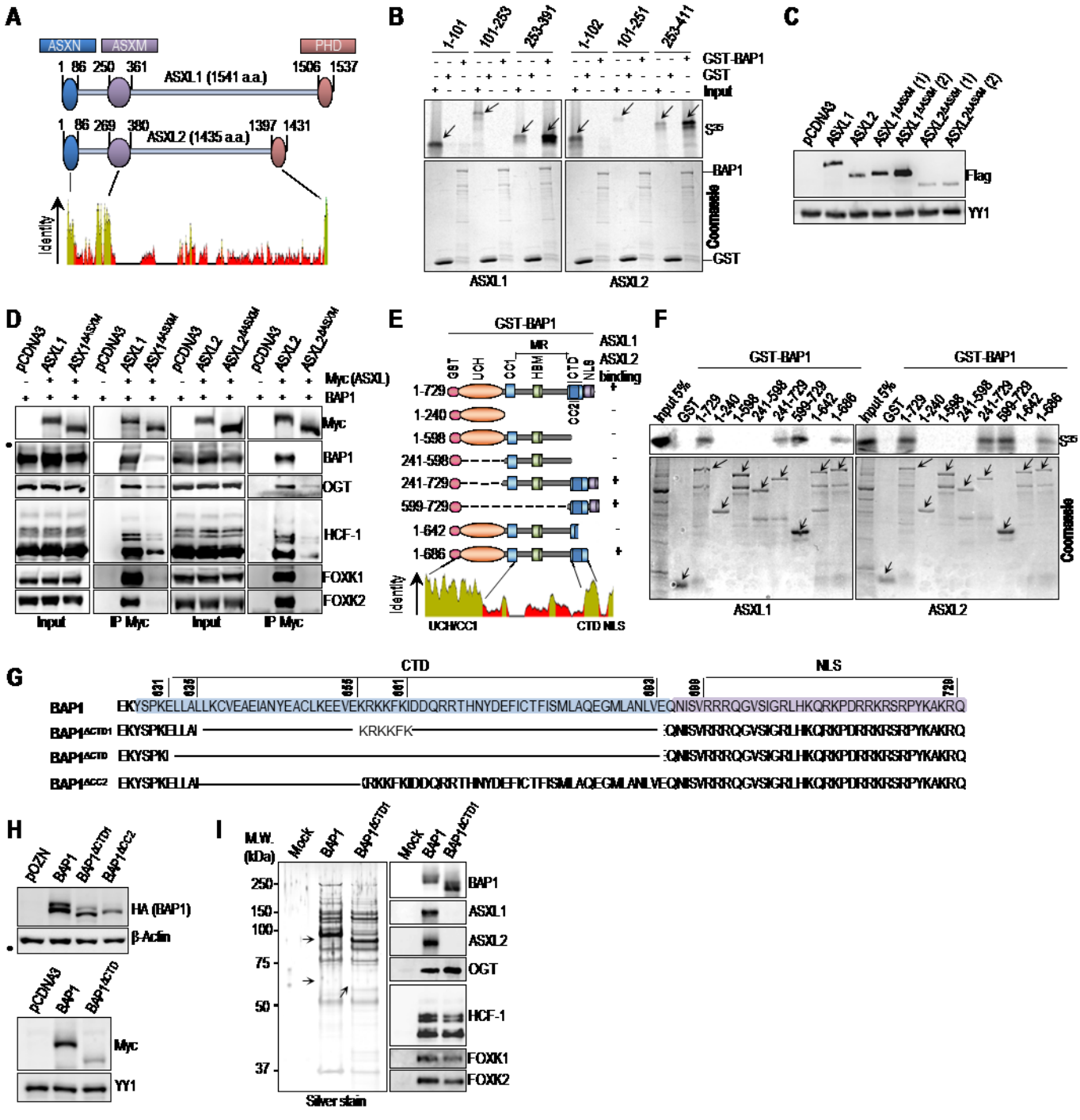
A
ASXN
ASXM
PHD
1 86 250 361
ASXL1 (1541 a.a.)
1506 1537
1 86 269 380
ASXL2 (1435 a.a.)
1397 1431
Identity
B
1-101
101-253
253-391
1-102
101-251
253-411
GST-BAP1
GST
Input
S35
BAP1
Coomassie
GST
ASXL1
ASXL2
C
pCDNA3
ASXL1
ASXL2
ASXL1ΔASXM (1)
ASXL1ΔASXM (2)
ASXL2ΔASXM (1)
ASXL2ΔASXM (2)
Flag
YY1
D
pCDNA3
ASXL1
ASXL1ΔASXM
ASXL2
ASXL2ΔASXM
Myc (ASXL)
BAP1
Myc
BAP1
OGT
HCF-1
FOXK1
FOXK2
Input
IP Myc
E
GST-BAP1
MR
ASXL1
ASXL2
binding
GST
UCH
CC1
HBM
CTD
NLS
CC2
1-729
1-240
1-598
241-598
241-729
599-729
1-642
1-686
Identity
UCH/CC1
CTD NLS
F
GST-BAP1
Input 5%
GST
S35
Coomassie
ASXL1
ASXL2
G
CTD
NLS
BAP1
BAP1ΔCTD1
BAP1ΔCTD
BAP1ΔCC2
EKYSPKELLALLKCVEAEIANYEACLKEEVEKRKKFKIDDQRRTHNYDEFICTFISMLAQEGMLANLVEQNISVRRRQGVSIGRLHKQRKPDRRKRSRPYKAKRQ
EKYSPKELLAI
KRKKFK
QNISVRRRQGVSIGRLHKQRKPDRRKRSRPYKAKRQ
EKYSPKI
QNISVRRRQGVSIGRLHKQRKPDRRKRSRPYKAKRQ
EKYSPKELLAI
RKKFKIDDQRRTHNYDEFICTFISMLAQEGMLANLVEQNISVRRRQGVSIGRLHKQRKPDRRKRSRPYKAKRQ
H
pOZN
BAP1
BAP1ΔCTD1
BAP1ΔCC2
HA (BAP1)
β-Actin
pCDNA3
BAP1
BAP1ΔCTD
Myc
YY1
I
M.W. (kDa)
Mock
BAP1
BAP1ΔCTD1
250
150
100
75
50
37
Silver stain
BAP1
ASXL1
ASXL2
OGT
HCF-1
FOXK1
FOXK2

Figure 3

Figure 3. ASXL1/2 use their ASXM domain to interact with the CTD domain of BAP1. (**A**) Schematic representation and conservation of ASXL1/2. (**B**) GST-pull down assay using GST-BAP1 and methionine S^{35}-labeled ASXL1 or ASXL2 fragments. The arrows indicate the full length forms of the fragments. **C**) ASXM is required for ASXL2, but not ASXL1, stability. Flag-ASXL1/2 and their respective Flag-ASXL1/2 ΔASXM mutants (3 μg each) were transfected in 293T cells which were harvested, three days post-transfection, for immunoblotting. A duplicate of transfection is shown for Flag-ASXL1/2 ΔASXM mutants. (**D**) 293T cells were transfected with Myc-ASXL1 (4 μg), Myc-ASXL1 ΔASXM (4 μg), Myc-ASXL2 (4 μg), or Myc-ASXL2 ΔASXM (6 μg), along with BAP1 (1 μg) vectors and harvested, three days post-transfection, for IP with anti-Myc. (**E)** Schematic representation of the BAP1 fragments used for *in vitro* pull down in panel **F.** (**F**) GST-pull down assay using GST-BAP1 fragments and methionine S^{35}-labeled ASXM domains of ASXL1 or ASXL2. The arrows indicate the full length forms of the fragments**.** (**G**) Schema of the different deletions in the CTD domain used to generate BAP1 mutants. $BAP1^{\Delta CTD1}$ represents a deletion of the CTD from 635 up to 693 amino acids except the KRKKFK motif which is suggested to function as an NLS [314]. We also generated a $BAP1^{\Delta CTD}$ which represents a mutant with a deletion of the CTD domain (Δ631-693 amino acids). $BAP1^{\Delta CC2}$ represents a mutant with a smaller deletion within the CTD domain (Δ635-655 amino acids). (**H**) A functional CTD is required for proper protein stability of BAP1. Protein expression levels of BAP1 and its CTD deletion mutant form in stable HeLa S cell lines (Top panel). Myc-BAP1, Myc-BAP1 ΔCTD expression constructs (3 μg each) were transfected in 293T cells, which were harvested, three days post-transfection, for immunoblotting (Bottom panel). (**I**) Left panel, silver stain of the immunopurified BAP1 and $BAP1^{\Delta CTD1}$ complexes. Right panel, western blot detection of components of the BAP1 complexes. The high and low arrows indicate the position of ASXL2 and BAP1 (WT and $BAP1^{\Delta CTD1}$) respectively. β-Actin or YY1 are used as protein loading controls. The dot indicates a monoubiquitinated form of BAP1 (panel **D**, **H**) [9].

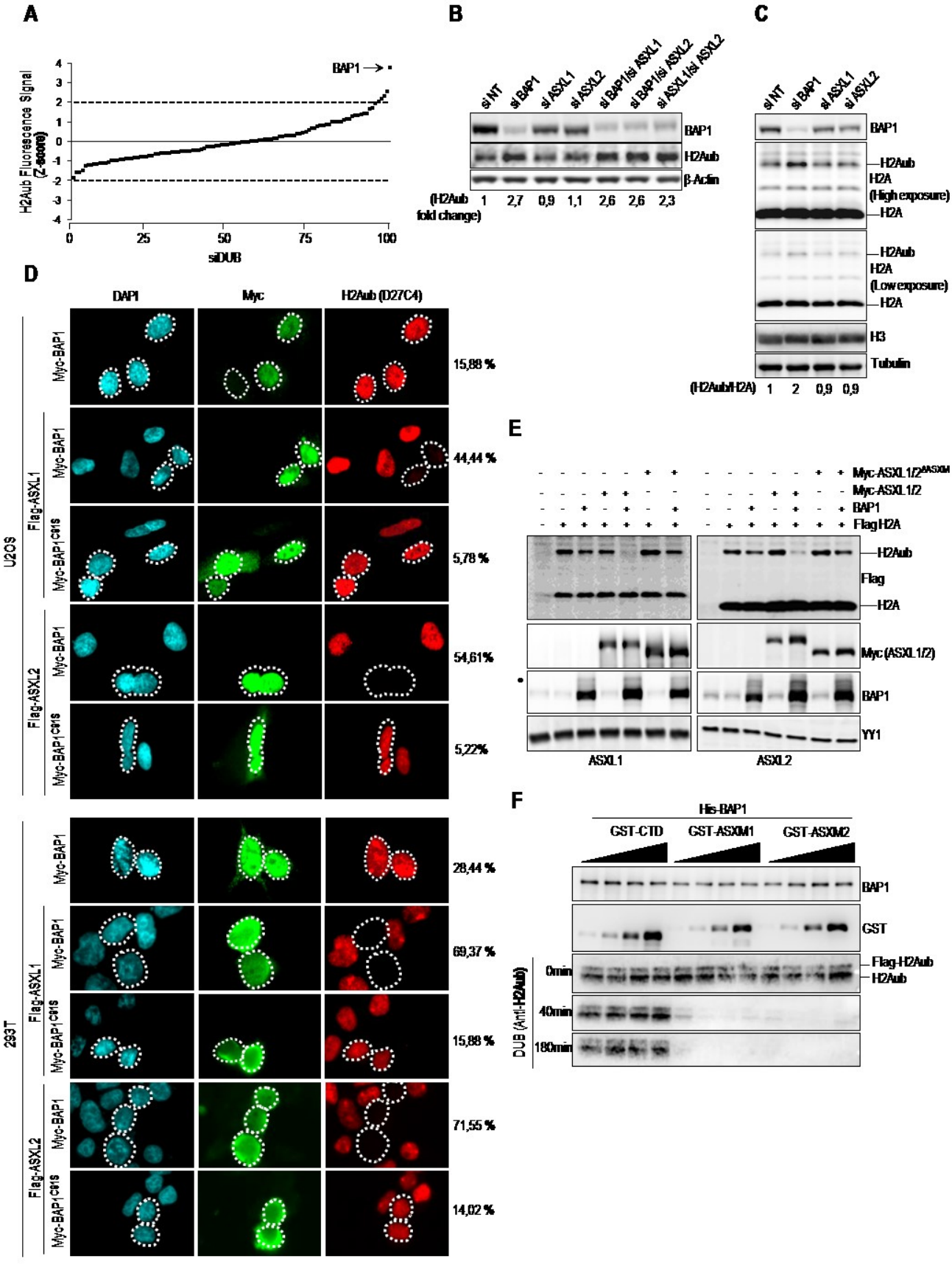
A
H2Aub Fluorescence Signal (Z-scores)
BAP1
siDUB
B
si NT
si BAP1
si ASXL1
si ASXL2
si BAP1/si ASXL1
si BAP1/si ASXL2
si ASXL1/si ASXL2
BAP1
H2Aub
β-Actin
(H2Aub fold change) 1 2,7 0,9 1,1 2,6 2,6 2,3
C
si NT
si BAP1
si ASXL1
si ASXL2
BAP1
H2Aub
H2A
(High exposure)
H2A
H2Aub
H2A
(Low exposure)
H2A
H3
Tubulin
(H2Aub/H2A) 1 2 0,9 0,9
D
DAPI
Myc
H2Aub (D27C4)
U2OS
Flag-ASXL1
Myc-BAP1
Myc-BAP1C91S
Flag-ASXL2
Myc-BAP1
Myc-BAP1C91S
15,88 %
44,44 %
5,78 %
54,61%
5,22%
293T
Flag-ASXL1
Myc-BAP1
Myc-BAP1C91S
Flag-ASXL2
Myc-BAP1
Myc-BAP1C91S
28,44 %
69,37 %
15,88 %
71,55 %
14,02 %
E
Myc-ASXL1/2ΔASXM
Myc-ASXL1/2
BAP1
Flag H2A
H2Aub
Flag
H2A
Myc (ASXL1/2)
BAP1
YY1
ASXL1
ASXL2
F
His-BAP1
GST-CTD
GST-ASXM1
GST-ASXM2
BAP1
GST
Flag-H2Aub
H2Aub
DUB (Anti-H2Aub)
0min
40min
180min

Figure 4

Figure 4. ASXM of ASXL1/2 stimulates BAP1 DUB activity. (**A**) siRNA screen for DUBs that coordinate H2Aub levels. Following transfection with siRNA DUB library, HeLa cells were fixed and immunostained for H2Aub K119 (H2Aub). The fluorescence signal was determined and the values used to derive the Z-scores. (**B**) Knockdown of BAP1 or concomitant Knockdown of ASXL1 and ASXL2 induces a significant increase of the global level of H2Aub. U2OS cells were transfected with siRNA as indicated and harvested four days post-transfection for immunoblotting using the indicated antibodies. Quantification of band intensity for H2Aub was conducted relative to the non-target siRNA control (siNT). (**C**) Increase of H2Aub levels following BAP1 depletion is not due to a global increase of H2A. U2OS cells were transfected with siRNA of BAP1, ASXL1 and ASXL2 and harvested, four days post-transfection, for immunoblotting using the respective antibodies. Tubulin was used a loading control for soluble proteins and histone H3 as a loading control for histones levels. Quantification of band intensity for H2Aub was conducted relative to the non-modified histone H2A and the values were then normalized to the non-target siRNA control (siNT). (**D**) ASXL1/2 promote BAP1 DUB activity toward H2Aub *in vivo*. U2OS cells (top panel) or 293T cells (bottom panel) were transfected with either Myc-BAP1 (0.5 µg) or Myc-BAP1 C91S (0.5 µg) expression constructs in the presence or absence of Flag-ASXL1/2 (4 µg) expression constructs. Three days post-transfection, cells were harvested for Immunostaining using the indicated antibodies. The cells overexpressing BAP1 and BAP1^{C91S} were encircled. Note that the transfections were conducted with plasmid ratios optimized to ensure that most BAP1 transfected cells also express ASXL1 or ASXL2. Cells overexpressing BAP1 were counted for change in H2Aub signal. The percentages at the right of the panel represent the number of cells showing very low signal of H2Aub versus the total number of BAP1 expressing cells. (**E**) 293T cells were transfected as indicated using Flag H2A (0.2 µg), BAP1 (1 µg), Myc-ASXL1 (4 µg) or Myc-ASXL1 ΔASXM (4 µg) vectors (left panel); Myc-ASXL2 (4 µg) or Myc-ASXL2 ΔASXM (6 µg) vectors (right panel) and harvested, three days later, for immunoblotting. (**F**) *In vitro* DUB assay of nucleosomal H2A using recombinant His-BAP1 (8 ng, 2 pM) in presence of increasing amounts of recombinant GST-CTD, GST-ASXM1 or GST-ASXM2 (0.6 pM, 1.2 pM, 2pM and 4 pM). β-Actin, Tubulin or YY1 were used as loading controls.

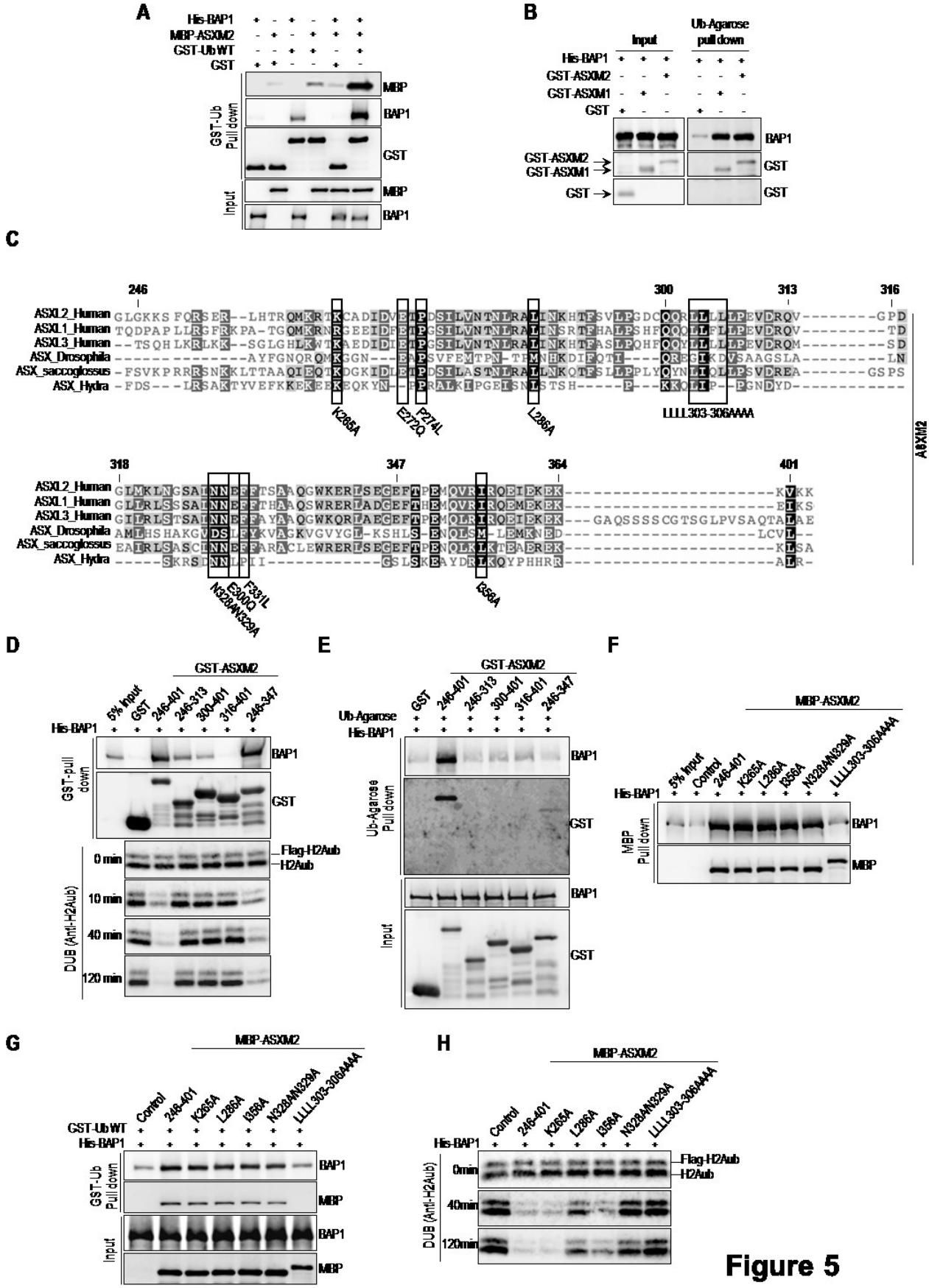
A
His-BAP1
MBP-ASXM2
GST-Ub WT
GST
GST-Ub Pull down
MBP
BAP1
GST
Input
B
Input
Ub-Agarose pull down
His-BAP1
GST-ASXM2
GST-ASXM1
GST
C
246
300
313
316
318
347
364
401
ASXL2_Human
ASXL1_Human
ASXL3_Human
ASX_Drosophila
ASX_saccoglossus
ASX_Hydra
K265A
E272Q
F274L
L286A
LLLL303-306AAAA
E300Q
F331L
N328AN329A
I356A
ASXM2
D
GST-ASXM2
5% Input
GST
246-401
246-313
300-401
316-401
246-347
His-BAP1
GST-pull down
BAP1
GST
Flag-H2Aub
H2Aub
DUB (Anti-H2Aub)
0 min
10 min
40 min
120 min
E
Ub-Agarose
Ub-Agarose Pull down
Input
F
MBP-ASXM2
Control
MBP Pull down
MBP
G
GST-Ub WT
H
0min
40min
120min

Figure 5

Figure 5. ASXM enhances BAP1 binding to ubiquitin.
(**A**) Recombinant His-BAP1 (1.6 µg, 20 nM) and MBP-ASXM2 (2 µg, 30 nM) were incubated with either GST or GST-Ubiquitin-Agarose beads (3 µg, 80 nM) and the pulled down fractions were analysed by immunoblotting. (**B**) Recombinant His-BAP1 (1.6 µg, 20 nM) and GST-ASXM1 or GST-ASXM2 (2 µg, 40 nM) were incubated with ubiquitin-agarose beads and the pulled down fractions were analyzed by immunoblotting. (**C**) Multiple sequence alignment between the ASXM domains of human ASXL1/2, Drosophila ASX and other orthologs of ASX. The mutants of ASXM2 including the cancer-associated mutants used in panels **F**, **G**, **H** and Fig.**8** are shown. (**D**) GST pull down interaction assay and *in vitro* DUB reactions of H2A using His-BAP1 and GST-ASXM2 (full length and deletion mutant forms). For the pull down assay, His-BAP1 (1.6 µg, 20 nM) was incubated with GST-ASXM2 (2 µg, 40 nM) or the different fragment of GST-ASXM2 (2 µg, 50 nM). His-BAP1 (8 ng, 2 pM) and the different recombinant ASXM2 fragments (10 ng, 4 pM) were used for the DUB reactions. (**E**) His-BAP1 (1.6 µg, 20 nM) and the different GST-fused fragments of ASXM2 (2 µg, 40 nM) were subjected to ubiquitin-Agarose pull down assay followed by immunoblotting. (**F**) MBP-pull down interaction assay using recombinant MBP-ASXM2 (full length and mutant forms) (2 µg, 30 nM) and His-BAP1 (1.6 µg, 20 nM). (**G**) GST-Ubiquitin pull down assay using MBP-ASXM2 full length and the different mutant forms with His-BAP1. The pull down was done as in (**A**). (**H**) *In vitro* DUB reactions of H2A using His-BAP1 (8 ng, 2 pM) and the different recombinant MBP-ASXM2 (10 ng, 2,8 pM).

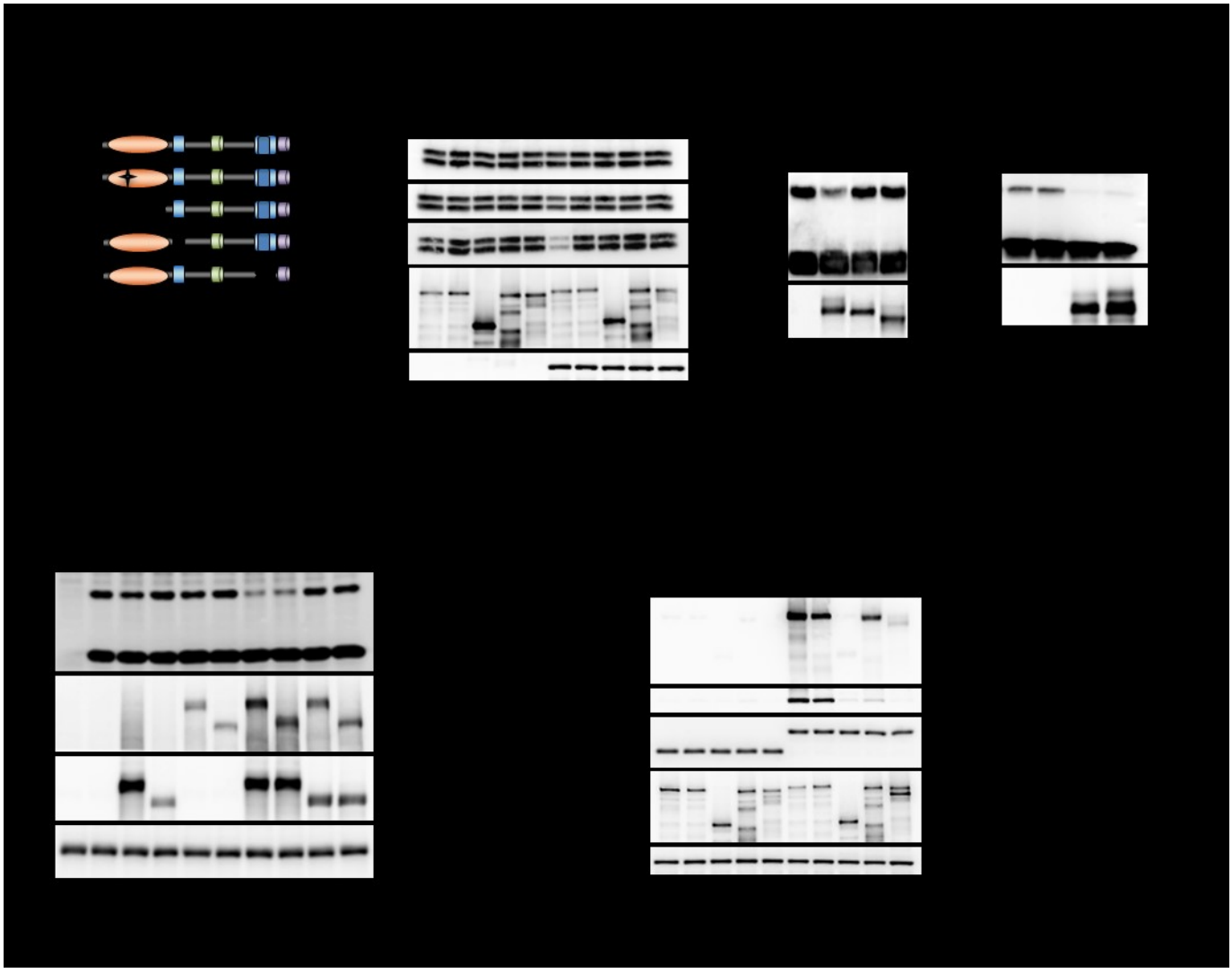

Figure 6. Intramolecular interaction in BAP1 is required to create an ASXM-inducible composite ubiquitin binding interface (CUBI).
(**A**) Schematic representation of the different BAP1 mutants generated for *in vitro* experiments done in panel **B**. **B)** *In vitro* DUB reaction of nucleosomal H2A using His-BAP1 or its mutant forms (8 ng, 2 pM) in presence or absence of MBP-ASXM2 (10 ng, 2,8 pM). **C-D)** *In vitro* deubiquitination assay of nucleosomal histone H2A using purified Flag-HA BAP1, BAP1$^{\Delta CTD1}$ or BAP1$^{\Delta CC2}$ complexes. BAP1$^{\Delta HBM}$ was used as a control since HCF-1 is not required for BAP1 DUB activity. **E)** *In vivo* DUB activity of BAP1$^{\Delta CTD}$ is abolished due to the lack of interaction with ASXL1/2. Flag-H2A (0.2 µg) expression construct was co-expressed in 293T cells with either Myc-BAP1 (1 µg) or Myc-BAP1 ΔCTD (1 µg) with or without Myc-ASXL1 (4 µg) or Myc-ASXL2 (6 µg) expression constructs. Three days post-transfection, cells were harvested for immunoblotting. YY1 is used as a loading control. **F)** His-BAP1 mutants (1.6 µg, 20 nM) and MBP-ASXM2 (2 µg, 30 nM) were subjected to GST-Ubiquitin pull down assay followed by immunoblotting.

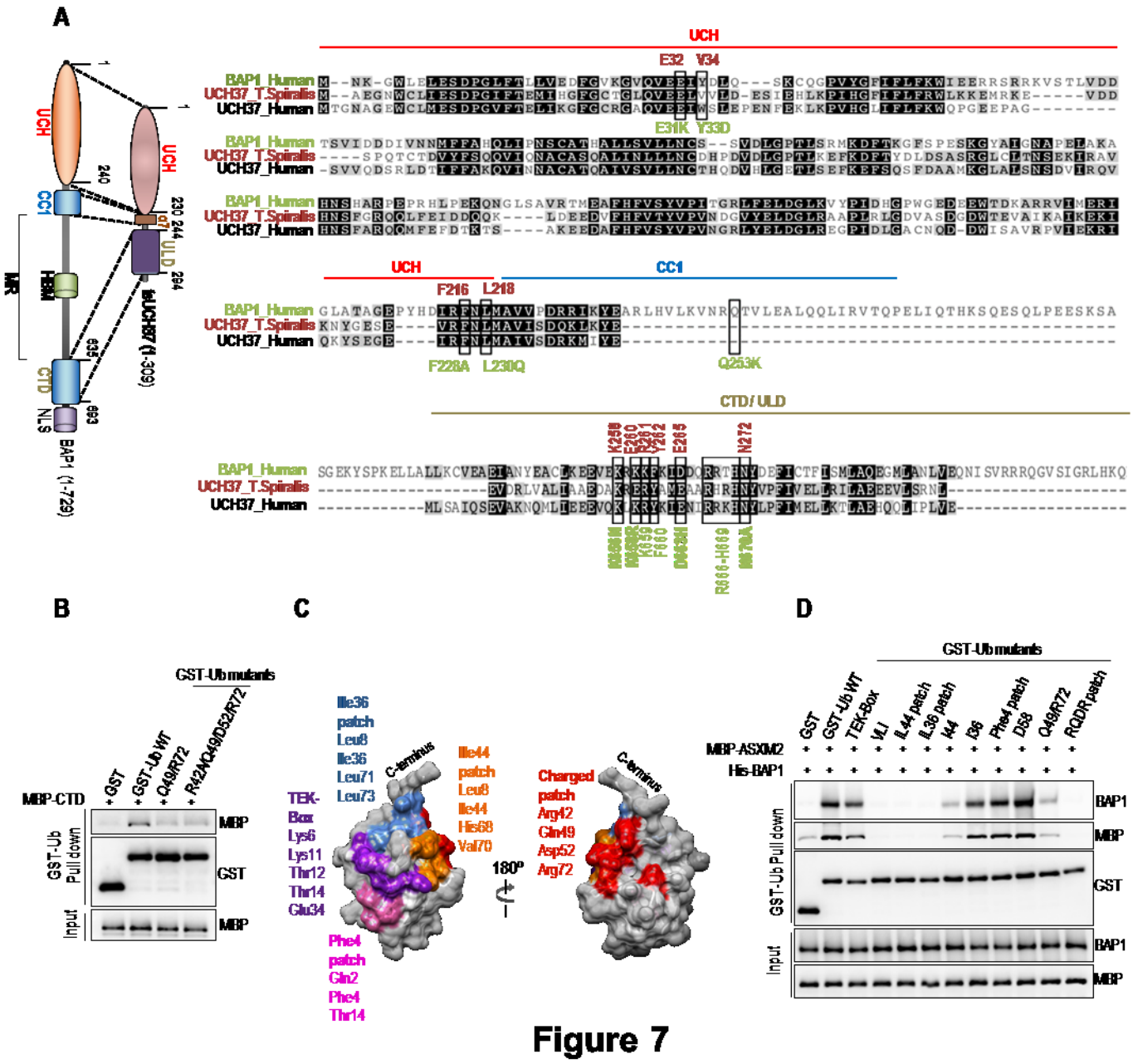

Figure 7

Figure 7. BAP1 CTD is an ubiquitin-interacting motif.
A) Comparison between BAP1 and UCH37. tsUCH37 of the worm *Trichinella spiralis* whose crystal structure was recently reported (38), was aligned with human UCH37 and BAP1. The functional conserved domains between BAP1 and tsUCH37 are shown in the left panel. The alignment (right panel) show conserved motifs and residues in the UCH, CC1 and CTD domains. The mutants of BAP1 including the cancer-associated mutants used in **Fig. 8** are shown. Note the presence in the CTD of the cancer mutant BAP1$^{R666\text{-}H669}$ with a deletion of the R666 to H669 amino acids. **B)** MBP-CTD (3 µg, 40 nM) of BAP1 was subjected to GST-Ubiquitin pull down assay using GST-Ubiquitin wild type or its mutant forms (3 µg, 80 nM)

(all residues were converted to alanines) and then analysed by immunoblotting. **C)** Ubiquitin structure showing the various interaction interfaces**. D)** GST-Ubiquitin pull down interaction assays using GST-Ubiquitin wild type or its different mutant forms (all residues of each path were converted to alanines) and His-BAP1 with MBP-ASXM2 followed by immunoblotting. The pull down was done as in **Fig. 6F**.

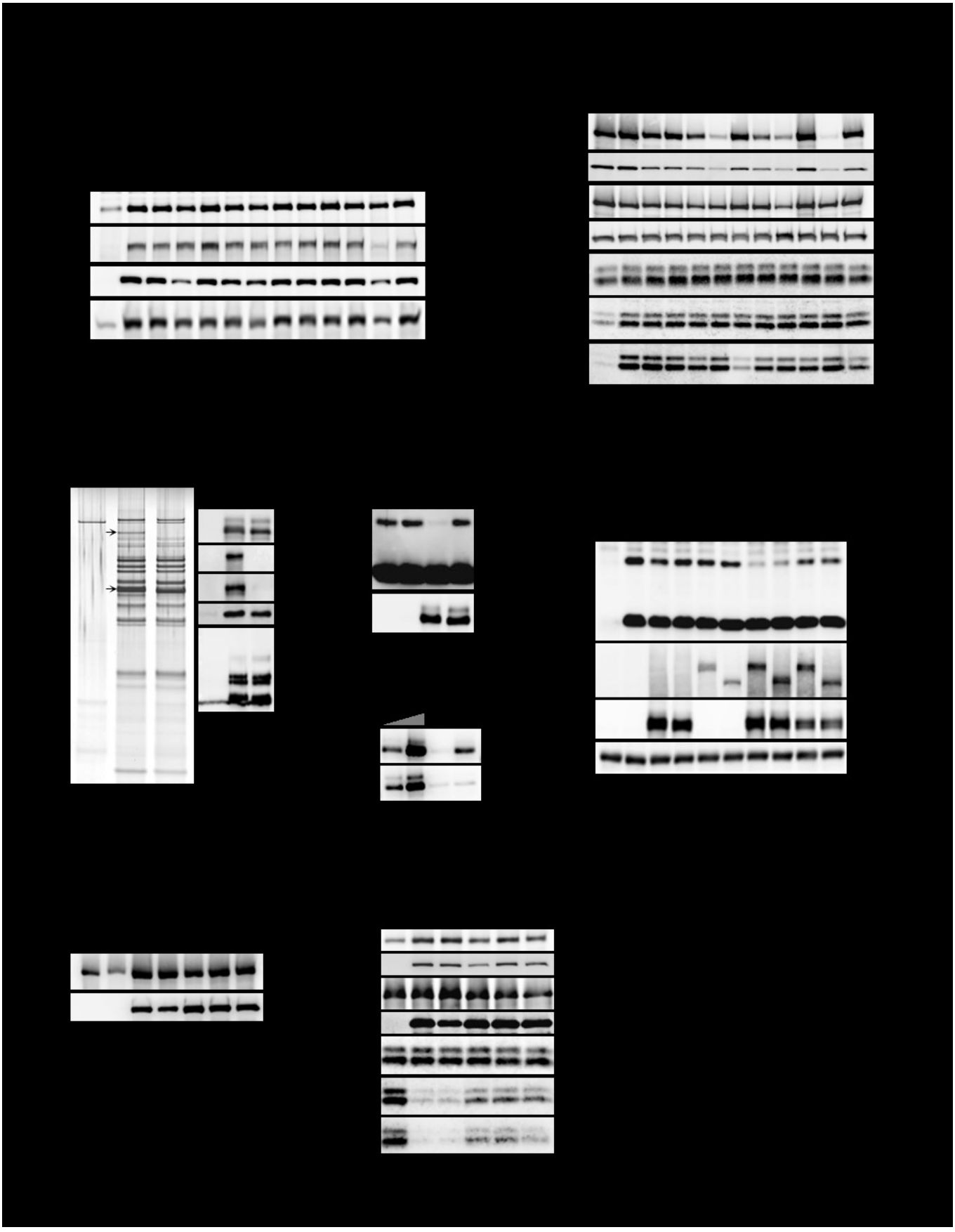

Figure 8. Disruption of BAP1 ubiquitin binding and DUB activity by cancer-associated mutations of BAP1 and ASXL2.

A) R666-H669 BAP1 cancer mutation abolishes its interaction with ASXL2. Myc-ASXL2 (6 μg) construct was co-transfected in 293T with either Flag-BAP1, Flag-BAP1 C91S or Flag-BAP1 mutants constructs (1 μg) and cells were harvested for Flag IP of BAP1 followed by immunoblotting. **B)** Ubiquitin pull down and *in vitro* DUB assays of nucleosomal H2A using GST-ASXM2 and His-BAP1, His-BAP1^{C91S} or the different recombinant mutant forms of BAP1. The same amounts of recombinant proteins as presented in **Fig. 4**, **5** and **6** were used for the *in vitro* reactions. **C)** BAP1 complexes were purified from HeLa cells stably expressing Flag-HA-BAP1 or Flag-HA-BAP1R666-H669. Left panel, silver stain shows the profiles of the complexes. Right panel, western blot detection of the major components of the BAP1 complexes. The high and low arrows indicate the position of ASXL2 and BAP1 respectively. **D)** *In vitro* DUB assay of nucleosomal H2A (top panel) and Ubiquitin pull down assay (bottom panel) using BAP1 and BAP1R666-H669 complexes. **E)** R666-H669 cancer mutation results in the abrogation of its DUB activity *in vivo*. Flag-H2A (0.2 μg) construct was co-expressed in 293T cells with either Myc-BAP1 (1 μg) or Myc-BAP1 R666-H669 (1 μg) with or without Myc-ASXL1 (4 μg) or Myc-ASXL2 (6 μg) expression constructs. Three days post-transfection, cells were harvested for immunoblotting. **F)** His-BAP1 (1.6 μg, 20 nM) and MBP-cancer associated mutants forms of ASXM2 (2 μg, 30 nM) were subjected to MBP pull down interaction assays. **G)** His-BAP1 and MBP-ASXM2 mutants were subjected as done in **Fig. 5**, **6** and **7** to GST-Ubiquitin pull down assay and *in vitro* DUB assay using nucleosomal H2A. The reactions were analyzed by immunoblotting. YY1 is used as a loading control. The dot indicates a monoubiquitinated form of BAP1 [9] (panels **C**, **D**).

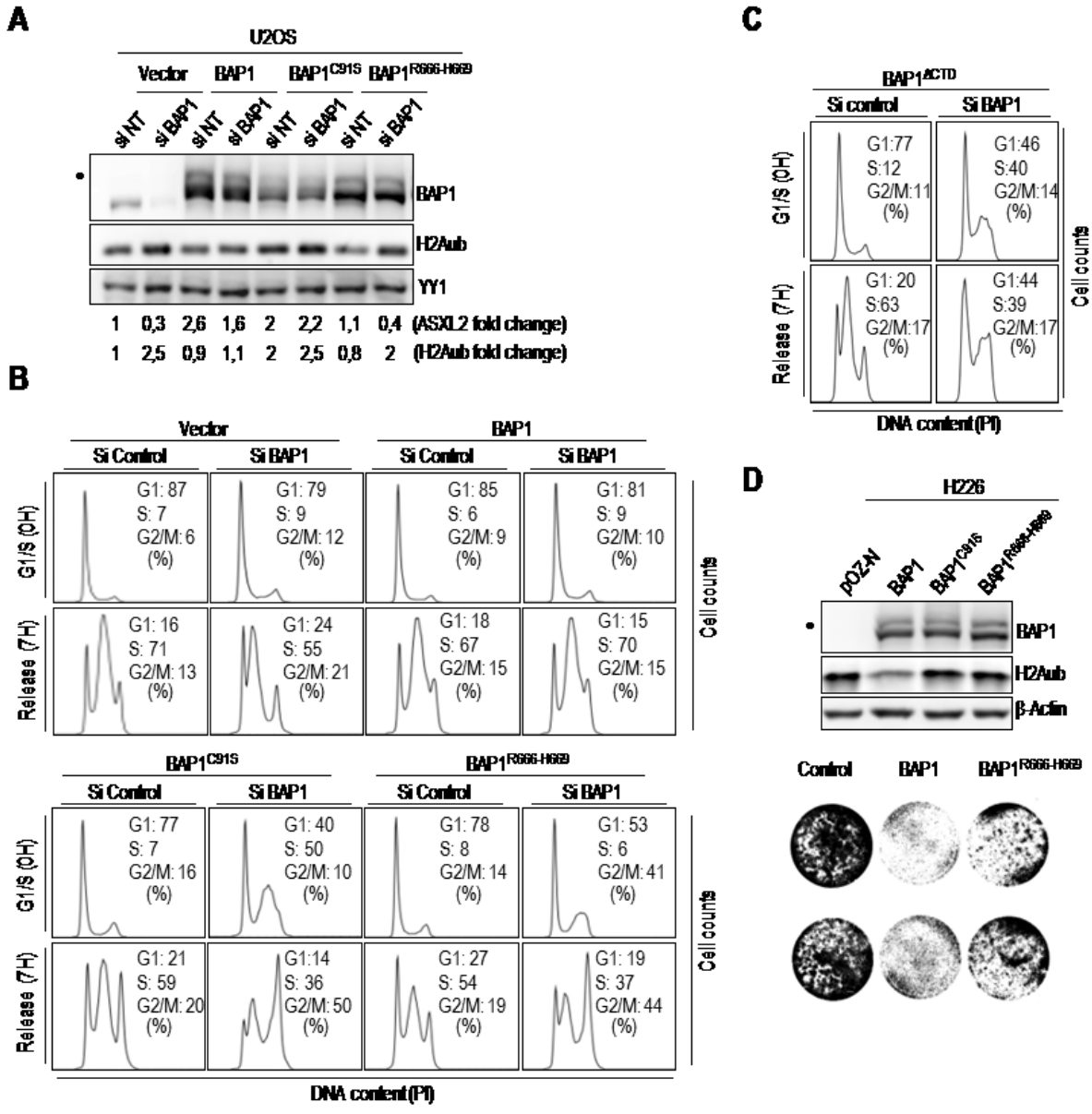

Figure 9

Figure 9. BAP1 regulates cell cycle progression in CTD-dependent manner.

A) Protein levels following depletion of endogenous BAP1 using siRNA in U2OS cells stably expressing siRNA-resistant BAP1, BAP1^{C91S} or BAP1$^{R666\text{-}H669}$. B-C) Mutations of CTD disrupts BAP1 function in regulating cell proliferation. Following siRNA for endogenous BAP1, U2OS cells stably expressing siRNA-resistant BAP1, BAP1^{C91S}, BAP1$^{R666\text{-}H669}$ or BAP1$^{\Delta CTD}$ were synchronized by double thymidine block at the G1/S boundary and released 7 hours to progress through S phase and were then subjected to FACS analysis. D) H226 BAP1-null cells stably expressing BAP1, BAP1^{C91S} or BAP1$^{R666\text{-}H669}$ was analysed by immunoblotting (top panel). Similar numbers of cells were plated and cultured for 5 days prior staining with crystal violet dye (bottom panel). YY1 and β-Actin were used as a protein loading controls. The dot indicates a monoubiquitinated form of BAP1 [9] (panels A, D).

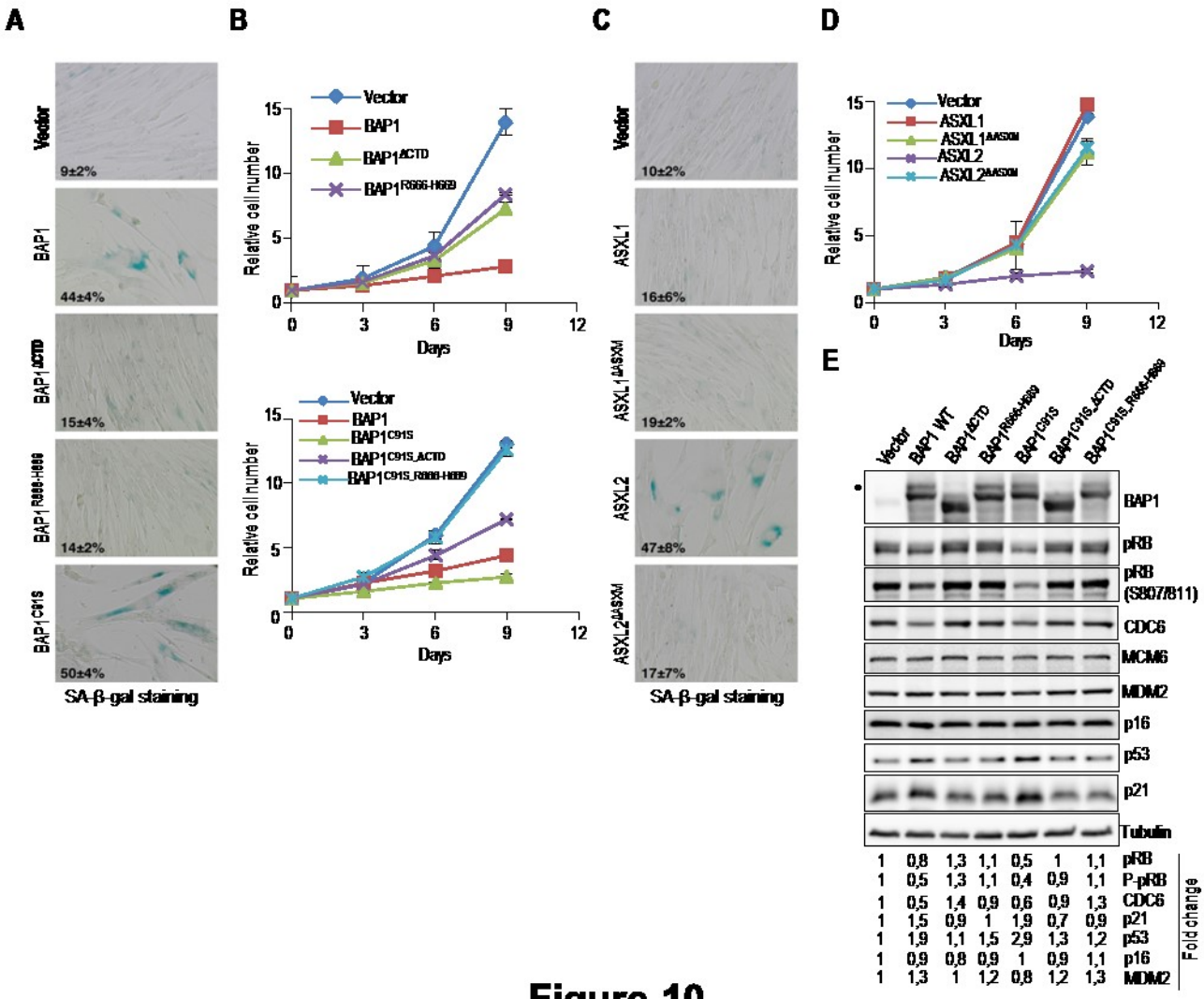

Figure 10

Figure 10. ASXL2 and BAP1 overexpression induce senescence in an ASXM- and CTD-dependent manner respectively.

A) IMR90 cells were infected using retroviral expression vectors for BAP1 and its respective mutant forms. Eight days post-selection the cells were fixed for staining of senescence-associated β-galactosidase assay (SA-β-gal). **B)** Cells were also transduced with retroviral expression vectors for BAP1, $BAP1^{C91S}$ and their respective mutant forms and counted every three days after selection to follow cell proliferation. 100 cells were counted in triplicate and data presented as percentage of positive cells, average ± SD. **C-D)** IMR90 cells were transduced using retroviral expression vectors for ASXL1, ASXL2 and their mutant forms. Eight days post-selection the cells were fixed for SA-β-gal staining **(C)** Cells were counted as in **(B)** every three days after selection to follow cell proliferation **(D)**. **E)** BAP1 overexpression triggers cellular senescence and induces the p53/p21 DNA damage response in ASXL1/2 dependent manner. Eight days post-selection the senescent cells were harvested for immunoblotting. Quantification of band intensity was conducted relative to the empty vector transduced cells. Tubulin was used as a protein loading controls. The dot indicates a monoubiquitinated form of BAP1 [9] (panels **E**).

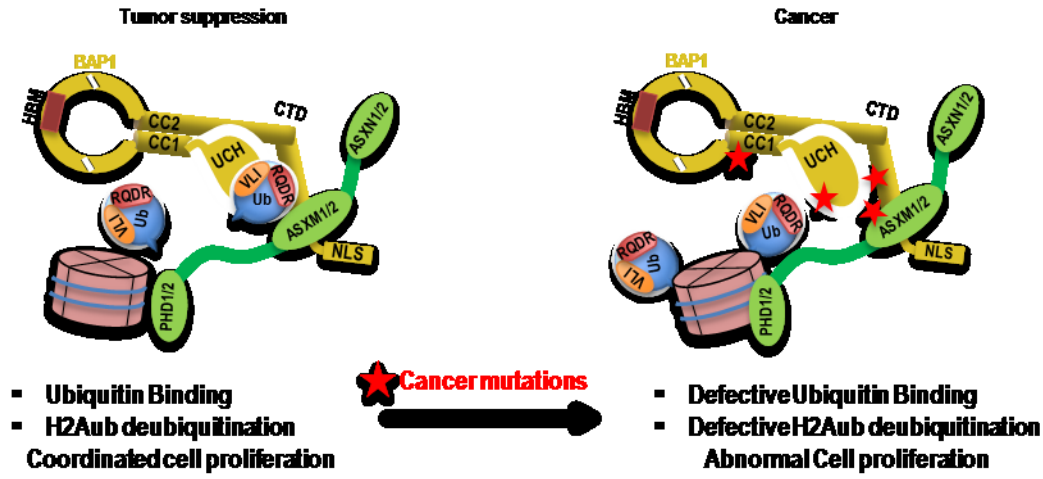

Figure 11

Figure 11. Model for the regulation of BAP1-mediated deubiquitination by ASXL1/2. An intramolecular interaction involving UCH/CC1 and CTD domains of BAP1 creates an ASXM-inducible composite ubiquitin binding interface (CUBI) that facilitates ubiquitin binding and catalysis. The red stars indicate cancer-associated mutations of BAP1 or ASXM that disrupt the CUBI.